

PYROLYSIS AND PARTIAL OXIDATION OF N-BUTANE

Thesis by

James Edwin Blakemore

In Partial Fulfillment of the Requirements

**For the Degree of
Doctor of Philosophy**

**California Institute of Technology
Pasadena, California**

1970

(Submitted May 7, 1970)

ACKNOWLEDGEMENTS

The patience, encouragement, and guidance with which Dr. William H. Corcoran has advised me in this research endeavor is reflected in the respect that I hold for him both as a man and as an educator. I would also like to thank other members of the faculty who have helped broaden my education. From a laboratory standpoint, Hollis Reamer was always helpful in discussions of equipment and mechanical problems.

Financial support from the National Science Foundation in the form of a graduate fellowship and the California Institute of Technology in research assistantships was greatly appreciated. Support of the research project by Shell Oil Company is also gratefully acknowledged.

Design and fabrication of the experimental apparatus was greatly expedited by the assistance and cooperation of George Griffith, Chick Nakawatase, Bill Schuelke, and Ray Reed. The talents and attitudes of these men toward their work are an asset of immeasurable value to the department.

I would like to thank Roger Barker for his constructive discussions on hydrocarbon reactions and for his "breaking me in" in the lab. To other fellow graduate students, I feel indebted for their having made the past four years in Pasadena an enjoyable experience.

My education is primarily a result of the encouragement and financial sacrifice of my parents. For them, I will be eternally grateful.

An acknowledgement would not be complete without thanking my wife, Frances, for her devotion, patience, and understanding. She was especially helpful in the preparation of this thesis.

ABSTRACT

A gas-chromatograph network capable of the analysis of possible products in the gas-phase pyrolysis, oxidative pyrolysis, and partial oxidation of n-butane was developed. Low-molecular-weight paraffins, olefins, alcohols, esters, aldehydes, ketones, organic acids, carbon oxides, fixed gases, and water could be identified and measured in the parts-per-million range of product mixtures.

The pyrolysis of n-butane was examined in tubular-flow, gold micro-reactors having lengths of twelve inches and an inside diameter of 0.0625 inch. Partial pressures of butane were varied from 0.5 to 12 psia, with the total pressure being maintained at fifteen psia by use of an argon diluent. Conversions of butane were less than 2.5 per cent. The overall rate of reaction of the butane was accurately described by kinetics of three-halves order. An average activation energy of 65 kcal mole⁻¹ was observed. Approximately equal molar quantities of methane and propylene were observed in the products. Formation of ethane, ethylene, and hydrogen varied with temperature and concentration of butane. The pyrolysis varied only slightly in untreated and in acid-treated reactors.

The influence of trace quantities of oxygen on moderate-temperature (500 to 600°C) pyrolysis of butane was investigated using gold micro-reactors having lengths of twelve inches and inside diameters of 0.0625 and 0.125 inch. Partial pressures of butane from one to twelve psia were used, with the total pressure being maintained at fifteen psia.

Oxygen, present from 7 to 800 parts-per-million in the reactants, inhibited the overall pyrolysis rate and increased the olefin content of the product mixture which was predominantly paraffins and olefins.

The investigation of the oxidative dehydrogenation of n-butane was also examined from 460 to 595°C. Concentration of oxygen in the reactants was varied from 0.04 to 1.0 per cent by volume. At the lower temperatures, isomers of butene, 1,3-butadiene, water, and carbon dioxide comprised over 97 per cent of the products. At higher temperatures, formation of the cracked products of the pyrolysis increased. The overall rate of the disappearance of n-butane was correlated on the basis of a power-law expression of three-halves order with respect to the butane and one-half order with respect to oxygen. The Arrhenius activation energy of the overall dehydrogenation of n-butane was 23.1 kcal mole⁻¹ compared to a value of 65 kcal mole⁻¹ for the pyrolysis.

The partial oxidation of n-butane to oxygenated-organic products was totally suppressed at temperatures of 400 and 440°C for contact times of 20 seconds and less.

TABLE OF CONTENTS

<u>TITLE</u>	<u>PAGE</u>
INTRODUCTION	1
LITERATURE SURVEY	4
The pyrolysis of n-butane	4
The pyrolysis in the presence of traces of oxygen	8
The oxidative dehydrogenation of n-butane	9
The oxidative dehydrogenation of other alkanes	13
The low-temperature partial oxidation of n-butane	15
The low-temperature oxidation of other hydrocarbons	17
APPARATUS	21
Reactants	22
Flow control	25
Auxilliary equipment	26
Reactor	27
Thermostat	31
Analysis of product mixture	37
EXPERIMENTAL PROCEDURE	50
TREATMENT OF DATA	52
RESULTS AND DISCUSSION	57
Pyrolysis of n-Butane	57
Reactor operation and energy transfer	57
Pyrolysis of n-butane	63
Pretreatment of the reactor with oxygen	75

TABLE OF CONTENTS, CONT'D.

<u>TITLE</u>	<u>PAGE</u>
Pyrolysis in a stabilized acid-treated reactor	81
The mechanism of the pyrolysis of n-butane	93
Pyrolysis in the Presence of Trace Amounts of Oxygen	102
Distribution of hydrocarbon products	102
Distribution of cracked products	109
Rate of formation of cracked products	116
Inhibition or acceleration	119
Oxidative Dehydrogenation of Butane	124
Distribution of products	124
Relative formation of C ₄ unsaturates	143
Relative formation of the cracked products	148
Stoichiometry of the overall reaction	151
Overall rate of the reaction	154
The mechanism of the oxidative dehydrogenation	166
Partial Oxidation of Butane at Lower Temperatures	171
CONCLUSIONS	172
RECOMMENDATIONS FOR FUTURE STUDY	176
NOMENCLATURE	179
REFERENCES	180
APPENDIX A	185
APPENDIX B	223
APPENDIX C	231

TABLE OF CONTENTS, CONT'D.

<u>TITLE</u>	<u>PAGE</u>
APPENDIX D	239
PROPOSITIONS	244

INTRODUCTION

The pyrolysis and partial oxidation of paraffin hydrocarbons frequently present economical means of upgrading petroleum fractions. Trends in the petroleum industry indicate an annual growth rate in the supply of n-butane of about 4 per cent per year over the next five years. Coupled with the present excess supply, this will add to the pressure to find new outlets for n-butane.

Currently over 80 per cent of the consumption of n-butane is in gasoline as a blend-stock for volatility. Increasing use of butane is expected in the production of olefins by means of thermal cracking. Propylene, methane, ethylene and ethane are the primary products of the pyrolysis of n-butane. Commercial units for thermal cracking of butane are operated at temperatures from 800 to 900°C.

The partial oxidation of n-butane may be divided into three ranges according to temperature: (1) a high-temperature region, (2) a region of negative temperature coefficient, characterized by an increase in overall reaction rate with a decrease in temperature, and (3) a low-temperature region. The precise limits of each region are dependent upon the pressure and composition of the reactants and surface effects of the reactor; however, near atmospheric pressure the upper limit of the second region is approximately 440 to 480°C while the lower boundary is generally 370 to 400°C.

In the upper range in partial oxidation, the primary products of the reaction are olefins and water. Commercial advantage may be taken

of this fact by introducing oxygen into conventional pyrolysis units. A result is the absence of soot and carbon deposits on the reactor surface.

In the low-temperature range, oxygenated hydrocarbons such as aldehydes, ketones, acids, oxides and alcohols are the major products. Industrially, the partial oxidation of n-butane and other paraffins in this region represents an economical route to the production of these compounds. Celanese Corporation operates a full-scale process, in which n-butane and propane are used as feedstocks, for the production of methanol, formaldehyde, acetaldehyde and acetone. The diversification of products and thus increased outlay for often complicated separation processes is a disadvantage; however, the outlay is frequently offset by the relatively low cost of paraffin feedstocks. Ample commercial impetus, therefore, exists for a detailed study of the pyrolysis and the partial oxidation of n-butane.

There are also academic incentives for a thorough examination of the reactions as many fundamental questions remain unsatisfactorily answered and open to debate. Aspects of the pyrolysis in which additional work would be desirable include the influence of trace amounts of oxygen on the overall rate of pyrolysis, the nature and extent of surface effects, and the inhibition of the reaction by the products. The partial oxidation of n-butane has been studied less than the pyrolysis. Variation of the product distribution with temperature, pressure, and concentration of reactants, the effect of additives on

the reaction, the role of surfaces, order of the reaction, and the mechanism by which the oxidation takes place are but a few of the controversial areas.

The basic aim of the present work was to study the thermal cracking of n-butane and the reaction between oxygen and butane in a gold micro-reactor at atmospheric pressure and at temperatures from 460 to 630°C. Objectives of the study were the characterization of the initial stages of the reactions in terms of the reaction rate and the distribution of products as functions of temperature, concentrations of reactants, and extent of the reactions. Correlation of the experimental results with plausible mechanisms is of primary interest.

LITERATURE SURVEY

Many investigators have studied the pyrolysis and vapor-phase oxidation of hydrocarbons. Attention has been focused on the pyrolysis of methane, ethane and, to a lesser extent, propane and n-butane. Primarily, the oxidation work has been directed towards ethane and propane. Little research has been devoted to the pyrolysis of any hydrocarbon in the presence of trace amounts of oxygen.

In the following section, a review is given of the literature related to the pyrolysis and gas-phase oxidation of n-butane. Work dealing with other paraffins is presented in areas where studies involving butane are incomplete.

The pyrolysis of n-butane

The thermal decomposition of n-butane was examined using a gold tubular reactor by Barker and Corcoran (1). Data were taken under the following conditions: temperatures from 530 to 595°C, pressures from 5 to 20 psia, contact times from 0.55 to 4.0 sec and conversions of butane less than 2 per cent. Continual monitoring of the reactants insured less than 2 ppm oxygen. Products were analyzed by gas chromatography.

Generally, the kinetics of the pyrolysis could be accurately described by the following expression:

$$-R_{C_4H_{10}} = k [C_4H_{10}]^{1.5}$$

where $k = 2.27 \times 10^7 \exp(-66,000/RT) \text{ cc}^{1/2} \text{ mole}^{-1/2} \text{ sec}^{-1}$. With an excess of diluent in the system (mole fraction of butane less than 0.3) the rate of disappearance of butane became substantially greater than that predicted by the above expression. Although several hypotheses were developed, the exact cause of this phenomena was not determined.

Surface-to-volume ratio (hereafter referred to S/V) was varied from 64 in^{-1} to 165 in^{-1} by packing the reactor with lengths of gold wire. Although the rate data were approximately 11 per cent lower in the packed reactor, the reaction otherwise possessed the same characteristics as in the unpacked reactor. Comparison of this work with other investigations (2, 3) conducted in pyrex or quartz supported the homogeneity of the pyrolysis. This is not to imply that the surface could not be made to significantly effect the pyrolysis. On the contrary, after exposure of the surface to oxygen at temperatures above 400°C , the rate of pyrolysis was sharply depressed. This was explained by the presence of oxidizable impurities such as copper or silver in the gold. After removing such impurities by nitric-acid etching, the reaction rate returned to its original level.

The product distribution was unaffected by changes in contact time and was affected only slightly by temperature and pressure in the ranges studied. Methane and propylene yields were essentially identical, each representing about 33 per cent of the product mixture. Ethylene, 18 per cent, and ethane, 12 per cent, and hydrogen, 3 per cent, were the other major products. Isomers of butene composed the

remaining 1 per cent of the product mixture. A free-radical mechanism, similar to that originally proposed by Rice (4), satisfactorily accounted for the distribution of products.

The present work is considered a complement to the work of Barker and Corcoran. The reader is referred to the original thesis for an extensive review of the available literature on hydrocarbon pyrolyses. For convenience a brief review of other work is given herein.

Early investigations into the pyrolysis of butane were conducted by Pease and Durgen (5), Steacie and Puddington (6), Crawford and Steacie (7), Hepp and Frey (8), and Nehaus and Marek (9). In these and other early studies, the products were seldom measured at conversions of butane below 10 per cent. As secondary reactions involving propylene undoubtedly occur at high conversions of butane (10, 11), the kinetic correlation of the reaction was complex. Thus some authors described the decomposition on the basis of a first-order dependence on butane concentration while others chose to use a second-order model. The major products of methane, propylene, ethylene, and ethane were identified.

Using a batch reactor Purnell and Quinn (2, 12, 13, 14) extensively studied the thermal decomposition of butane over the temperature range 420 to 530°C, at initial pressures between 10 and 150 mm Hg, and conversions of butane from 4 to 11 per cent. The products contained methane and propylene in equal molar amounts, ethylene, ethane, and hydrogen. Minor amounts of butenes, butadiene, and 1-pentene were observed

at butane conversions above 10 per cent. The production of hydrogen was found to equal one half the difference in yields of the ethylene and ethane. The rate of decomposition of butane was approximately proportional to the three-halves power of the butane concentration. The rate of formation of each product was also described by a power law expression of the butane concentration. Exponents from 1.25 for hydrogen to 1.60 for ethane were calculated. A free-radical mechanism incorporating the pressure dependence of the ethyl radical accounted for the experimental data.

The effects of changing the S/V ratio of the pyrex reactor from 3.0 to 11.0 in^{-1} were noted. In the case of clean, KCl-coated and acid-etched vessels, identical and reproducible rates were obtained for all values of S/V. A magnesium-perchlorate coating led to a large initial acceleration of the rate. Conditioning of the vessel surface with carbon considerably reduced the reaction rate. It was concluded that the reaction was homogeneous in the clean, KCl-coated and acid-etched reactors but that in the magnesium perchlorate or carbon-coated vessels heterogeneous termination processes may be important.

Sagert and Laidler (3) investigated the pyrolysis of n-butane at temperatures from 520 to 590°C and at pressures from 30 to 600 mm Hg. Experiments were conducted in batch reactors of quartz. The rate of reaction was followed manometrically and by gas chromatography. The reaction was accurately predicted by three-halves order kinetics; the activation energy was found to be 59.9 kcal mole⁻¹, and the frequency factor $3.24 \times 10^{15} \text{ cc}^{1/2} \text{ mole}^{-1/2} \text{ sec}^{-1}$. Packing the vessel with quartz

tubing increased the activation energy to $62.3 \text{ kcal mole}^{-1}$. The surface effect was attributed to a certain amount of initiation and termination of chains involving surface reactions. It was concluded that the surface reactions represented only a small portion of the total reaction and that the reaction was thus largely homogeneous. Products reported included methane, propylene, ethylene, ethane, and butenes. No analysis was made for hydrogen. The product distribution was predicted from a free-radical mechanism.

Wang and Corcoran (15, 16) employed a ceramic reactor in the study of the pyrolysis of butane. The reactor possessed a S/V ratio of 4.0 in^{-1} and was operated at atmospheric pressure over the temperature range 460 to 560°C . Energy, mass and momentum transport were considered in the treatment of the rate data. Velocity and temperature distributions within the one-inch-diameter reactor were measured. Although the data could be correlated equally well with a first or second-order rate expression, the product distribution was in agreement with other work (2, 3).

The pyrolysis in the presence of traces of oxygen

Essentially no literature exists for the influence of oxygen in concentrations of less than 100 ppm on the pyrolysis of n-butane. Appleby (17), working with concentrations of oxygen greater than 0.5 per cent, suggested that oxygen concentrations as low as 1 ppm could significantly affect pyrolysis rates. Concentrations of 0.5 per cent oxygen had increased the rate of pyrolysis of n-butane a hundred-fold.

Voevodsky (18) observed that with propane the effect of oxygen was to accelerate the pyrolysis up to a limiting value.

Niclause, et al (19, 20, 21, 22) reported the effects of small quantities of oxygen on the pyrolysis of propane, isopentane and isobutane. Oxygen concentrations from 0.001 to 1.0 per cent were involved in the experiments. The data, largely qualitative in nature, revealed several surprising features. Depending upon the S/V ratio and nature of the reactor surface, oxygen exhibited either an accelerating or inhibiting effect on the pyrolysis of the hydrocarbon. For propane, oxygen concentrations of 0.5 per cent increased the rate of pyrolysis in a pyrex reactor with $S/V = 1.8 \text{ in}^{-1}$ while decreasing the rate in a pyrex reactor with $S/V = 23.8 \text{ in}^{-1}$. The treatment of the reactor surface with PbO or KCl also accented the inhibitory effect.

A detailed analysis of the product mixture was not given; however, a general mechanism was presented to explain the dual role--inhibition or acceleration-- of oxygen in the pyrolysis. No attempt was made to kinetically describe the reaction or to estimate the temperature dependence of the pyrolysis in the presence of oxygen.

The oxidative dehydrogenation of n-butane

The reaction of butane and oxygen was studied in the temperature range 486 to 526°C by Appleby et al (17). The S/V ratios of the pyrex and KCl-coated reactors were 6.8 in^{-1} . The products of the reaction were analyzed by a method of multi-isothermal distillation. Oxygen concentrations from 0 to 35 per cent by volume were employed in the reactor

feed. At oxygen concentrations below about 8 per cent, the reaction products consisted of only water and hydrocarbons, primarily butenes; however, the sensitivity of the analysis was limited. Even at concentrations of oxygen up to 35 per cent, no carbon dioxide or hydrogen peroxide were detected in the products. In runs with high oxygen concentrations and conversions of butane above 30 per cent, appreciable amounts of carbon monoxide, in addition to water and hydrocarbons, were detected in the products.

The rate of reaction was found to be approximately proportional to the square root of the oxygen concentration and to the three-halves power of the butane concentration. The temperature dependence of the rate was found to be slight, an activation energy of 21 kcal mole⁻¹ being obtained.

Several significant observations were also made in the study. When compared to the thermal decomposition of butane, oxygen had a pronounced accelerating effect on the decomposition. Generally, nearly all the oxygen was consumed in about 5 seconds. Below 10 per cent by volume of oxygen, the number of moles of butane which reacted per mole of oxygen consumed decreased from a value of fifteen in mixtures containing 0.5 per cent oxygen to a value of 2 in mixtures containing 10 per cent oxygen. Water, a major product, had no noticeable inhibiting effect on the reaction; however, the addition of 1-butene sharply reduced the rate of conversion of butane.

Surface effects were noted as influencing the rate of the reaction

although the surface of the reactor was not studied in detail. Attempts at studying the reaction below butane conversions of 1 per cent met with little success as the data were inconclusive.

Barker and Corcoran (1), in a preliminary study of the oxidative dehydrogenation of n-butane, examined the reaction in a gold tubular reactor ($S/V = 64 \text{ in}^{-1}$) at temperatures of the order of 500°C . Butane partial pressures from 2.5 to 8.0 psi and oxygen concentrations of 4 per cent by volume were primarily employed in the tests. However, because of the unexpected appearance of large amounts of carbon dioxide in the products, a complete analysis of the products was not made. Faint but positive tests were obtained for the presence of aldehydes in the products.

Butene isomers were among the initial products at high levels of oxygen but were rapidly attacked further by oxygen. Water was not detected chromatographically, but its presence was noted by condensate in the effluent lines.

Several runs with trace levels (30 ppm) of oxygen in the reactants were made. In general the production of cracked products was sharply depressed while the formation of butenes was slightly enhanced. All of the oxygen was consumed in the first few milli-seconds of the reaction. No attempt was made of a correlation between the overall rate and the reactant concentrations because of limited data.

Kalvinskas and Corcoran (23) studied the partial oxidation of n-butane in a 1-inch-diameter, porcelain, flow reactor whose length could

be varied from 0 to 30 inches. The range of experimental conditions covered were one atmosphere pressure, 360 to 760°C, and inlet oxygen concentrations of 0 to 25 per cent. Conversions of n-butane were from 5 to 45 per cent based on inlet conditions. Reaction rate data were correlated on the basis of the following equation which was also proposed by Appleby (17):

$$-R_{C_4H_{10}} = k[C_4H_{10}]^{1.5}[O_2]^{0.5}$$

A minimum reaction rate was observed at 425°C. The products were analyzed for carbon oxides, olefins, paraffins, hydrogen, and water. Carbon dioxide and carbon monoxide were produced in roughly the same amounts. Carbon was found in significant quantities at the higher conversions of butane.

Baldwin and Walker (24) gained insight into the reaction of H• and •OH radicals with n-butane in a study of the inhibition of hydrocarbons on the hydrogen-oxygen reaction. The study was conducted in pyrex reactors, S/V ratios from 2.0 to 4.2 in⁻¹, over the temperature range 480 to 520°C. The consumption of butane was most easily explained by reaction with the hydroxyl radical, •OH, to form water and an alkyl radical. The alkyl radical then reacts predominantly with oxygen to form an olefin and the hydroperoxide radical, HO₂•, which is destroyed without continuing the chain. The following rate constants at 520°C were obtained from this work:



The oxidative dehydrogenation of other alkanes

In a comparison of the high-temperature oxidation of butane with other paraffins, common conclusions can often be reached as all alkane oxidations are known to be of a free-radical nature.

Jones, Daubert, and Fenske (25) have investigated the vapor phase oxidation and oxidative dehydrogenation of ethane and propane in the presence of a countercurrent "rain" of noncatalytic, dispersed, particulate solids. As conversions of butane ranged from 5 to 50 per cent, the "rain" of solids provided a means of rapid energy transport necessary for the maintenance of nearly isothermal conditions. Product distributions were determined as a function of temperature (310 to 560°C), oxygen-hydrocarbon molar ratios (0.05 to 0.6), pressure (0 to 150 psig), solids flow rate, and contact time (1 to 28 sec).

No attempt was made to treat the data kinetically or to postulate definitive reaction mechanisms. However, similarities and differences in the behavior of ethane and propane upon oxidation were noted. The analogous olefin appeared as the major product in both instances. At temperatures of 500 to 560°C and atmospheric pressure, virtually no carbon monoxide was formed in the oxidation of ethane while carbon dioxide appeared as a major product. The CO_2/CO ratio for propane under similar conditions was about 10 : 1. Increasing the flow rate of particulate solids and hence the total surface area further depressed the

formation of carbon monoxide and the overall rate of butane consumption and increased the selectivity of carbon dioxide.

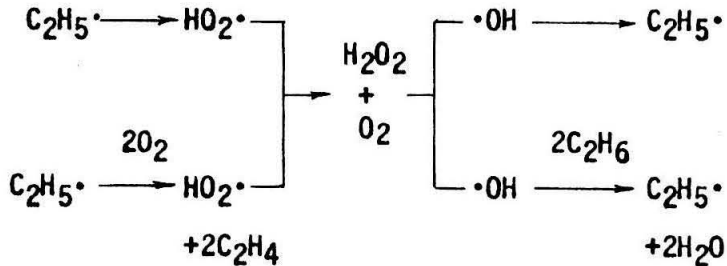
The effect of increasing the pressure was to decrease the CO_2/CO ratio, decrease the production of olefins and increase the formation of paraffins. In all the work at temperatures above 500°C , formaldehyde and other oxygenated hydrocarbons were not observed in the products. Neither was hydrogen peroxide detected.

The use of air or oxygen as the oxidant had little effect on the overall reaction for oxygen-hydrocarbon molar ratios of less than 0.3. As the contact time was increased, the primary result was an increase in the formation of carbon oxides and a decrease in the formation of olefins.

Sampson (26) using a fused silica reactor ($S/V = 5.0 \text{ in}^{-1}$) studied the reaction between ethane and oxygen at 600 to 630°C . Ethane-oxygen ratios between 2.5 and 10 were used and conversion of ethane was kept below 3 per cent. Primarily ethylene and water (no measurement of the water concentration was attempted) were found in the products although significant amounts of hydrogen, hydrogen peroxide, formaldehyde, carbon monoxide, and other oxygenated hydrocarbons were detected. No carbon dioxide was reported in the product mixture.

A mechanism, depicted below, was proposed in which a primary feature was the formation and decomposition of hydrogen peroxide. Although the amounts of hydrogen peroxide isolated were invariably less than might be expected with such a mechanism, the small yields were attributed

to decomposition of hydrogen peroxide on the walls rather than to its nonformation.



The low-temperature partial oxidation, n-butane

Over the temperature range 300 to 460°C and with significant oxygen-butane molar ratios, the reaction results in the formation of formaldehyde, methanol, acetadehyde, hydrogen peroxide, and other organic oxygenated compounds. As little of the present work was involved in this region, only a brief review of the pertinent literature is presented. General knowledge of this area of oxidation is important for a complete understanding of the oxidative dehydrogenation at higher temperatures.

Comprehensive studies of the effects of temperature, residence time, initial oxygen concentrations, and reactor surface on the partial oxidation of n-butane have been published by Steitz (27) of Pan American Petroleum Corporation, Lemon (28) of Union Carbide, and Harris (29) of DuPont. These data have, in general, been industrially oriented toward high butane conversion and operating conditions for maximum product yields and, as such, have contributed only a small part to a better understanding of the basic reaction sequence.

Skrivan and Hoelscher (30), using a stainless-steel flow reactor, made a kinetic study of the partial oxidation of n-butane at atmospheric pressure, 257 to 350°C, and initial oxygen concentrations of 20 per cent and 40 per cent. From 6 to 30 per cent conversion of the n-butane was effected. An interesting observation was the presence of periodic cool flames at the higher oxygen level. Carbon monoxide, carbon dioxide, low-molecular-weight olefins and paraffins, hydrogen, water, formaldehyde, acetaldehyde, methanol, and acetone were measured in the products.

Employing a batch reactor, Norikov and Blyumberg (31) investigated the oxidation of n-butane at 250°C and 550 mm Hg. The reaction vessel was constructed of quartz. Acetaldehyde, formaldehyde, acetone, methanol ethanol, acetic acid, formic acid, carbon monoxide, and carbon dioxide were reported as the major products. Addition of acetaldehyde to a reactant mixture increased the rate of n-butane decomposition. Quartz and stainless-steel reactor vessels were studied with the result that the oxidation of butane took place much more rapidly in the quartz vessel (32). In the stainless-steel vessels, the reaction took place more slowly in a new reactor than in one which had been in operation for a few days.

Slavinskaya (33), using a quartz reactor, examined the effect on n-butane oxidation of small amounts of ozone in the low temperature region (190 to 303°C, 300 mm Hg). The ozone increased the production of aldehydes. Another interesting observation was the production of CO₂ at higher temperatures. Nieman (34), using radioactive tracer

molecules, concluded that at a temperature of 400°C formation of CO₂ from oxidation of CO was negligible. This is in agreement with Barker (1) whose work around 500°C showed no CO but significant amounts of CO₂.

The low-temperature oxidation of other hydrocarbons

Working with ethane and propane, Jones, et al (25) observed the effects of contact time (1 to 28 sec), pressure (0 to 150 psig), oxygen-hydrocarbon molar ratios (0.05 to 0.6), and temperature (300 to 420°C) on the product composition. This study, in conjunction with work on the high-temperature dehydrogenation noted earlier, was conducted in a steel, tubular reactor in the presence of a countercurrent "rain" of dispersed solids. Formaldehyde, acetaldehyde, and methanol were the primary oxygenated products and together with the olefins composed the major products. In addition smaller amounts of ethanol, acetals, epoxides, etc. were detected. The sum of these compounds were referred to as organic oxys. The production of organic oxys increased with increasing pressure, decreasing temperature and decreasing oxygen-hydrocarbon molar ratios.

A striking observation was the complete suppression of the reaction leading to organic oxys when a packed bed was utilized as the reactor. This was probably a result of surface destruction of the oxygenated chain carriers.

Propane was partially oxidized with oxygen in both flow and batch glass reactors by Albright and Winter (35). The flow reactor possessed

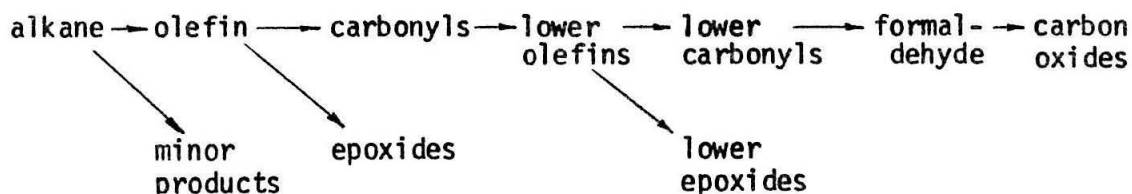
a S/V ratio of 2.1 in⁻¹ while that of the batch system was about 1.5 in⁻¹. Most tests were performed at 335°C and pressures from 3 to 15 psia. Water, methanol, formaldehyde, methylal, carbon monoxide, carbon dioxide, propylene, and ethylene constituted the bulk of the products. Analysis was accomplished using gas chromatography. The flow experiments produced more water, carbon monoxide and propylene than did the batch runs for similar conditions. Of significance was the formation of cool flames and a hysteresis loop in this region using the flow apparatus. The activity of the reactor surfaces was observed to change with aging of the vessel.

Satterfield and Reid (36) emphasized the importance of surfaces on product distributions formed in the oxidation of propane. Temperatures of 375 to 475°C were employed as were flow reactors of various materials. Inlet propane-oxygen molar ratios varied from 5.5 to 6.5 and the total pressure was near atmospheric. Propylene, ethylene, carbon monoxide, carbon dioxide, formaldehyde, acetaldehyde, methanol, hydrogen peroxide, and water were measured in the product mixture. Borosilicate glass reactors with various surface treatments yielded a slight variation in product composition; however, the striking difference was found between the glass and stainless-steel reactors. In the stainless-steel reactor, more carbon dioxide was formed than carbon monoxide. Hydrogen peroxide was not detected in the product mixture and formaldehyde, acetaldehyde and methanol were present only in minute amounts.

In a summary of the oxidation of hydrocarbons in the temperature

range 300 to 400°C, Knox (37) stressed the importance of a sequence involving the conversion of $\text{HO}_2\cdot$ to $\cdot\text{OH}$ radicals. Competitive oxidations of ethane and propane were examined by Knox (38). The experimental radical selectivities were in close agreement with those of an $\cdot\text{OH}$ or $\cdot\text{O}$ radical obtained in independent experiments by Baldwin (39). Similarly the selectivities differed from those expected of an $\text{HO}_2\cdot$ radical. This led Knox to believe that the $\text{HO}_2\cdot$ could not be the abstracting radical in alkane oxidations.

It was also concluded that any discussion of the oxidation of a paraffin must involve the co-oxidation of the conjugate olefin, the primary oxidation product of most alkanes. In support of this view were studies conducted by Knox (40, 41, 42) on ethane, propane and isobutane in which about 80 per cent of the initial oxidation product was the olefin. Zeelenberg (43) also obtained similar results on isobutane. The following sequence was then suggested as a plausible mechanism for hydrocarbon oxidations in the temperature range from 300 to 400°C.



The Knox scheme accounts for aspects of alkane oxidations such as

the initial high yield of olefins, the decrease in radical selectivity as the reaction proceeds, the importance of surface reactions, the strong promoting effects of olefins and the negative temperature coefficient.

Yet several points may be made which question the Knox mechanism. Albright (44), acknowledging that olefins are intermediates for a portion of the oxygenated compounds, suggests that undue importance is placed on the role of olefins. As a basis, he cites the work of Satterfield and Reid (45). Working with the partial oxidation of propane-propylene mixtures, they found that although the same products were formed upon oxidation regardless of the inlet hydrocarbon composition, the proportion of each component in the product mixture depended upon the initial propane-propylene composition. Albright concluded that isomerization and fragmentation of peroxy and hydroperoxy radicals might be an alternate route for the formation of the major products.

Semenov (46) has also made calculations which show that the Knox scheme predicts excessively long reaction times and that the acceleration from low to high rates of reactions, characteristic of hydrocarbon oxidations, is not properly predicted.

APPARATUS

The focal point of any system designed to obtain fundamental information on the nature of chemical reactions is the experimental reactor. It is not necessary that the experimental reactor be of the same type as industrial reactors. More important is that one of the model types of reactors is approached and that it is operated isothermally.

Previous investigators of paraffin pyrolyses and oxidations have generally chosen batch reactors. Several reasons for these selections are obvious. Large variations in the surface to volume ratio may be obtained. The reaction may easily be examined at high conversions of the reactants. In the case of low-temperature oxidations where a significant inhibition period often exists, sufficient time may be allowed for the reaction to measurably occur. But perhaps most important, direct measurement of the conversion rate may be made using a static reactor.

With a tubular flow reactor the conversion rate is not measured in a straightforward manner but an average rate over the length of the reactor is obtained, i.e. an integral reactor. This difficulty may often be avoided with the use of a microreactor, so characterized by its small size and often accompanying low conversions of the reactants. With low conversions and near constant conditions throughout the reactor, i.e. a differential reactor, simplification of the data analyses result. A tubular flow reactor is well-suited to the study of gas-phase reactions and to relatively fast reactions.

Since a basic objective of this research was the investigation of the initial rates of reaction, tubular-flow microreactors were selected. Gold tubing, 99.99 per cent, was used in construction of the reactors. The flow of n-butane, oxygen, and an inert diluent were adjusted to yield the reactor feed. The effluent of the reactor was quenched and analyzed for possible products. Figure 1 is a schematic of the experimental system.

Reactants

Research grade n-butane, 99.90 to 99.97 mole per cent minimum purity, was obtained from the Phillips Petroleum Company. Instrument grade n-butane, 99.5 mole per cent minimum purity, was purchased from the Matheson Company. Continuous operation of the reactor was economically possible by alternate use of research grade and instrument grade reactants for tests and interim use, respectively. Impurities detected in the research grade butane, in decreasing order of importance, were isobutane, 1-butene, c-2-butene, t-2-butene, and propylene. In addition, the instrument grade material contained varying amounts of 1,3-butadiene and 2,2-dimethyl propane. Representative analyses of the research grade butane are listed in Table 1.

Research grade c-2-butene, 99.94 mole per cent minimum purity, was obtained from the Phillips Petroleum Company and used in preliminary checks on the rate of isomerization of butene. Impurities included t-2-butene, 1-butene, n-butane, and 1,3-butadiene. Argon, used as an inert diluent, and oxygen were obtained from Linde in cylinders of 99.99 mole per cent minimum purity. Water, oxygen (in gases other than oxygen), and

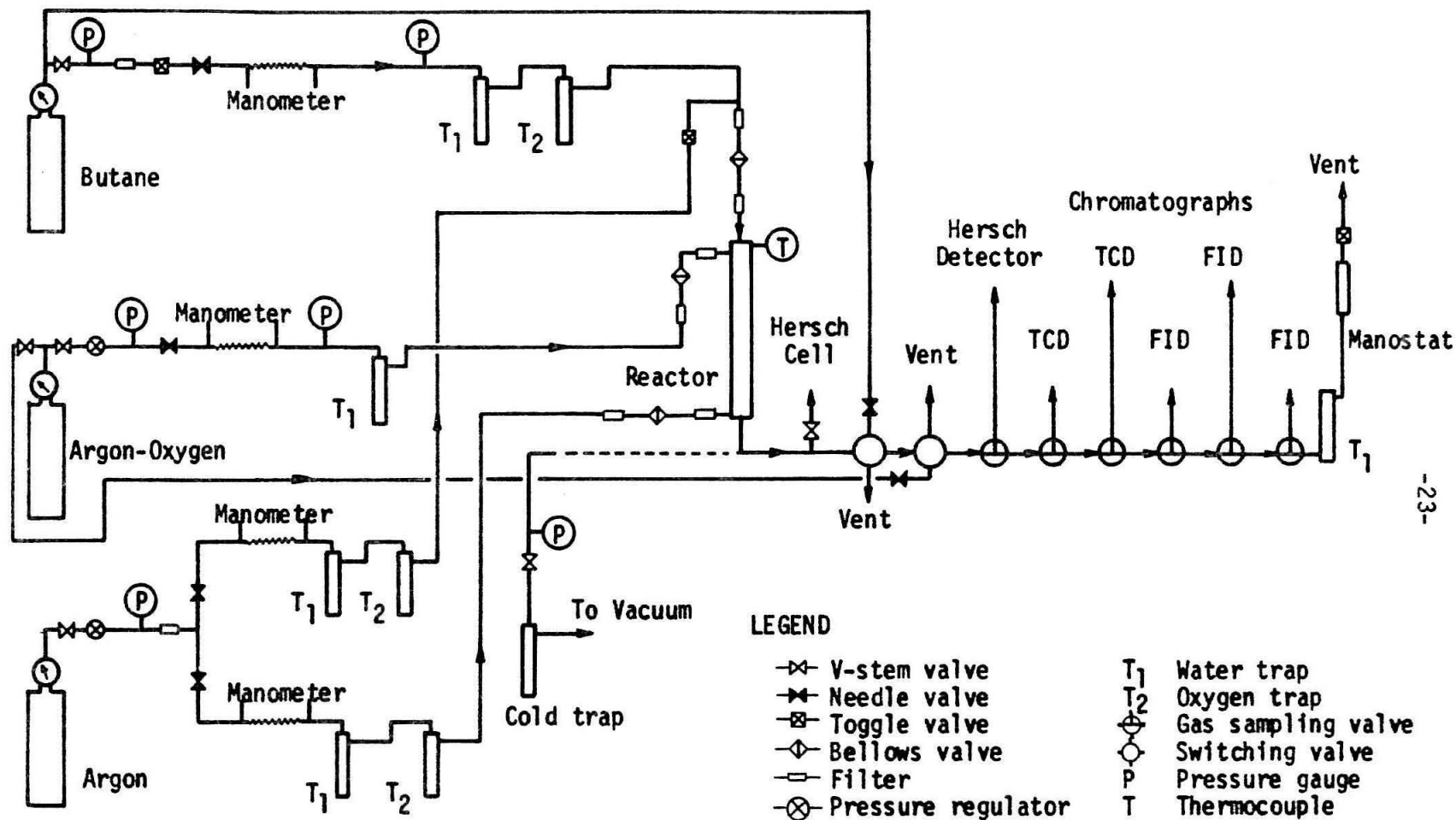


Figure 1. Schematic of the experimental apparatus.

Table 1. Representative Analysis of the Research Grade N-Butane.

Cylinder	Molar Percentage of N-Butane					
	$i\text{-C}_4\text{H}_{10}$	$1\text{-C}_4\text{H}_8$	$t\text{-2-C}_4\text{H}_8$	$c\text{-2-C}_4\text{H}_8$	C_3H_6	C_3H_8
1	0.0625	---	---	---	---	0.0121
2	0.0110	---	---	---	---	0.00134
3	0.0225	0.00805	0.00304	0.00090	0.0030	---
4	0.00413	0.0149	0.0306	0.00535	0.00027	0.00044
5	0.00321	0.0140	0.0280	0.00539	0.00032	0.00082
6	0.00264	0.0121	0.0282	0.00627	---	0.00017

nitrogen were present in trace amounts in each of the gases.

Effective removal of water, a product in the partial oxidation studies, from the argon and oxygen lines was accomplished using traps containing indicating silica-gel. Drierite (anhydrous calcium sulphate) was used in the butane stream because of irregular adsorption of the butane on the silica-gel.

Oxygen was removed from the argon and butane lines by means of traps of manganous oxide. The removal of oxygen was necessary because of its marked influence on the pyrolysis.

Flow control

Matheson (model 8) and Victor (model VTS 400 D) two-stage cylinder regulators were used to deliver oxygen and argon at near-constant pressure. Further reduction and control of the pressure was accomplished using Kendall (model 30) pressure regulators. A Matheson (model 40) single-stage line regulator was used for the butane.

Small-bore needle valves (Nupro, type 1 SA) were used to adjust flows of the gas streams. With pressure drops from 2 to 4 psi across a valve, the flow rate of gas could be adjusted from 0.5 ± 0.025 to 10.0 ± 0.1 ml/min.

Flow rates were indirectly measured by observing manometrically the pressure drops through columns filled with glass beads (Minnesota Mining and Manufacturing Company, type 100-5005). The columns were made from 10 to 15-inch lengths of 1/8 inch or 1/4 inch tubing. The manometers were calibrated and checked periodically using a soap-film flowmeter.

Correction was made for the presence of water vapor. The volumetric flow rate was approximately linear with pressure drop and was independent of the absolute pressure, 15 to 20 psia.

Silicone oil (Dow-Corning, type 200-500) was selected as the manometer fluid because of its density, flow characteristics and low vapor pressure. The silicone oil was degassed under vacuum before being placed in the manometers as selective absorption and desorption of gases could cause appreciable error in the flow rate. Reservoirs were installed in the manometer lines to avoid contamination of gas lines with silicone oil in the event of sudden surges of gas flow throughout the system.

Auxilliary equipment

A vacuum of less than 10 microns could be exerted on the reactor by connecting the reactor outlet directly to a vacuum pump (Welch Scientific Company, Duo-Seal). Leak-tight bellows valves (Nupro, type 554BG) and a Televac vacuum gauge were installed in the inlet lines of the reactor for this purpose.

Liberal use was made of screen filters (Nupro, 7 micron elements) to protect critical valves and to exclude fine particles or metal filings from the reactor.

For a measure of the reactor pressure, a calibrated Bourdon-tube pressure gauge (Wallace and Tiernan, type FA-145) was inserted in the butane and argon lines prior to the traps. In this manner impurities, entering the reactant lines through the gauge and its connections, would be removed.

A cartesian manostat (Manostat Corporation, model 6A) was used for precise control of the system pressure. The manostat fluid was mercury. Near atmospheric pressure and at low flow rates, this device was capable of controlling the pressure to within 0.05 psia of its set point. A problem was encountered when using the manostat with gas streams that were supersaturated with water vapor. Water would condense inside the manostat, collect on top of the mercury pool and interfere with the normal operation of the diver. A trap containing Drierite was inserted in the line prior to the manostat for removal of the water. Effluent from the manostat could be connected to a vacuum pump for control of pressures below atmospheric.

Reactor

Microreactors, having inside diameters of 0.0625 inch and lengths of 12 inches, were constructed from 99.99 per cent pure gold obtained locally from the Wilkinson Company. Gold was chosen primarily for two reasons. First, the pyrolysis and oxidation of n-butane had not been studied previously in gold vessels. For complete discussions on the homogeneity or heterogeneity of the reactions, the nature and type of reactor surface must be varied as well as the surface-to-volume ratio of the reactor. In this manner, the present work will supplement previous work as reactors of pyrex, quartz and stainless steel have been used. Secondly, gold does not form a stable oxide and weakly adsorbs oxygen at the high temperatures of interest. The inertness of gold to oxygen facilitates the controlled introduction of trace quantities of

oxygen into the reactor.

Design of the microreactors was based on the following considerations:

1. The reactor length should be sharply defined.
2. Configuration of the reactor should be such that isothermal operation is facilitated.
3. Hot butane or oxygen should contact only gold surfaces.
4. Thorough mixing of the reactants should be accomplished.
5. The reactor should be kept simple in design for ease of construction and absolute leak tightness.

In Figure 2 is a schematic of the reactor. A twelve-inch length of 3/16 inch O.D. (0.125 inch I.D.) or 1/8 inch O.D. (0.0625 inch I.D.) gold tubing bent into a U formed the reactor. In the inlet of the reactor, provision was made for mixing a preheated argon or argon-oxygen stream with the butane to effect a rapid approach to the reaction temperature. Similarly in order to freeze the reaction at the reactor exit, provision was made for mixing the product mixture with an argon quench stream. Figure 3 gives a detailed drawing of the inlet and exit heads for the 3/16 inch O.D. reactor. The 1/8 inch O.D. reactor heads are similar except for reduced dimensions. As gold is a good conductor of heat, the mass of material in the inlet and exit heads was kept to a minimum.

To insure that hot butane or oxygen contacted only gold surfaces, twelve-inch lengths of gold tubing were placed in lines adjacent to the

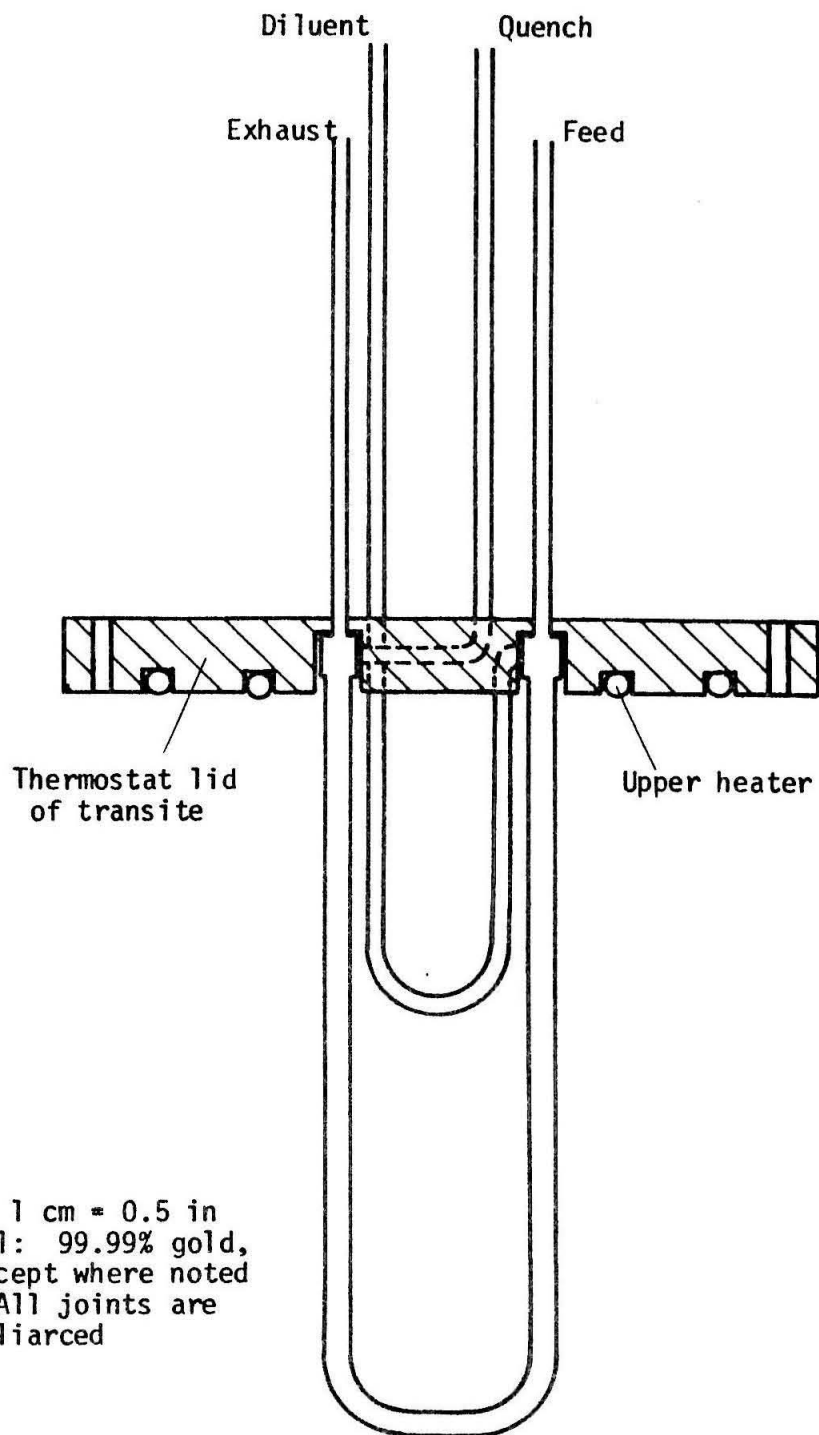
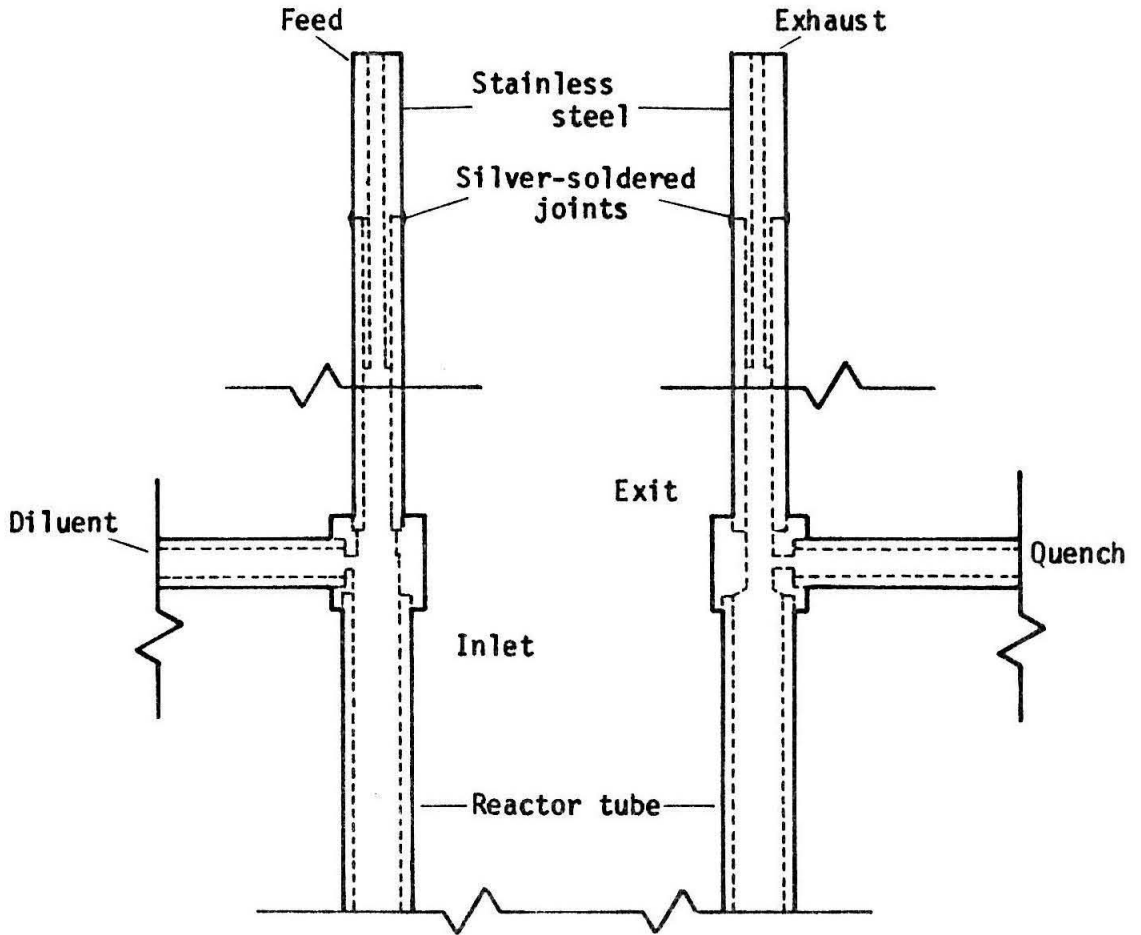


Figure 2. Schematic of the 3/16 inch O.D. gold microreactor.



Scale: 2" = 1"
Material: 99.99% Gold, except
where noted
Note: All joints are heliarced
unless otherwise noted

Figure 3. Inlet and exit heads for the 3/16" O.D. reactor.

reactor. Gold joints were heli-arc'd to provide leak tightness. As the assembled reactor was extremely prone to damage owing to the softness of gold, extreme care had to be exercised in the insertion and removal of the reactor from the thermostat. Pin-hole leaks, resulting from fatigue of the gold, could be closed with silver solder if the hole was not directly in the thermostated section of the reactor. Since the thermostated section attained temperatures of 650°C (near the softening point of the silver solder), holes in this section had to be heli-arc'd. Successfully heli-arc'ing the pin holes without further damage to the reactor was difficult.

Because of the softness of gold, a problem was encountered in trying to connect the gold tubing to other parts of the system. Since these connections had to be leak-tight and easily disconnected for reactor removal, 1/8 inch stainless-steel tubing was silver soldered to the gold tubing. Leak-tight connections using Swagelock fittings and teflon ferrules could then be made from the stainless-steel tubing.

Thermostat

The microreactor was encased in a recirculating-air thermostat, a schematic of which is given in Figure 4. Two concentric cylinders of stainless steel formed the chamber which housed the reactor. The inner cylinder, 1.5 inches in diameter, was suspended inside the outer cylinder, 3.5 inches in diameter. The ends of the housing were constructed of 0.5-inch thick transite to minimize heat losses. The upper transite end contained a heater, rated 135 watts at 38 volts, and the reactor inlet and exits.

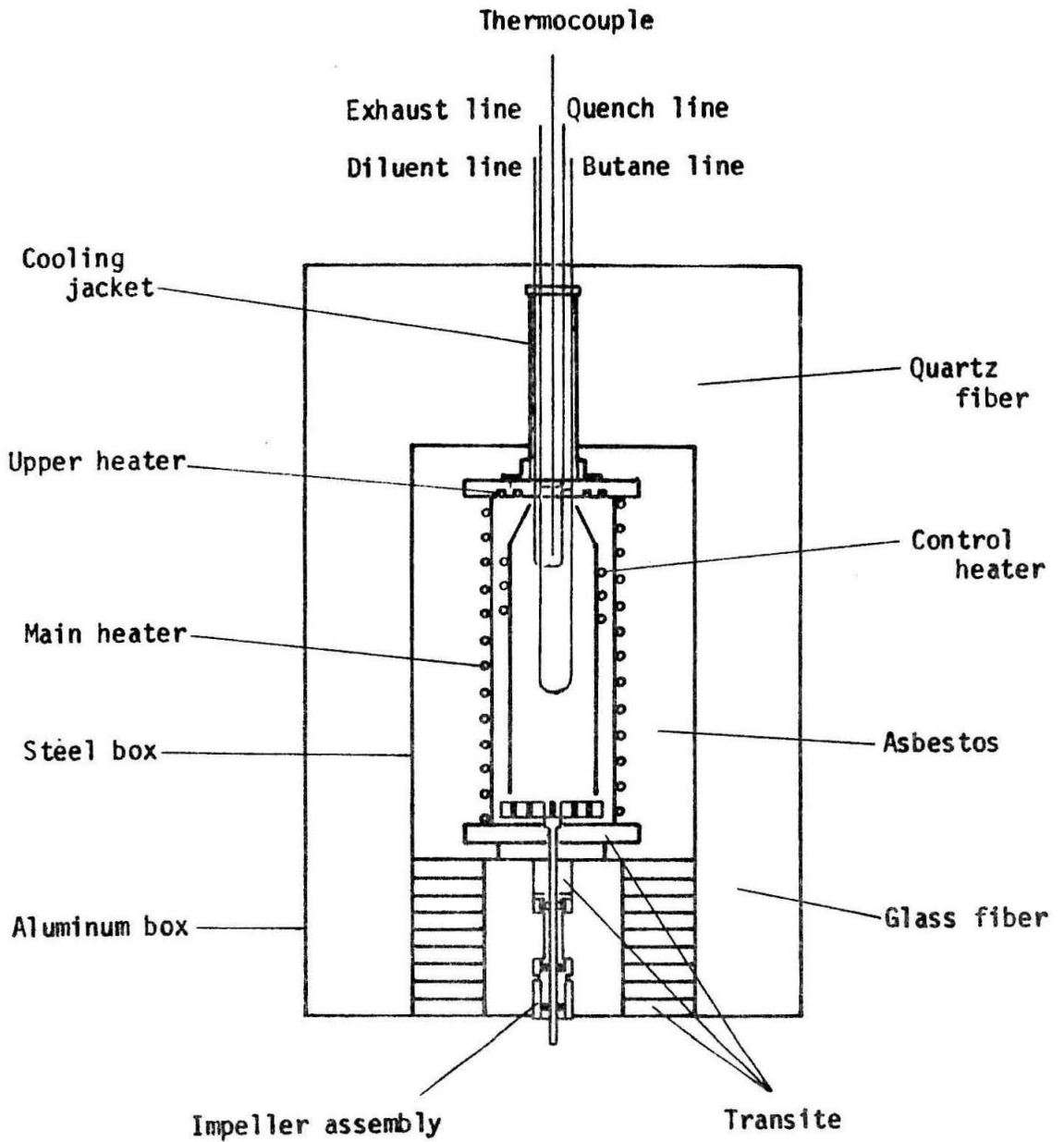


Figure 4. Schematic of the recirculating-air thermostat.

Air was forced up the annulus and down the center cylinder by a centrifugal impeller. To direct the air close to the transite end and toward the center of the thermostat where the reactor was situated, a cone of stainless steel was placed on top of the inner cylinder. The space between the cone and the transite was about 0.25 inch.

A control heater, rated 125 watts at 35 volts, was wrapped around the inner cylinder. Using a thyatron temperature controller (Chem. Eng. #26533), control of the thermostat temperature could be achieved within $\pm 0.08^{\circ}\text{C}$. The main heater, rated 800 watts at 155 volts, was wound around the outer cylinder. All heaters were of Nichrome V resistance wire and insulated with ball and socket ceramic beads (Cole-Parmer). Maximum temperature for continuous operation of the heaters was 1093°C . Power for the heaters was drawn from a 115-volt regulated supply and adjusted with the use of Variacs.

The impeller was located below the inner cylinder with a clearance of about 0.125 inch. Previous attempts in this lab to operate a recirculating-air system at 500 to 650°C for prolonged periods of time had been unsuccessful. Using self-lubricating bearings (Bemol Company, type FSR-4 ball bearings with a Feuralon retainer) and an improved design of the impeller assembly, a system was developed that has operated trouble-free since its inception. The design of the assembly is pictured in Figure 5.

Use was made of transite, a poor conductor of heat, to remove the air-cooled bearing assembly from the actual thermostat. The Bemol bearings were not recommended for continuous use in air above 400°C . A

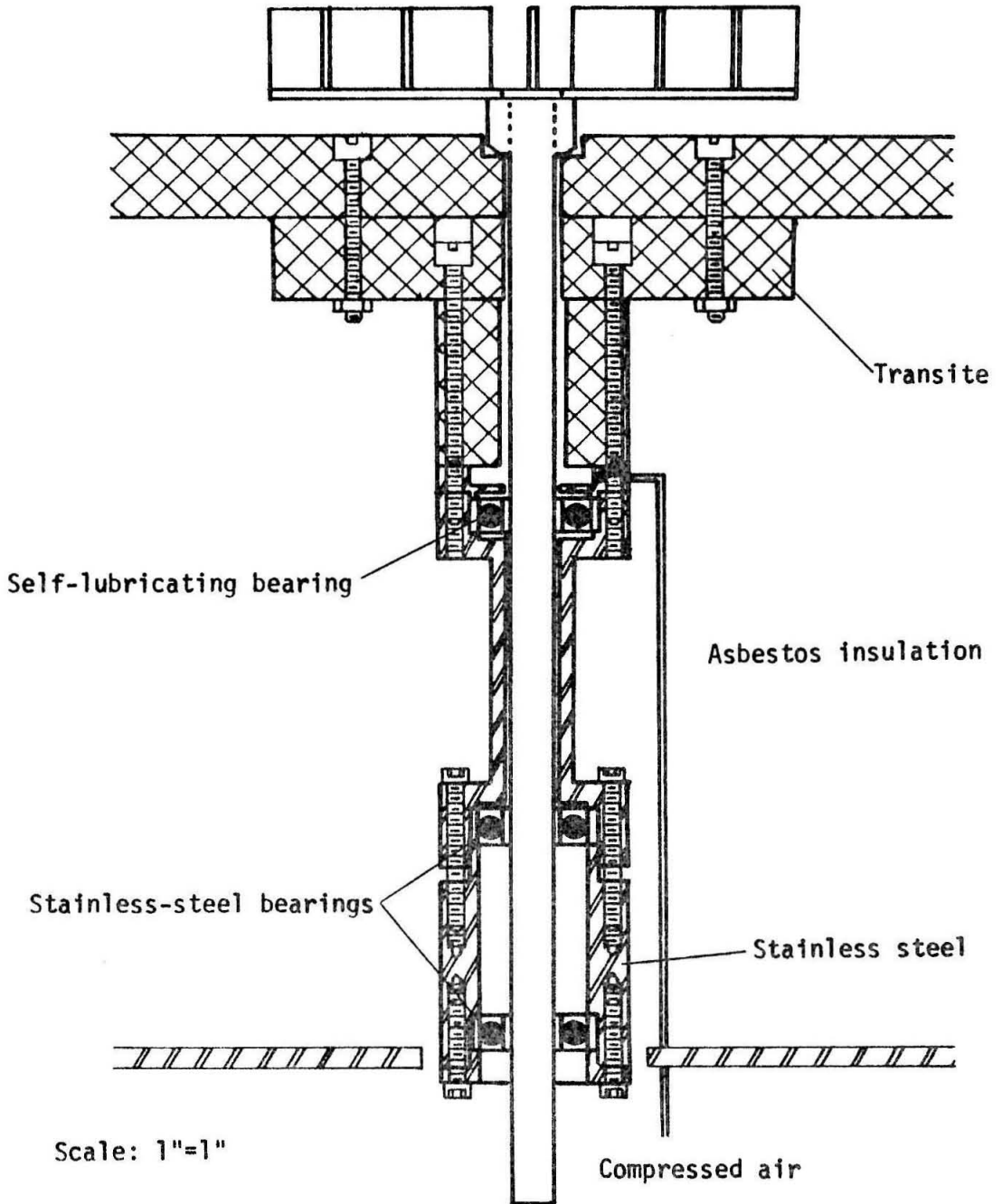


Figure 5. Impeller assembly for the recirculating-air thermostat.

lower set of stainless-steel ball bearings (New Departure, No. SS/R4A) were incorporated to assist in support of the impeller assembly.

The impeller base had ten vertical blades and was machined from a single block of stainless steel. The base was press fitted to the shaft and held rigidly in place by a set screw. Through a finger coupling, the lower end of the impeller shaft was connected directly to a shunt-wound motor (Bodine No. NSH-12) equipped with a full-wave-variable-speed motor control (Minarik Electrical Company, No. SL-14). The impeller could be operated from 0 to 3600 rpm.

Asbestos fiber and quartz fiber insulation was placed around the reactor housing which was mounted in a stainless-steel box. This box, resting on transite blocks within an aluminum box, was surrounded by glass fiber and quartz fiber insulation. A total of about 4.5 inches of insulation surrounded the reactor housing. The entire assembly was mounted in a Unistrut steel frame for ease of maintenance.

Temperature of the thermostat was measured vertically along the centerline of the inner cylinder with a chromelalumel thermocouple (Ceramo, 0.125-inch diameter, sheathed). The emf was measured within ± 0.001 by using a potentiometer (Leeds and Northrup Company, type K-3). The thermocouple, employing a ice-point reference junction, was calibrated at the tin, lead and zinc melting points using A.C.S. grade chemicals.

Temperature profiles of the thermostat were recorded at various impeller speeds. The results are portrayed in Figure 6. An impeller

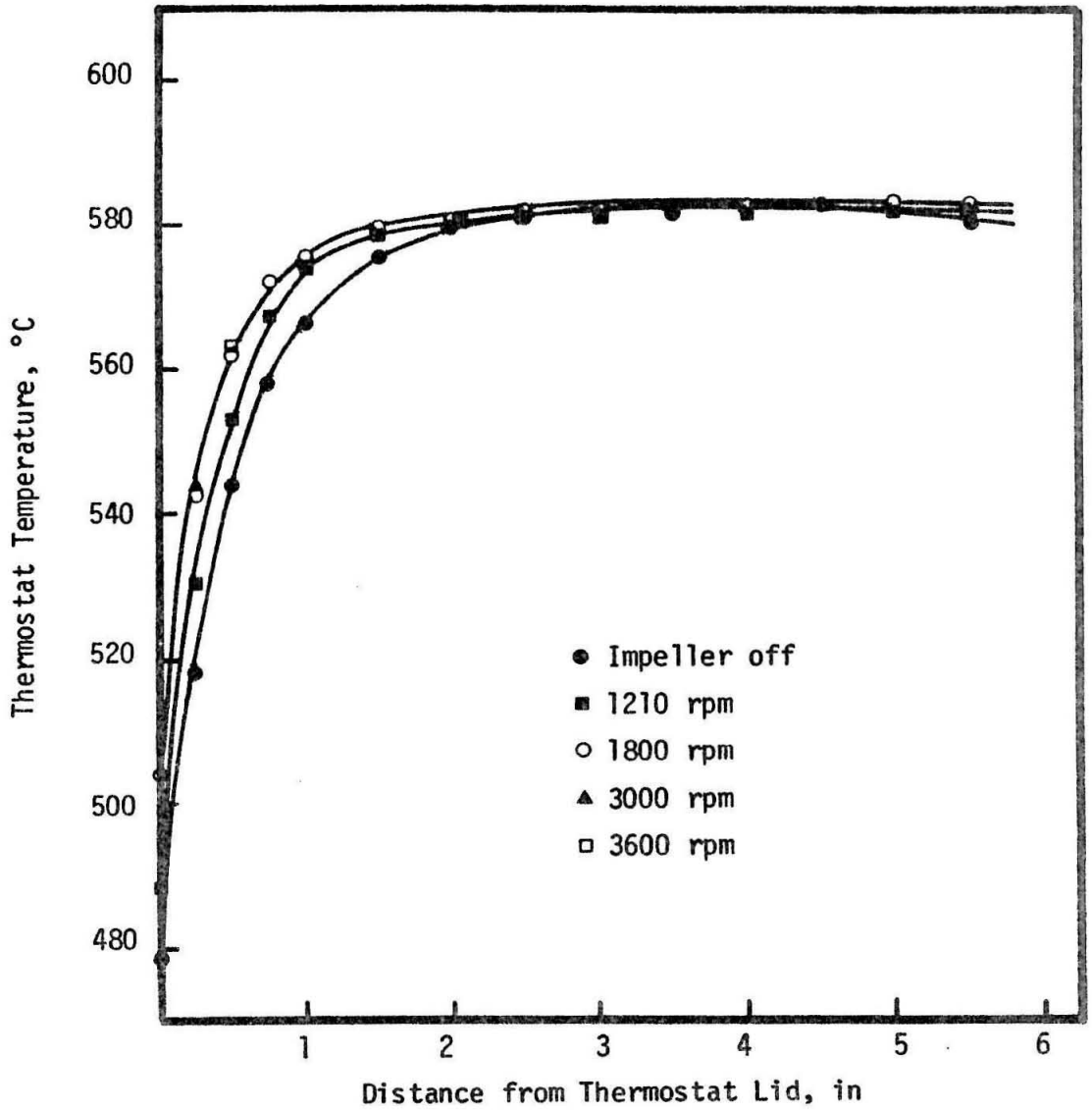


Figure 6. Temperature profile of recirculating-air thermostat, measured along the center line of the thermostat, as a function of the impeller speed.

speed of 1800 rpm was selected for all experimental kinetic tests and the temperature measured at a distance of two inches from the lower side of the transite end was taken as the reactor temperature. The temperature profile in the gold reactor tube should be more uniform as the thermal conductivity of gold is three orders of magnitude greater than that of air.

Analysis of product mixture

The reactor effluent was analyzed using gas-liquid and gas-solid chromatography in conjunction with a galvanic analyzer for oxygen. Design of the chromatographic network was based on consideration of possible products of the oxidation and pyrolysis of n-butane. Products in the high-temperature oxidation of n-butane include low-molecular-weight paraffins and olefins as well as carbon monoxide, carbon dioxide, hydrogen, and water. In the lower-temperature partial oxidations of n-butane, oxygenated compounds such as formaldehyde, acetaldehyde, methanol, and acetone are also probable products. As the temperature regions of the two processes are not precisely defined, a system capable of the analysis of all such products was desired.

Analysis of all possible products allows not only a quantitative determination of compounds found in the product mixture but also a qualitative check of compounds excluded from the products. The latter in butane-oxygen reactions may be of considerable significance in a mechanistic sense.

A schematic of the analytical network is given in Figure 7. Three chromatograph units listed below were employed in the analytical system.

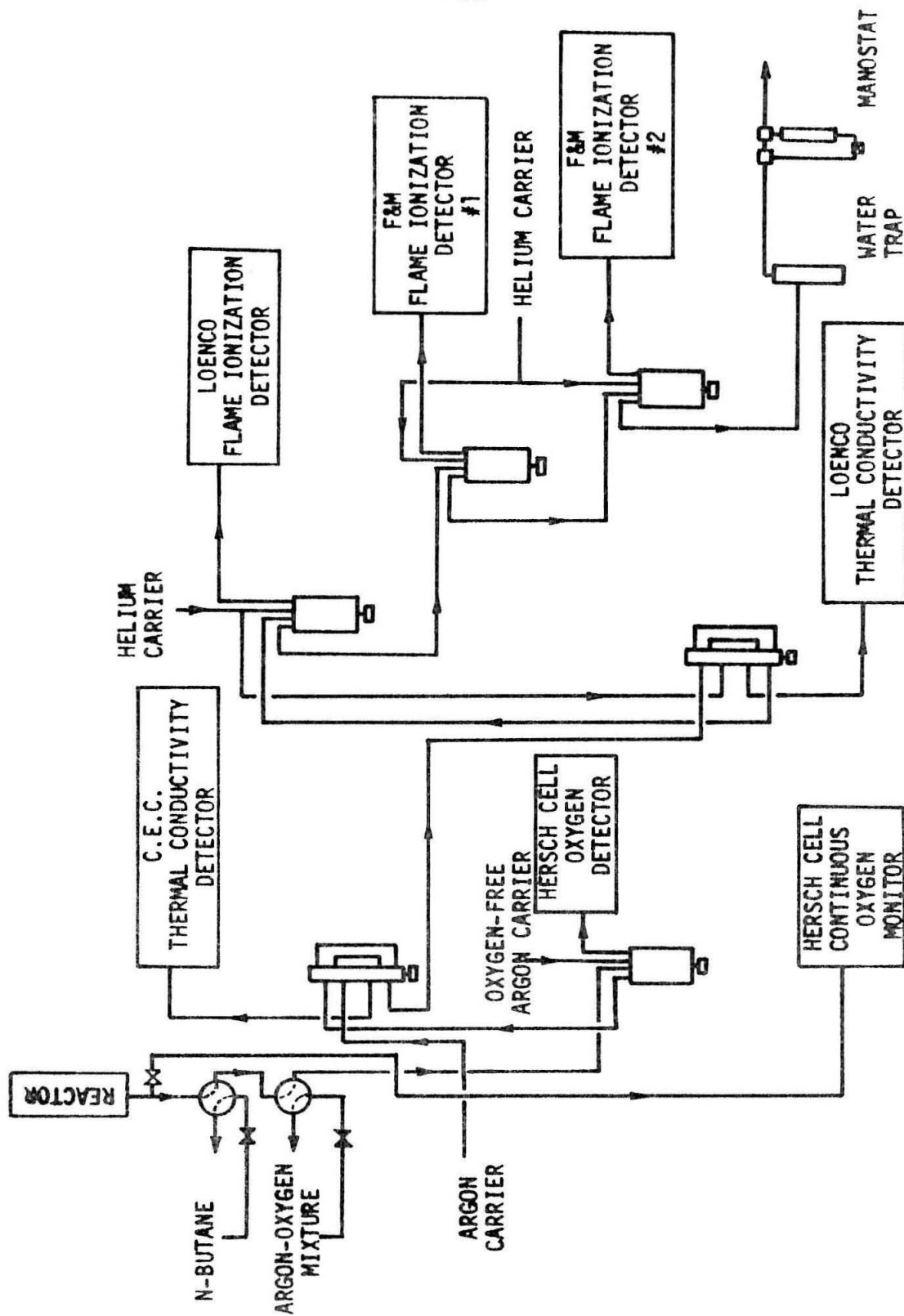


Figure 7. Schematic of the system used for analysis of the products.

1. Loenco Model 70 Hi-Flex Gas Chromatograph, containing a single flame ionization detector and a thermal conductivity cell, used in conjunction with a Cary Model 31 vibrating-reed electrometer from the Applied Physics Corporation.

2. Consolidated Electrodynamics Corporation Model No. 26-014 Chromatograph housing a thermal conductivity detector and used in conjunction with a Harrison Labs Model 865 C power supply.

3. F & M Scientific Model 5750 Research Chromatograph containing a dual flame ionization detection, each channel of which could be operated independently.

Accessory chromatograph equipment included the following:

1. Carle, gas sampling valves, model 2014.
2. Loenco, gas sampling valves, model
3. Beckman potentiometric recorder, model 1005, equipped with Disc integrator.
4. Two Honeywell potentiometric recorders, model Y 143X(58), each equipped with a Disc integrator.

Six chromatographic determinations were required for a complete analysis of the reacting mixture. Chromatograms of prepared samples are reproduced in Figures 8-13. The conditions under which the chromatograms were taken are noted on each figure. As may be seen peaks such as methane and ethylene appear on several of the traces and thus serve as a basis for determining the relative composition of the entire product mixture.

Legend for Figures 8-13.

<u>Component</u>	<u>Identification</u>
methane	1
ethane	2
ethylene	3
propane	4
isobutane	5
propylene	6
n-butane	7
1-butene	8
t-2-butene	9
c-2-butene	10
1-pentene	11
1,3-butadiene	12
hydrogen	13
oxygen	14
nitrogen	15
carbon monoxide	16
carbon dioxide	17
water	18
formaldehyde	19
methanol	20
acetaldehyde	21
formic acid	22
ethanol	23
propionaldehyde	24
acetone	25
2-propanol	26
methyl acetate	27
acetic acid	28
1-propanol	29
methyl ethyl ketone	30
ethyl acetate	31
2-butanol	32
crotonaldehyde	33
1-butanol	34
diethyl ketone	35
argon	36

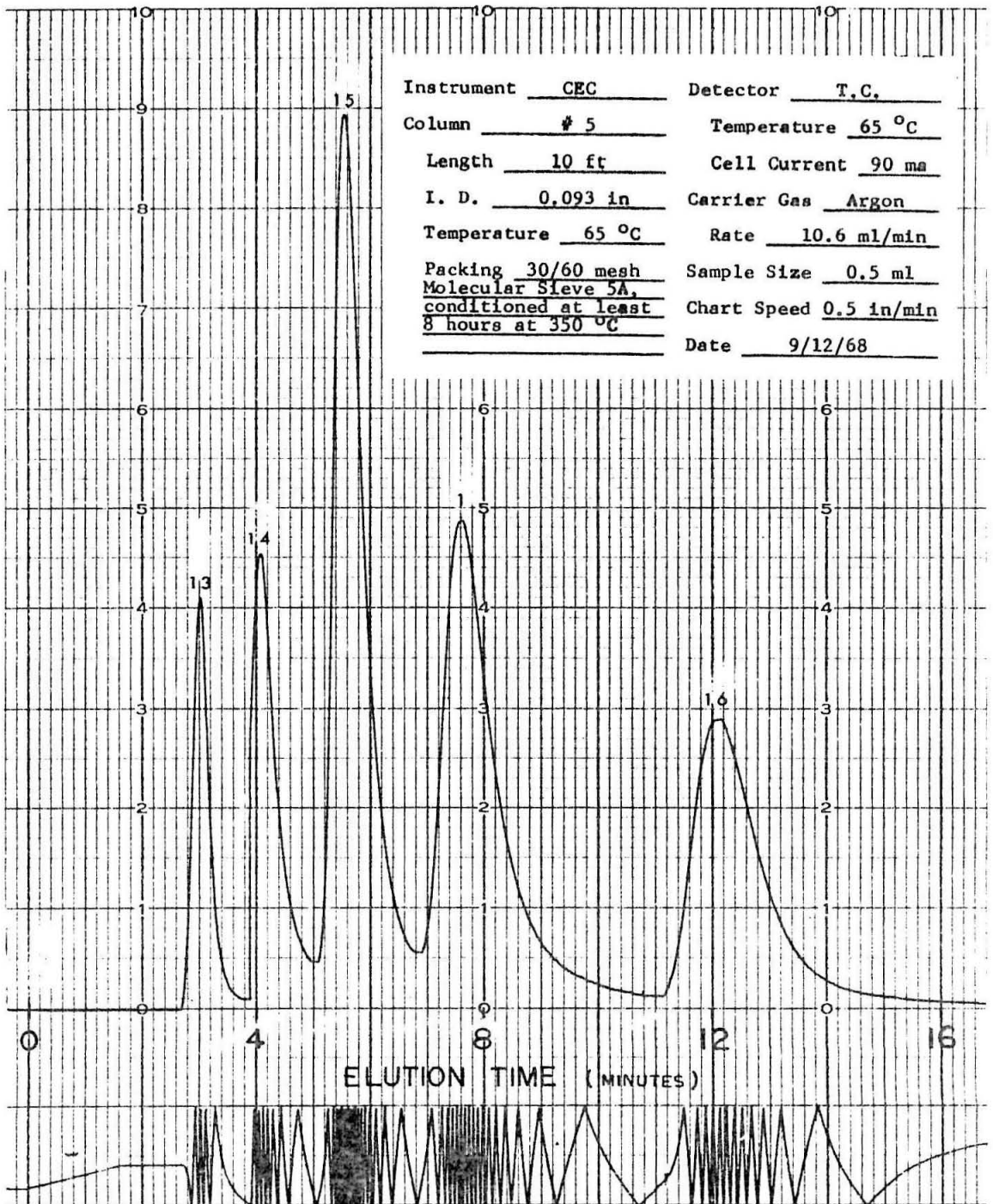


Figure 8. Fixed gases.

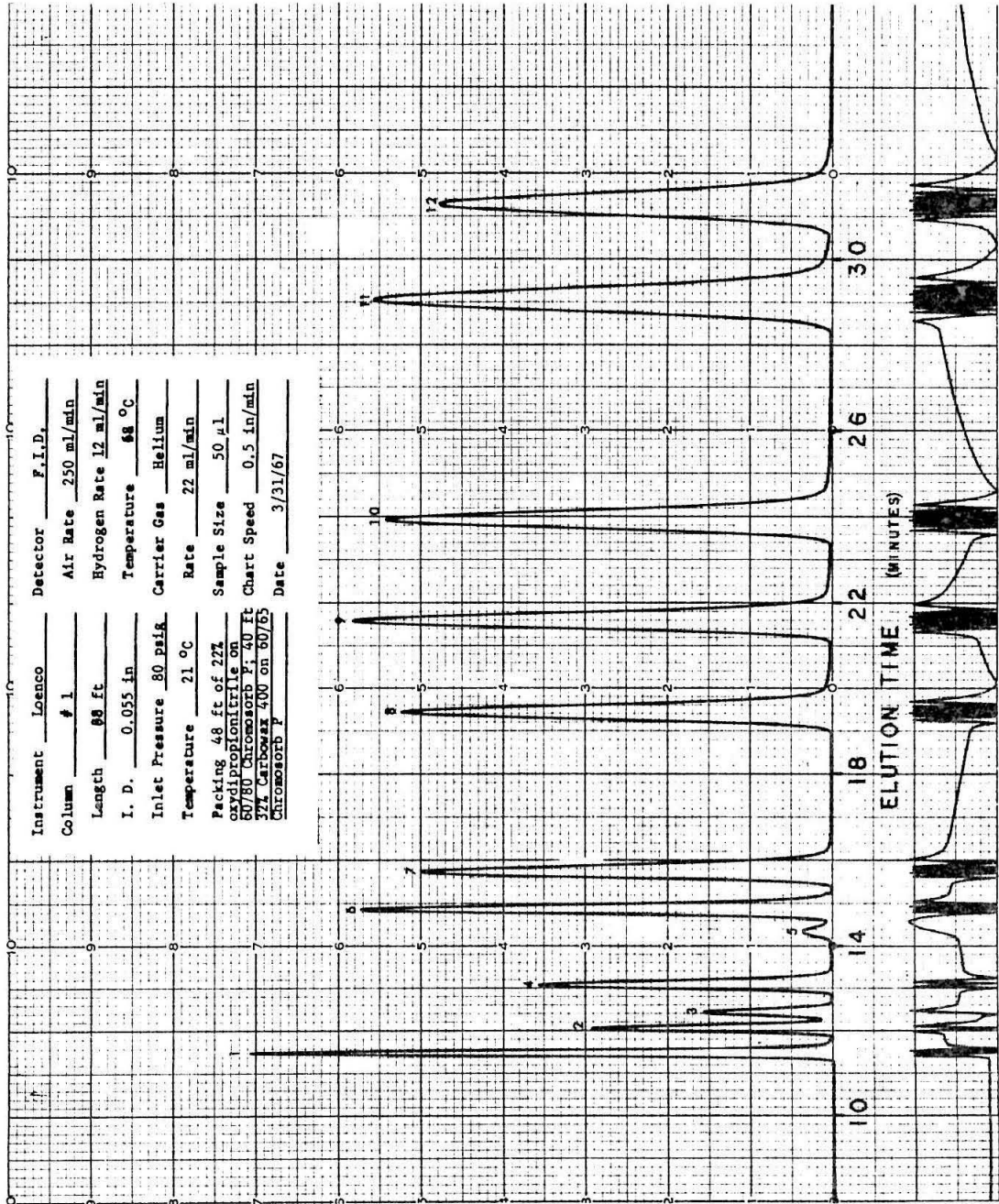


Figure 9. Paraffins and olefins.

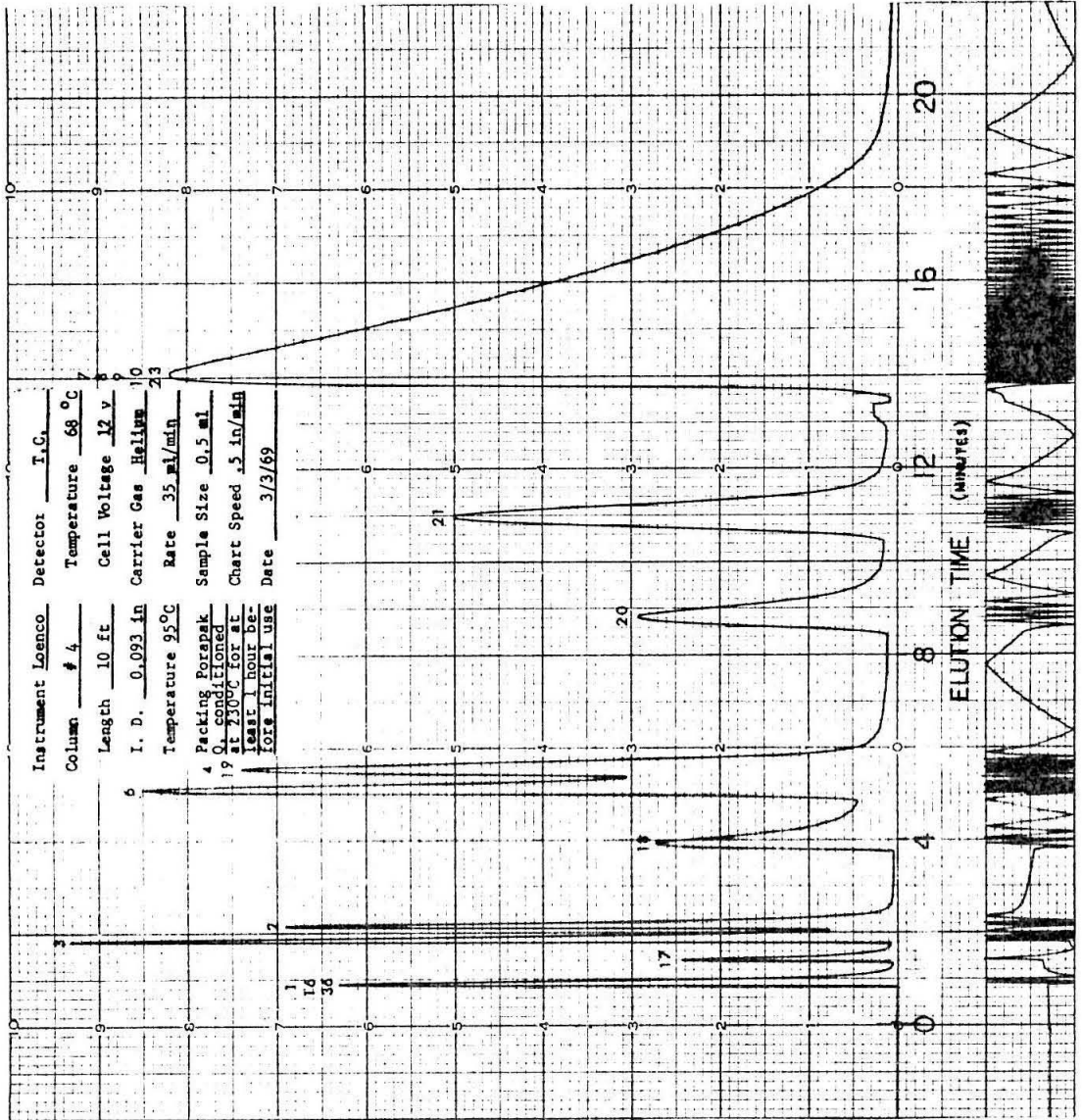


Figure 10. Paraffins, olefins and oxygenated compounds of low molecular weight.

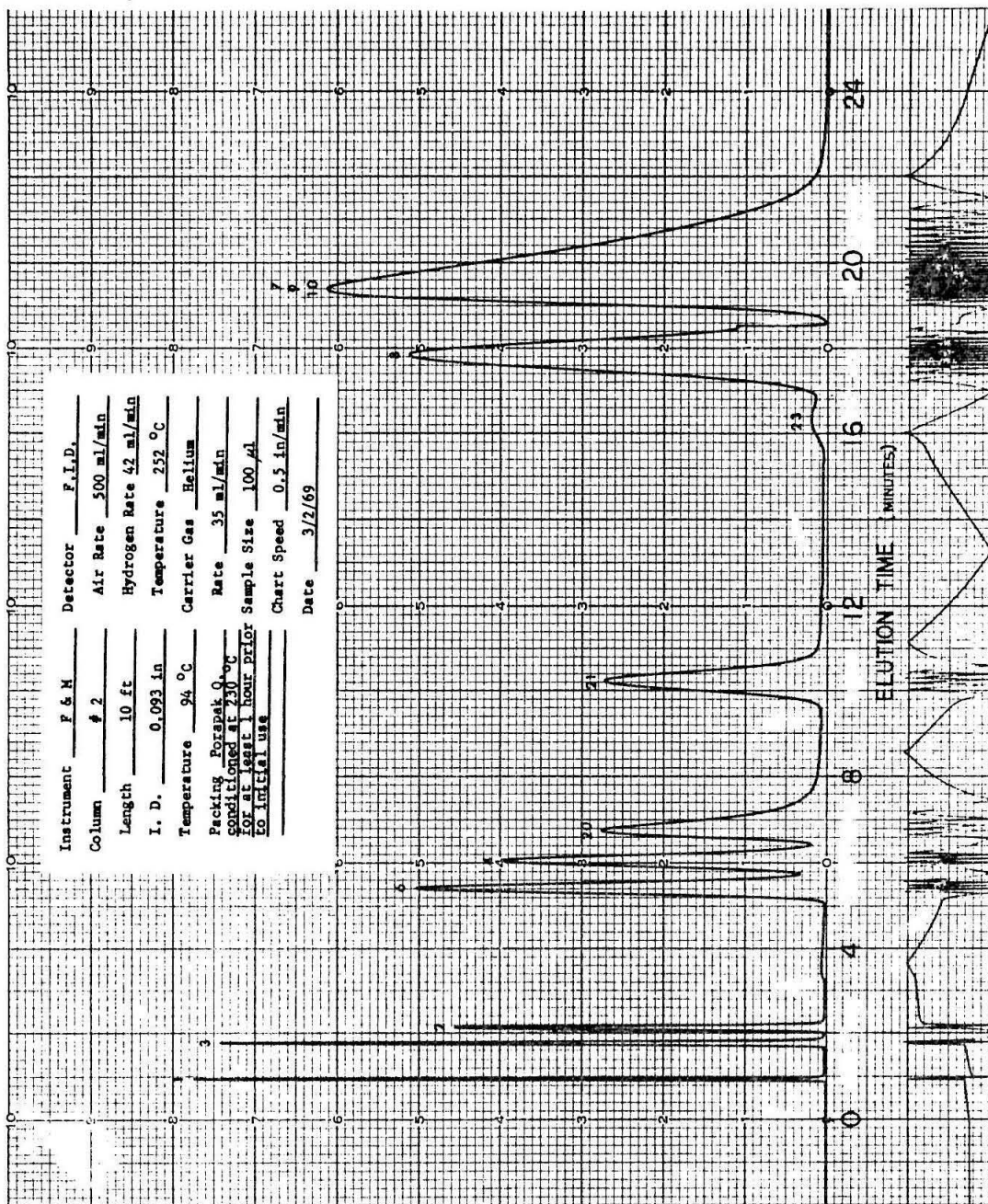


Figure 11. Paraffins, olefins and selected oxygenated compounds of low molecular weight.

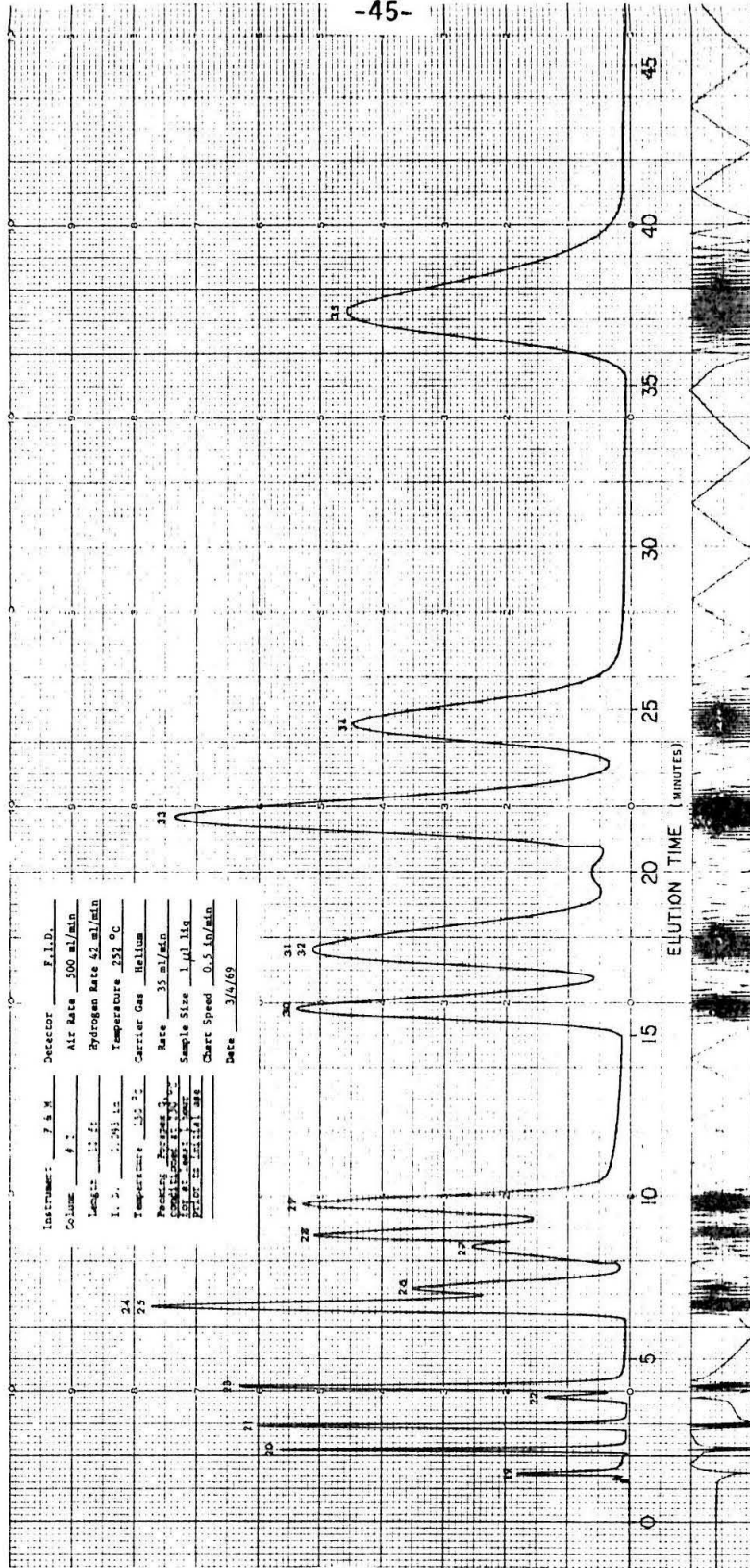


Figure 12. Oxygenated compounds of higher molecular weight.

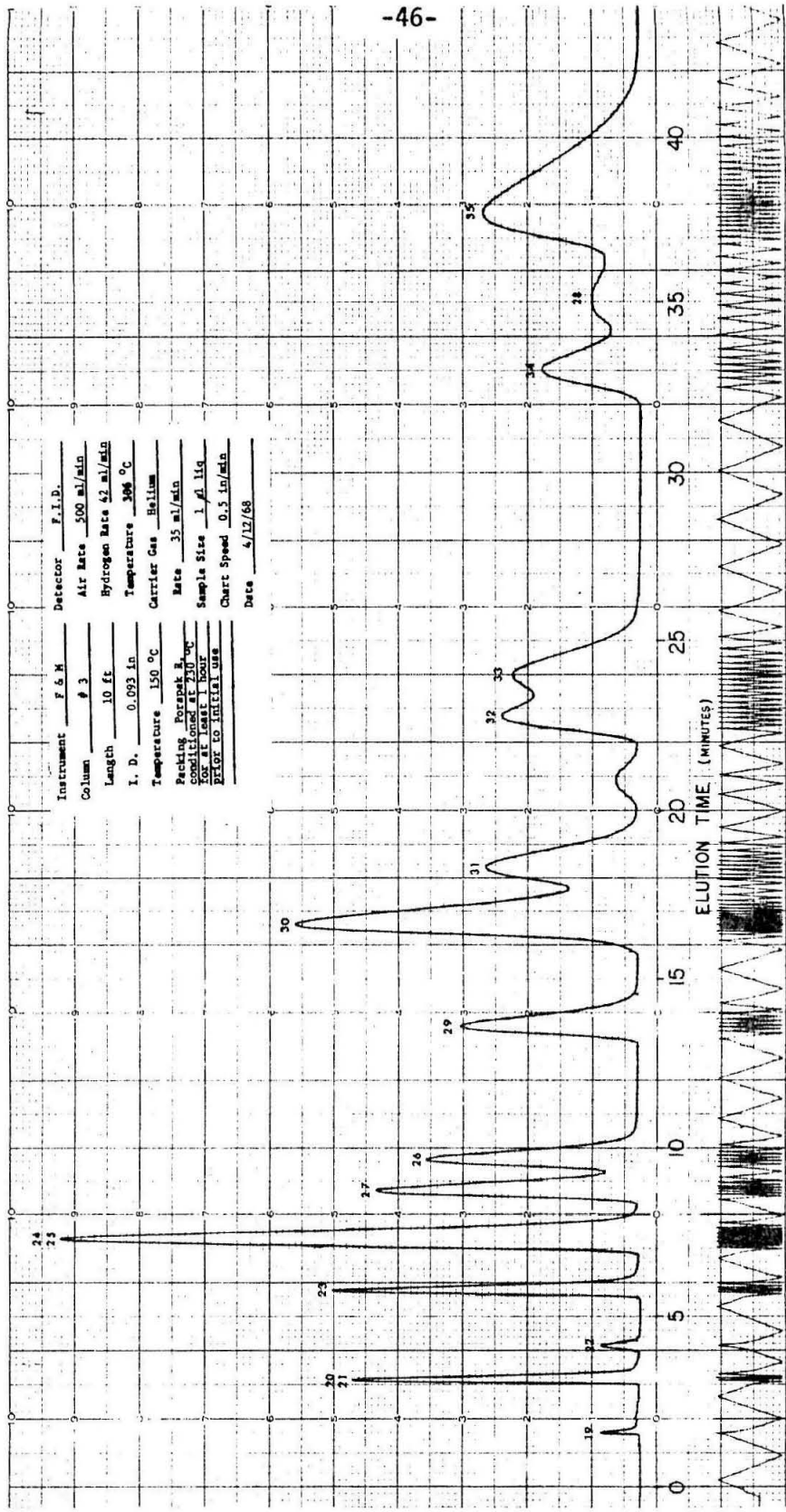


Figure 13. Oxygenated compounds of higher molecular weight.

In Table 2 are listed the minimum measurable quantities (MMQ) of individual components. The MMQ is defined as that volume fraction of a particular compound which produces a peak height signal 5x the noise level under average operating conditions. A factor of 2x the noise level is taken to be the minimum detection limit (MDL). Thus if in Table 2 the MMQ of methanol is 0.52 ppm, the smallest detectable concentration under average operating conditions would be 0.21 ppm. It should be noted that the sensitivity to a particular component depends on its elution time, relative response, carrier flow rate, column temperature and detector type. Thus while under equivalent operating conditions a flame detector is two to three orders of magnitude more sensitive than a thermal conductivity detector, the MMQ of a compound may be less using a flame detector if the parameters mentioned are varied.

In Appendix B is presented a detailed summary of the chromatograph columns, detectors and calibration procedures.

In order to measure accurately small concentrations of oxygen in the reactant and product mixtures, a galvanic analyzer, first proposed by Hersch (47), was designed and built. The cell, consisting of a lead anode and silver cathode separated by a suitable electrolyte such as potassium hydroxide, could be used either for continuous monitoring of a gas stream or as a chromatograph detector. In either case the current generated by the cell was indicative of the amount of oxygen passing through the cell.

The cell is highly specific to oxygen and theoretically the lower

Table 2. Estimated Minimum Measurable Quantities (MMQ) for Chromatograph Network.

<u>Component</u>	<u>MMQ, ppm</u>
methane	0.45
ethane	0.53
ethylene	0.47
propane	0.43
isobutane	0.40
propylene	0.50
1-butene	0.70
t-2-butene	0.72
c-2-butene	0.92
hydrogen	10
oxygen	50
nitrogen	100
carbon monoxide	200
carbon dioxide	13
water	26
formaldehyde	15
methanol	0.52
acetaldehyde	0.50
formic acid	10
ethanol	1.0
propionaldehyde	1.4
acetone	1.4
2-propanol	0.47
methyl acetate	0.50
acetic acid	0.90
1-propanol	0.64
methyl ethyl ketone	0.52
ethyl acetate	1.2
2-butanol	1.2
crotonaldehyde	0.84
1-butanol	1.2
diethyl ketone	1.0

limit of detection is zero oxygen. However, in practice because of leakage the lower limit is of the order of 1 part oxygen per million parts gas. Cell life and linearity of response combine to fix the upper limit of detection at 150 ppm oxygen for the continuous analyzer and 2.0 per cent oxygen by volume for the detector. Because of the greater range of linearity and rapid response, a cell used as a detector was employed in most analyses. A detailed description of the Hersch cells and their operation may be found in Appendix C.

The n-butane or argon-oxygen mixture could be diverted directly to the analytical network, thus bypassing the reactor. Frequent analysis of the reactants was desirable for two reasons. First, the level of impurities, namely butenes, in the n-butane varied over a period of time. Secondly, daily calibration of the Hersch detector was necessary for best results.

EXPERIMENTAL PROCEDURE

A period of 12 to 16 hours was required to raise the temperature of the reactor from room temperature to a constant value in the range 500 to 600°C. Similarly, a period of several hours was required for the column ovens of some chromatographs to achieve constant temperature. As a result, this equipment was left on continuously.

At the beginning of each day, the impeller to the thermostat was set at 1800 rpm and the temperature controller was turned on. A period of two hours was allowed for adjustment of the temperature to the desired value for the day. Meanwhile, the following operations were performed.

1. Vacuum pumps were turned on.
2. Gas flows to the analytical system were adjusted and the detectors were activated.
3. An ice bath for the reference junction of the thermocouple was prepared.
4. Gas flows through the reactor were adjusted for the first point.

A chromatographic analysis of the impurities in the unreacted butane was made prior to taking data on the reaction. For oxidation work, calibration of the Hersch detector with a standard argon-oxygen mixture was generally made at this time.

For the remainder of the day, data were collected on the reaction under study. Record was kept of the temperature, pressure, flow rates

of gas to the reactor, and the composition of the effluent from the reactor. A complete analysis of the products required about 45 minutes. From 30 to 45 minutes were allowed between points for attainment of steady-state operation at the new conditions.

At the end of the day, the impeller and temperature controller were turned off. Approximate power settings were made to the thermostat heaters for the desired temperature of the next day. The analytical equipment was placed on stand-by for overnight. Flows of butane and argon through the reactor were maintained at all times but at a reduced rate when a run was not in progress.

Gas chromatographs, recorders and electrical equipment were serviced every six months as part of a preventative maintenance program. Water traps and oxygen traps were replaced or regenerated as required or every two months.

TREATMENT OF DATA

Calculations by Barker and Corcoran (1), using equations derived by Trombetta and Happel (48), indicated that the microreactor could be described accurately by an isothermal, plug-flow model. Data required for a kinetic analysis of the reaction included the following:

1. Temperature of the reactor,
2. Pressure in the reactor,
3. Flow rates of the butane, oxygen, diluent and quench streams,
4. Composition of the reactor feed and effluent,
5. Dimensions of the reactor,
6. Nature of the reactor surface.

The duration of operation of the reactor was also important in studies on the aging of the reactor surface.

The composition of the reactor feed was calculated knowing the volumetric flow rates of the various components of the feed and assuming Dalton's law and the ideal gas law. The concentration of component i in the feed was given as

$$C_i^{\circ} = \frac{f_i}{f_R} \left[\frac{P_T}{RT} \right], \quad (1)$$

where C_i° = inlet concentration of the i^{th} component, [=] moles cc^{-1}
 f_i = flow rate of the i^{th} component into the reactor measured at the temperature and pressure of the reactor, [=] cc sec^{-1}

f_R = total flow rate of inlet gas measured at the temperature and pressure of the reactor, [=] cc sec⁻¹

P_T = reactor pressure, [=] psi

T = reactor temperature, [=] °K

R = universal gas constant = 1205.9 psi cc °K⁻¹ moles⁻¹.

The composition of the reactor effluent was measured using gas chromatography and a galvanic analyzer. For a chromatogram, the peak area of component i is related to the moles of i in the sample in the following manner:

$$n_i = k \frac{A_i}{R_i} \quad (2)$$

where n_i = moles of the i^{th} component in the reactor effluent, [=] moles

k = constant of proportionality, [=] moles (integrator units)⁻¹

A_i = peak area of component i , [=] integrator units

R = relative molar response of component i , dimensionless

The amount of component i in the product mixture relative to the amount of butane could be computed as

$$N_i = \frac{A_i}{A_B} M_i \quad (3)$$

where N_i = moles of component i per mole of butane in the product mixture, dimensionless

$M_i = R_B/R_i$ = multiplier factor for component i , dimensionless

As conversions of butane were generally less than 1 per cent, N_i represents, within the accuracy of the analysis, the moles of product i

formed per mole of butane in the reactor feed. For appreciable conversions of butane, a correction to the peak area must be made using a carbon balance over the products. If the mass density is assumed constant throughout the reactor, i.e. neglecting the expansion of gases caused by reaction, the concentration of component i at the reactor exit may be computed as

$$C_i = N_i C_B^0 . \quad (4)$$

The concentration of oxygen in the effluent was measured directly using galvanic cell, calibrated on the basis of peak height. The current generated by reduction of the oxygen was indicative of the amount of oxygen in the sample. The concentration of oxygen at the exit of the reactor was related to the concentration of oxygen measured in the quenched effluent by

$$C_0 = \left[\frac{f_R + f_Q}{f_R} \right] C_0^1 \quad (5)$$

where f_Q = quench flow rate measured at the temperature and pressure of the reactor, [=] cc sec^{-1}

C_0^1 = concentration of oxygen in the diluted product mixture, [=] ppm or moles cc^{-1}

A mean contact time or space time was defined as

$$\tau = \frac{V}{f_R} , \quad (6)$$

where τ = mean contact time, [=] sec^{-1}

V = volume of the reactor, [=] cc

Assuming plug flow, a mass balance on reactant i yields for a tubular reactor the following equation:

$$\frac{d\tau}{C_i} = \frac{dX_i}{-r_i} \quad (7)$$

where X_i = fraction of reactant i converted into product, dimensionless

$-r_i$ = rate of disappearance of reactant i by chemical reaction,

[=] $\text{moles cc}^{-1} \text{sec}^{-1}$

Upon consideration of constant mass density throughout the reactor, as is the case with either no change in the number of moles with reaction or at very low conversion of reactants

$$dX_i = \frac{dC_i}{C_i^0} \quad (8)$$

and equation (7) becomes

$$\frac{dC_i}{d\tau} = -r_i \quad (9)$$

Equation (9) may be integrated over the reactor length to obtain

$$\tau = \int_{C_i^0}^{C_i} \frac{dC_i}{-r_i} \quad (10)$$

Possible rate expressions may be evaluated using the above equations and appropriate experimental data. Specific application of these equations are described in the discussion of results.

RESULTS AND DISCUSSION

Reactor operation and energy transfer

Barker and Corcoran (1) studied the pyrolysis of n-butane using a gold, tubular-flow microreactor. The reaction was examined at conversions of butane less than 2 per cent, temperatures from 529 to 595°C and total pressures from 5 to 20 psia. The results satisfactorily agreed with the work of Sagert and Laidler (3) and Purnell and Quinn (2) taken in quartz and pyrex reactors, respectively, with one striking exception. For a given pressure and temperature, departure from the expected three-halves order for the reaction was observed as the partial pressure of butane was decreased.

At the higher concentrations of butane, the overall rate of the pyrolysis exhibited an order of three halves with respect to the concentration of butane. Typical rate data are given in Figure 14 where the order of the reaction is equal to the slope of the curve at a given concentration of butane. The order gradually decreased with decreasing concentration of butane to the extent that at a butane concentration of 5.5×10^{-6} moles cc^{-1} , the order was as low as 0.25. A primary objective of the present work is to resolve the question of reaction order with respect to the pyrolysis of butane in a gold microreactor.

A schematic of the reactor used by Barker is reproduced in Figure 15 and may be compared with the similar assembly of Figure 2 used in this investigation. The major revisions in the reactor design are listed below and were aimed at reducing energy transfer near the inlet

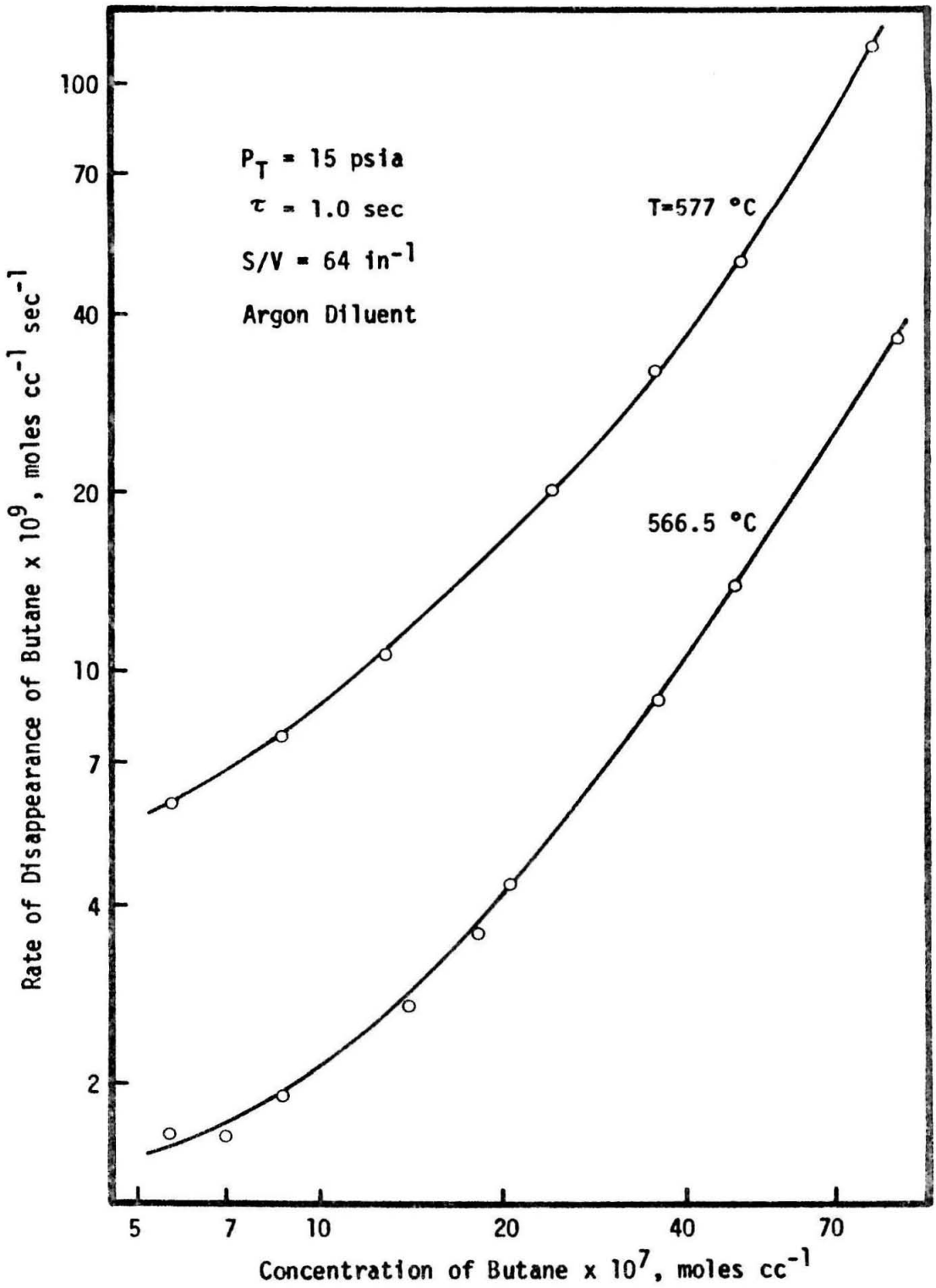
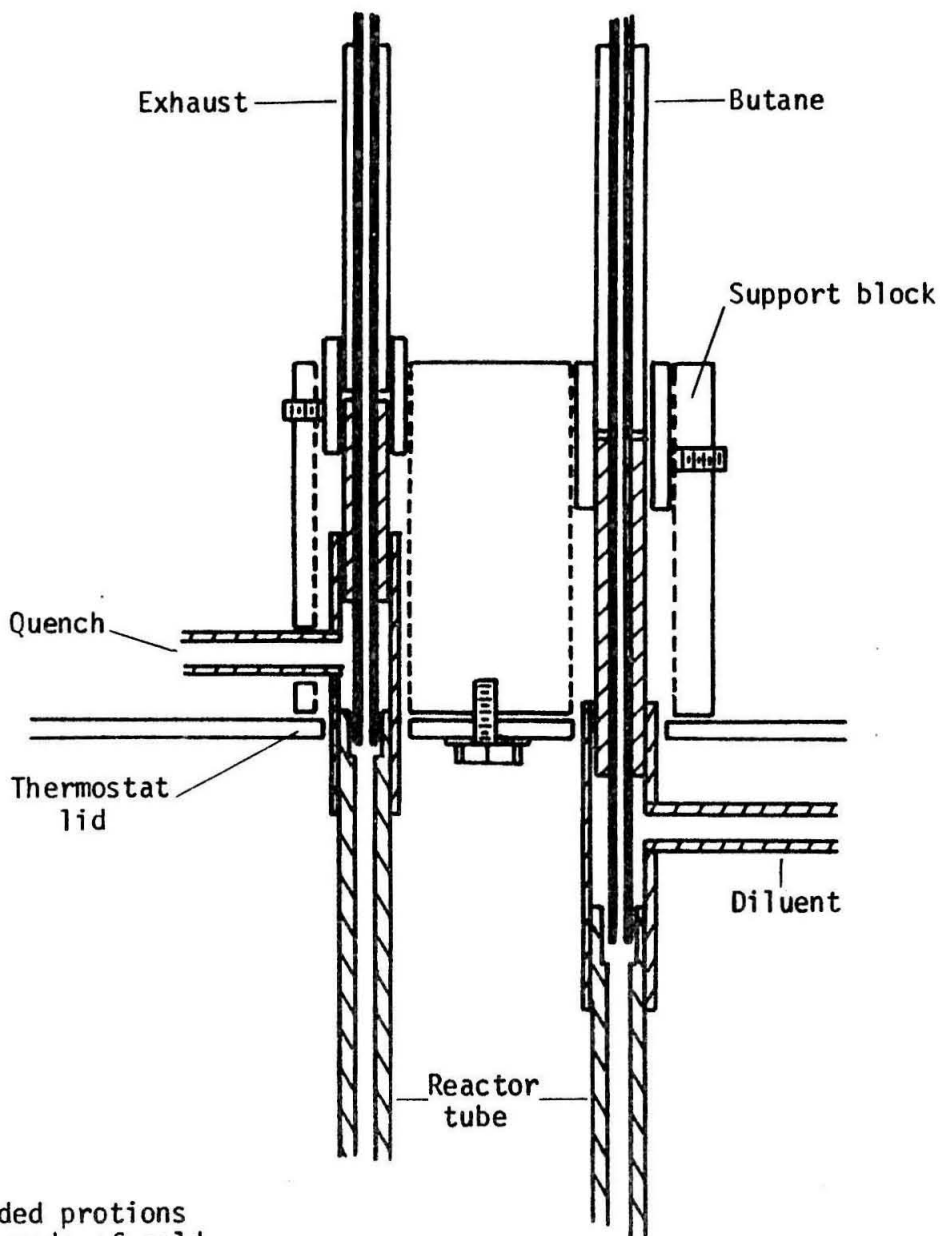


Figure 14. Rate data from the work of Barker and Corcoran (1).



Shaded portions
are made of gold.
All other components
are stainless steel.

Figure 15. Schematic of the reactor used by Barker and Corcoran.

of the reactor.

1. The point of intersection of the argon diluent and butane lines was removed from direct exposure to the thermostat.

2. The mass of metal in contact with the inlet lines and the thermostat was minimized.

The total pressure of the system was maintained near 15 psia. For partial pressures of butane below 15 psia, argon was mixed with the butane stream. Provisions were made for diluting the butane at the entrance of the reactor and/or at a point well-ahead of the entrance. By altering the point of mixing and measuring the rate of reaction for several concentrations of butane, an estimate of the effect of energy transfer in the entrance region could be obtained.

Positioning the diluent line one-eighth of an inch below the thermostat as had been required in the apparatus of Barker, the data shown in Figure 16 were taken at 575°C. The point of dilution of the butane is seen to exert a pronounced effect on the observed rate. For the completely premixed feed, the rate of disappearance of butane at a concentration of butane of 1.3×10^{-6} moles cc^{-1} is approximately 50 per cent of that for mixing at the reactor entrance. Moreover, the reaction accurately follows three-halves-order kinetics over the entire range of butane concentrations provided the butane is diluted prior to the "hot" inlet region of the reactor.

The influence of the point of mixing is more pronounced at higher temperatures. This is expected as a simplified analysis of the system

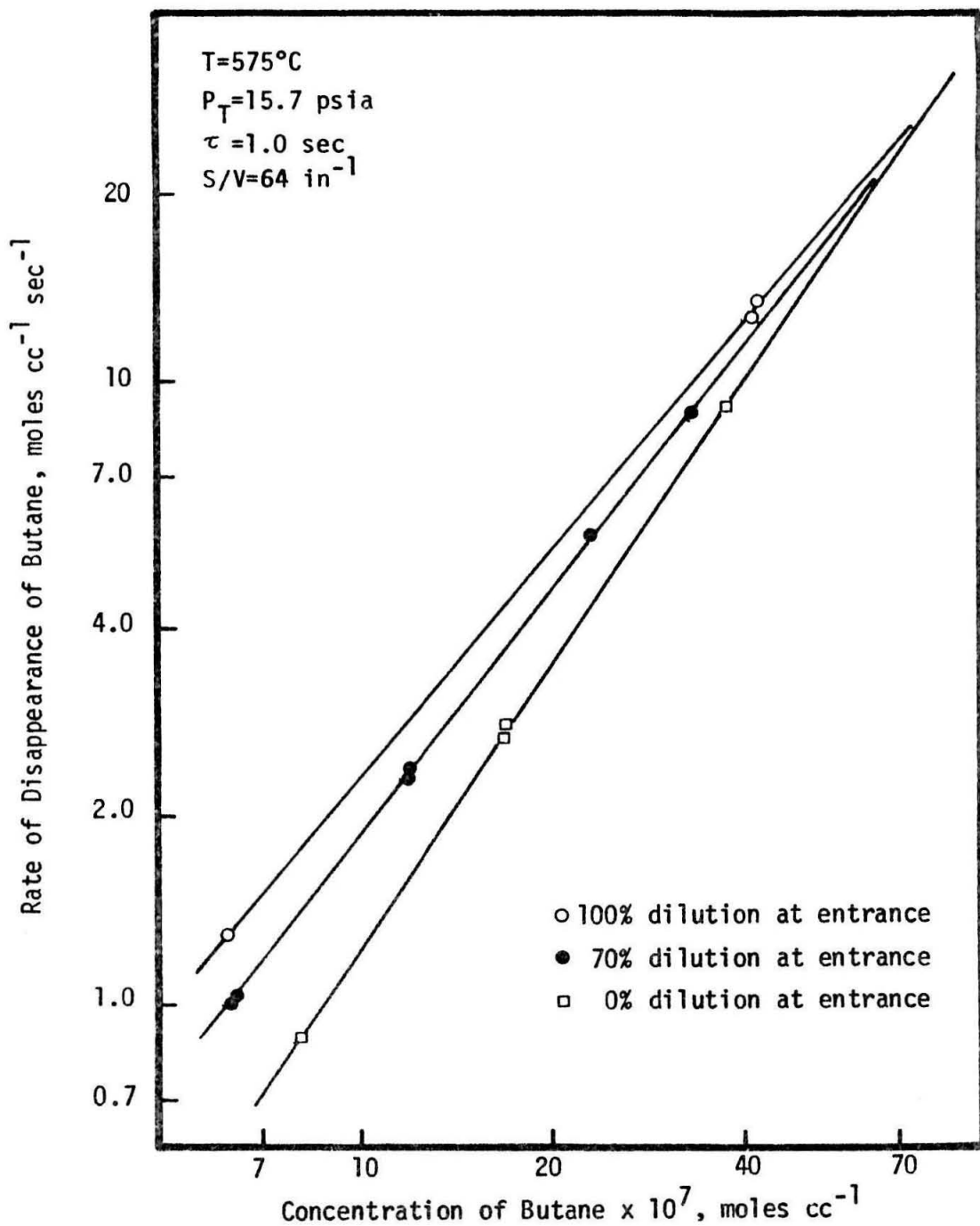


Figure 16. Effect of the point of dilution on the pyrolysis of butane.

is to consider the reaction as occurring in two "reactors". One is the reactor tube in which the temperature is nearly constant at the experimentally observed temperature for the reactor. The other, a short section of the butane line prior to dilution, possesses a non-uniform temperature which is less than that of the reactor. The observed rate of reaction may be represented as follows:

$$-R_{C_4H_{10}} = k' [C_4H_{10}]_{inlet}^{3/2} + k [C_4H_{10}]_{reactor}^{3/2} \quad (11)$$

For the case where 100 per cent of the argon is mixed with the butane at the entrance of the reactor, the concentration of butane in the inlet section may be 25 times that of the reactor. Assuming an activation energy of 65 kcal mole⁻¹, it can be shown using the above equation that the average temperature of the inlet section would have to be about 125 degrees less than the temperature of the reactor for a inlet contribution of less than 5 per cent to the overall rate. Ideally, the temperature of the inlet lines would at all points be much less than the temperature of the reactor, but because of heat transfer along the gold tubing such is not always the case.

In the present work, the point of dilution at the reactor entrance was contained in the transite lid of the thermostat and not directly exposed to the thermostat. This significantly diminished the rate of reaction in the undiluted butane stream. In the majority of tests, the proportion of argon metered at the inlet of the reactor was less than 20 per cent of the total argon in the feed. A small proportion of "hot"

argon was mixed at the entrance in order to affect a rapid approach of the reactants to the operating temperature.

Pyrolysis of n-butane

The pyrolysis was studied in both untreated and acid-treated reactors. By untreated is meant that, aside from rinsing the tubes with acetone and subsequent drying, the reactor surface was as received from the manufacturer. Acid-treatment of the reactor, primarily for the purpose of removing oxides or chemisorbed oxygen of impurities in the 99.99 per cent pure gold, was accomplished in the following steps.

1. Nitric acid, 70 per cent by volume, was continually pumped through the reactor lines for a period of 30 to 40 minutes.
2. Triple-distilled water was flushed through the lines until the water exiting the reactor was of neutral pH. The pH was monitored using a color-indicating pH paper.
3. A vacuum was pulled on the reactor as the temperature of the system was gradually raised to normal operating levels, about 550°C.
4. The vacuum was terminated when the reactor pressure leveled at less than 10 microns. Generally the vacuum procedure took from 8 to 12 hours.
5. Flow of argon through the reactor was initiated and maintained at atmospheric pressure until tests were commenced.

Care was taken in all pyrolysis tests to prevent exposure of the reactor to oxygen at high temperatures. As indicated by a Hersch cell,

the level of oxygen in the reactor was at all times less than 2 ppm.

The rate expression for the disappearance of butane was assumed to be of the following form:

$$-R_{C_4H_{10}} = k [C_4H_{10}]^m, \quad (12)$$

where

$$k = A \exp [-E_c/RT] . \quad (13)$$

For a differential reactor, a logarithmic plot of the rate of disappearance of butane against the concentration of butane will allow a straightforward determination of m , the order of the overall reaction. Figure 17 is a summary of the data taken over the temperature range 535 to 595°C in an untreated reactor. The order, m , equal to the slope of the isotherm, is found to be 1.50 ± 0.05 . At the highest temperature, 595°C, the order is slightly less (1.41 at the higher concentrations of butane); however, this most likely was a result of mixing the argon diluent and butane at the entrance of the reactor. Over a period of several weeks, the data varied less than 5 per cent.

An Arrhenius plot of the data for the untreated reactor is shown in Figure 18. The frequency factor, A , and the activation energy, E_c , of the rate constant were computed as $1.75 \times 10^{17} \text{ cc}^{1/2} \text{ moles}^{-1/2} \text{ sec}^{-1}$ and $66.6 \text{ kcal mole}^{-1}$, respectively. An activation energy of $65.4 \text{ kcal mole}^{-1}$ was reported by Barker for a gold reactor under similar conditions. Sagert and Laidler (3) observed an activation energy of $59.9 \text{ kcal mole}^{-1}$ in a quartz reactor. Conditioning of the

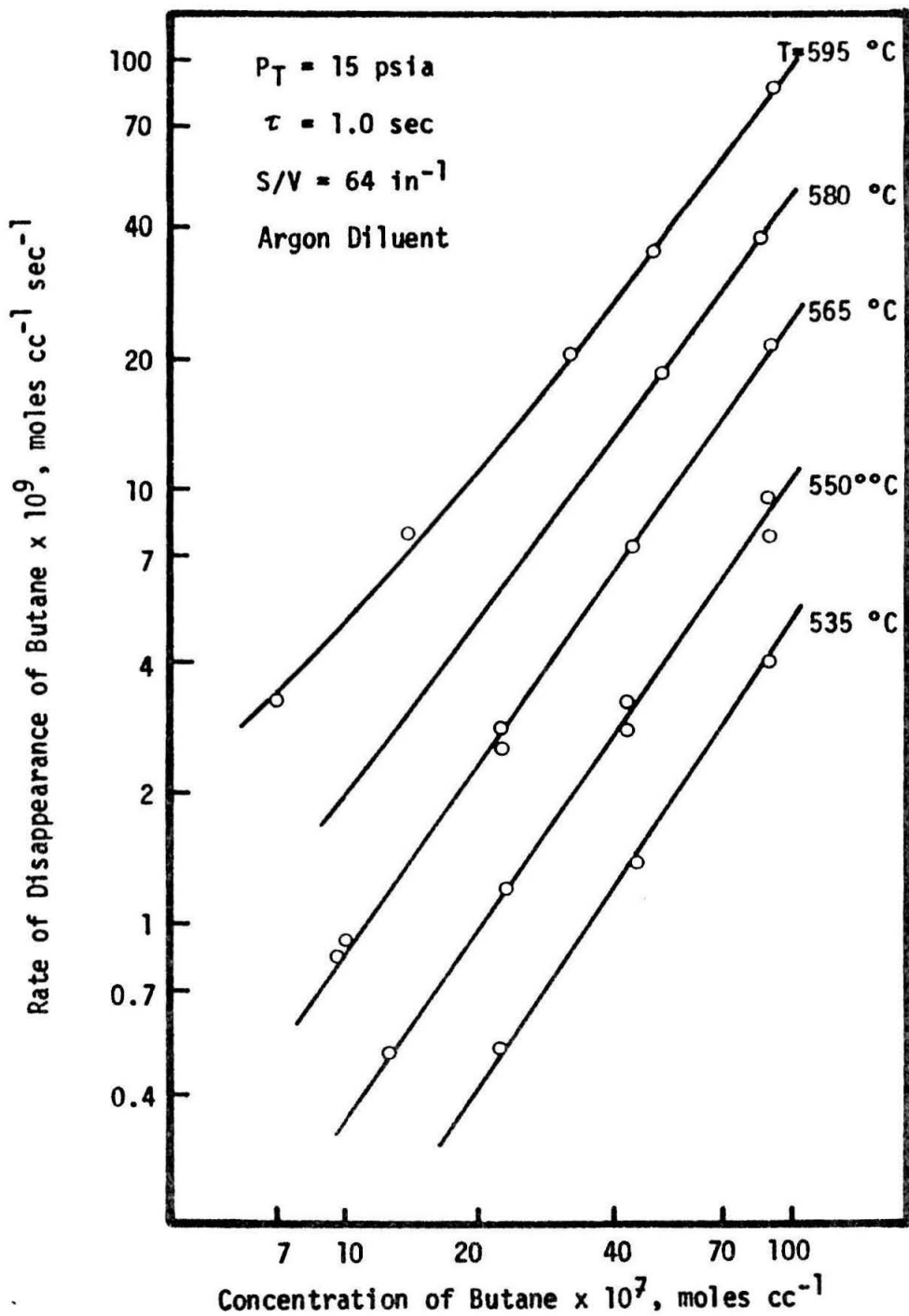


Figure 17. Pyrolysis of butane as a function of temperature and concentration of butane in an untreated reactor.

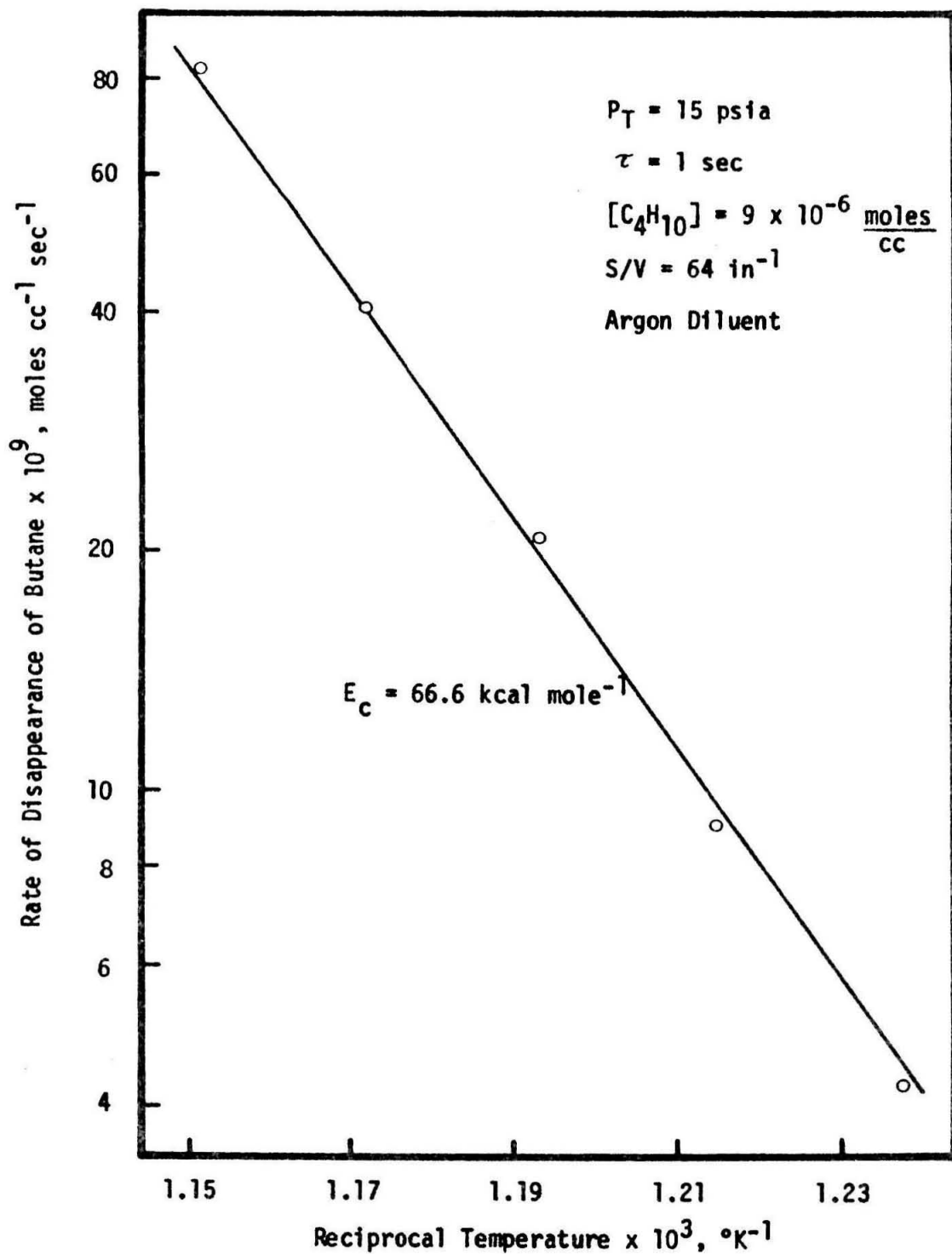


Figure 18. Arrhenius plot for the pyrolysis in an untreated reactor.

vessel or packing with quartz tubing resulted in higher activation energies. A value of $62.3 \text{ kcal mole}^{-1}$ was given for a packed reactor.

The product mixture consisted primarily of methane, propylene, ethylene and ethane. Hydrogen, present in smaller quantities, could not be accurately measured at the low conversions of butane (0.02 to 0.93 per cent) employed in the tests. Representing less than 1 per cent of the total products were 1-butene, c-2-butene and t-2-butene. No 1, 3-butadiene or propane were observed in the products.

The distribution of products is shown in Figure 19 as a function of the concentration of butane for several temperatures. In each instance, methane and propylene were produced in approximately equal molar amounts and together represented from 68 to 71 per cent of the major products. The proportion of ethane and ethylene varied with temperature and concentration of butane. In Figure 20 is a plot of α , the ratio of ethylene to ethane in the products, as a function of temperature and concentration of butane. High temperatures and low concentrations of butane favor formation of ethylene. The variation of α with temperature and pressure served as a basis for the hypothesis of Purnell and Quinn (2) that the decomposition of the ethyl radical is in its pressure dependent region, Figure 21.

The proportion of C_2 hydrocarbons in the product mixture is relatively constant throughout the range of butane concentrations for a given temperature. The function β , defined as

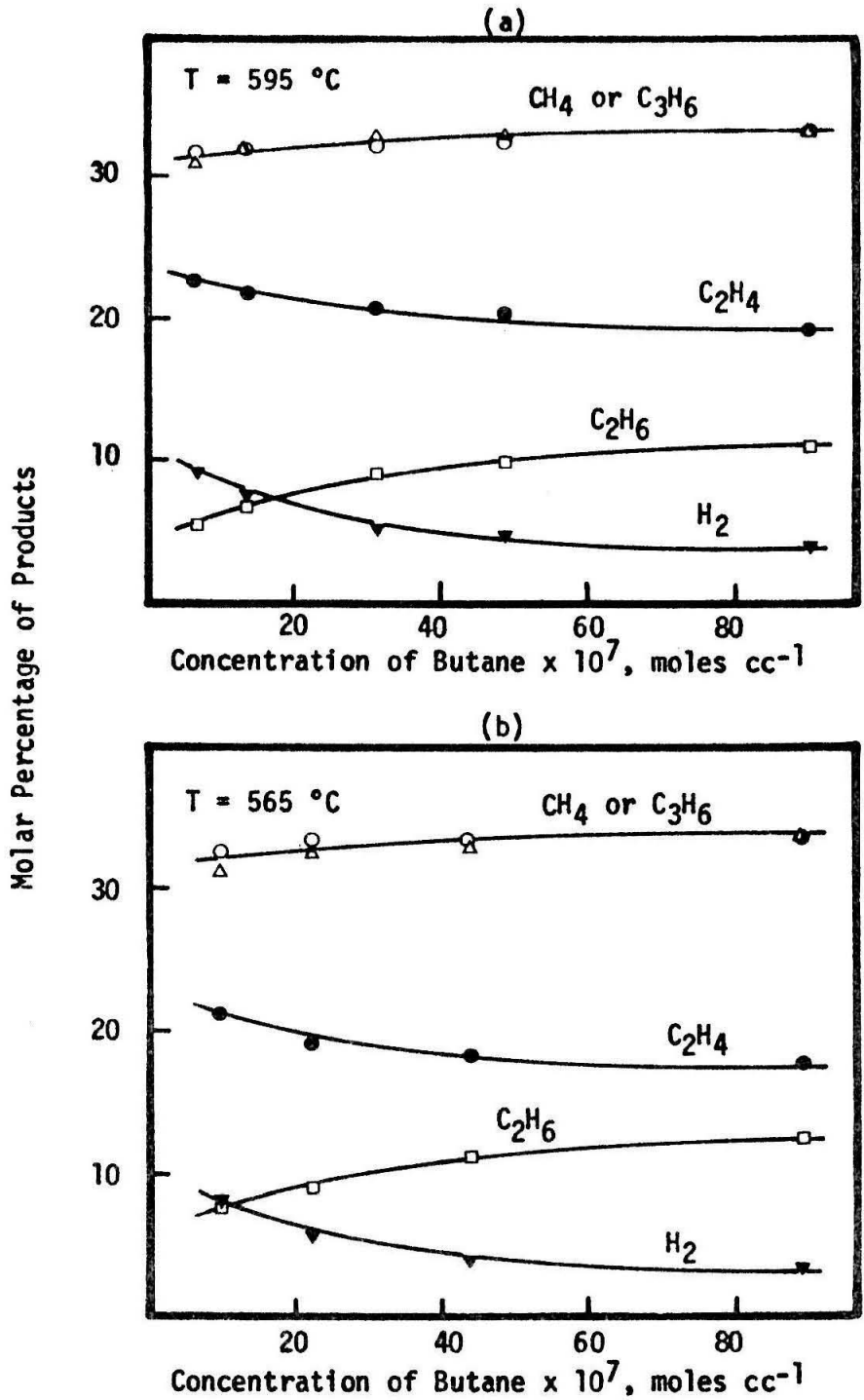


Figure 19. Distribution of products for the pyrolysis in an untreated reactor.

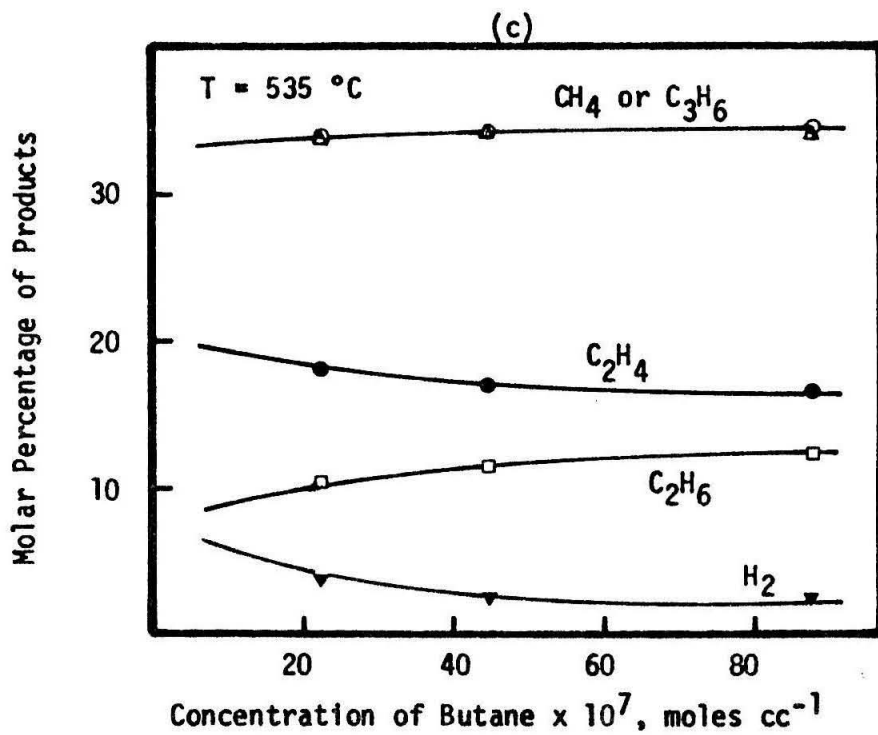


Figure 19, continued.

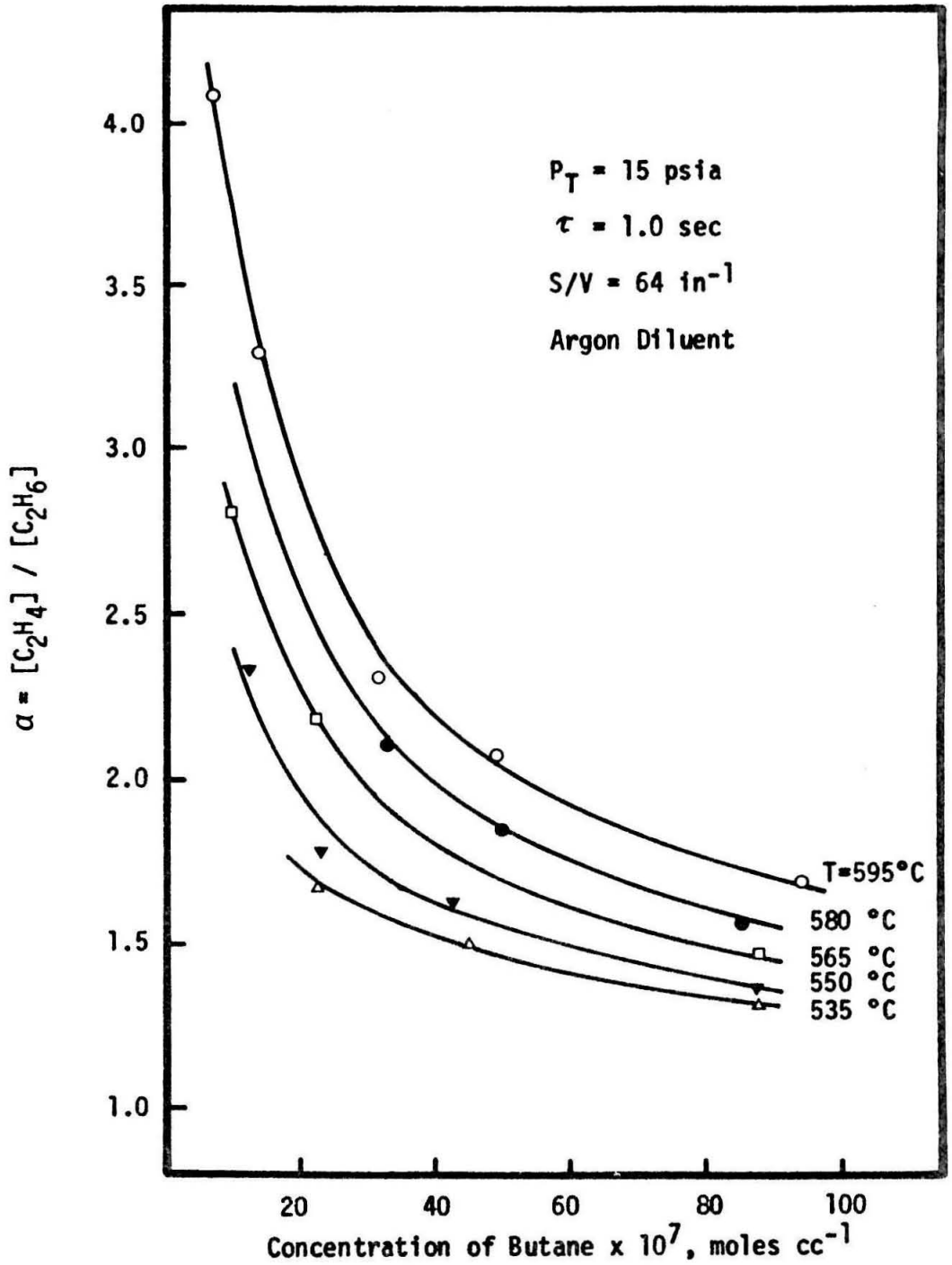


Figure 20. Ethylene/ethane yield for the pyrolysis in an untreated reactor.

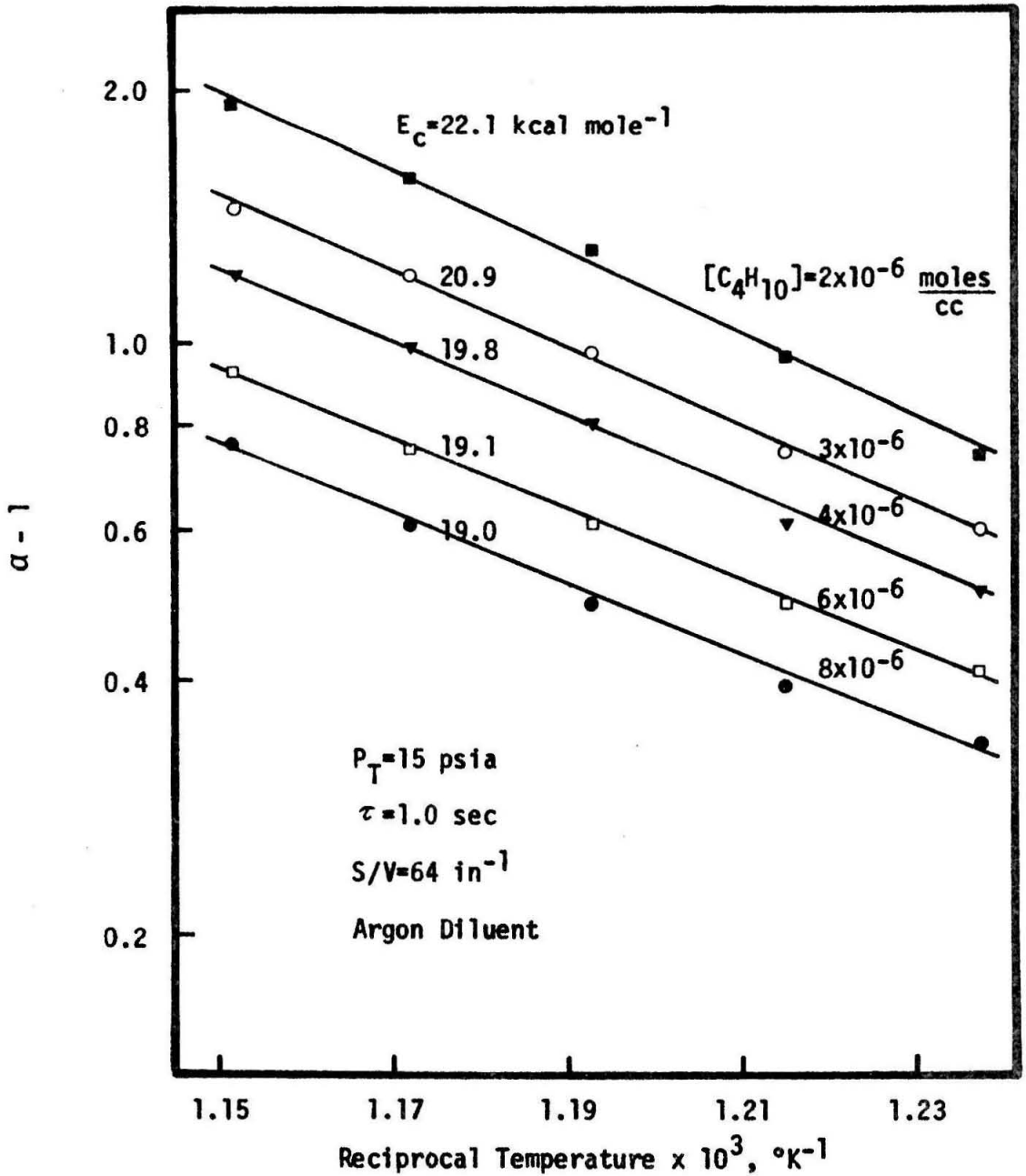


Figure 21. Arrhenius temperature dependence of the function $(\alpha - 1)$ for the pyrolysis in an untreated reactor.

$$\beta = \frac{[C_2H_4] + [C_2H_6]}{[CH_4] + [C_3H_6]} \quad (14)$$

is plotted against butane concentration for several temperatures in Figure 22. Although there is considerable scatter in the data, β is seen to be a weak function of temperature. The Arrhenius plot of Figure 23 reveals an activation energy of approximately 2.33 kcal mole⁻¹.

Although hydrogen could not accurately be measured in the products, a mass balance on the major products indicates that hydrogen is produced according to the following relationship:

$$[H_2] = 0.50 \left([C_2H_4] - [C_2H_6] \right) + 0.75 \left([C_3H_6] - [CH_4] \right). \quad (15)$$

Assuming equal molar amounts of methane and propylene in the products, equation (15) reduces to the following:

$$[H_2] = 0.5 \left([C_2H_4] - [C_2H_6] \right) \quad (16)$$

Purnell and Quinn (2) observed the formation of hydrogen in agreement, within ± 10 per cent, with the simplified equation. For the present work, hydrogen is computed to represent from 3 to 8 per cent of the total products.

The isomers of butene which were detected in the products represented less than 1 per cent of the total products. Little variation of the percentage was observed with changes in temperature or concentration of butane.

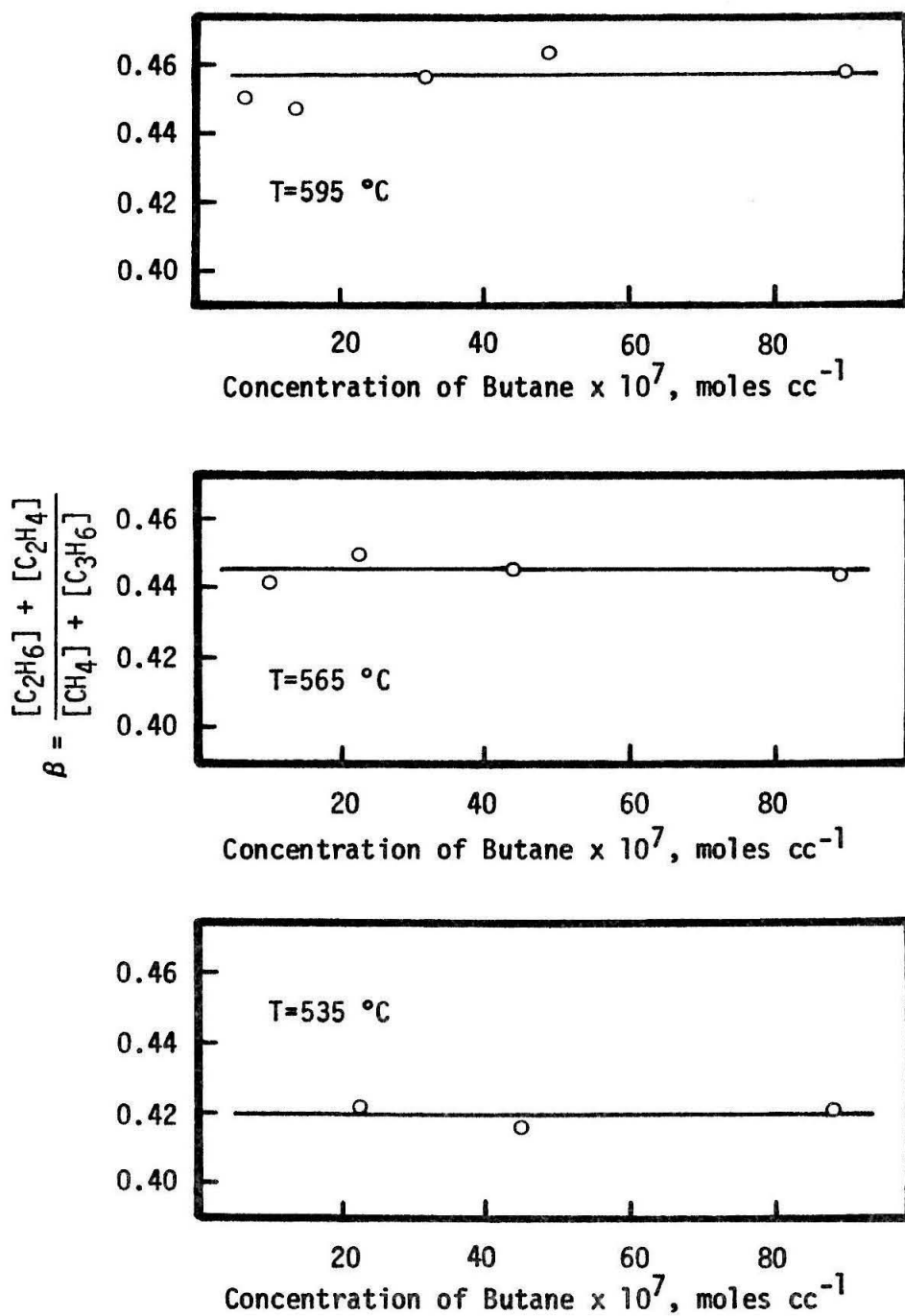


Figure 22. Variation of the proportion of C₂ hydrocarbons in the products for the pyrolysis in an untreated reactor.

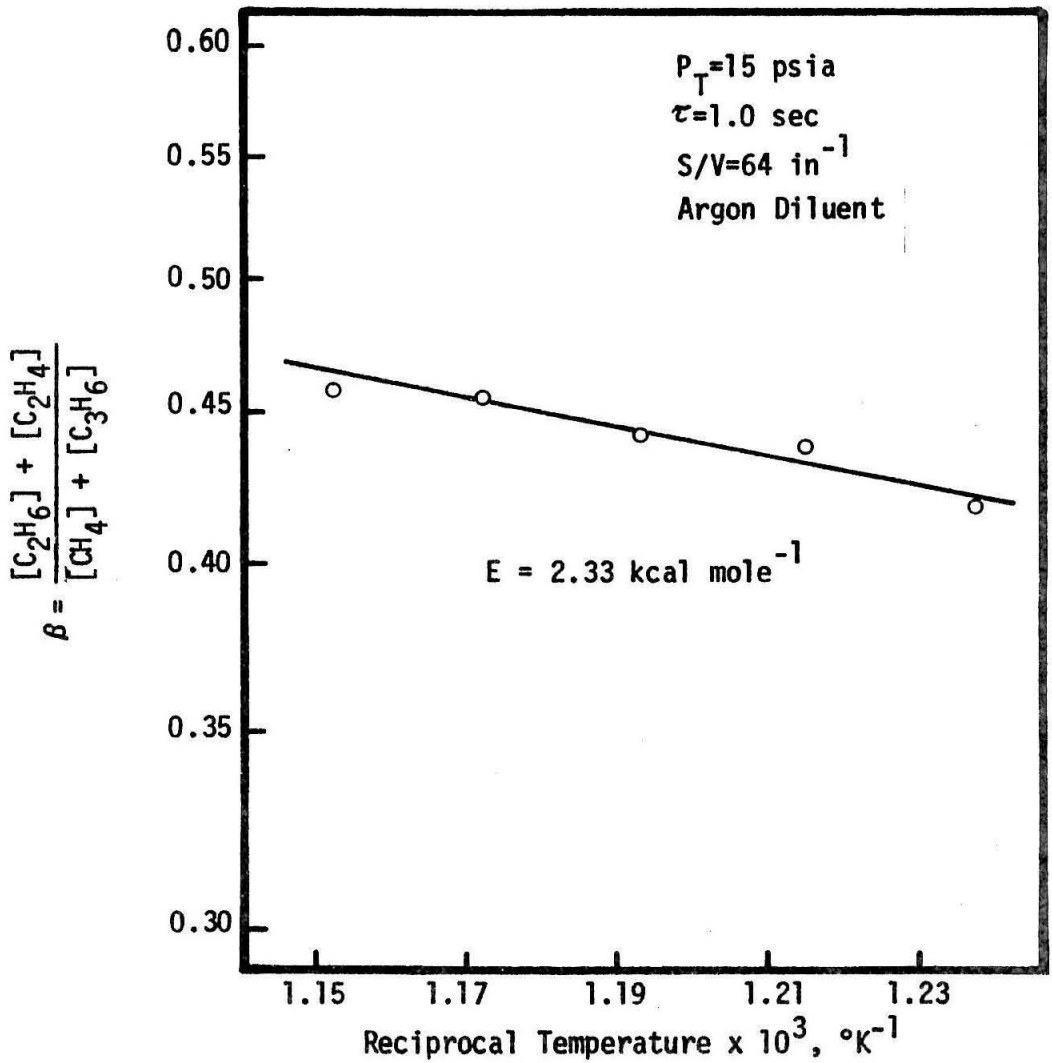


Figure 23. Arrhenius plot of the function β for the pyrolysis in an untreated reactor.

Pretreatment of the reactor with oxygen

The extent of the reaction was significantly altered after the gold reactor had been treated with oxygen. Figure 24 presents results obtained after the reactor had been exposed to a stream of pure oxygen at 500°C for a period of several hours.

The rate of pyrolysis was roughly 30 per cent of that in the untreated reactor. Composition of the products was comparable to that in the untreated reactor. A vacuum of less than 10 microns was exerted on the reactor at 580°C in an effort to remove any oxygen that might have been adsorbed on the surface. The attempt failed to restore the pyrolysis rate to the original level.

Washing the surface with nitric acid did return the rate of pyrolysis to a level comparable to that in the untreated reactor. However, after acid-treatment, operation of the reactor for several days, at conversions of butane of near 1 per cent, was necessary in order to achieve steady state. The rate of decomposition of the butane, as measured by a mass balance on the observed products, is shown in Figure 25 as a function of time from initial operation of the acid-treated reactor. The initial rate of pyrolysis is depressed 50 per cent and only after 60 hours of operation did it reach a steady value. No such unsteady-state conditions were ever observed in the untreated reactors.

The composition of the products during the start-up period changed drastically. The rates of formation of the various products as a function of time are presented in Figure 26. Initially 1-butene, t-2-butene

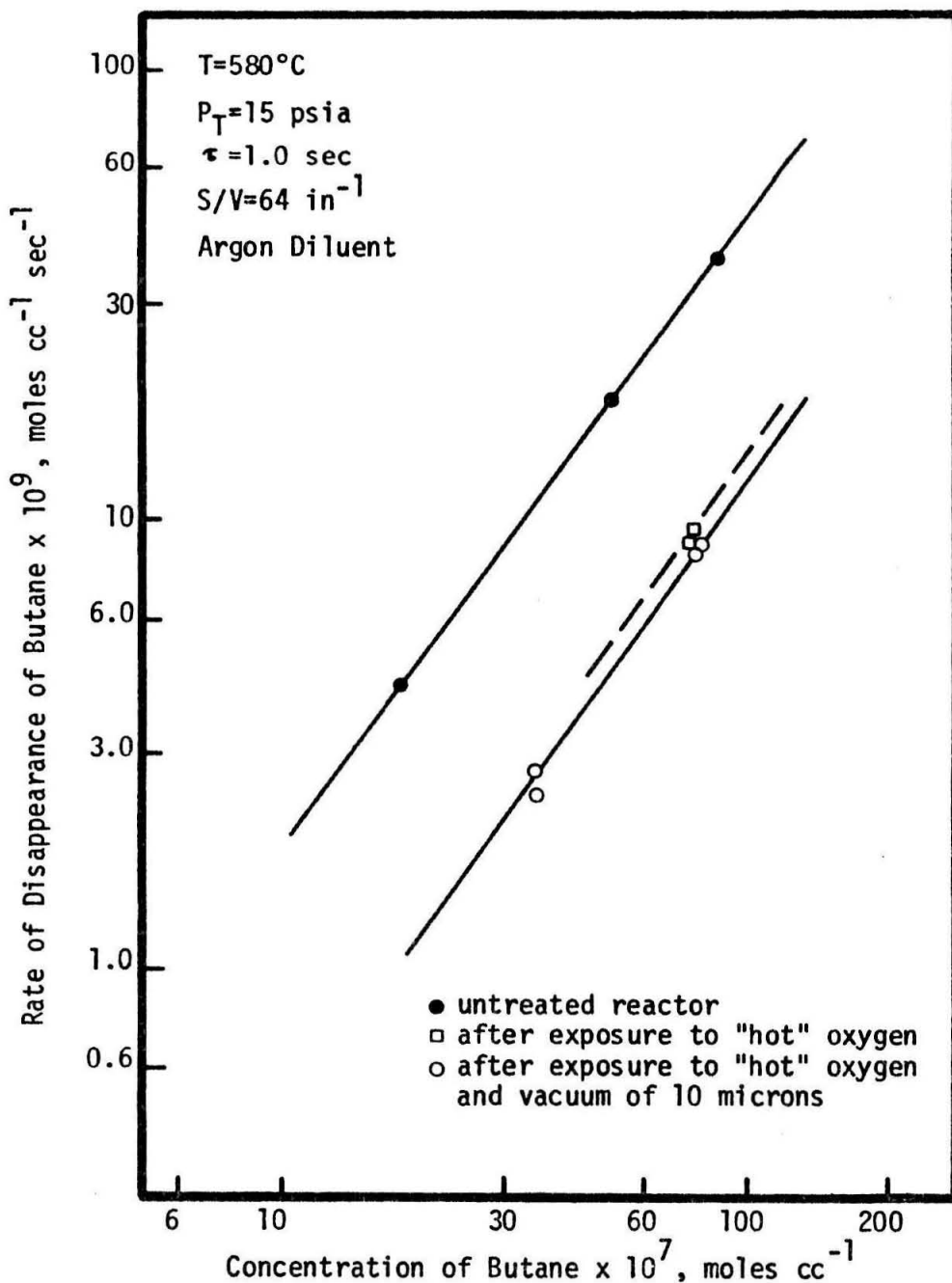


Figure 24. A comparison of the pyrolysis in an untreated reactor, before and after exposure to "hot" oxygen.

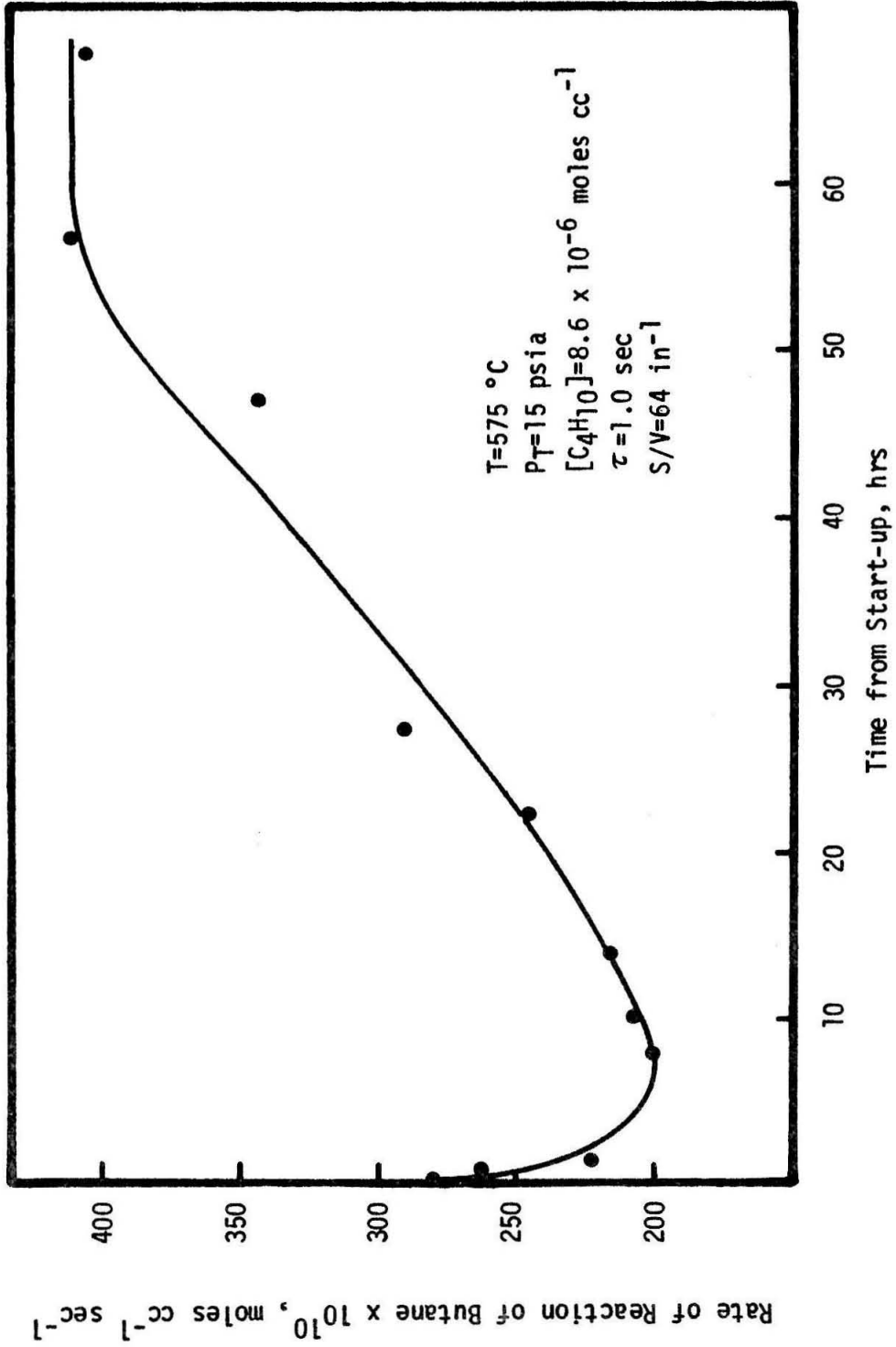


Figure 25. The pyrolysis of butane during the initial operation of a reactor that had been washed with nitric acid.

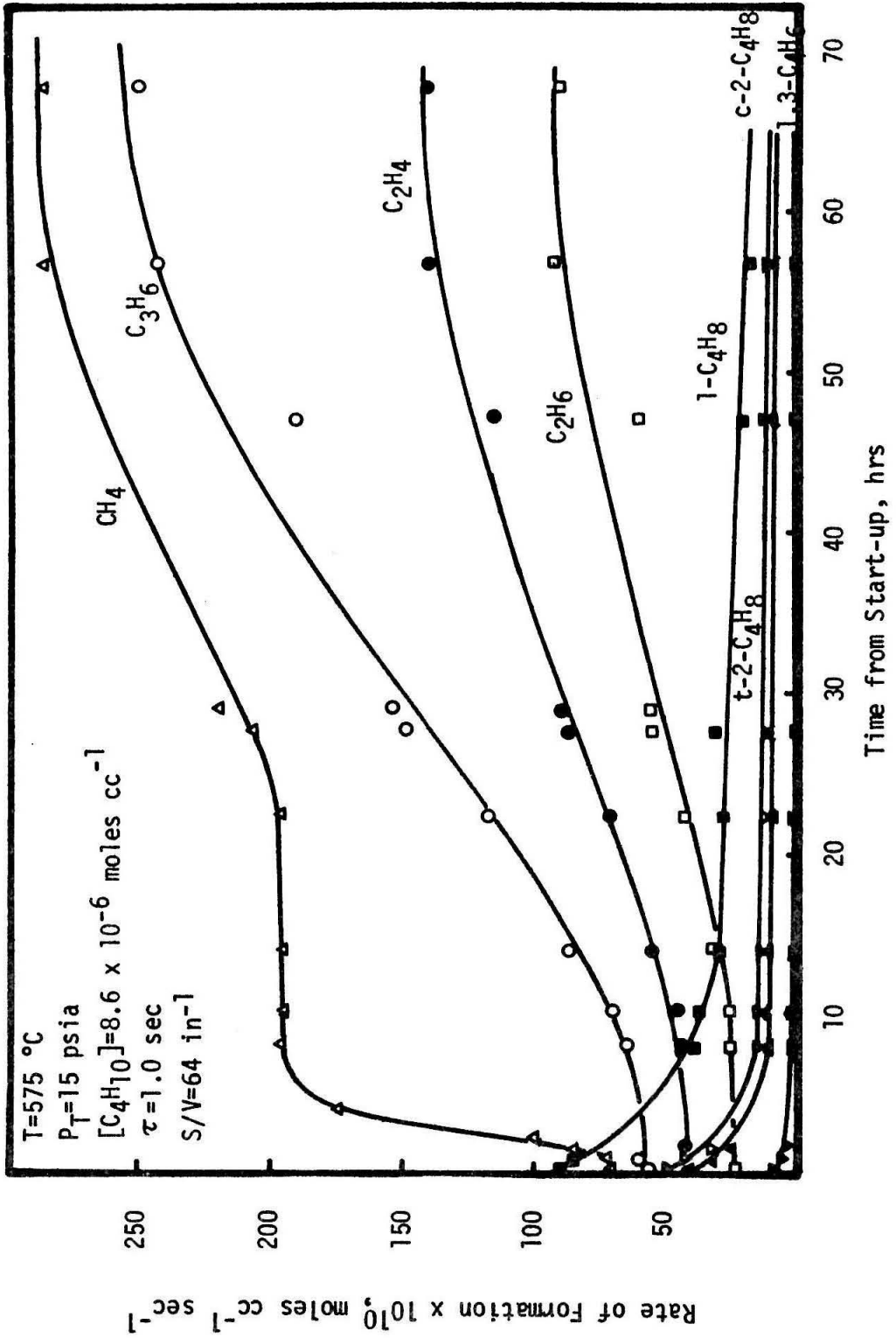


Figure 26. Formation of the products during the initial operation of a reactor that had been washed with nitric acid.

and c-2-butene represented 47 per cent of the products; however, after 60 hours of operation, they constituted about 5 per cent of the products. This latter value is more in line, although slightly high, with that expected in the pyrolysis. The presence of 1,3-butadiene in the products is in contrast to the results of the untreated reactor although Purnell and Quinn (2) had noted the formation of 1,3-butadiene in a pyrex reactor.

Production of methane rapidly increased in the initial stages of operation while the yield of propylene slowly increased. This may be a result of the deposition of carbon on the wall of the reactor. The yield of hydrogen, calculated from a mass balance, represented as high as 30 per cent of the products initially but decreased to a value of 8 per cent when steady state was attained. The initial yield may have been greater provided carbon was formed during the initial stages of the start-up. After steady state was attained the composition of the products approximated the values for the untreated reactor.

Apparently exposure of the reactor to oxygen removes a carbonaceous layer deposited in previous pyrolyses. Evidence of this was noted in the oxygen pretreatment. During the first 15 minutes of treatment, carbon dioxide was observed in the oxygen exiting the reactor.

After removing the carbonaceous layer, oxygen is chemisorbed or forms an oxide with the impurities in the gold, notably copper and silver. Gold, itself, does not chemisorb oxygen nor does it form a

stable oxide at the conditions of pyrolyses (49, 50). The acid-treatment then removes the oxygen from the surface. Kummer (51), working with surface potentials, reported that oxygen did chemisorb on the impurities in a gold cylinder and that removal of the oxygen and impurities could be achieved by repeatedly etching the surface with nitric acid and heating to 500°C.

In the start-up period of the acid-treated reactor, the carbonaceous layer is deposited and any acid or water which may have been adsorbed on the surface is removed. The above scheme is plausible and consistent with the available data. Studies involving surface measurements and the pyrolysis under controlled conditions would aid in a better understanding of the role of the reactor surface.

Crynes and Albright (52) observed a similar phenomena associated with the cracking of propane at 700°C after their stainless-steel reactor had been pretreated with oxygen. A reduction in the rate of pyrolysis of propane was initially observed; however, after 140 minutes of operation, values of conversion and product composition approximated those of runs in untreated stainless-steel reactors. The rapid return to kinetics comparable to the untreated reactors is probably a result of the high conversions (30 to 40 per cent) of propane employed. Material balances during the early operation of the treated reactor always indicated less carbon leaving than entering the reactor. This confirmed the formation of carbon or a carbonaceous layer in the reactor. Formation of cracked hydrocarbons steadily increased during the start-

up period but hydrogen decreased from 50 per cent to 8 per cent of the total products. This was comparable to the situation for the gold reactor.

Pyrolysis in a stabilized acid-treated reactor

After the rate of pyrolysis had reached a steady value in the acid-treated reactor, a series of tests were conducted for a comparison of the kinetics with that of the untreated reactor. Temperatures from 535 to 595°C and total pressures near atmospheric were used in the tests. The rate of decomposition of the butane is shown in Figure 27 as a function of the concentration of butane. The order of the reaction with respect to butane was 1.51 ± 0.03 over the entire range of experimental conditions. In these runs, the butane and argon were primarily premixed. As a result the order for the highest temperature did not decrease at the lower concentrations of butane. Within the accuracy of the data, the order was identical to that observed in the untreated reactor.

The variation of the pyrolysis rate with temperature is presented in Figure 28 for a concentration of butane of 9.0×10^{-6} mole cc^{-1} . An activation energy of $63.3 \text{ kcal mole}^{-1}$ was computed; a frequency factor of $2.45 \times 10^{16} \text{ cc}^{1/2} \text{ mole}^{-1/2} \text{ sec}^{-1}$. The activation energy is slightly less than the $66.6 \text{ kcal mole}^{-1}$ for the untreated reactor. Hence the reaction was found to be less sensitive to temperature in the acid-treated reactor. The variation among reactors of the same type is often 3 kcal mole^{-1} . Barker and Corcoran (1) reported a value of 66.0 kcal

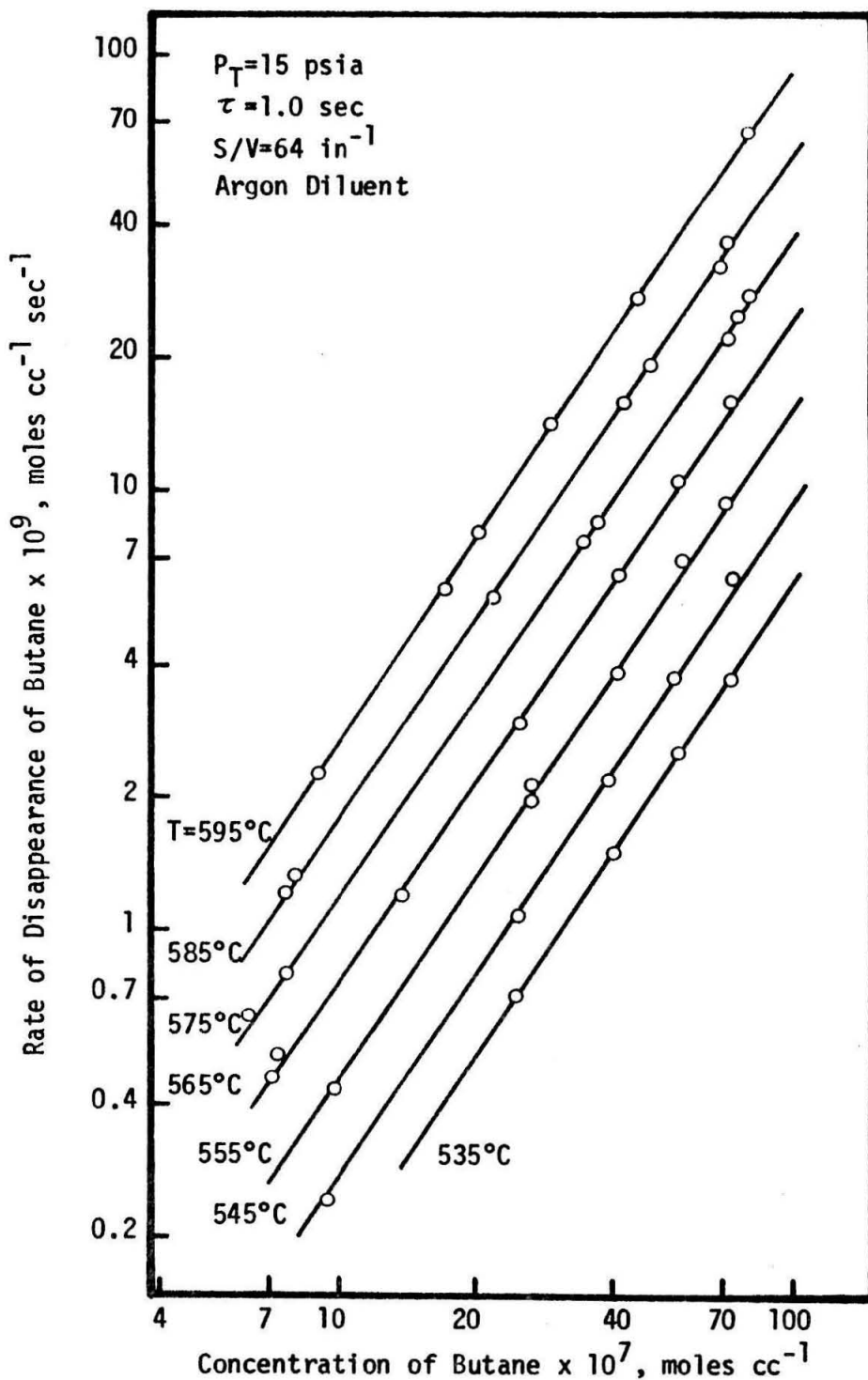


Figure 27. Pyrolysis of butane as a function of temperature and concentration of butane in an acid-treated reactor.

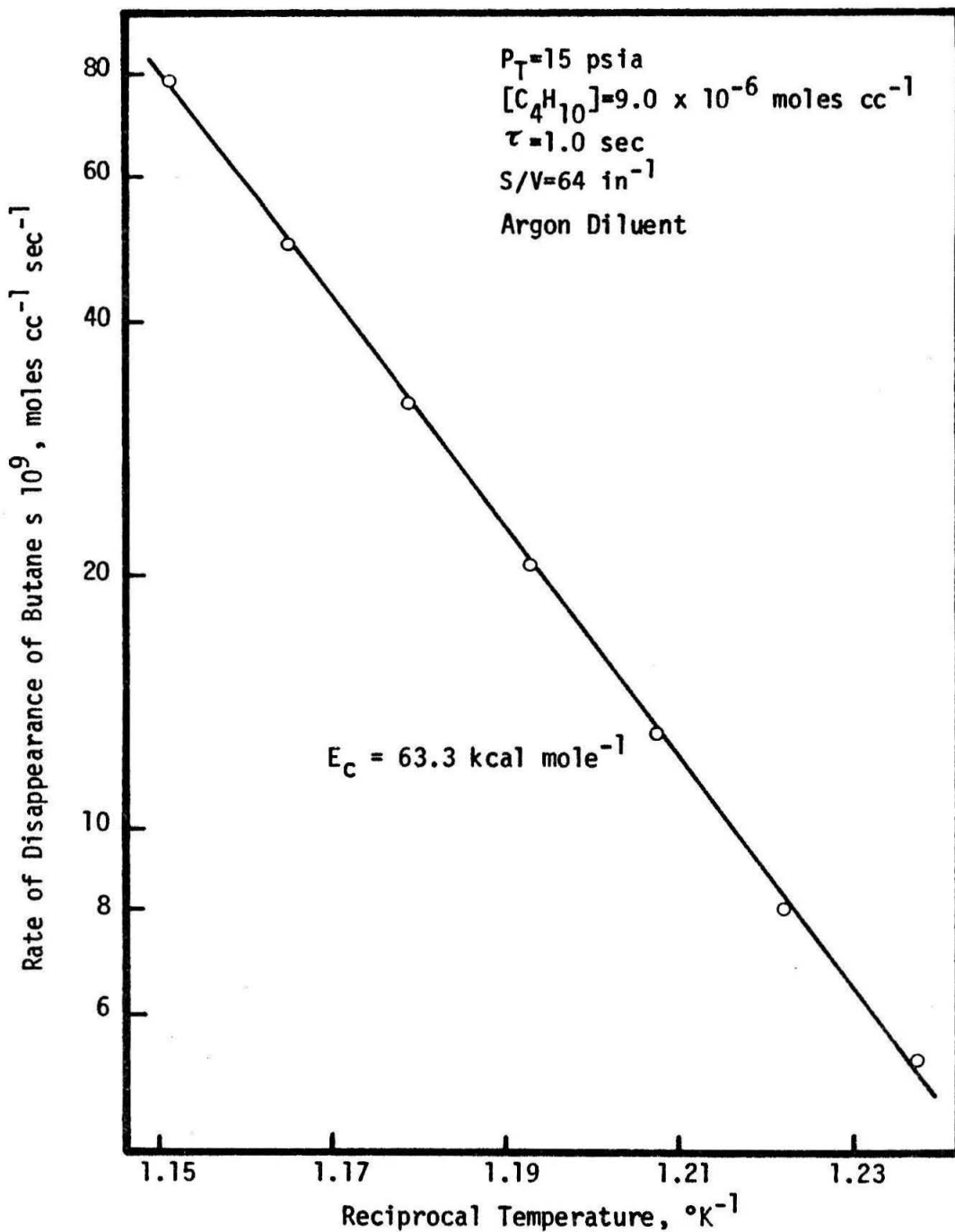


Figure 28. Arrhenius plot for the pyrolysis in an acid-treated reactor.

mole⁻¹ for an acid-treated gold reactor of the same dimensions ($S/V = 64 \text{ in}^{-1}$) as the present reactor. For chain reactions possessing long chains, the order and apparent activation energy of the overall reaction are determined by the dominant chain terminating processes. Thus it may be concluded that termination of the chains occur by similar processes in both the untreated and acid-treated reactors. This is not surprising for a reaction that is considered to proceed primarily in a homogeneous manner.

The distribution of the products was also similar for the acid-treated and untreated reactors. The data were not as consistent in the acid-treated reactor. Methane and propylene were formed in approximately equal yields at concentrations of butane above 8.0×10^{-6} moles cc⁻¹.

In several cases at lower concentrations of butane and particularly in the early runs in the "stabilized" reactor, methane was formed in much greater amounts than was propylene. This is shown in Figure 29. As may be seen when comparing Figure 29(a) and Figure 29(c), the yields of methane and propylene became closer with aging of the reactor. It is likely that although the rate of pyrolysis had reached a steady value, the product mix was still affected by the reactor pretreatment and acid-wash. Crynes and Albright (52) reported that the oxygen-treated surface catalyzed the pyrolysis of ethylene and especially propylene. If in the present work the "excess" methane is assumed to be formed at the expense of propylene (on a carbon basis), the calcu-

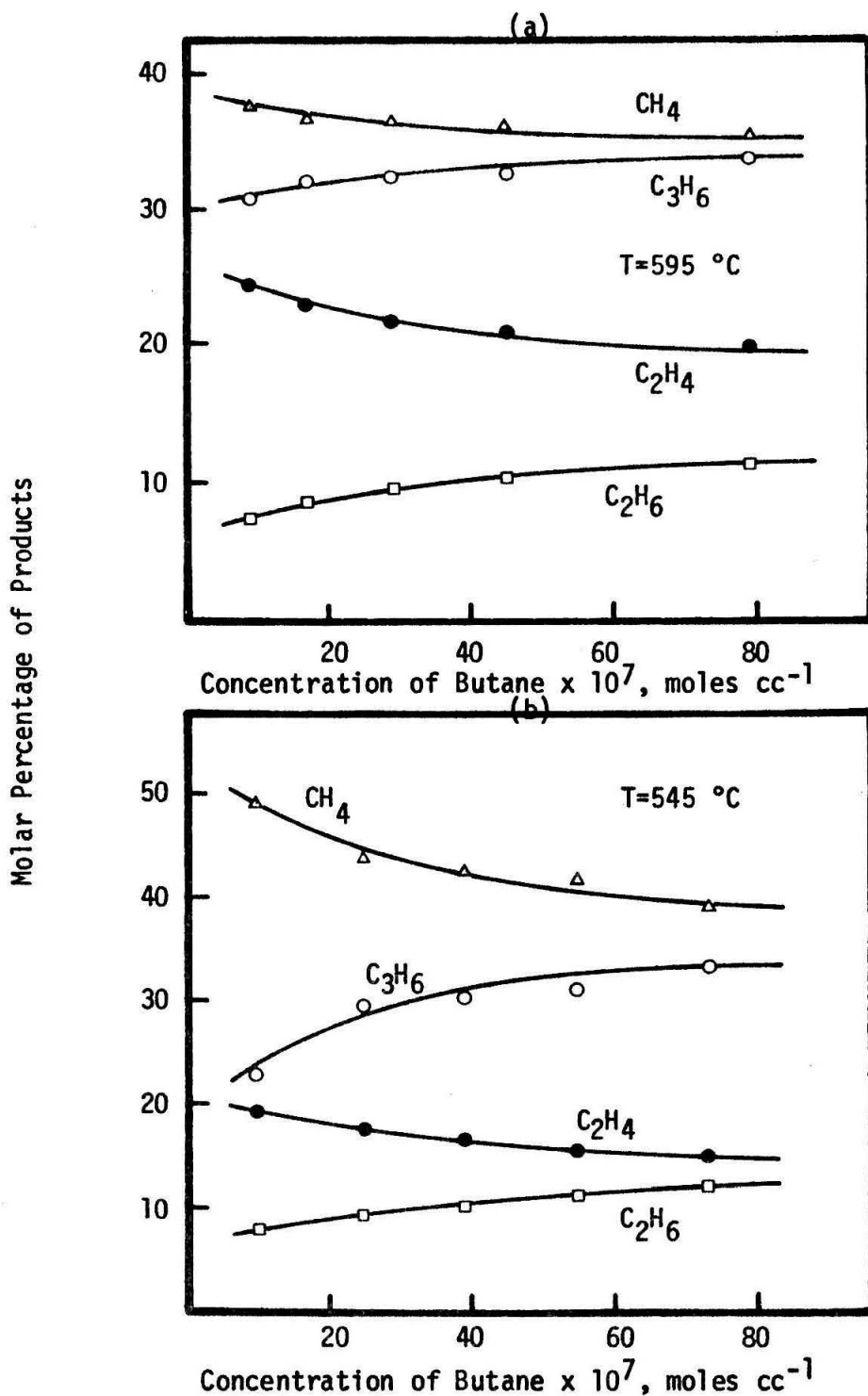


Figure 29. Distribution of products for the pyrolysis in an acid-treated reactor.

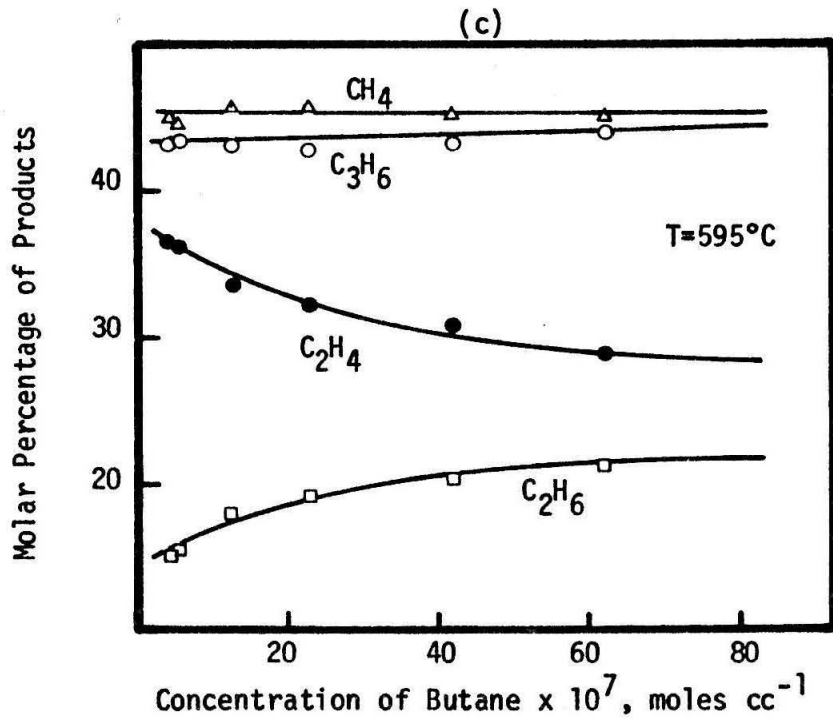


Figure 29, cont'd. Distribution of products for the pyrolysis in an aged acid-treated reactor.

lated product distribution is the same as that for the untreated reactor.

Barker and Corcoran (1) reported identical product composition for the reaction in untreated and acid-treated reactors. It is highly probable that with continued operation of the acid-treated reactor of the present work, the product mix would approach that for the untreated reactor. The distribution of products for long chains is primarily determined by the propagation steps. Therefore, the propagating sequence may differ slightly on the two surfaces in the early periods of operation. In aged vessels the propagation steps are more nearly the same for untreated and treated reactors. Possibly this is a result of a carbonaceous coating of the wall of the reactor in both cases.

Figure 30 shows α , the ratio of ethylene to ethane in the products, as a function of the concentration of butane for several temperatures. The curves are strikingly similar to those of Figure 20 for the untreated reactor. Barker and Corcoran (1) indicated that the function α exhibited a maximum at a concentration of butane near 2.0×10^{-6} mole cc^{-1} . A possible explanation might lie in the care that must be exercised in the measurement of the ethane concentration at the extremely low conversions of butane (0.05 per cent) below a concentration of 1.0×10^{-6} mole cc^{-1} . Measurement of the products on the chromatographic column of Barker was difficult under these conditions. Using a column of Porapak Q, sensitivity of the analysis was increased with respect to both ethane and ethylene. In the present

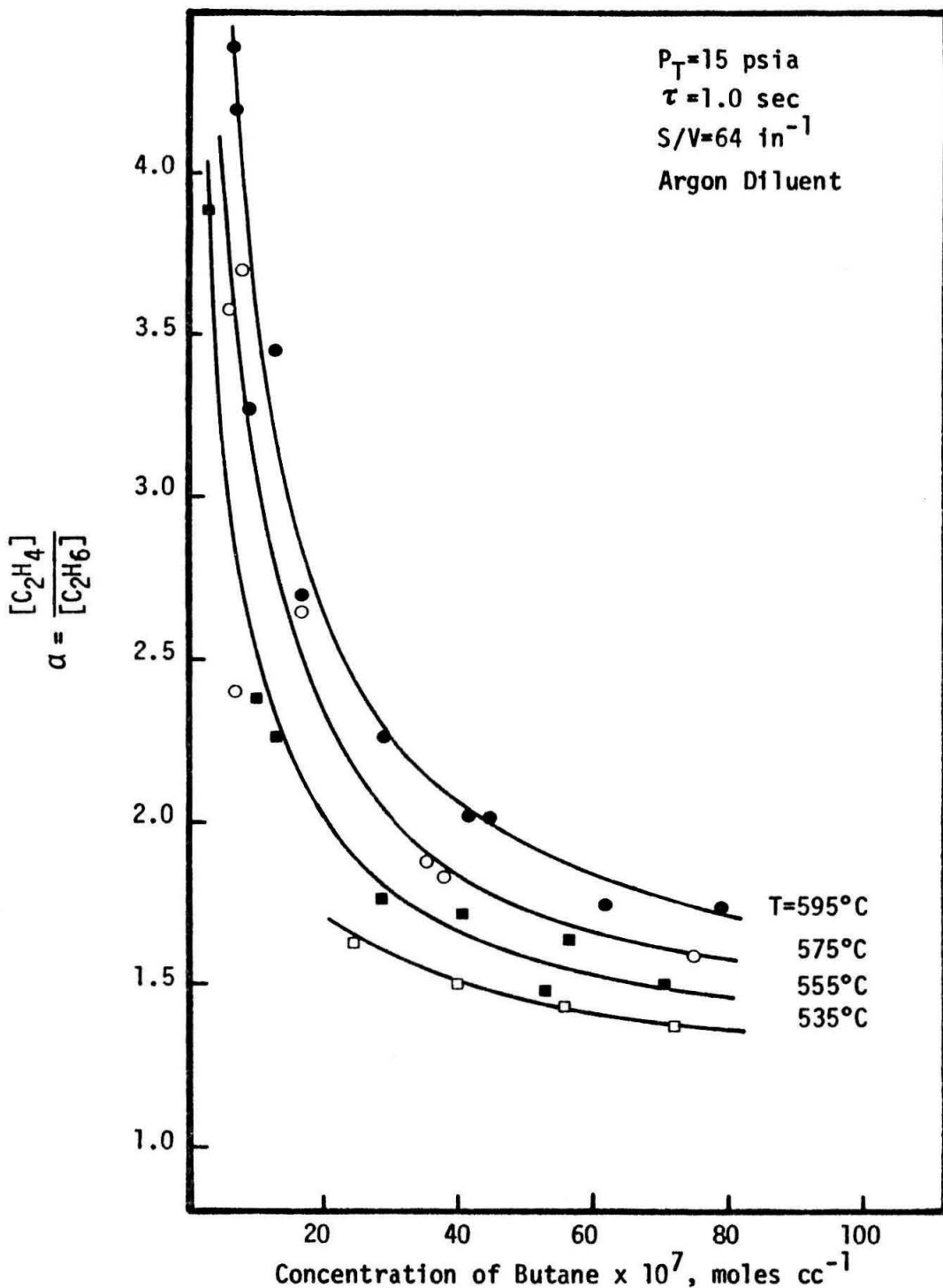


Figure 30. Ethylene/ethane yield for the pyrolysis in an acid-treated reactor.

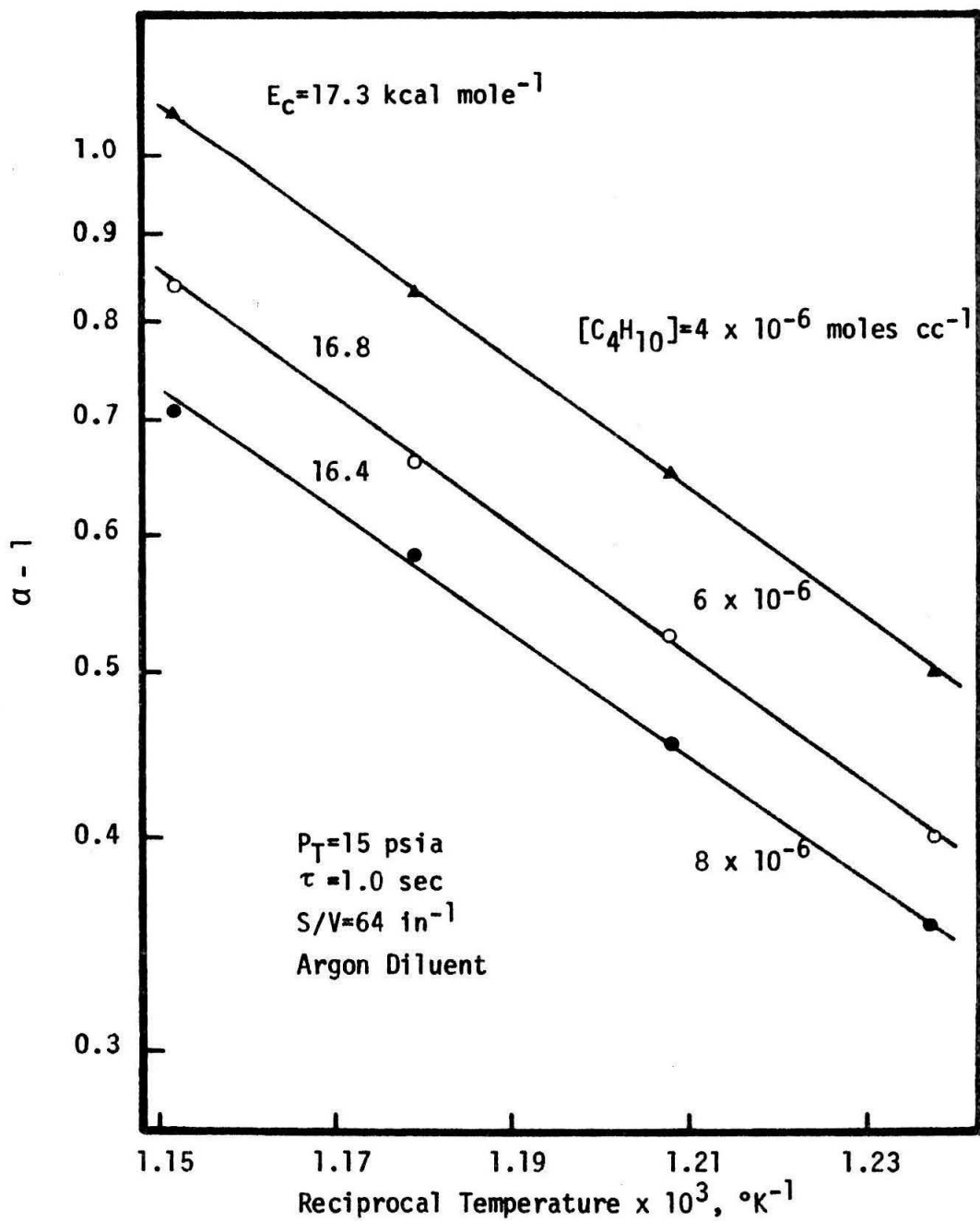


Figure 31. Arrhenius plot for the function $(\alpha - 1)$ for the pyrolysis in an acid-treated reactor.

work, measurements were made using both columns, and in light of the data, no maximum in the function α was found at the lower concentrations of butane.

An Arrhenius plot of the function $(\alpha - 1)$ yields values of the activation energy between 16 and 18 kcal mole⁻¹. These may be compared with an average value of 19.5 kcal mole⁻¹ for the untreated reactor. Within the limits of error, ± 2 kcal mole⁻¹, these are in good agreement. The proportion of C₂ hydrocarbons in the products is presented in Figure 32. As in the case for the untreated reactor, the function, β , is nearly constant for a given temperature and is weakly a function of temperature. In the instances where methane was formed in excess of propylene, the values of β decreased. The average value of β for the acid-treated reactor is 0.45, in reasonable agreement with the value of 0.44 observed in the untreated reactor. Sagert and Laidler (3) reported values near 0.54 for their work in a quartz reactor.

In summary, studies conducted in the untreated reactor and in the acid-treated reactor are very similar. An exception is to be noted in the early stages of operation of the acid-treated reactor. The reaction is seen to be sensitive to the condition of the surface of the reactor. Nevertheless, the majority of the decomposition is believed to occur homogeneously in the gas phase. A comparison of this work with the work of previous investigators is given in Figure 33. The data for the untreated and acid-treated reactors ($S/V = 64$ in⁻¹)

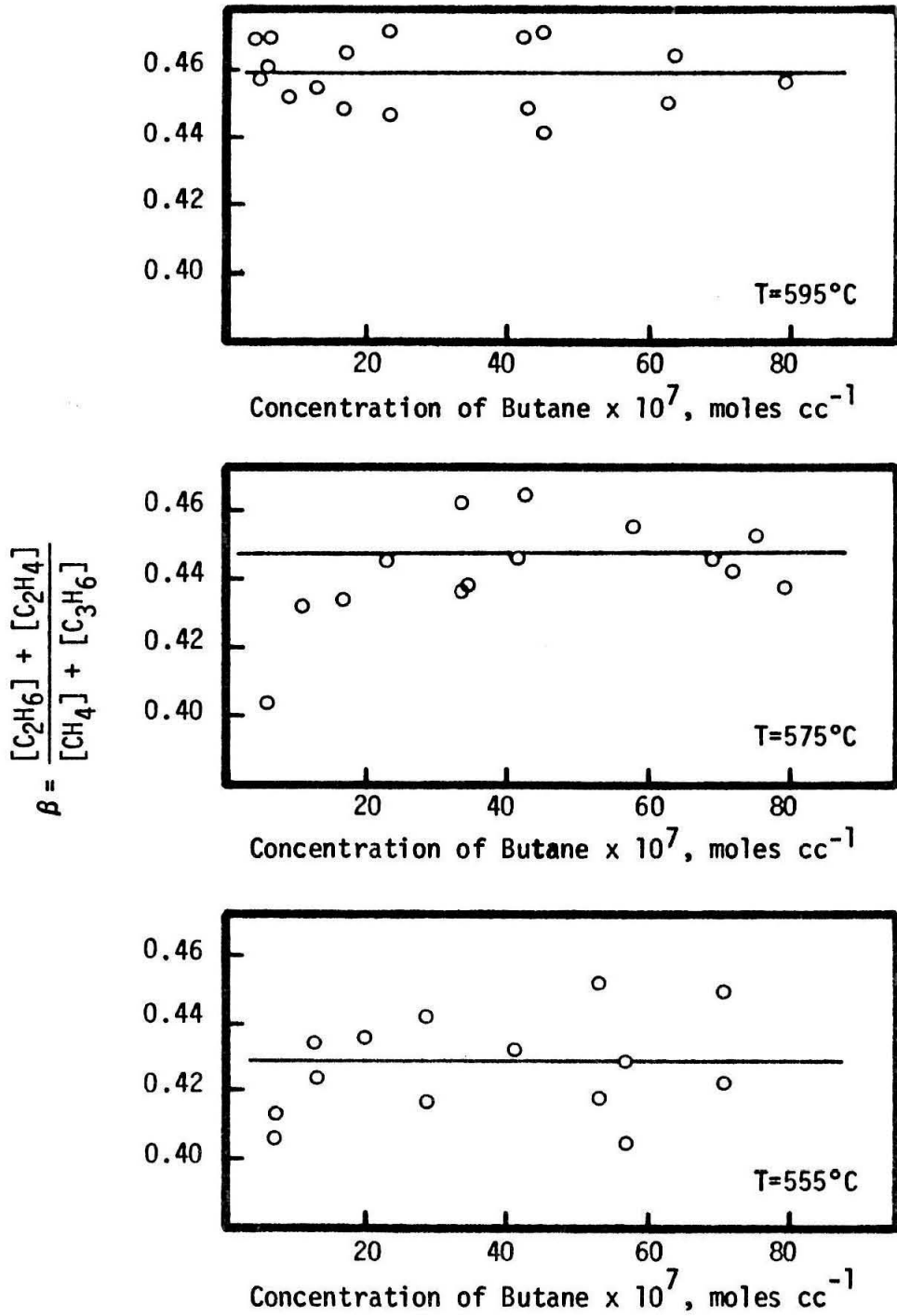


Figure 32. Variation of the proportion of C₂ hydrocarbons in the products for the pyrolysis in an acid-treated reactor.

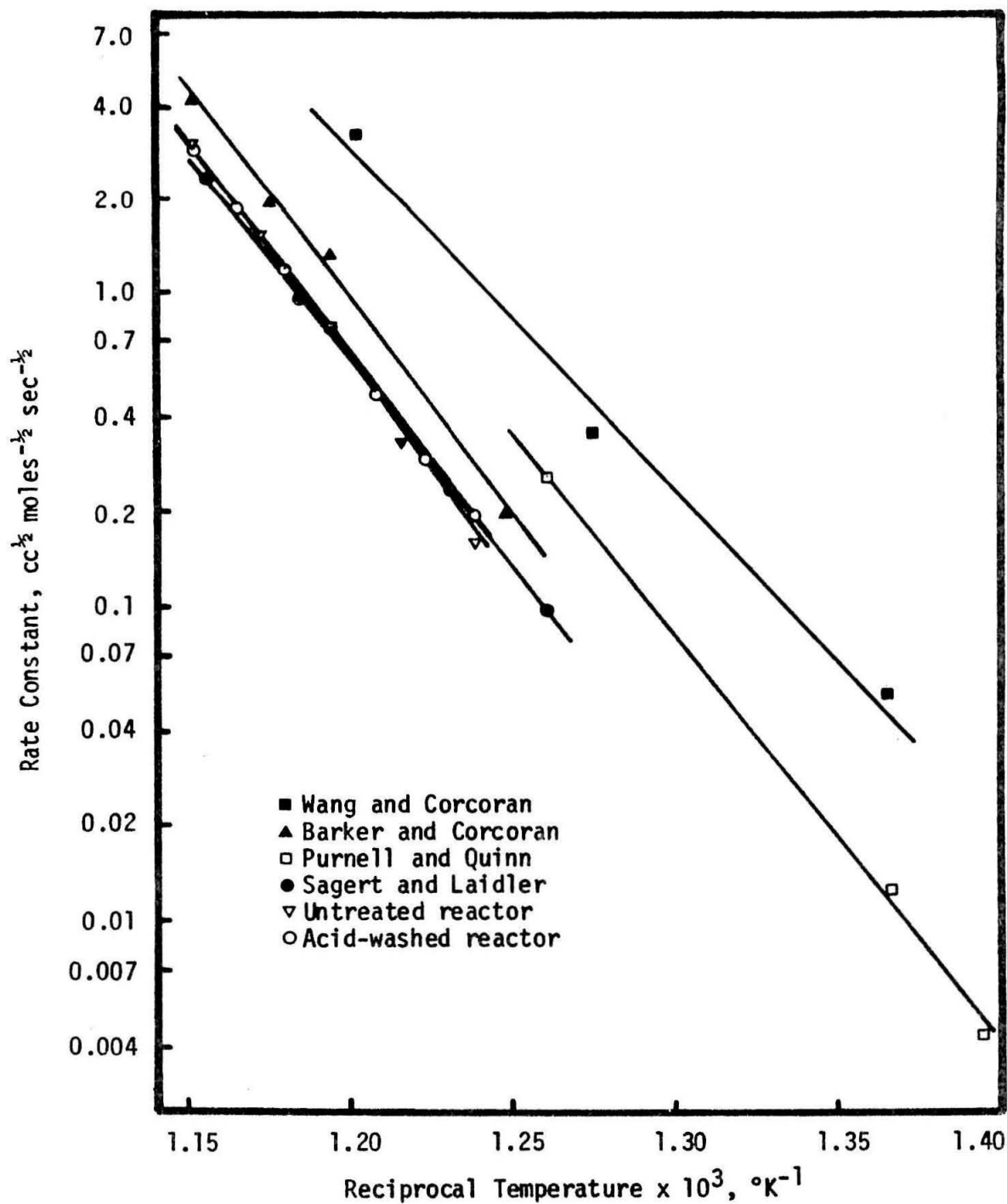


Figure 33. A comparison of the pyrolysis among various investigators.

are in good agreement with respect to the variation among workers. The data of Sagert and Laidler (3), using a quartz reactor with $S/V = 1.7 \text{ in}^{-1}$, also agrees with the present work. As Barker and Corcoran (1) were using a stagnant thermostat, the difference in the present work and that of Barker is believed to be primarily a difference in the measured temperature for the reaction.

The mechanism of the pyrolysis of n-butane

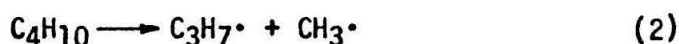
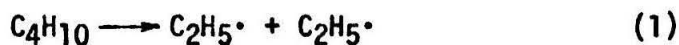
The pyrolyses of hydrocarbons are recognized as free-radical chain reactions. Rice (4) was first to propose the free-radical nature of the reaction. Others including Sagert and Laidler (3), Wang and Corcoran (15), Purnell and Quinn (2) and Barker and Corcoran (1) have presented mechanisms based on the concepts of Rice.

Free-radical reactions are easily discussed in terms of three distinct phases: initiation, propagation and termination. Initiation of the chains in the pyrolysis of butane is considered to be the homolytic decomposition of butane into two free radicals. Only a small percentage of the total butane which reacts is attributed to the initiation sequence. Decomposition of the butane primarily takes place in the propagation steps. The propagation reactions are recognizable in that free radicals are consumed and regenerated. Free radicals may be divided into two classes according to the type of propagation reactions in which they participate. Those that undergo monomolecular propagation steps are referred to as μ radicals. Free radicals involved in bimolecular propagation reactions are termed γ radicals. The disappearance of

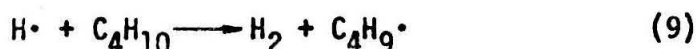
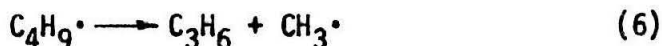
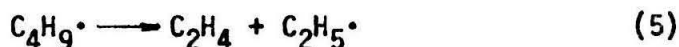
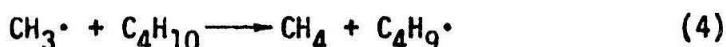
butane is primarily achieved by the reaction of butane with a γ radical. Chains are terminated with the recombination of free radicals.

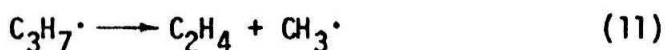
The lengthy mechanism proposed by Wang and Corcoran (15) is perhaps more nearly representative of the actual reaction than condensed schemes. The mechanism provided for secondary reactions of the products as well as additional alternative paths for free-radical participation by reaction. A serious disadvantage of such a mechanism is the difficulty in treating the mechanism mathematically. In an effort to present a mechanism that is in agreement with a majority of experimental results and one whose consequences may be easily derived, a condensed mechanism is given below. This mechanism is similar to that proposed by Purnell and Quinn (2) and Barker and Corcoran (1).

Initiation:

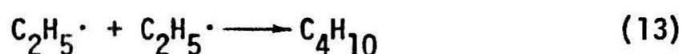
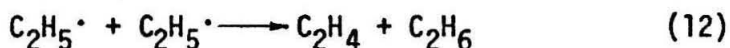


Propagation:





Termination:



Trotman-Dickenson (53) has estimated that step (1) is approximately 4 kcal mole^{-1} more favorable than step (2). This being the case, initiation by the first-order decomposition of butane into two ethyl radicals would predominate. Propyl radicals are generated only in initiation of the chains. Consequently, the concentration of propyl radicals, assuming long chains, should be extremely low and steps (9) and (10) should have little effect on the overall product distribution.

The recombination of two ethyl radicals is considered the predominate chain breaking process. Laidler and Wojciechowski (54) have recently shown that the recombination of two methyl radicals and the recombination of a methyl and ethyl radical are in their third order region at the conditions of pyrolysis.

According to the scheme of Goldfinger, Letort, and Niclause (55), overall kinetics of three-halves is predicted for a free-radical reaction which involves a first-order initiation and $\gamma\gamma$ recombination. The ethyl radical is considered primarily as a γ radical since step (3) is more rapid than step (8). Support for this mechanism is its agreement with the kinetics of three-halves order observed experimentally.

The assumption of steady state is frequently applied to the free radicals of the pyrolyses of hydrocarbons. Steady state implies that the concentration does not change with time. Numerical proof of the validity of the assumption of steady state as it applies to the pyrolysis of butane is given in Appendix D. Making use of the steady-state hypothesis, relationships may be derived which predict the experimental kinetics of the pyrolysis.

The rate of pyrolysis of the butane is predicted as follows from the mechanism:

$$\begin{aligned}
 -R_{C_4H_{10}} = & [C_4H_{10}]^{3/2} \left\{ k_3 \left(\frac{k_1+k_2}{k_{12}+k_{13}} \right)^{1/2} \left(1 + \frac{k_6}{k_5} + \frac{k_7}{k_5} \right) \right\} \\
 & + [C_4H_{10}] \left\{ k_1+k_2+2k_2 \left(1 + \frac{k_6}{k_5} + \frac{k_7}{k_5} \right) - k_{13} \left(\frac{k_1+k_2}{k_{12}+k_{13}} \right) \right\} \\
 & + [C_4H_{10}]^{1/2} \left\{ k_8 \left(\frac{k_1+k_2}{k_{12}+k_{13}} \right)^{1/2} \left(1 + \frac{k_6}{k_5} + \frac{k_7}{k_5} \right) \right\}, \quad (17)
 \end{aligned}$$

Approximate values of the rate constants are tabulated in Appendix D. Considerable variation in the value of several of the rate constants may be found in the literature. Substitution of the rate constants evaluated at 519°C into equation (17) reveals that the three-halves-order term is dominant although the one-half-order term contributes about 30 per cent to the overall rate. This percentage was calculated using the high-pressure or first-order rate constant for step (8), the

decomposition of the ethyl radical. Purnell and Quinn (2) postulated that the decomposition of the ethyl radical is in its second-order region. Loucks and Laidler (56) later experimentally confirmed this fact. This being the case, k_8 was overated in the above calculation. Thus the contribution to the overall rate from the one-half order term is less than 30 per cent. Experimentally, the reaction is precisely three-halves order.

The activation of the overall reaction may be estimated from the three-halves order term of equation (17). Insertion of the activation energies of Appendix D into the three-halves order term predicts a value between 50.4 and 59.4 kcal mole⁻¹. If the values of Purnell and Quinn (2) are used for activation energies, the apparent activation energy is predicted to be between 58.5 and 67.5 kcal mole⁻¹. The latter spread is in better agreement with the experimentally observed values of 63.3 kcal mole⁻¹ for the acid-treated reactor and 66.6 kcal mole⁻¹ for the untreated reactor.

Assuming long chains, an expression may be obtained from the mechanism which relates the ethylene and ethane yields in the products:

$$(\alpha - 1) [C_4H_{10}] = 2 \frac{k_8}{k_3} . \quad (18)$$

A plot of the function $(\alpha - 1)[C_4H_{10}]$ should be independent of the concentration of butane. Figure 34 is a display of the data at 595°C for pyrolysis in the untreated reactor. Indeed the function $(\alpha - 1)[C_4H_{10}]$ is found to be dependent on the concentration of butane. This

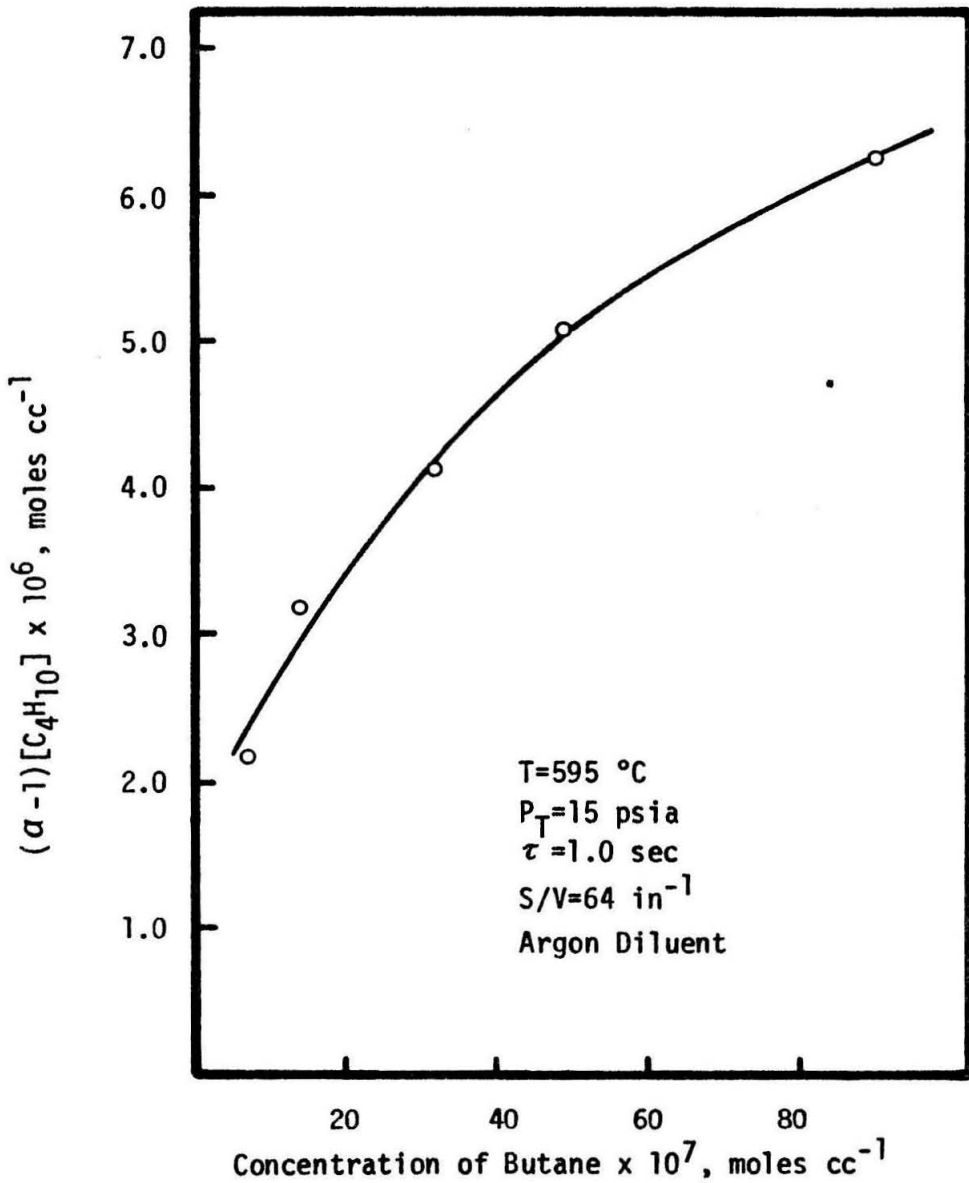


Figure 34. Variation of the function $(\alpha-1)[C_4H_{10}]$ as a function of the concentration of butane.

result led Purnell and Quinn (2) to postulate that step (8), the monomolecular decomposition of the ethyl radical, was in its pressure dependent region. Thus k_g would be a function of the pressure or concentration of the activating species.

The present work was performed at a constant total pressure near 15 psia by use of an inert gas, argon. The efficiency of argon in transferring energy for step (8) must be less than 5 to 10 per cent of that for butane. Argon possesses an efficiency of 7 per cent that of cyclopropane in the isomerization of cyclopropane at 492°C (57). Data for butane were not available. However, it is generally accepted that the inert gases are relatively inefficient and that the efficiency of energy transfer increases to a limit with increasing complexity of the molecule. Therefore, it is probable that the monomolecular decomposition of the ethyl radical is in its pressure dependent region.

Undoubtedly the $C_4H_9\cdot$ radicals are present as both primary and secondary radicals. The $C_4H_9\cdot$ are formed by abstraction of a hydrogen atom from butane. In abstraction, *s*- $C_4H_9\cdot$ are actually formed more easily than *p*- $C_4H_9\cdot$. Kuppermann and Larson (58) estimated that ratio of rate of primary abstraction to secondary abstraction is

$$\frac{k_p}{k_s} = 2.43 \exp [-2640/RT] \quad . \quad (19)$$

According to McNesby and Gordon (59), the ratio is

$$\frac{k_p}{k_s} = 1.50 \exp [-2100/RT] \quad . \quad (20)$$

At 595°C, these equations yield values of k_p/k_s of 0.52 and 0.44 respectively. Step (5) occurs most likely through a $p\text{-C}_4\text{H}_9\cdot$ and step (6) through a $s\text{-C}_4\text{H}_9\cdot$. Assuming that the rates of steps (5) and (6) are fast compared to the interconversion of the $p\text{-C}_4\text{H}_9\cdot$ and $s\text{-C}_4\text{H}_9\cdot$, the ratio of the C_2 hydrocarbons to the methane and propylene in the products, defined as β , should be comparable to the relative abstraction rates. For the untreated reactor, a value of 0.457 was observed at 595°C. In addition the activation energy for the function β was computed to be 2330 cal mole⁻¹ in good agreement with the above work.

The yields of methane and propylene are predicted to be equal from the mechanism. This was experimentally verified in the case of the untreated reactor and in the case of the aged acid-treated reactor.

No distinction was made among 1-butene, c-2-butene and t-2-butene in the mechanism. The formation of butenes is related to the yield of propylene by the following equation:

$$\frac{[\text{C}_3\text{H}_6]}{[\text{C}_4\text{H}_8]} = \frac{k_6}{k_7} \quad (21)$$

The decomposition of $\text{C}_4\text{H}_9\cdot$ by loss of hydrogen is known to be much slower than the decomposition involving severance of a carbon-carbon bond. However, much doubt exists to the exact values of k_6 and k_7 . Using values from Appendix D, the concentration of the butenes in the products should be approximately one-sixth of the propylene concentration or about 5 per cent of the total products. This was in agreement

with the results in the acid-washed reactor; however, total butene concentration was never greater than 2 per cent in the untreated reactor. Sagert and Laidler estimated that the activation energy for step (7) was about $40 \text{ kcal mole}^{-1}$ as compared with $31 \text{ kcal mole}^{-1}$ listed in Appendix D. Assuming the higher activation energy, butenes should represent only about 0.1 per cent of the total products. An accurate value for the rate constant of step (7) would greatly contribute to an understanding of the mechanism and the minor products of the reaction.

In summary, the proposed mechanism is in reasonable agreement with the observed kinetics of the pyrolysis. Product distribution can be approximated on the basis of the mechanism. The limited accuracy with which the rate constants of the elementary reactions are known, however, limits an accurate and complete comparison of the mechanism and the experimental results.

Pyrolysis of Butane in the Presence of Trace Amounts of Oxygen

Oxygen was observed to have a significant effect on the rate of decomposition of butane. In this section are discussed the experimental observations obtained when pyrolyzing butane in the presence of trace quantities of oxygen. The term "trace quantities of oxygen" refers to amounts small enough that the oxygen is totally consumed in a small fraction of the time in the reactor. Concentrations of oxygen in the inlet mixture to the reactor were varied from 7 to 870 ppm, with primary emphasis on the area below 50 ppm.

For a given inlet concentration of oxygen, the composition of the products of the reaction was studied as a function of temperature and concentration of butane. Temperatures from 535 to 625°C were employed and the concentration of butane was varied from 4×10^{-7} to 8×10^{-6} moles cc^{-1} . The total pressure of the reactor was maintained between 15 and 16 psia. All tests were conducted in a gold microreactor of $S/V = 32 \text{ in}^{-1}$ which had repeatedly been acid-washed and heated to 500°C to remove oxidizable impurities present in the gold.

Distribution of hydrocarbon products

Paraffins and olefins observed in the pyrolysis of butane were also found in the oxidative pyrolysis. In addition small amounts of water were present at all levels of oxygen. Above initial concentrations of oxygen of 400 ppm, carbon dioxide was also detected in the products.

The relative yields of the hydrocarbon products are shown in Figure 35 as a function of the initial concentration of oxygen for a temperature of 595°C. The concentration of butane was fixed at 7.15×10^{-6} mole cc^{-1} , and the product distributions were recorded for residence times of 2.6 sec. Conversions of butane were less than 1.2 per cent.

Increasingly larger fractions of 1-butene, t-2-butene, c-2-butene, and 1,3-butadiene appeared in the products as the oxygen level in the reactants was increased. Butenes constituted less than 2 per cent of the products for the pyrolysis in the absence of oxygen. At an initial oxygen level of 870 ppm, the butenes represented 17.5 per cent of the hydrocarbon products. 1,3-Butadiene comprised 1.5 per cent of the products, and traces of 1-pentene were detected in the products. The latter two compounds were not observed during the pyrolysis of butane in the absence of oxygen at conversions of butane below 2 per cent. Accompanying the relative increase of C_4 and C_5 olefins were decreases in the methane, propylene, ethylene, and ethane fractions.

Figures 36 and 37 show the variation of the products as a function of the concentration of butane for 595 and 555°C, respectively. The concentration of oxygen in the inlet mixture was 14.5 ppm in each case. The relative proportion of the C_4 olefins rapidly decreased with increasing concentration of butane. On the other hand, the relative proportions of methane, propylene, ethylene, and ethane increased with increasing concentration of butane. This rapid change of product

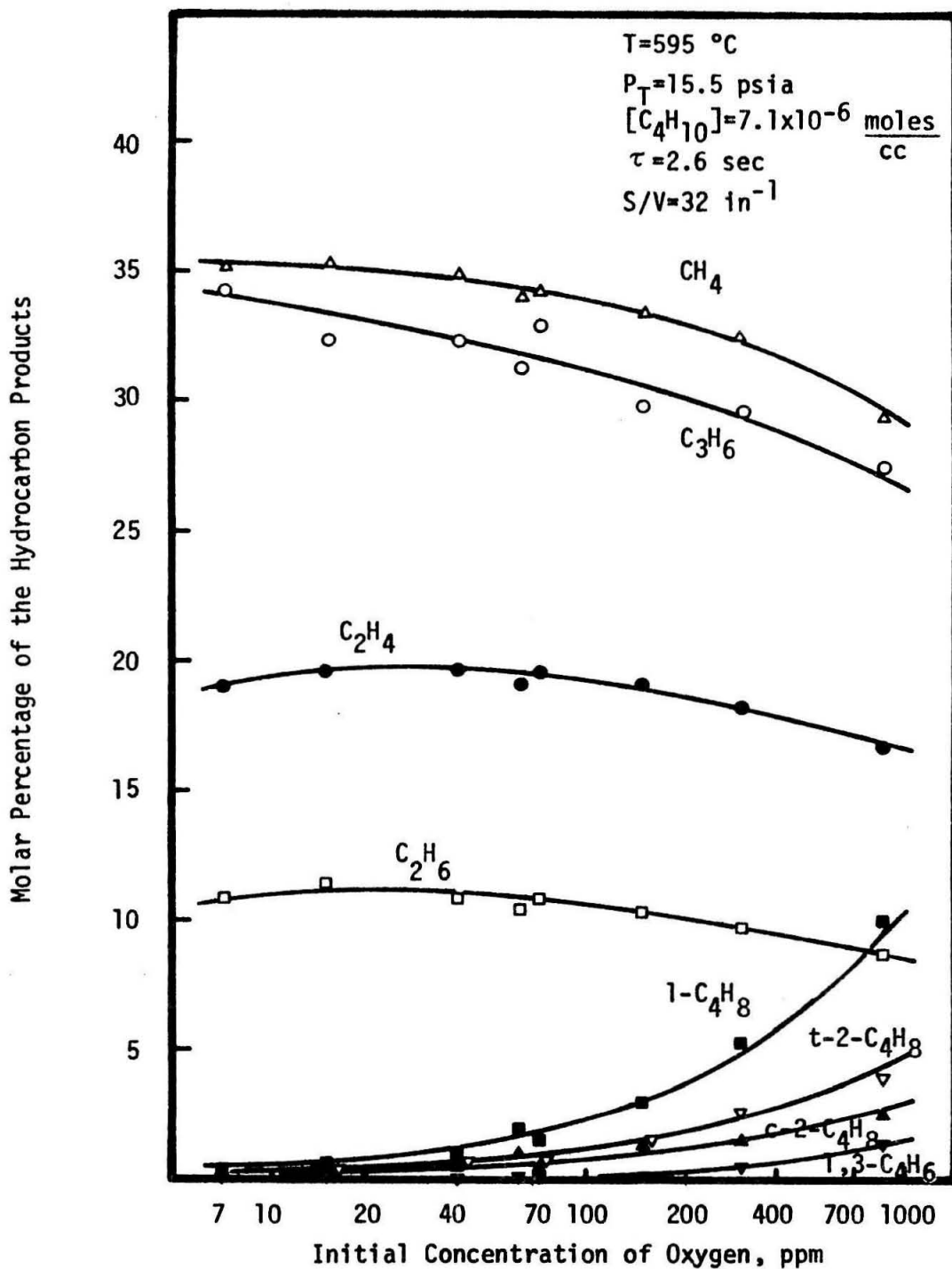


Figure 35. Distribution of hydrocarbon products as a function of the initial concentration of oxygen.

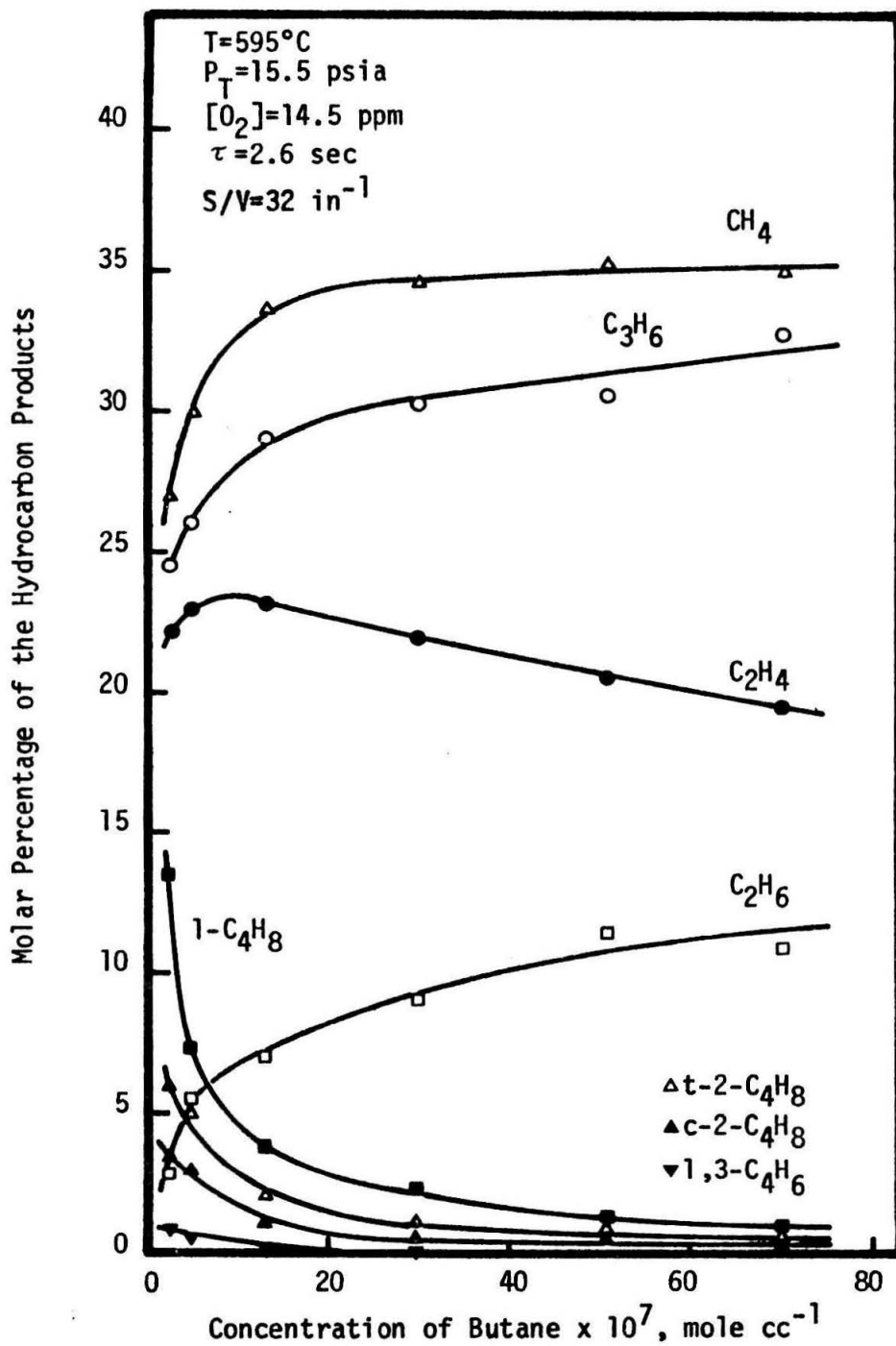


Figure 36. Distribution of hydrocarbon products at 595°C as a function of the concentration of butane.

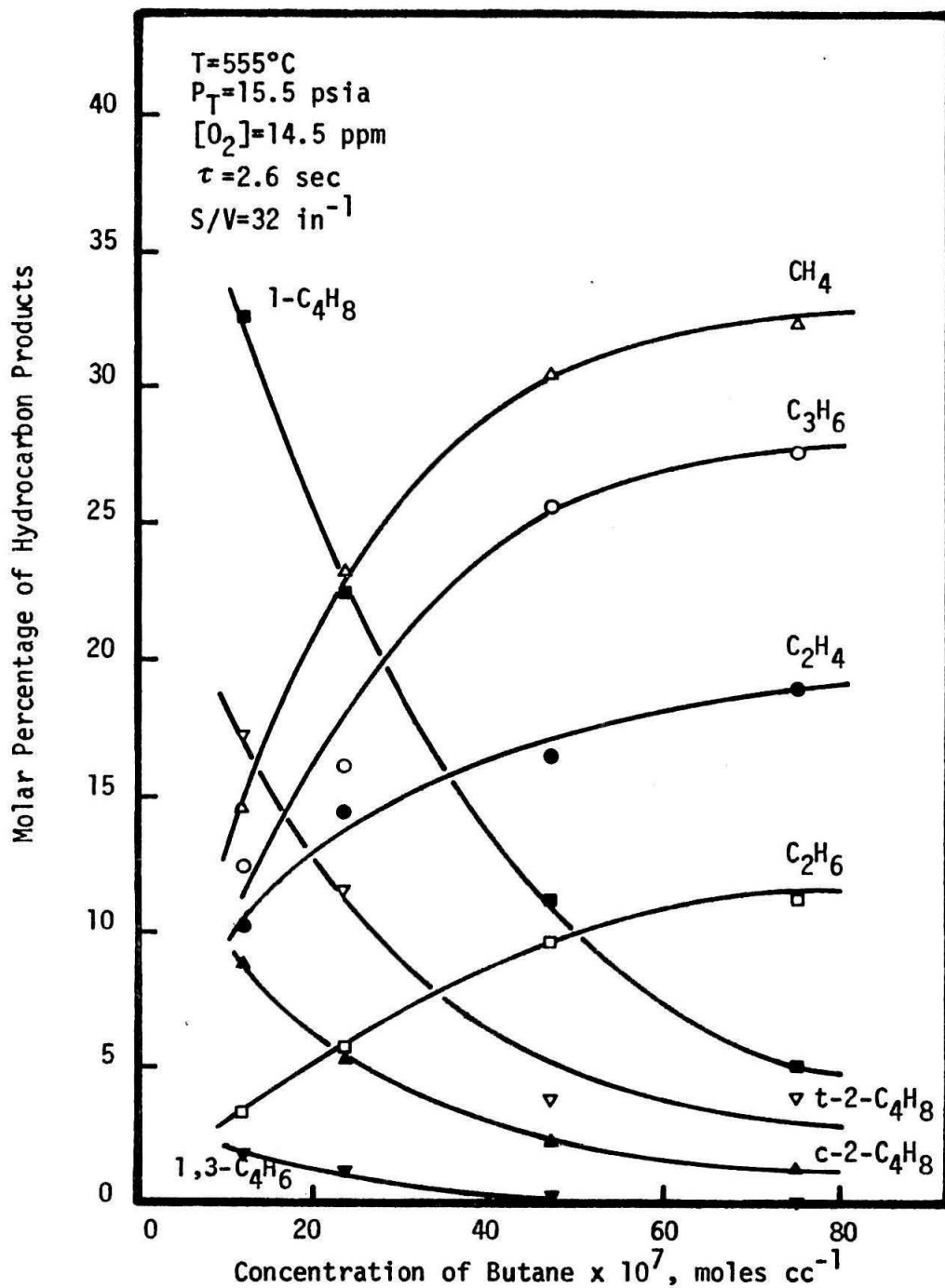


Figure 37. Distribution of the hydrocarbon products at 555°C as a function of the concentration of butane.

composition with concentration of butane was noted to be more severe at higher temperatures. These observations may be explained by consideration of the competitive pyrolysis and oxidative dehydrogenation of the butane. Butenes and water are the main products of the dehydrogenation while the lower-molecular-weight olefins and paraffins primarily result from the pyrolysis. The pyrolysis, possessing an activation energy of $65 \text{ kcal mole}^{-1}$, is much more sensitive to temperature changes than is the process of dehydrogenation, activation energy of $23 \text{ kcal mole}^{-1}$. At the higher temperatures the cracked products are formed more rapidly than the butenes. Consequently, the rapid change in product composition occurs at lower concentrations of butane. Once the oxygen has been completely consumed, incremental increases in the yield of butenes result from their role as a minor product in the pyrolysis. The selectivity of the overall reaction with respect to the butenes would be expected to increase with higher initial oxygen concentrations, lower concentrations of butane and relatively low temperatures. This is in agreement with the experimental observations.

The formation of C_4 olefins as a function of the oxygen concentration is shown in Figure 38 for 595°C . For a residence time of 2.6 sec, the average rate of formation of the C_4 olefins was approximately proportional to the square root of the initial concentration of oxygen. The data shown are for a concentration of butane of $7.15 \times 10^{-6} \text{ moles cc}^{-1}$. Similar data were obtained for other butane concentrations.

If the only products of the reaction between oxygen and butane

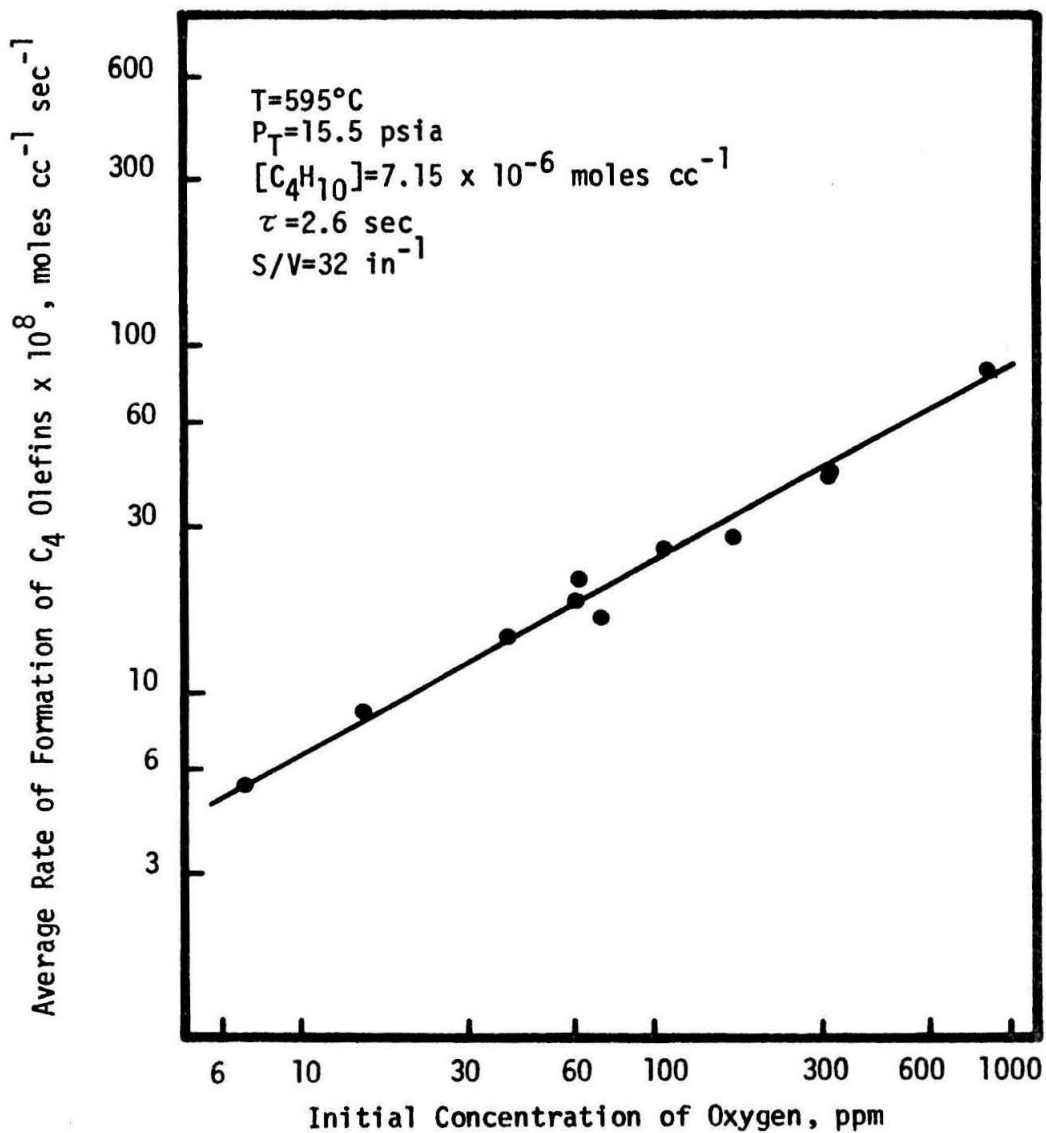


Figure 38. Formation of the C₄ olefins as a function of the initial concentration of oxygen.

are C₄ olefins and water, the molar ratio of the yield of C₄ olefins to the oxygen level of the reactants should be relatively independent of the inlet oxygen level. A plot of this ratio against the inlet oxygen level is given in Figure 39 for a concentration of butane of 7.15×10^{-6} moles cc⁻¹ and 595°C. Indeed the ratio was not independent of the oxygen concentration. At the lower concentrations of oxygen, butenes are the primary result of the interaction of oxygen with the butane. However, as the concentration of oxygen increases, alternate reactions between oxygen and the hydrocarbon become significant. These include the formation of carbon oxides as well as ethylene from the reaction with ethyl radicals.

Distribution of cracked products

Methane, ethane, ethylene and propylene are referred to as the cracked products because these are the primary products of the pyrolysis of butane in the absence of oxygen. It is interesting to compare the relative yields of the cracked products for the pyrolysis in the presence and absence of oxygen. Product distributions for the pyrolysis in the absence of oxygen were presented in Figure 19 of the preceding section. In Figure 40 are given the distributions of the cracked products as a function of the concentration of butane at 595°C for the reactants containing 14.5 and 8.0 ppm of oxygen. The curves are similar to those for the pyrolysis in the absence of oxygen with two exceptions. In the presence of oxygen, methane was formed in slightly greater yields than was propylene. As the concentration of

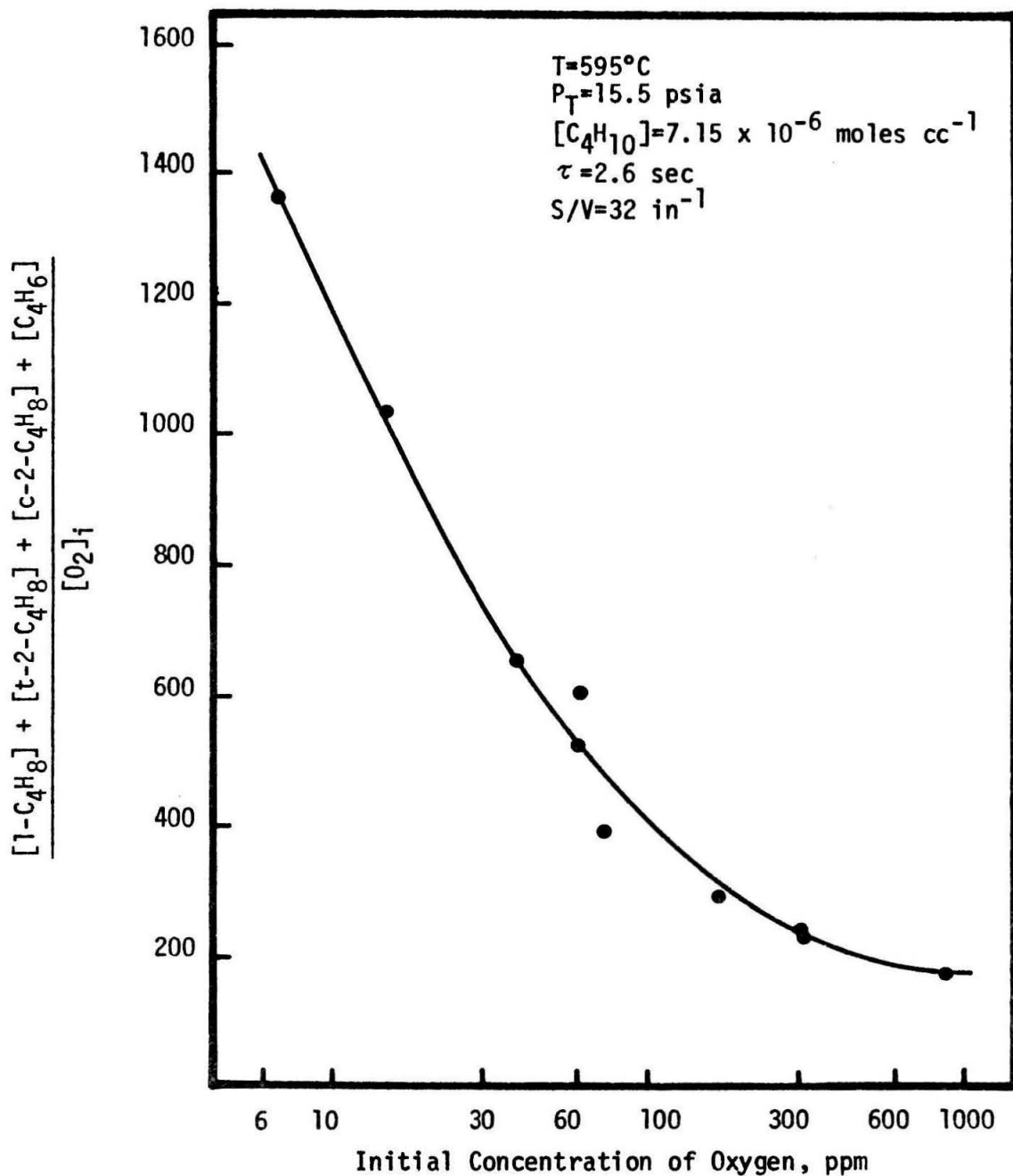


Figure 39. Ratio of the C₄ olefins to the initial concentration of oxygen as a function of the initial concentration of oxygen.

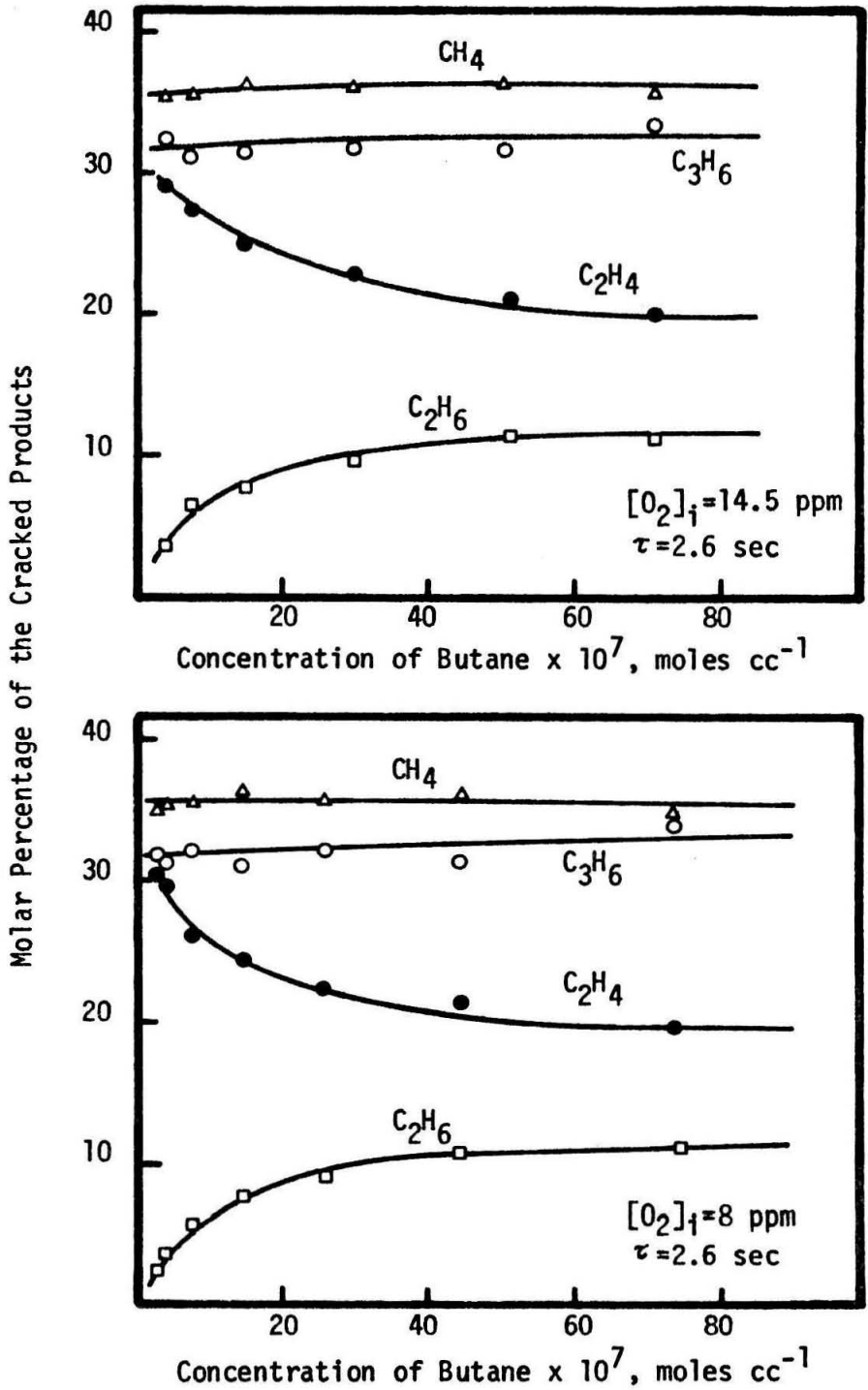


Figure 40. Distribution of the cracked products at 595°C as a function of the initial concentration of oxygen and the concentration of butane.

oxygen was increased, the relative yield of ethylene increased above that expected from the normal pyrolysis. The increase in formation of methane was also observed by Niclause, et al, (22) in studies of the pyrolysis of propane, isobutane and isopentane in the presence of oxygen.

A plot of α , the ratio of ethylene to ethane in the products, against the concentration of butane is given in Figure 41. The inlet oxygen level was recorded as 14.5 ppm. The isotherms possess the same characteristics as observed for the pyrolysis in the absence of oxygen. This includes a rapid increase in α at the lower concentrations of butane.

The distribution of the cracked products was relatively independent of the initial concentration of oxygen. Data for a concentration of butane of 7.15×10^{-6} moles cc^{-1} and 595°C are presented in Figure 42. The proportion of C_2 hydrocarbons in the cracked products was approximately that for pyrolysis in the absence of oxygen. The function β , defined as the ratio of the concentrations of ethane plus ethylene to the concentrations of methane plus propylene, varied between 0.44 and 0.51 for the pyrolysis in the presence of oxygen. In the absence of oxygen, β varied between 0.42 and 0.47. In Figure 43 are presented values of α and β as a function of the initial concentration of oxygen. The function β was independent of the initial concentration of oxygen; however, α was observed as a weak function of the concentration of oxygen. The increase of α with increasing

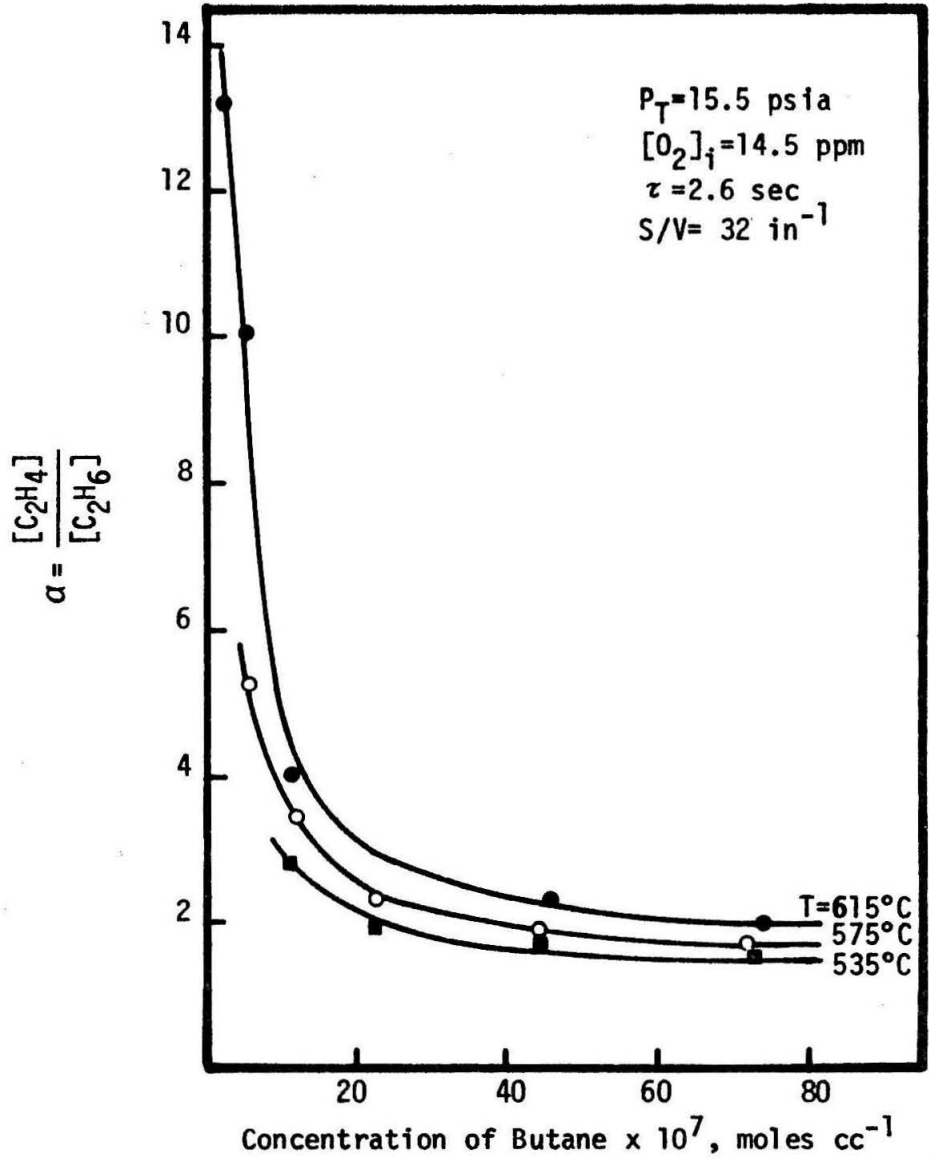


Figure 41. Variation of the function α with temperature and the concentration of butane for an initial concentration of oxygen of 14.5 ppm.

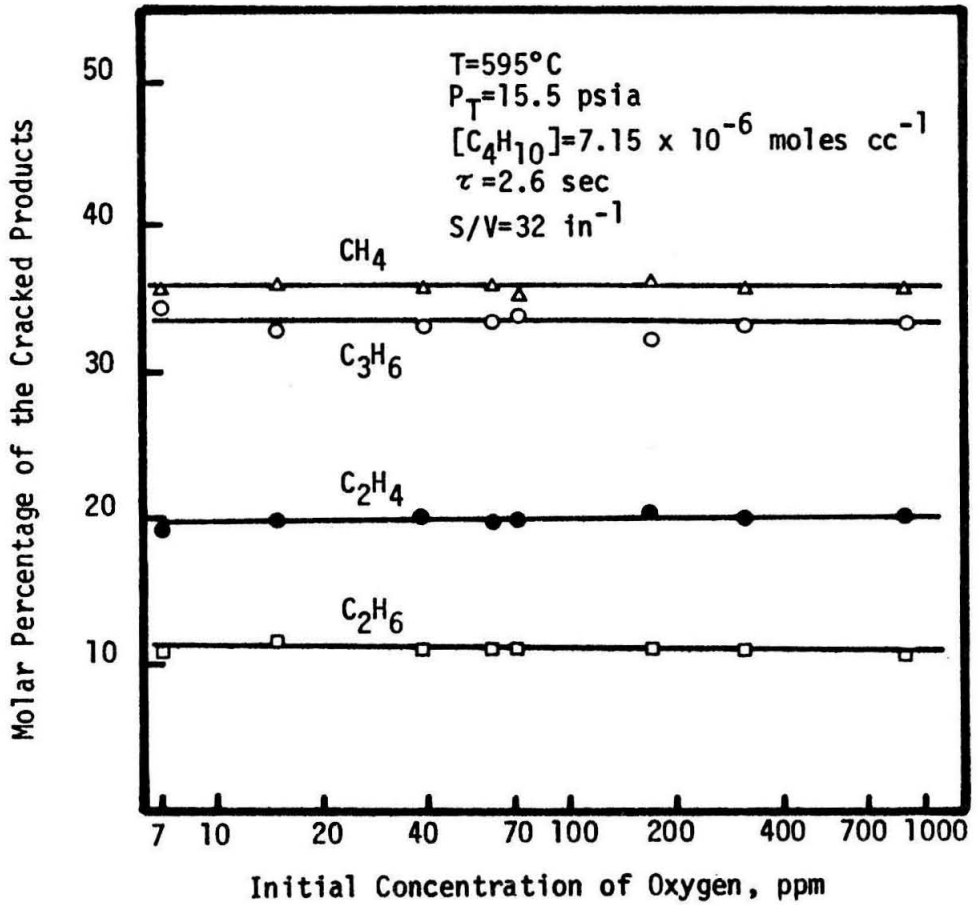


Figure 42. Distribution of the cracked products at 595°C as a function of the initial concentration of oxygen.

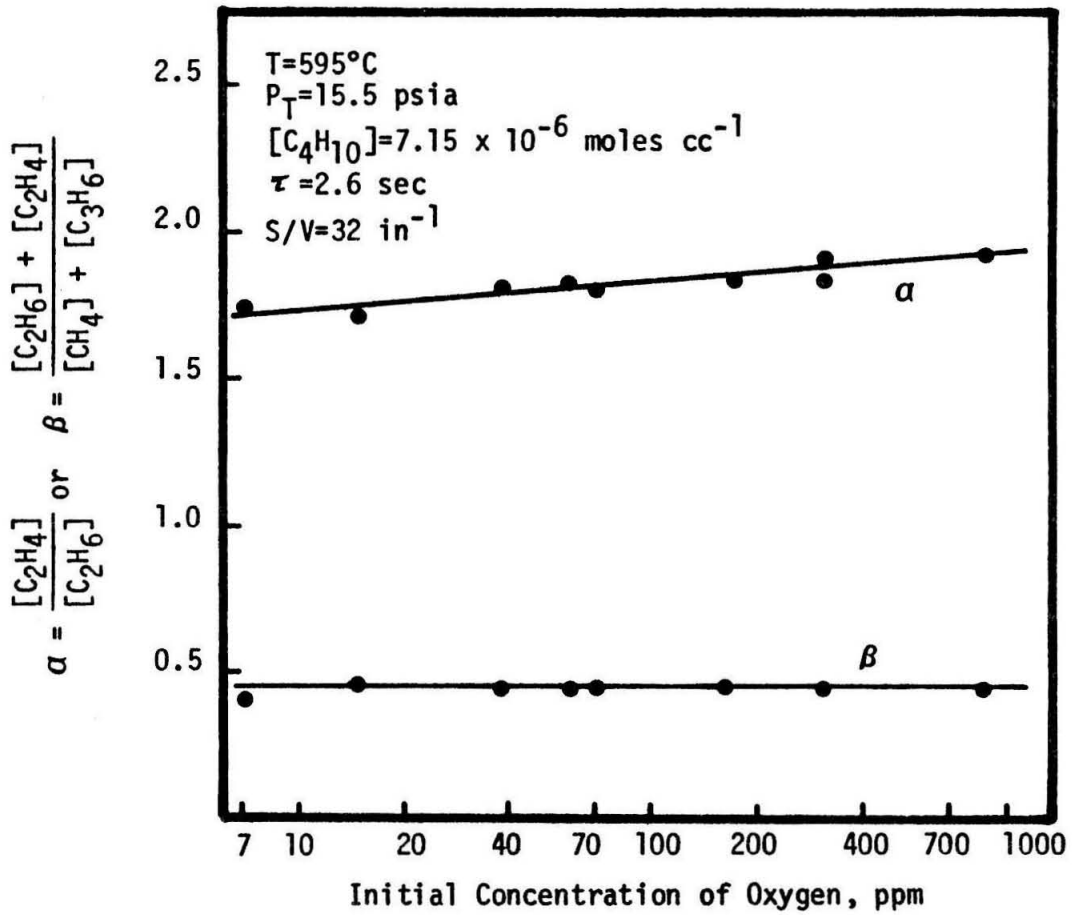
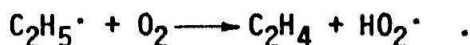


Figure 43. Variation of the functions α and β with initial concentration of oxygen at 595°C.

oxygen concentration is suggested to arise from the reaction of oxygen with the ethyl radicals as follows:



The similarities of the distributions of the cracked products for the pyrolysis in the absence or presence of oxygen is taken as evidence that these products are primarily formed by the same mechanism. That is to say, the cracked products resulting from the pyrolysis in the presence of oxygen are mainly formed from the chain reaction of alkyl radicals. The interaction of oxygen with the alkyl radicals leads to slightly higher yields of methane and ethylene in the oxidative pyrolysis.

Rate of the formation of cracked products

Assuming that the propagation steps are approximately the same for the formation of the cracked products in the absence or presence of oxygen, it is interesting to observe the effect of trace amounts of oxygen on the overall rate of formation of these products. Treating the reactor differentially, the rates of disappearance of butane based on the yields of the cracked products were calculated. These data are shown in Figure 44 as a function of the concentration of butane for an initial concentration of oxygen of 14.5 ppm. The order of the overall reaction was 1.50 ± 0.03 in agreement with the normal pyrolysis. The Arrhenius plot of Figure 45 reveals an activation energy of $81.3 \text{ kcal mole}^{-1}$, considerably greater than the $63 \text{ to } 66 \text{ kcal mole}^{-1}$ observed

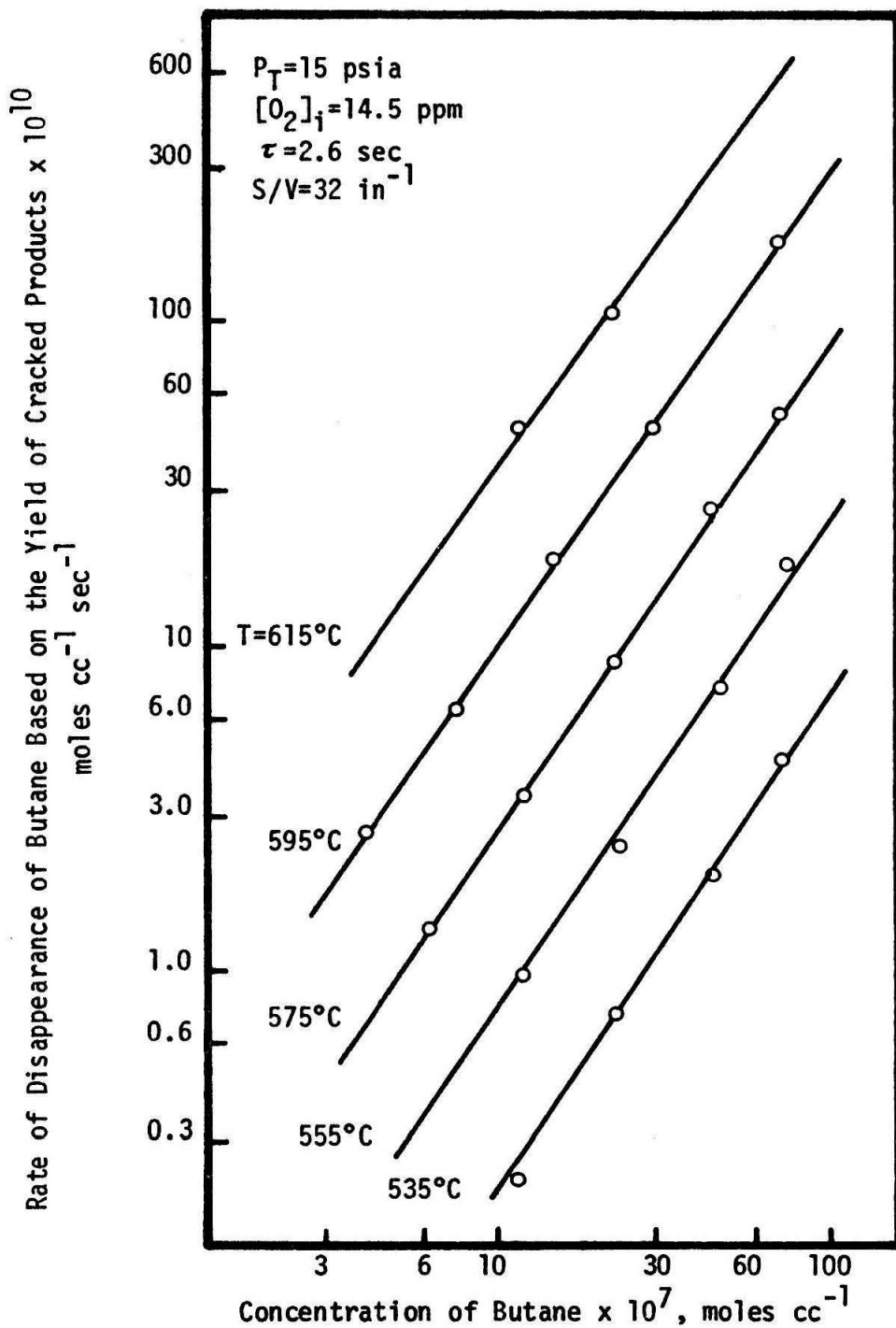


Figure 44. Rate of disappearance of butane base on the yield of cracked products as a function of temperature and the concentration of butane.

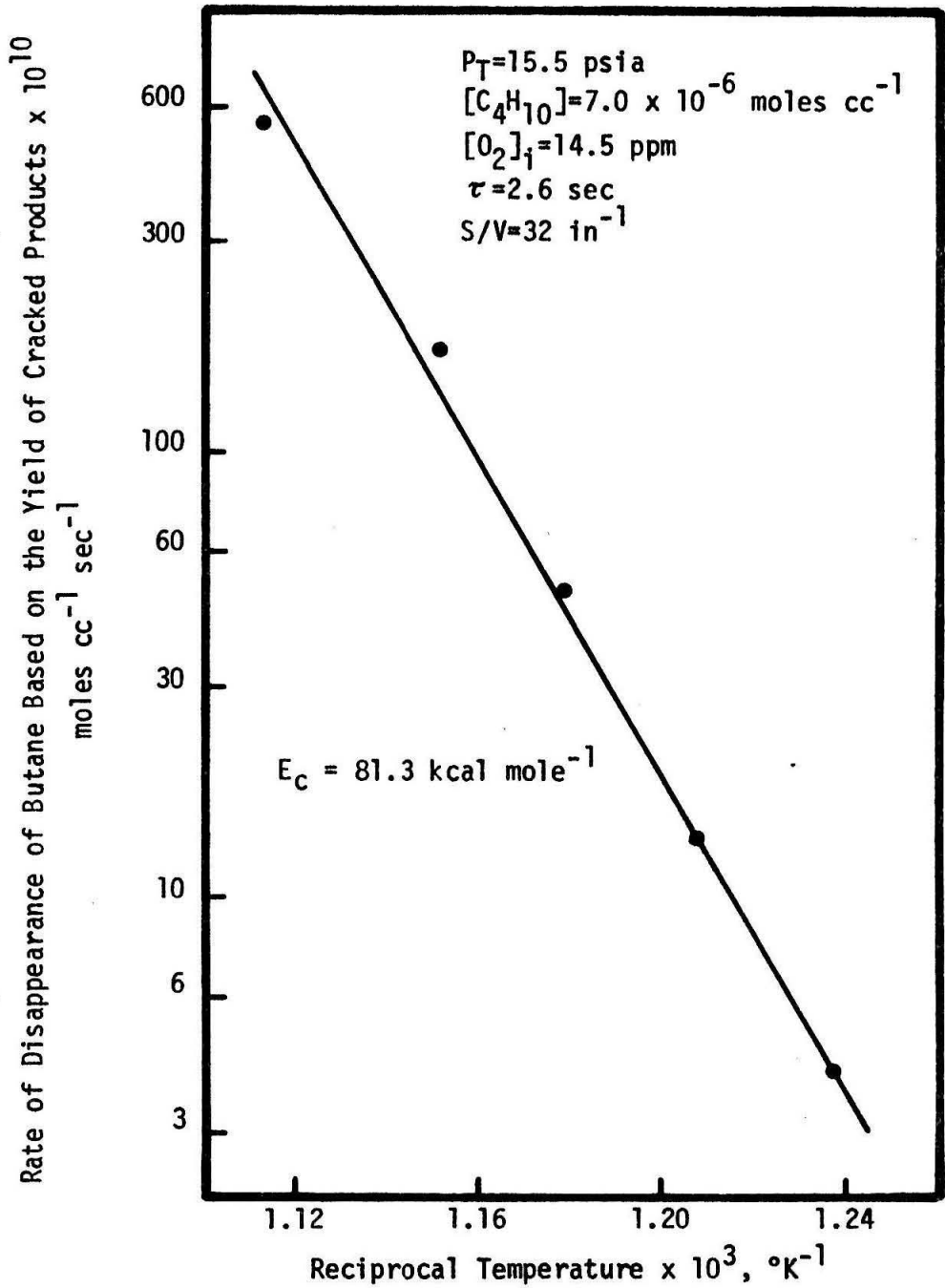


Figure 45. Arrhenius plot for the rate of disappearance of butane based on the yield of cracked products in the presence of 14.5 ppm of oxygen.

in the absence of oxygen. The net result is a reduction in the rate of formation of the cracked products in the presence of oxygen. The dominant initiation and termination steps influence the overall order of the reaction and the apparent activation energy. The presence of oxygen may influence both the initiation and termination steps.

Chain initiation is possible by the reaction of oxygen and butane to form butyl and hydroperoxide radicals. This process is 30 to 35 kcal mole⁻¹ more favorable than the homolytic decomposition of butane. However, at the high temperatures of pyrolysis and with quantities of oxygen in the ppm range, the homolytic decomposition of butane is thought to predominate.

The reaction of oxygen with an alkyl radical represents termination of chains which may lead to the cracked products. A reduction in the number of chain propagating radicals results and consequently a lower overall rate of reaction. Destruction of oxygenated free radicals on the surface of the reactor may also contribute to the reduction in the overall rate of the decomposition of butane.

Inhibition or acceleration

Niclause, et al, (22) found that the pyrolysis of propane, isobutane or isopentane in the presence of oxygen was drastically effected by the nature and extent of the surface of the reactor. Oxygen was observed to inhibit or accelerate the rate of decomposition of the hydrocarbon depending on the conditions of the reactor. In pyrex reactors

of relatively low surface-to-volume ratio ($S/V = 2.0 \text{ in}^{-1}$), the presence of oxygen accelerated the reaction whereas at higher surface-to-volume ratios inhibition was noted. Treatment of the surface of the reactor with PbO was also shown to effectively inhibit the reaction in the presence of oxygen.

As gold tubing of inside diameters greater than 0.125 inch was not available commercially, it was impractical to study the reaction in gold reactors of $S/V < 32 \text{ in}^{-1}$. For a gold reactor of $S/V=32 \text{ in}^{-1}$, the initial rate of decomposition of butane in the presence of oxygen was depressed in agreement with the work of Niclause. Data are shown in Figures 46 and 47 for temperatures of 595°C and 535°C respectively. At the lower temperature, the conversion of butane was approximately 0.03 per cent for a residence time of 2.6 sec. At such low conversions, measurement of the yields of products was difficult. Consequently, only a few points were taken in this region.

In each case, a significant depression of the reaction was noted for traces of oxygen less than 7 ppm. Depression of the pyrolysis in a reactor which had been exposed to oxygen was discussed earlier. By comparison with the pyrolysis in presence of 0 to 10 ppm of oxygen, it is concluded that the oxygen is probably consumed in the removal or partial removal of a carbonaceous layer that had been deposited on the wall of the reactor during pyrolysis.

It is commonly assumed (37, 66) that peroxy radicals, which may be formed by the direct combination of alkyl radicals and oxygen, are

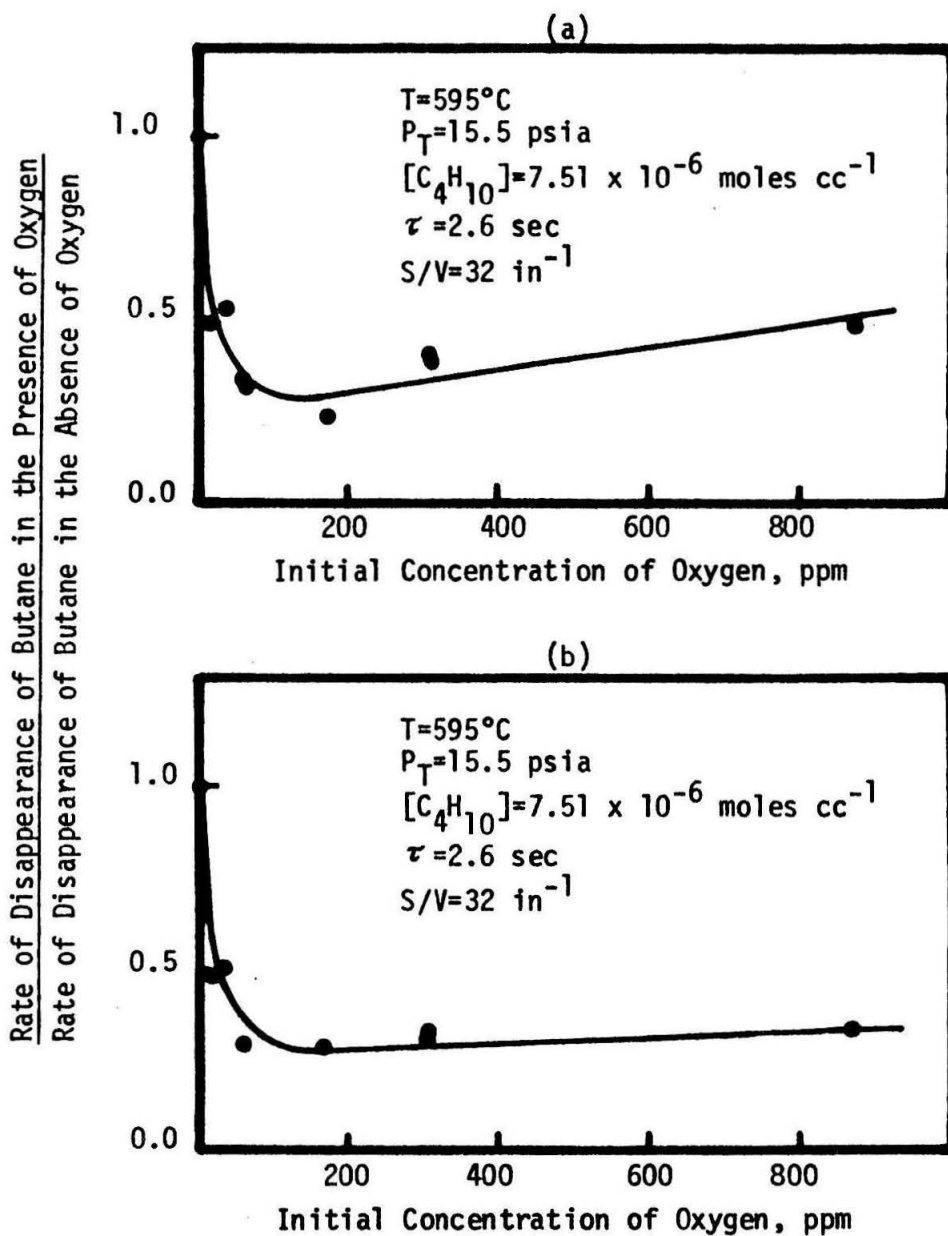


Figure 46. Rate of decomposition of butane in the presence of oxygen relative to that in the absence of oxygen at 595°; (a) decomposition based on all hydrocarbon products and (b) decomposition based on only the cracked products.

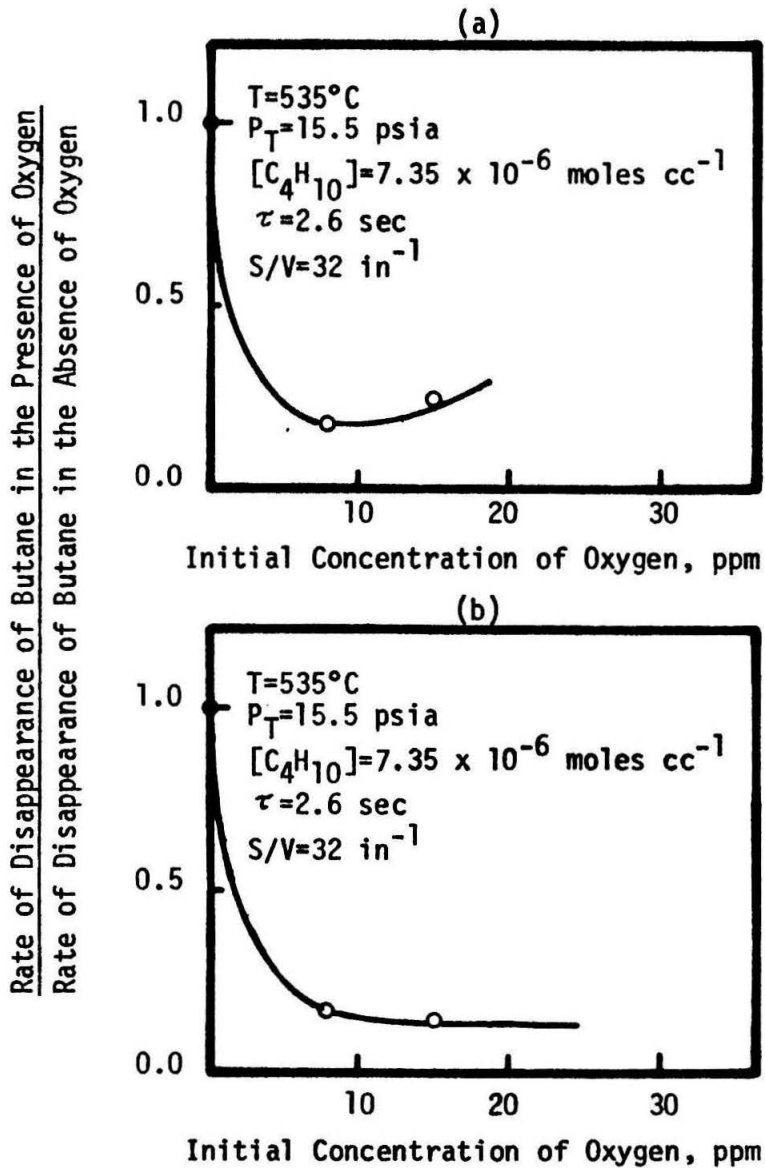


Figure 47. Relative rate of decomposition of butane in the presence of oxygen to that in the absence of oxygen at 535°C ; (a) decomposition based on all hydrocarbon products and (b) decomposition based on only the cracked products.

more easily destroyed on the wall of a reactor than are alkyl radicals. This being the case, a reduction in the rate of decomposition of butane in the presence of oxygen would be expected in reactors of relatively high surface-to-volume ratio. As noted by Purnell and Quinn (60), the inhibition processes of the pyrolyses of hydrocarbons may be extremely complex and depend on the physical conditions as well as the identity of the reactants.

Oxidative Dehydrogenation of Butane

The reaction between oxygen and butane in the temperature range 470 to 595°C was examined in a gold microreactor, $S/V = 32 \text{ in}^{-1}$. The surface of the reactor had been acid-stabilized as discussed in the previous sections. Initial concentrations of butane were varied from 0.6×10^{-6} to 7.5×10^{-6} moles cc^{-1} while the oxygen content of the feed was varied from 400 ppm to 1 per cent by volume.

In all runs, the conversion of butane was less than 1 per cent; the conversion of oxygen varied from 5 to 100 per cent. The total pressure was maintained between 14.8 and 16.5 psia in all tests.

Distribution of products

The primary products of the initial reaction were 1-butene, t-2-butene, c-2-butene and water. The formation of carbon dioxide increased rapidly with increasing contact times in the reactor. Ethylene, 1,3-butadiene, propylene, methane and ethane were also noted in the products. Carbon monoxide, which could be detected in concentrations as low as 200 ppm, was not found in the products.

The formation of water was calculated from a mass balance on oxygen, assuming that only water and carbon dioxide were formed from the oxygen. All other products were measured. Water could be measured chromatographically; however, for initial concentrations of oxygen of 1 per cent, the water analysis erratically yielded from 40 to 80 per cent of the amount predicted by a mass balance. For initial concentrations of oxygen of 400 ppm, the chromatograms indicated more water

than would result from 100 per cent conversion of the oxygen. It was concluded that water was condensing in the lines leading from the reactor. Evidence for this was the collection of water in the manostat during oxidation runs.

The formation of products as a function of space time are given in Figure 48 for 515°C, an initial concentration of oxygen of 9810 ppm and a concentration of butane of 2.3×10^{-6} moles cc^{-1} . These data are representative of all the runs. Of interest was the non-linear production of the C_4 unsaturates with space time. In large part, this was a result of the decreasing concentration of oxygen as the space time increased. However, the possibility of further reactions of the butenes is suggested. The formations of butenes were not observed to exhibit maxima with increasing space time as were noted by Barker and Corcoran (1). The maxima would be considered evidence of secondary reactions of the butenes.

The molar distribution of the products are shown in Figures 49, 50 and 51 as a function of space time and initial concentration of oxygen. In these figures, the percentage of water in the products is found by subtracting the total percentage of products shown from 100. The following conclusions may be drawn from a comparison of the three figures:

1. The relative formations of water and carbon dioxide increased rapidly with increasing space time and increasing concentrations of oxygen.

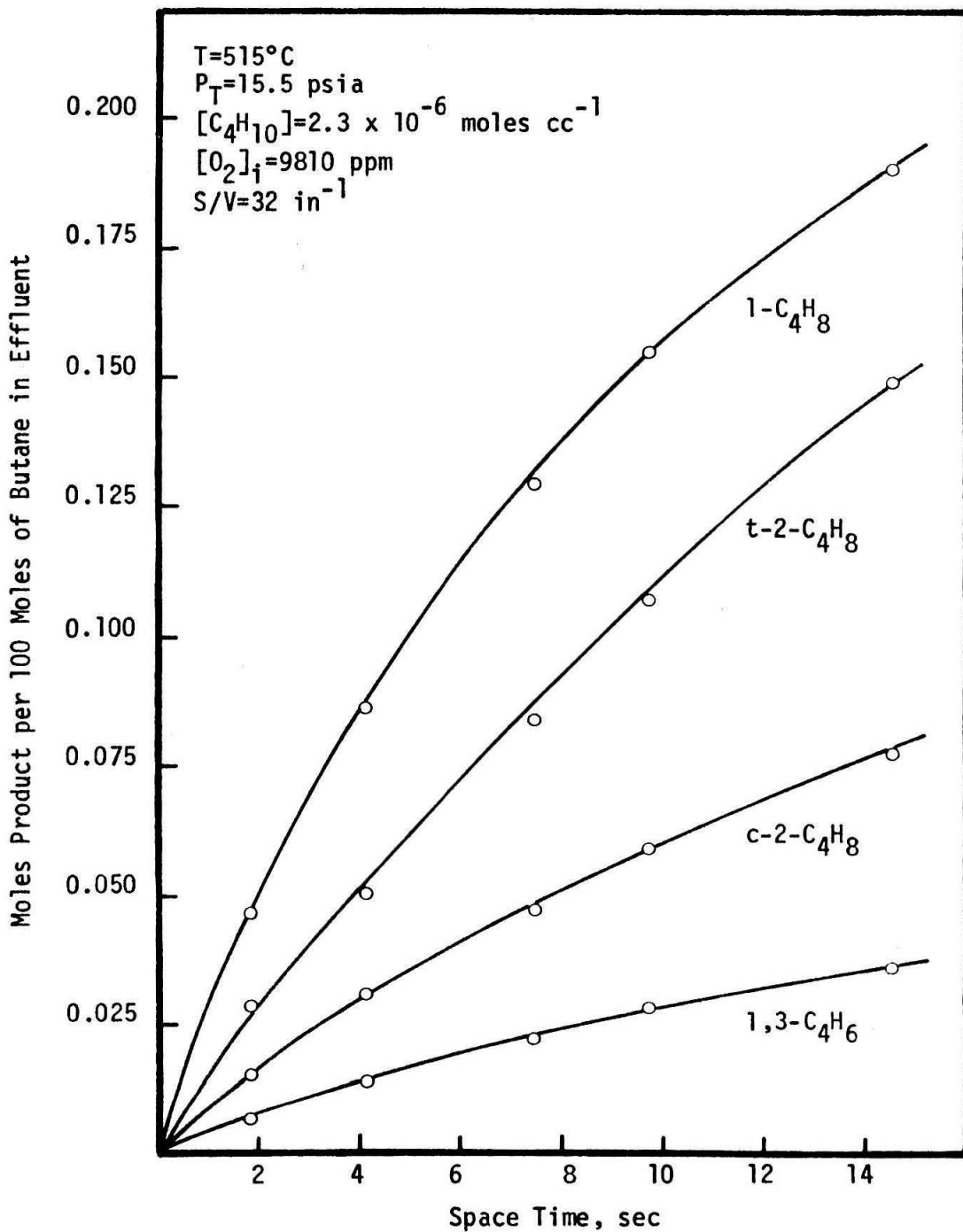


Figure 48. Formation of the products of the oxidative dehydrogenation of butane as a function of space time.

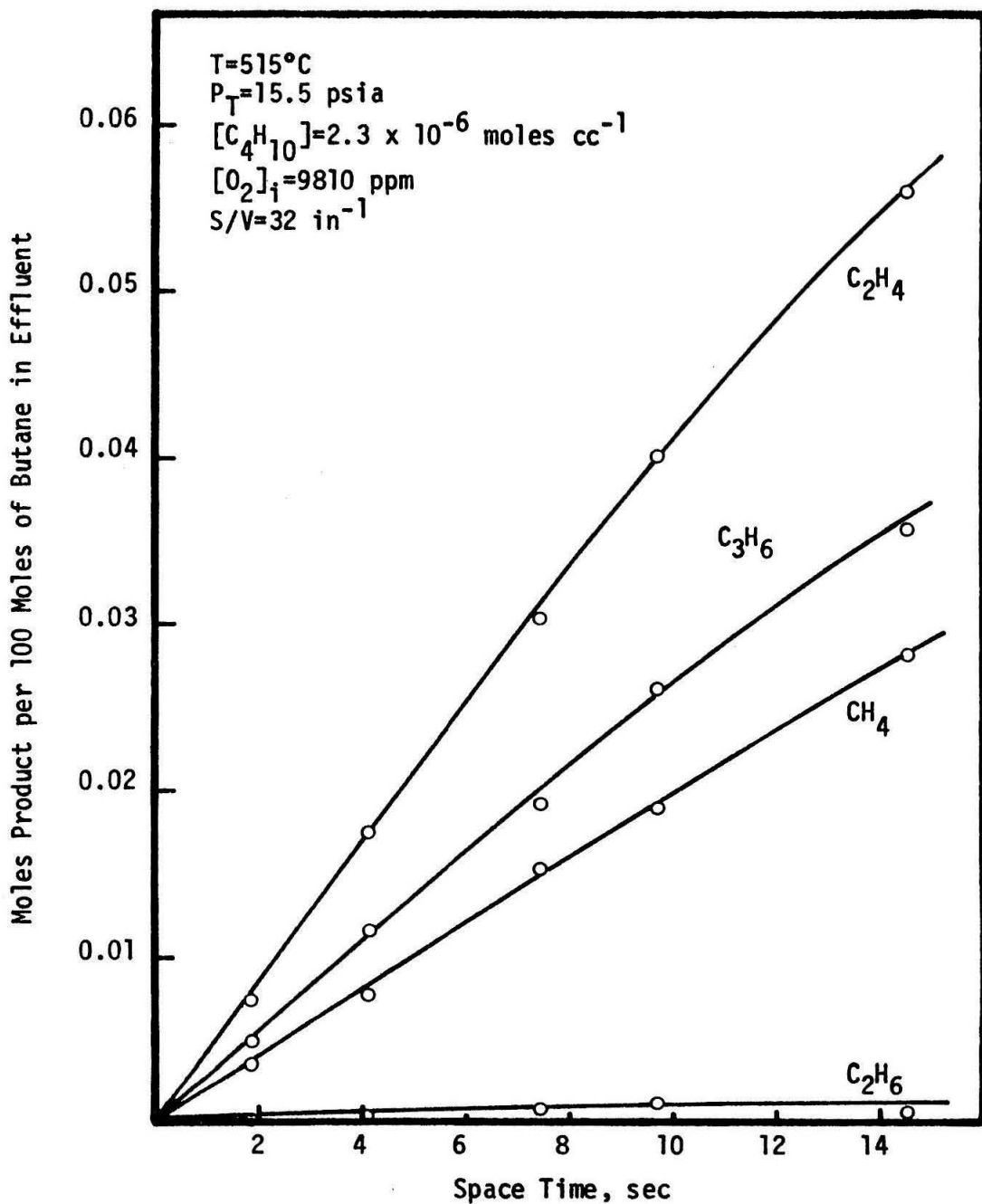


Figure 48, cont'd. Formation of the products of the oxidative dehydrogenation of butane as a function of space time.

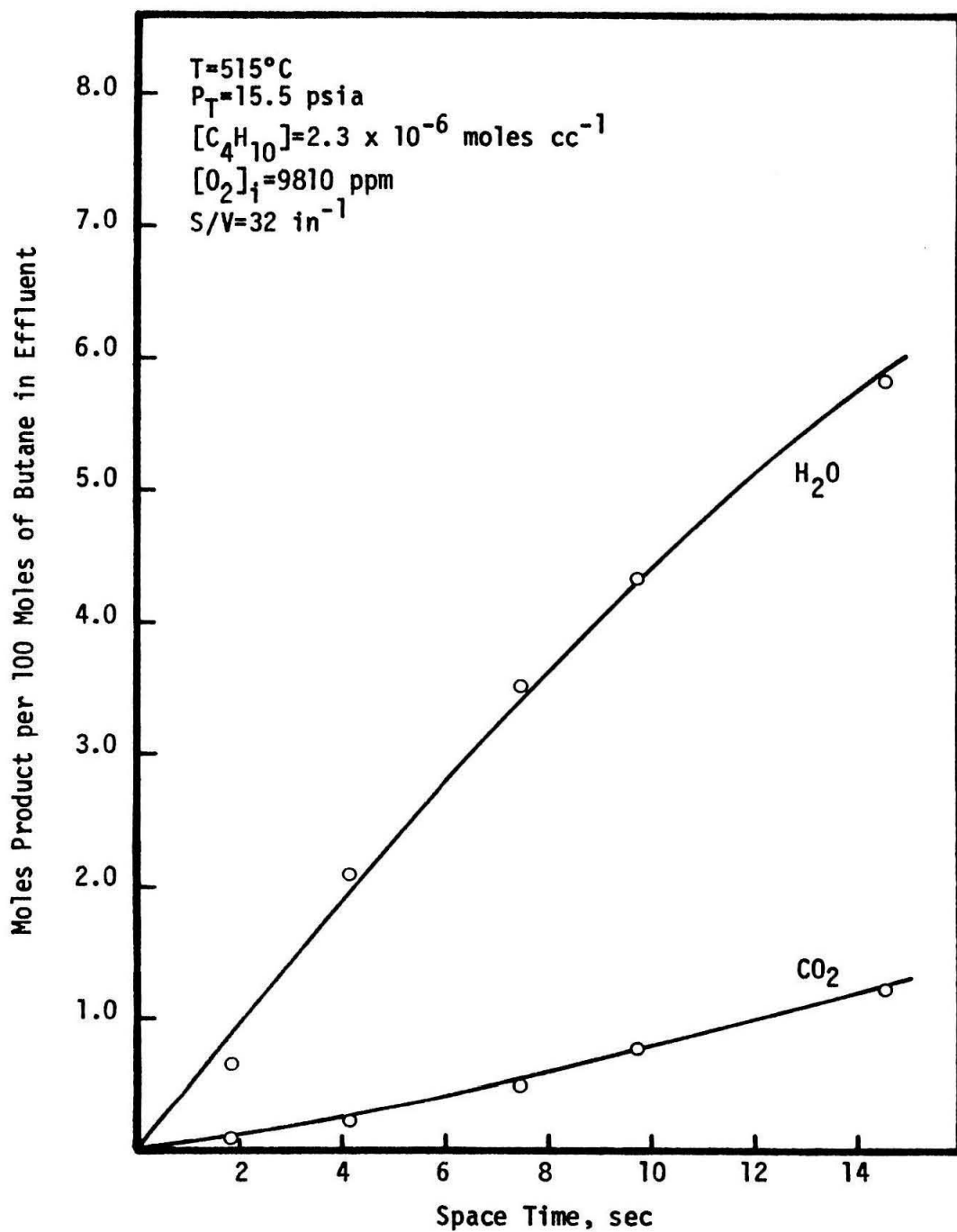


Figure 48, cont'd. Formation of the products of the oxidative dehydrogenation of butane as a function of space time.

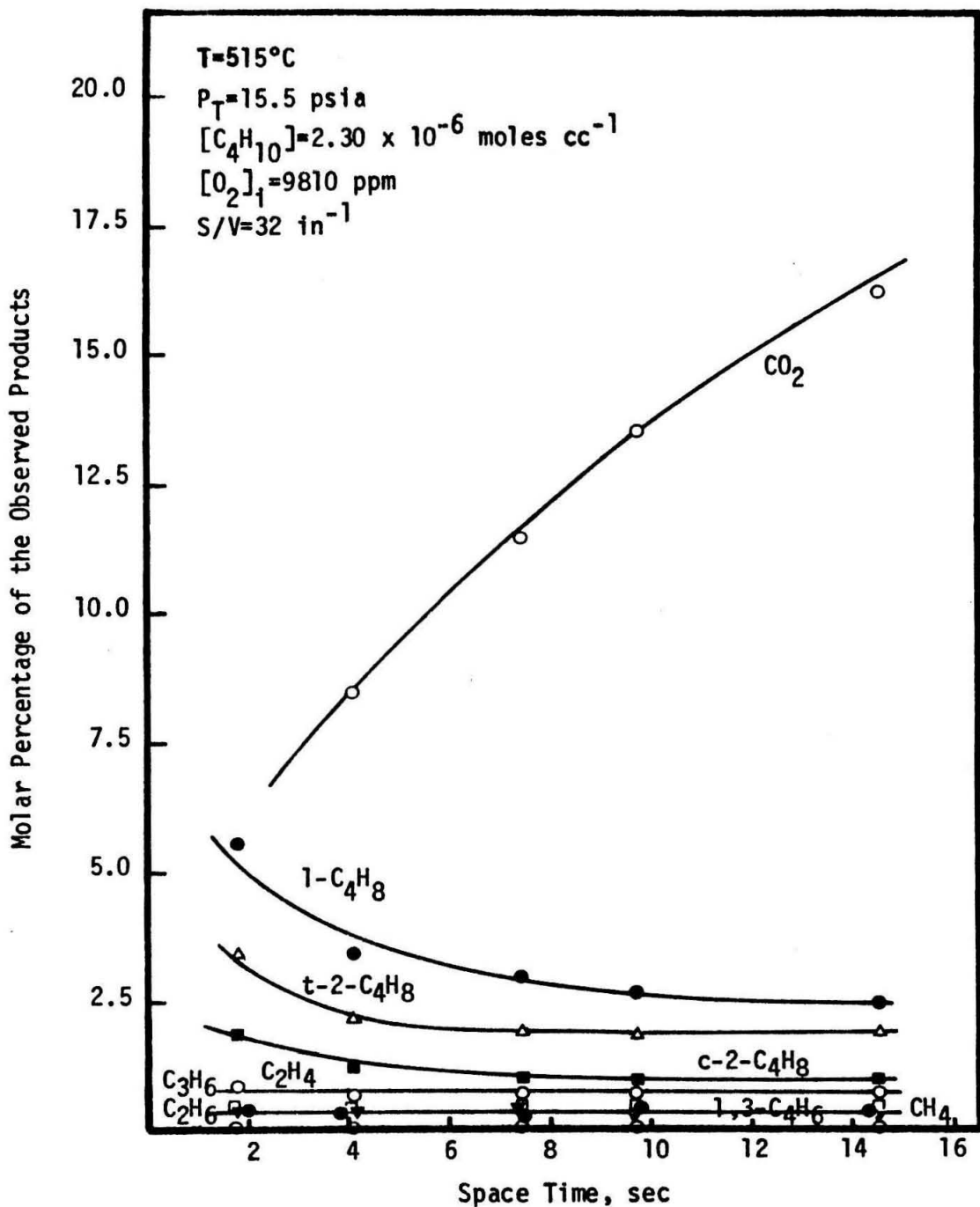


Figure 49. Distribution of observed products as a function of space time for an initial concentration of oxygen of 9810 ppm.

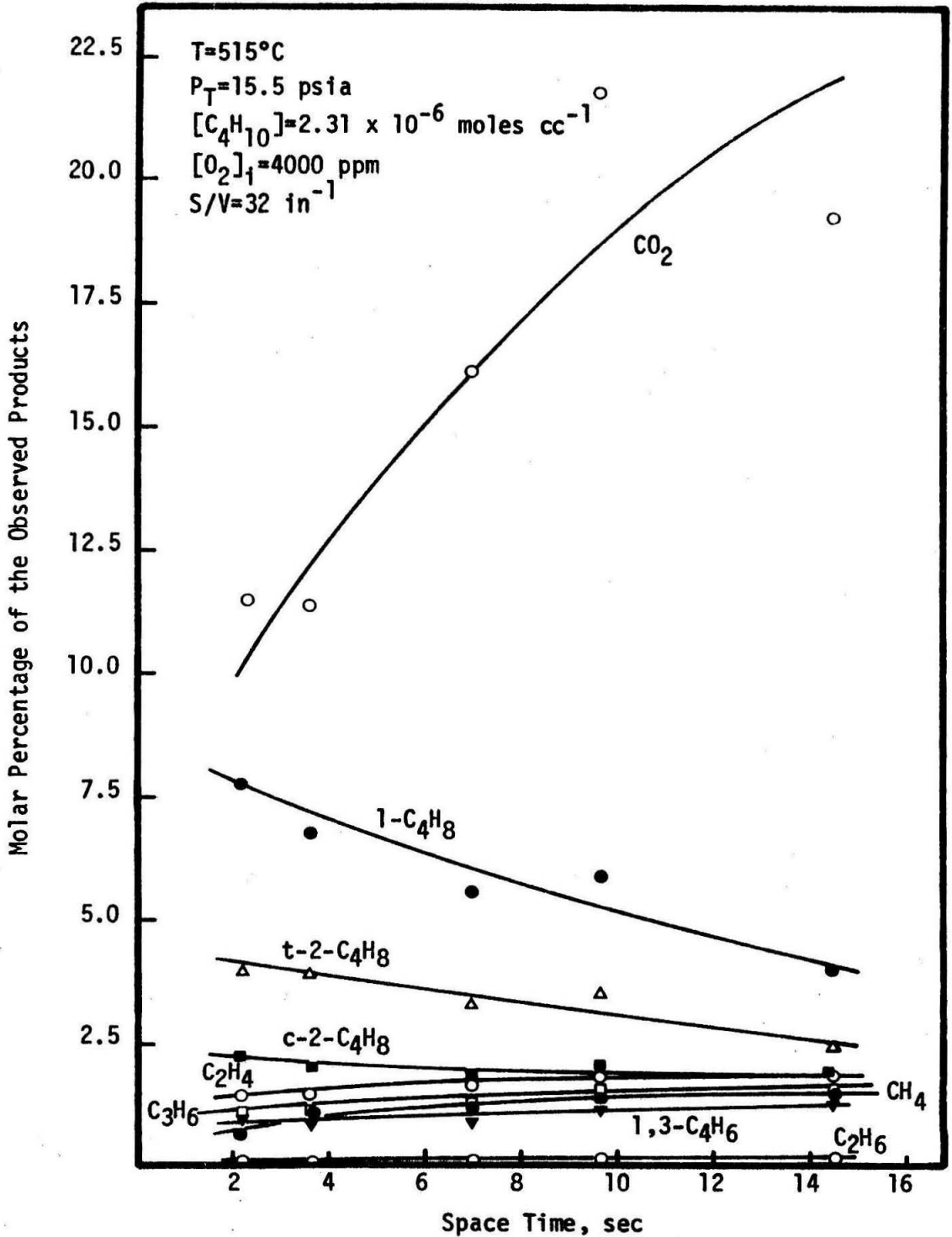


Figure 50. Distribution of observed products as a function of space time for an initial concentration of oxygen of 4000 ppm.

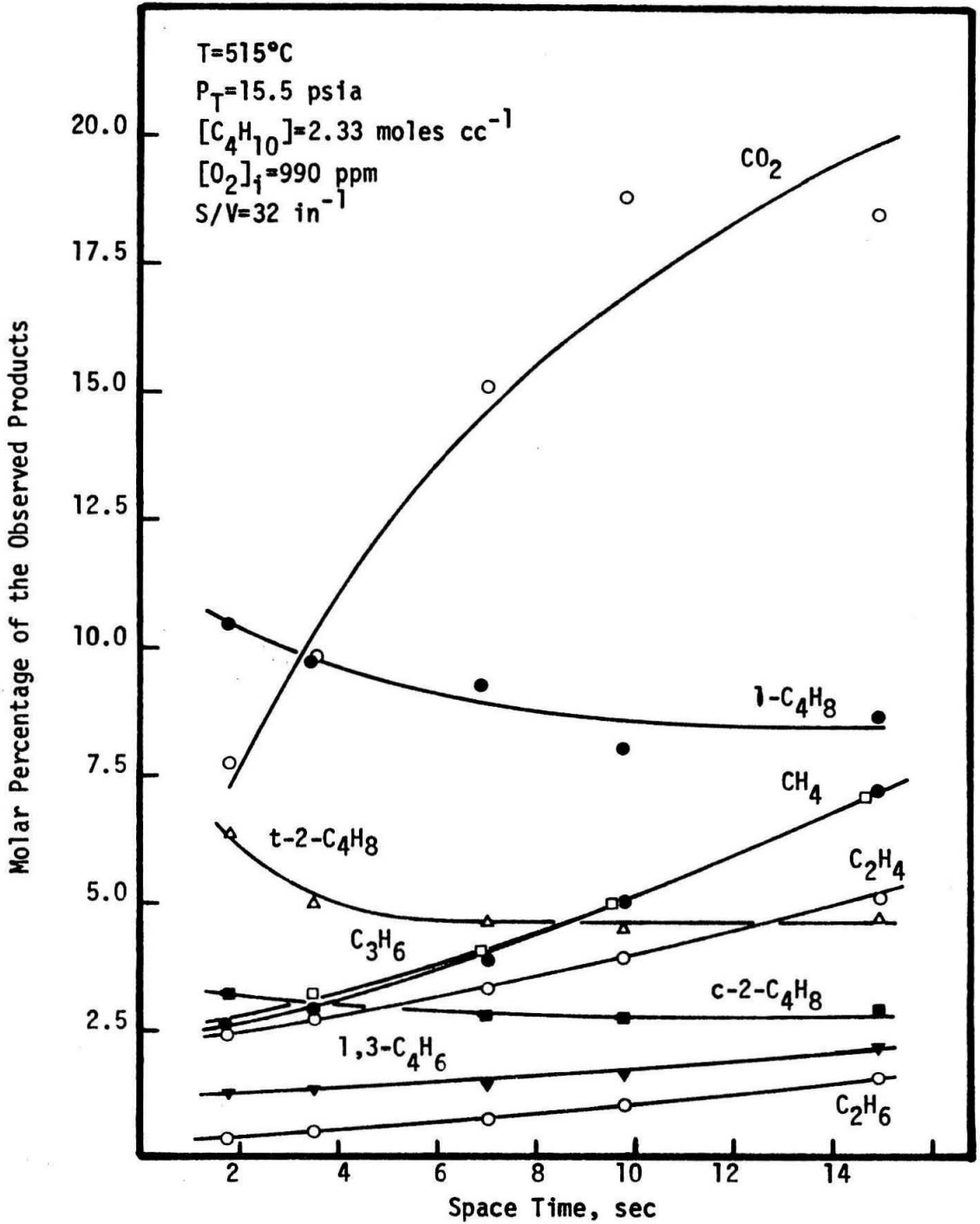


Figure 51. Distribution of observed products as a function of space time for an initial concentration of oxygen of 990 ppm.

2. The fractions of butenes in the products decreased with increasing space time.

3. The relative formations of methane, ethane, ethylene and propylene increased with increasing contact time; however, the fraction of these compounds in the products decreased with increasing concentrations of oxygen.

These trends are consistent with the concept that the product distribution is primarily determined by the reactions of the alkyl radicals. On the one hand, decomposition of the butyl radicals leads to formation of the cracked products as in the pyrolysis. On the other hand, reaction of butyl radicals with oxygen result in the formation of C_4 olefins.

In order to study the decomposition of the butane into various products, it is more instructive to examine the carbon selectivity of the products. The carbon selectivity of a given product is defined as its share of the total carbon appearing in the products. In Figures 52 through 60, the carbon selectivities of the various products are given as functions of temperature, space time and concentrations of oxygen and butane.

In Figures 52, 53, 54 and 55 the selectivities are shown as a function of space time for various initial concentrations of oxygen. In each figure, the selectivities for the butenes decreased as the space time increased. The selectivity for carbon dioxide increased rapidly with space time to a maximum limit. The maximum corresponded

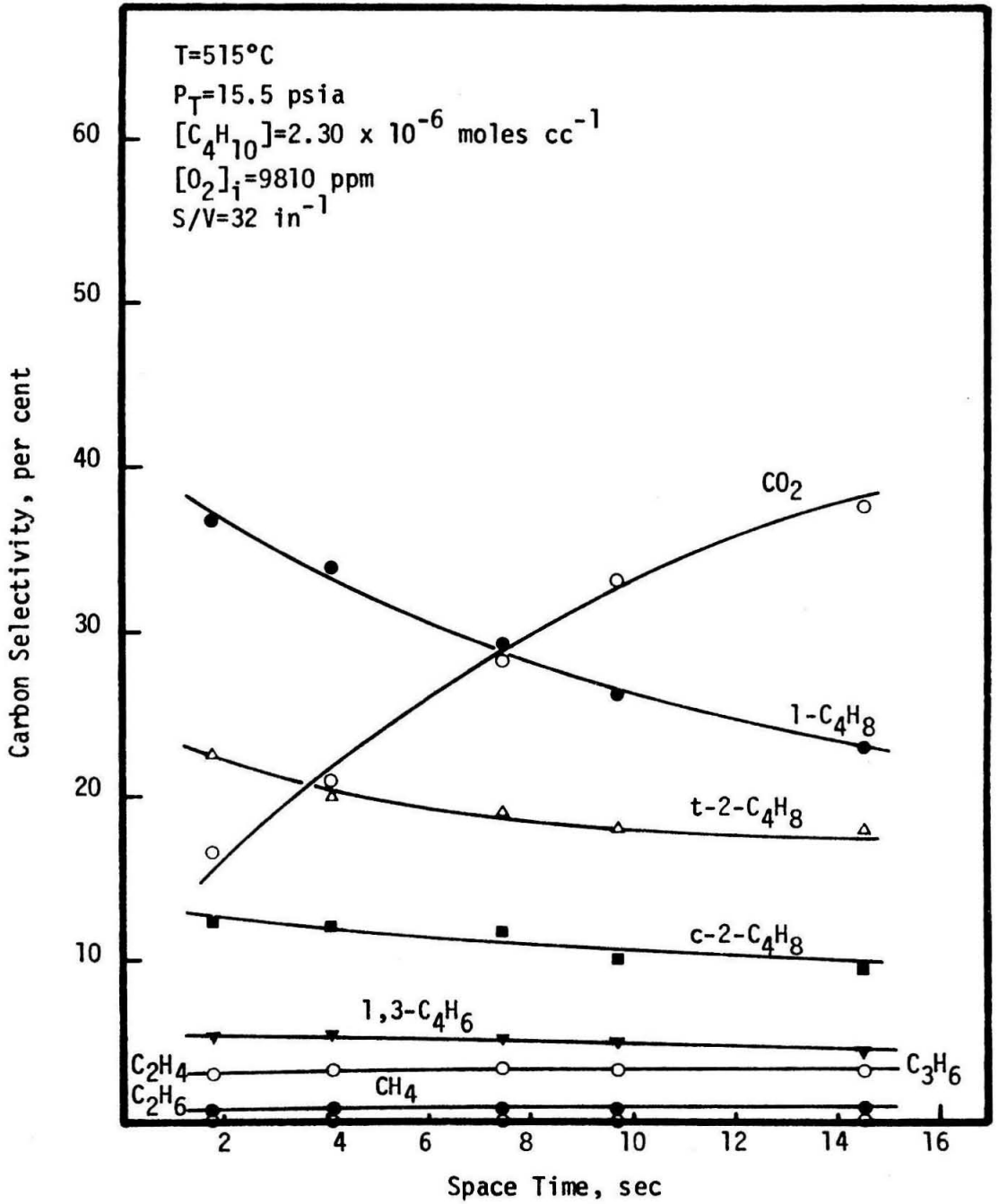


Figure 52. Carbon selectivity as a function of space time for T=515°C, [C₄H₁₀]=2.30 x 10⁻⁶ moles cc⁻¹ and [O₂]_i=9810 ppm.

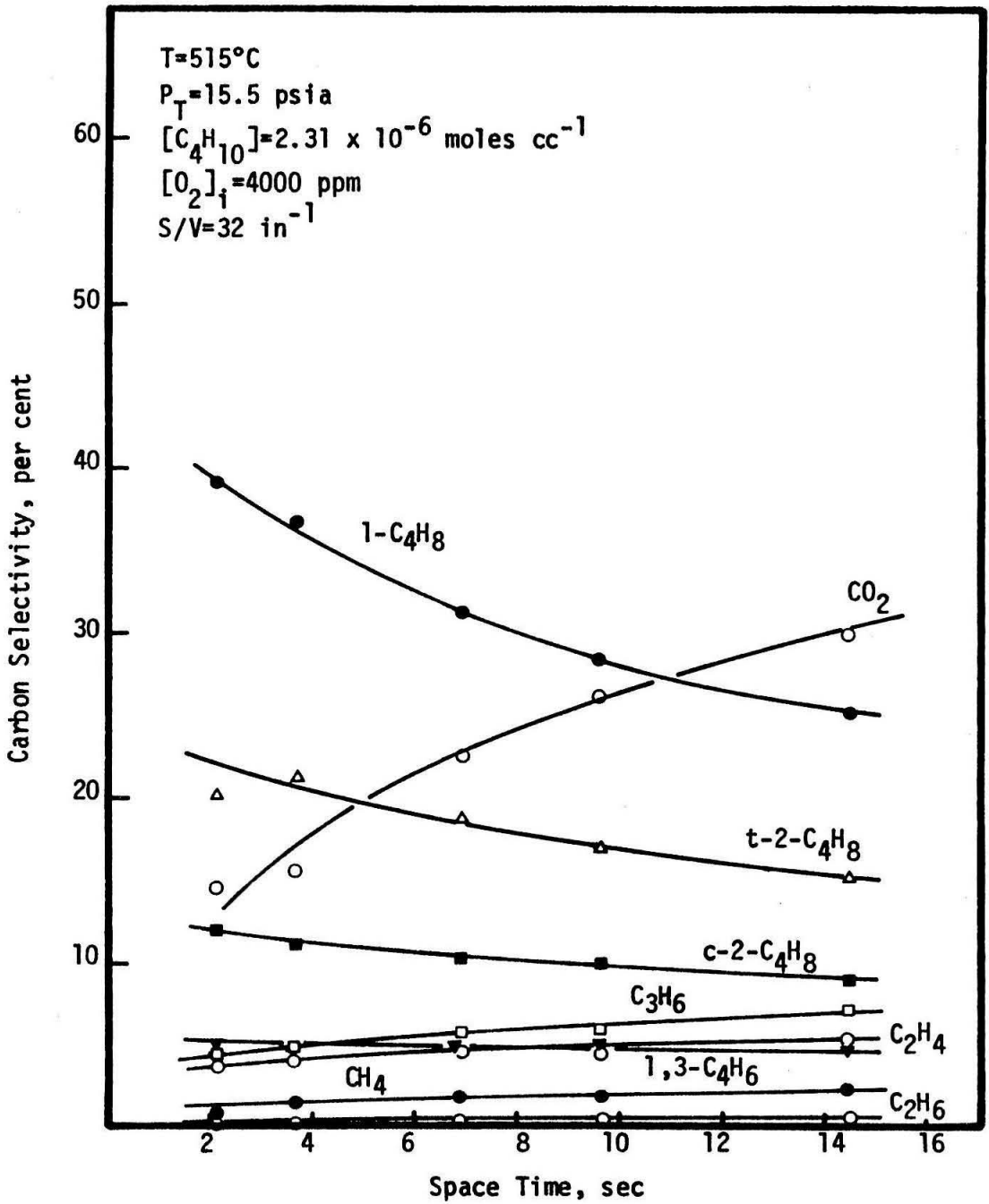


Figure 53. Carbon selectivity as a function of space time for $T=515^{\circ}\text{C}$, $[\text{C}_4\text{H}_{10}]=2.31 \times 10^{-6}\text{ moles cc}^{-1}$ and $[\text{O}_2]_i=4000\text{ ppm}$.

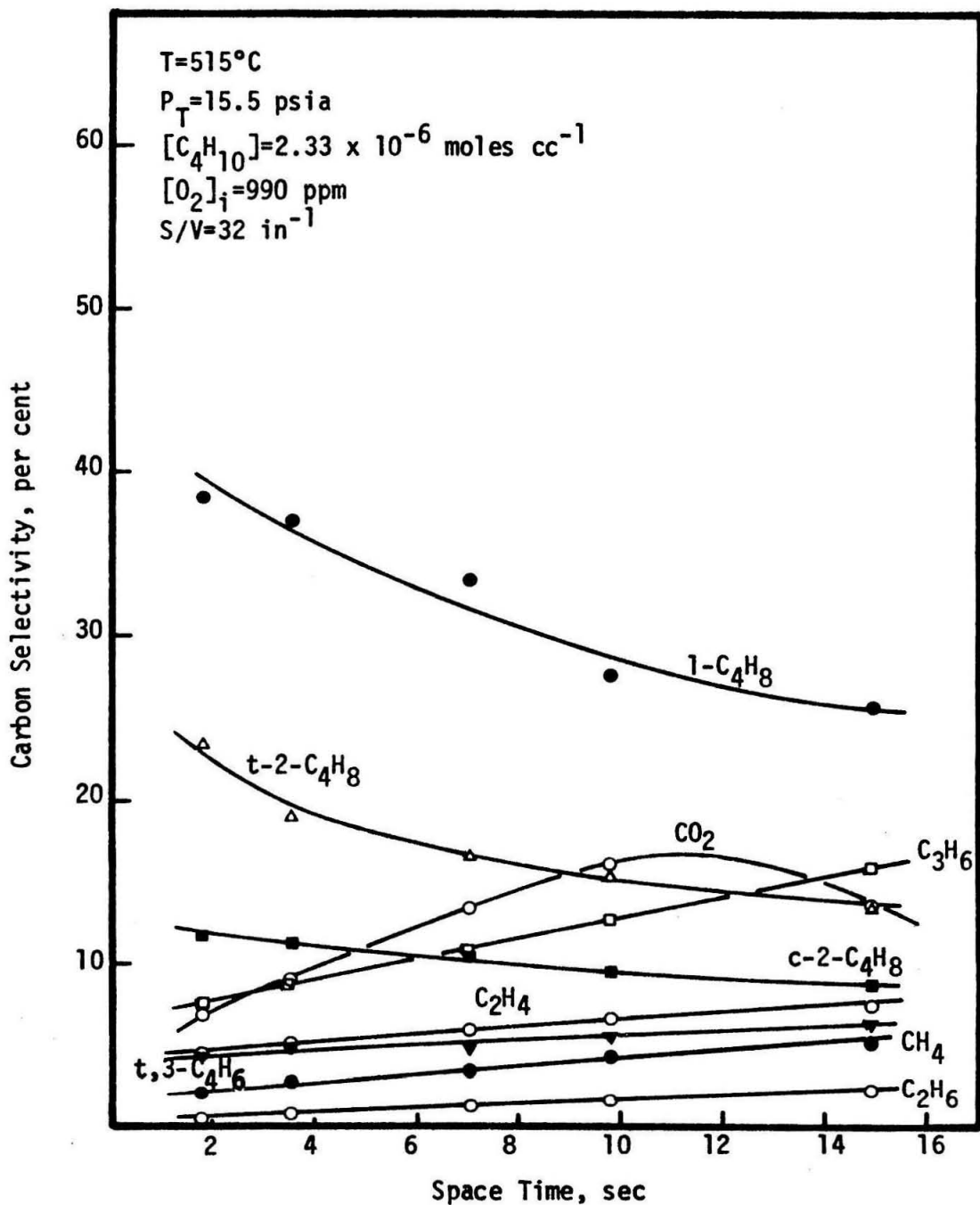


Figure 54. Carbon selectivity as a function of space time for $T=515^{\circ}\text{C}$, $[\text{C}_4\text{H}_{10}]=2.33 \times 10^{-6} \text{ moles cc}^{-1}$ and $[\text{O}_2]_i=990 \text{ ppm}$.

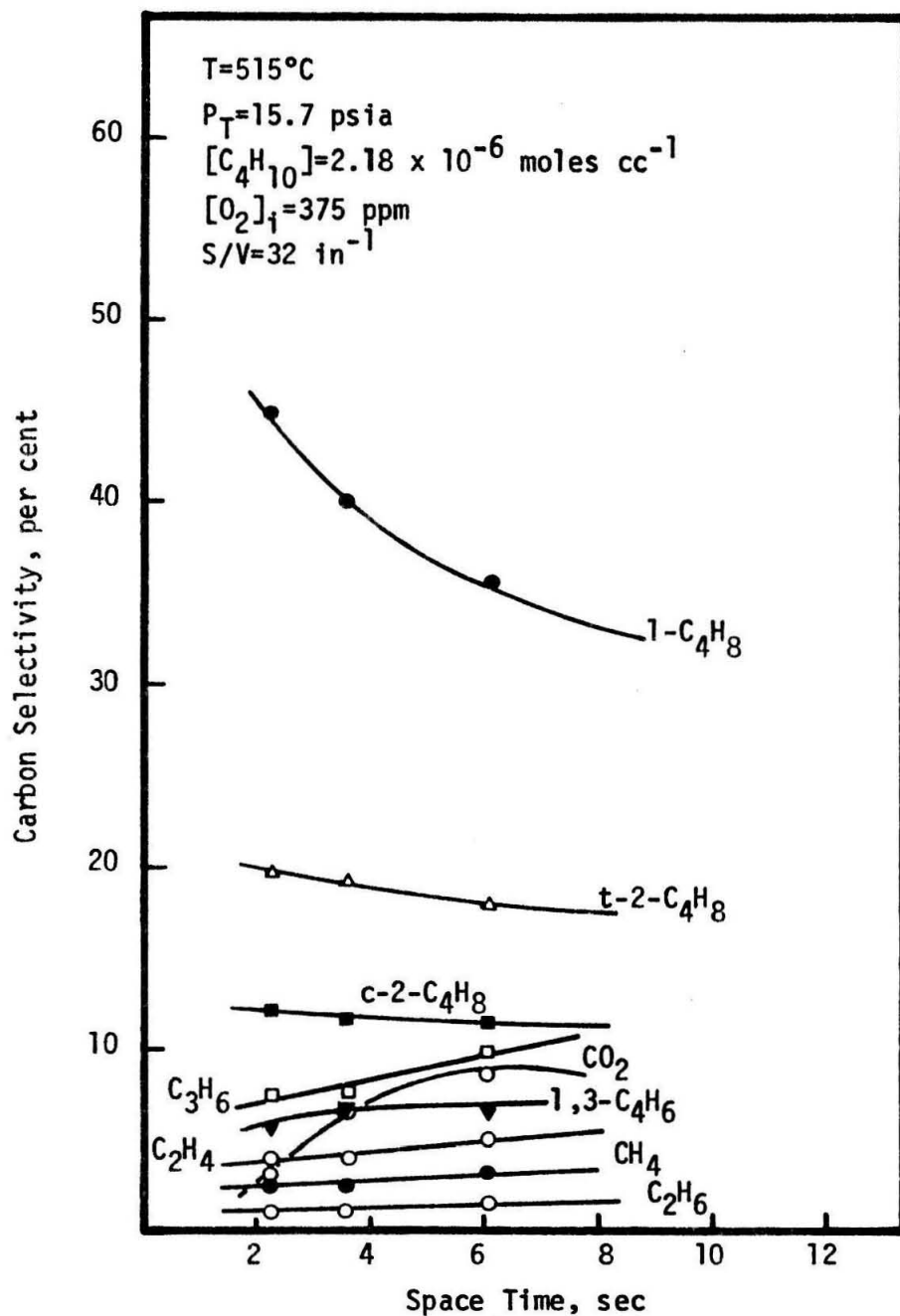


Figure 55. Carbon selectivity as a function of space time for $T=515^{\circ}\text{C}$, $[\text{C}_4\text{H}_{10}]=2.18 \times 10^{-6} \text{ moles cc}^{-1}$ and $[\text{O}_2]_i=375 \text{ ppm}$.

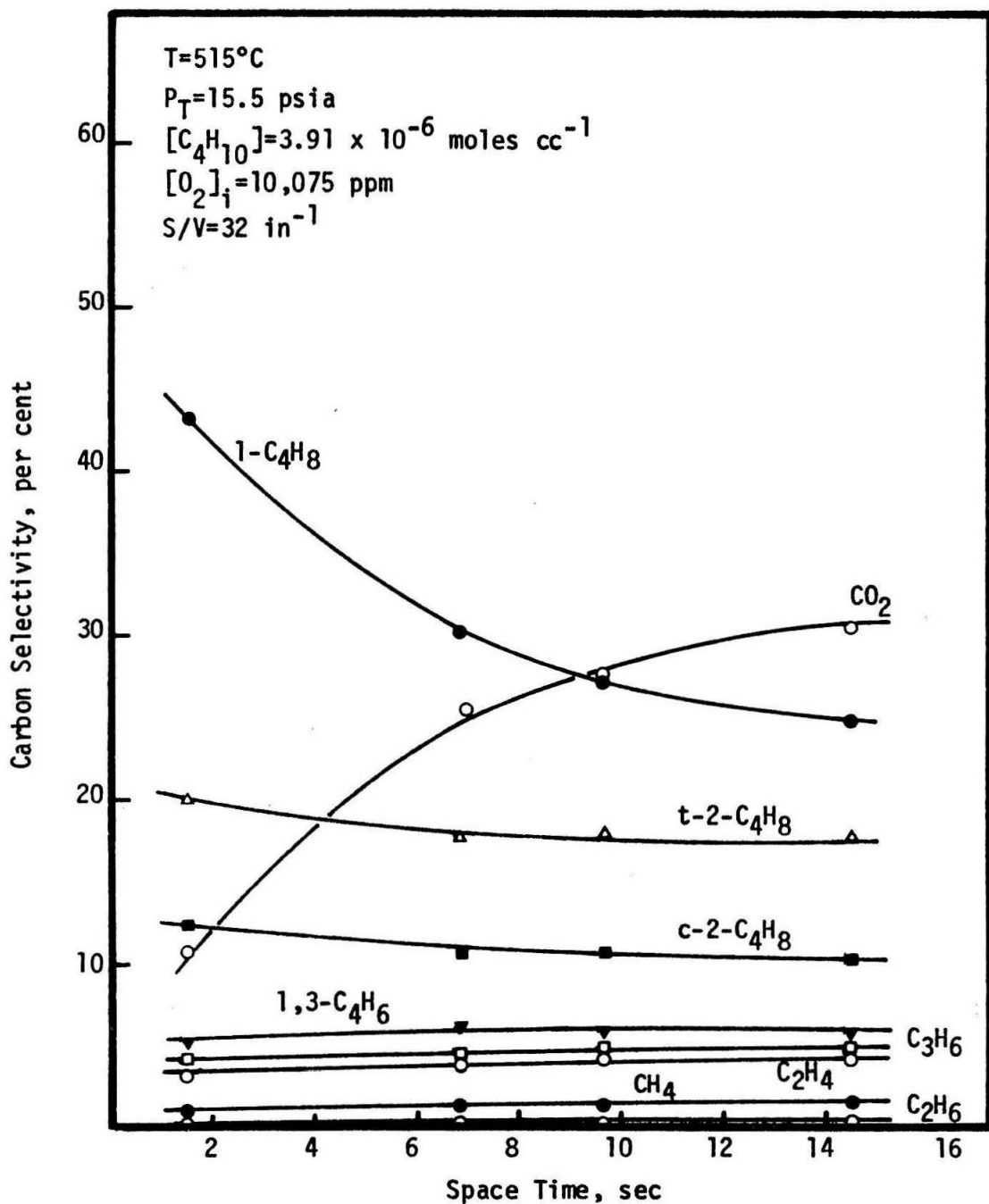


Figure 56. Carbon selectivity as a function of space time for $T=515^{\circ}\text{C}$, $[\text{C}_4\text{H}_{10}]=3.91 \times 10^{-6} \text{ moles cc}^{-1}$ and $[\text{O}_2]_i=10,075 \text{ ppm}$.

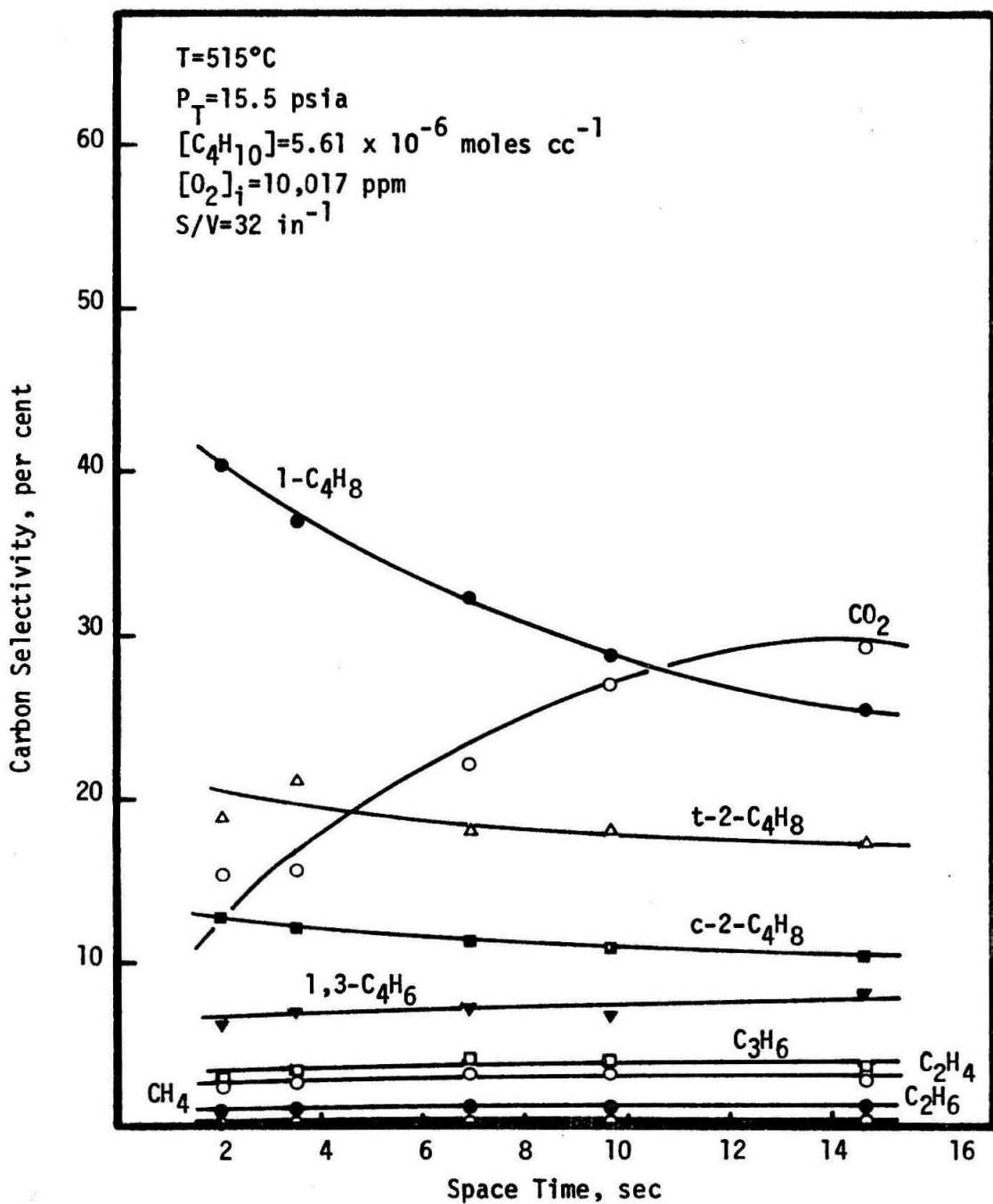


Figure 57. Carbon selectivity as a function of space time for $T=515^{\circ}\text{C}$, $[\text{C}_4\text{H}_{10}]=5.61 \times 10^{-6}\text{ moles cc}^{-1}$ and $[\text{O}_2]_i=10,017\text{ ppm}$.

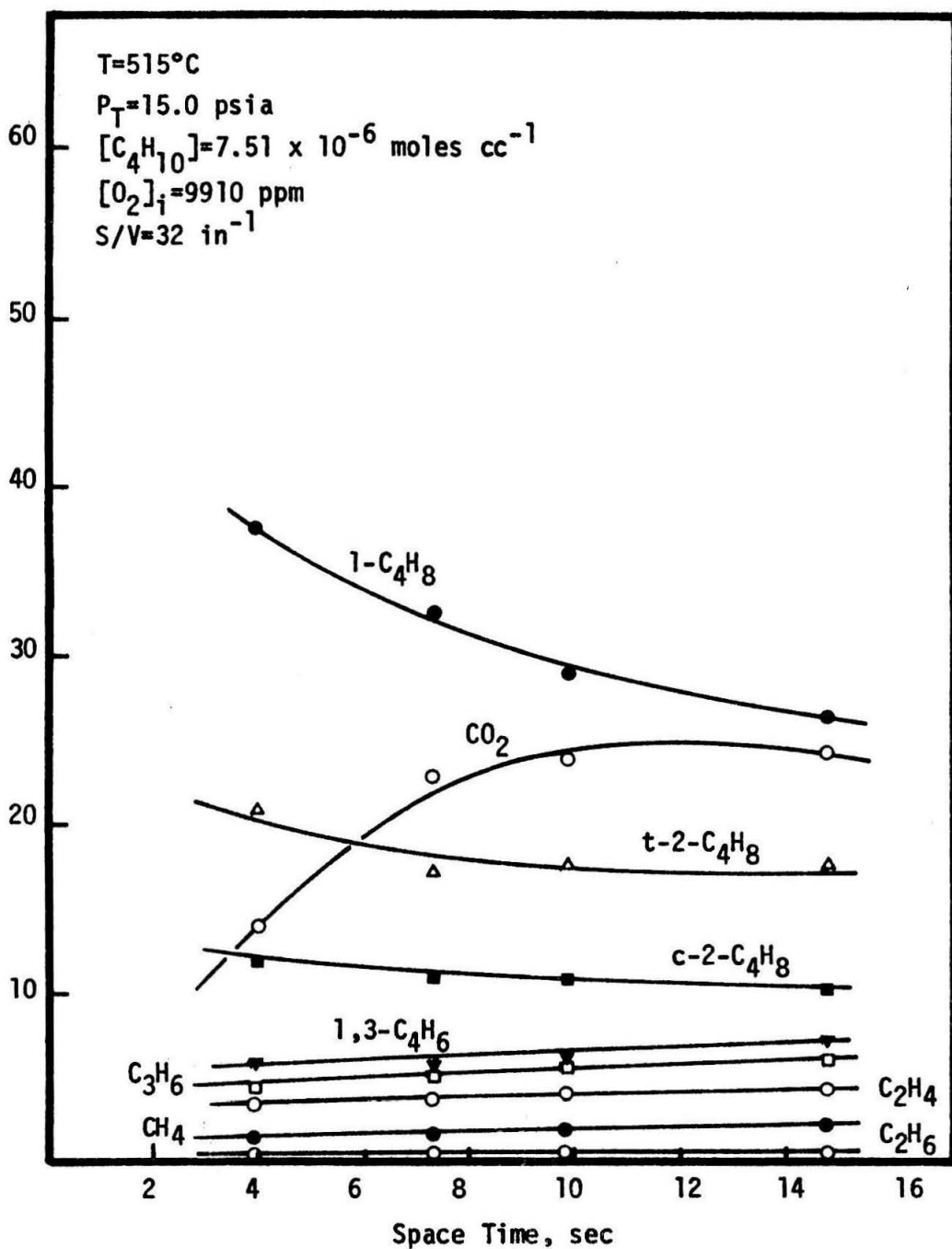


Figure 58. Carbon selectivity as a function of space time for $T=515^{\circ}\text{C}$, $[\text{C}_4\text{H}_{10}]=7.58 \times 10^{-6}\text{ moles cc}^{-1}$ and $[\text{O}_2]_i=9910\text{ ppm}$.

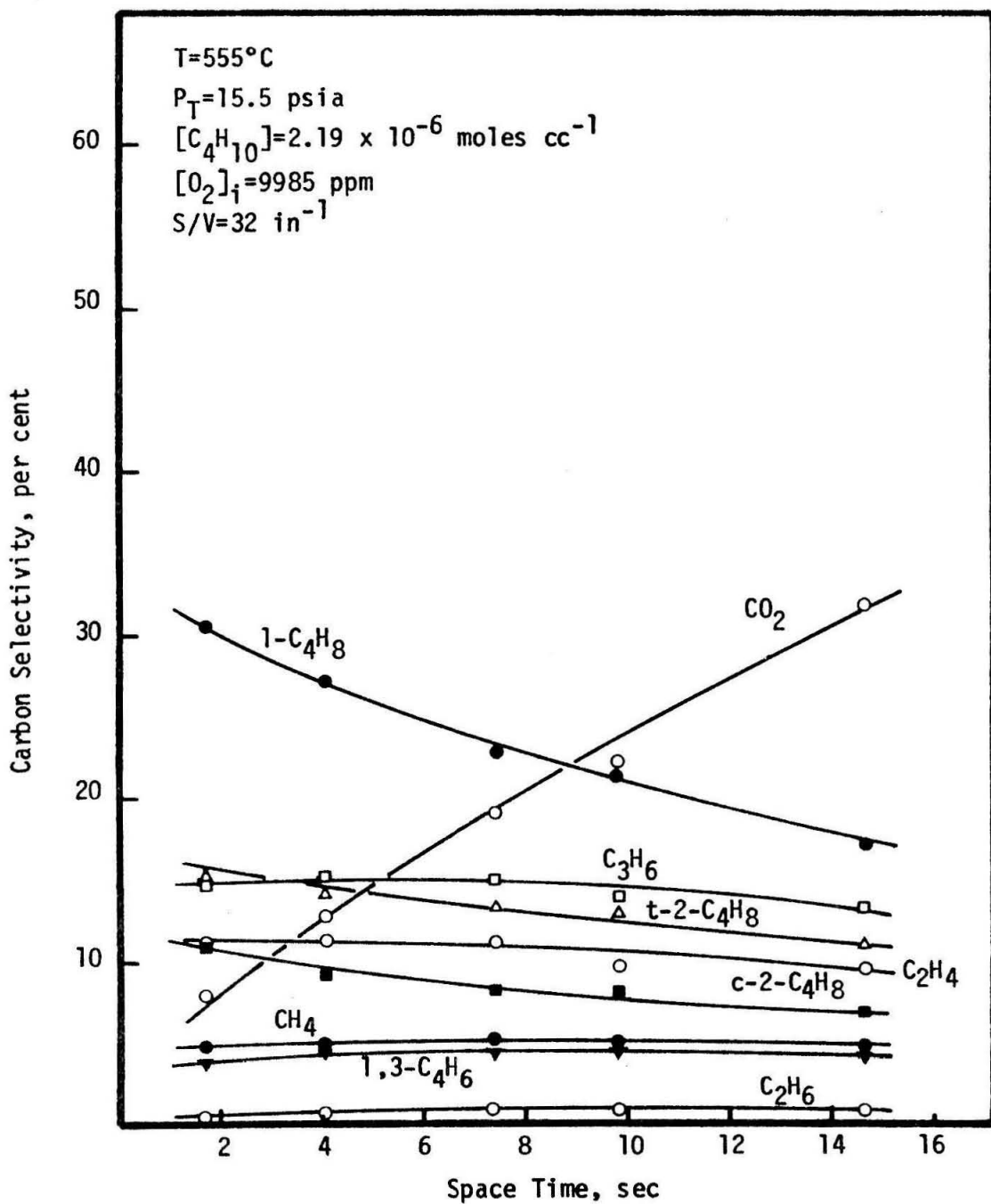


Figure 59. Carbon selectivity as a function of space time for $T=555^{\circ}\text{C}$, $[\text{C}_4\text{H}_{10}]=2.19 \times 10^{-6}\text{ moles cc}^{-1}$ and $[\text{O}_2]_i=9985\text{ ppm}$.

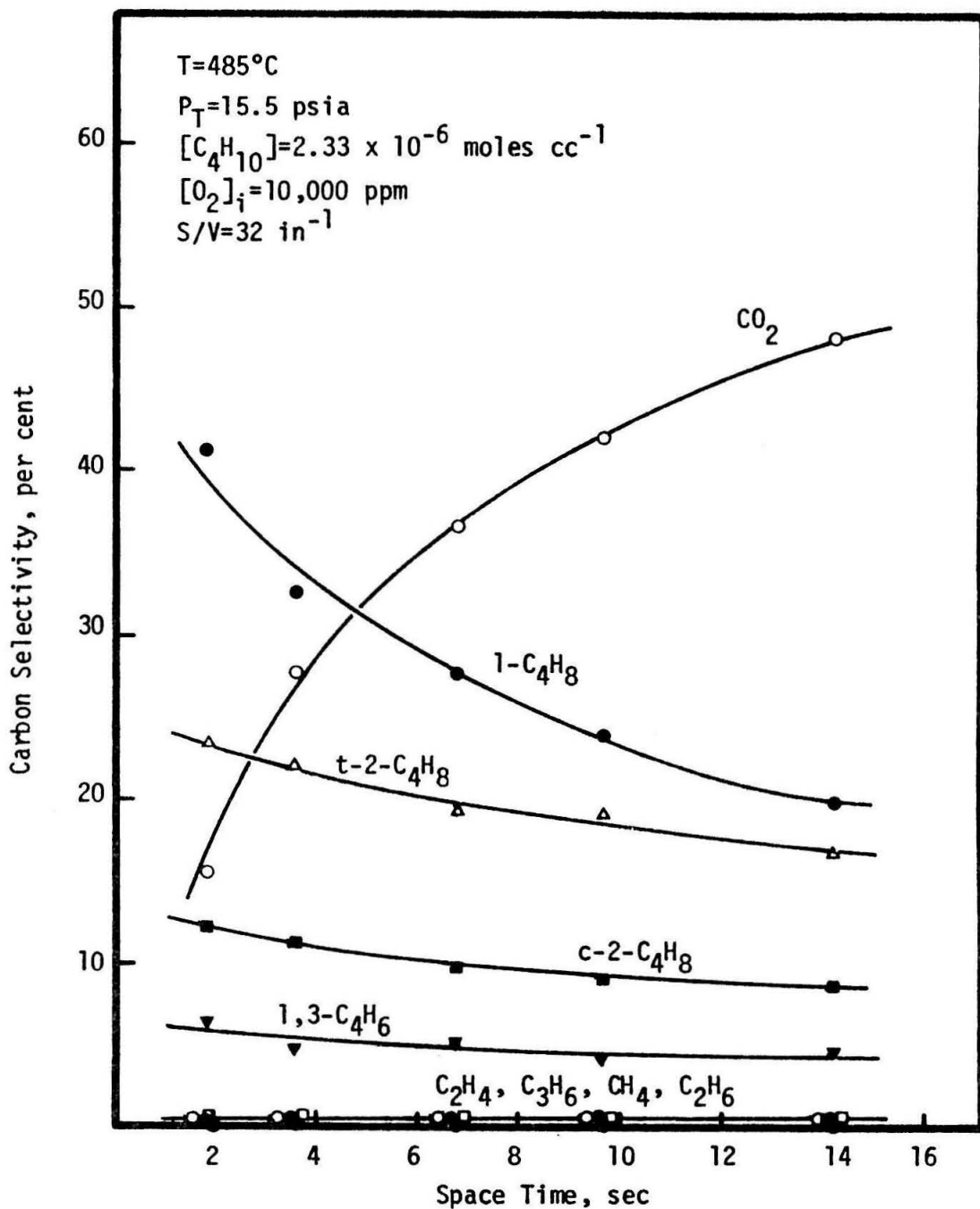


Figure 60. Carbon selectivity as a function of space time for $T=485^{\circ}\text{C}$, $[\text{C}_4\text{H}_{10}]=2.33 \times 10^{-6} \text{ moles cc}^{-1}$ and $[\text{O}_2]_i=10,000 \text{ ppm}$.

to complete conversion of the oxygen. Consequently, for lower initial concentrations of oxygen, the maximum level was reached at shorter contact times. At 515°C, the formation of C₄ olefins in preference to the cracked products was so favorable that for an initial concentration of oxygen of 9810 ppm the total selectivity of the cracked products was less than 10 per cent.

The effect of varying the concentration of butane may be seen by a comparison of Figures 52, 56, 57 and 58. Increased concentrations of butane effectively resulted in an increased rate of consumption of the oxygen for a given residence time. This was reflected in the selectivities by a decrease in the carbon dioxide value and increases in the values for the other products. The fact that the selectivity of 1-butene increased with an increase in the concentration of butane may be explained by assuming that an increased amount of oxygen was used in reaction with the butane. This would leave less oxygen available for secondary reactions with the olefin products to form carbon dioxide. Since both the selectivities of the C₄ olefins and the cracked products increased in roughly the same proportion with increasing concentration of butane, the possibility of the same kinetic dependence on butane was suggested for the two processes. As was previously shown, the formation of the products of the pyrolysis obey three-halves order kinetics with respect to the concentration of butane.

The effect of temperature may be gauged by a comparison of Figures

52, 59 and 60 which report the carbon selectivities for a given reactant mixture at 515, 555 and 485°C respectively. At 485°C, the carbon products were essentially C₄ unsaturates and carbon dioxide. At 485°C, the sum of selectivities for the cracked products was less than 1 per cent. In contrast, at 555°C this sum was approximately 32 per cent. The relative formation of cracked products increased markedly with increasing temperature. From these observations, it may be concluded that the activation energy of the process forming the cracked products is much greater than that of the process involving butene formation.

Of interest was the result of extrapolation of the selectivities to $\tau = 0$. In all of the cases the yield of carbon dioxide would be approximately zero. Thus, the consumption of oxygen in the initial reaction would result in complete conversion to water. The initial hydrocarbon products would appear to be primarily 1-butene, t-2-butene and c-2-butene. 1,3-Butadiene would be formed to a lesser extent. Only at temperatures above 550°C would the cracked products constitute a significant fraction of the products of the initial reaction.

Relative formation of the C₄ unsaturates

The relative molar formations of 1-butene, t-2-butene, c-2-butene and 1,3-butadiene are presented in Figure 61 for 515°C. The data were taken for concentrations of butane from 2.18×10^{-6} to 7.51×10^{-6} moles cc⁻¹ and initial concentrations of oxygen from 375 to 9810 ppm. As may be noted, the relative composition of the C₄ unsaturates was

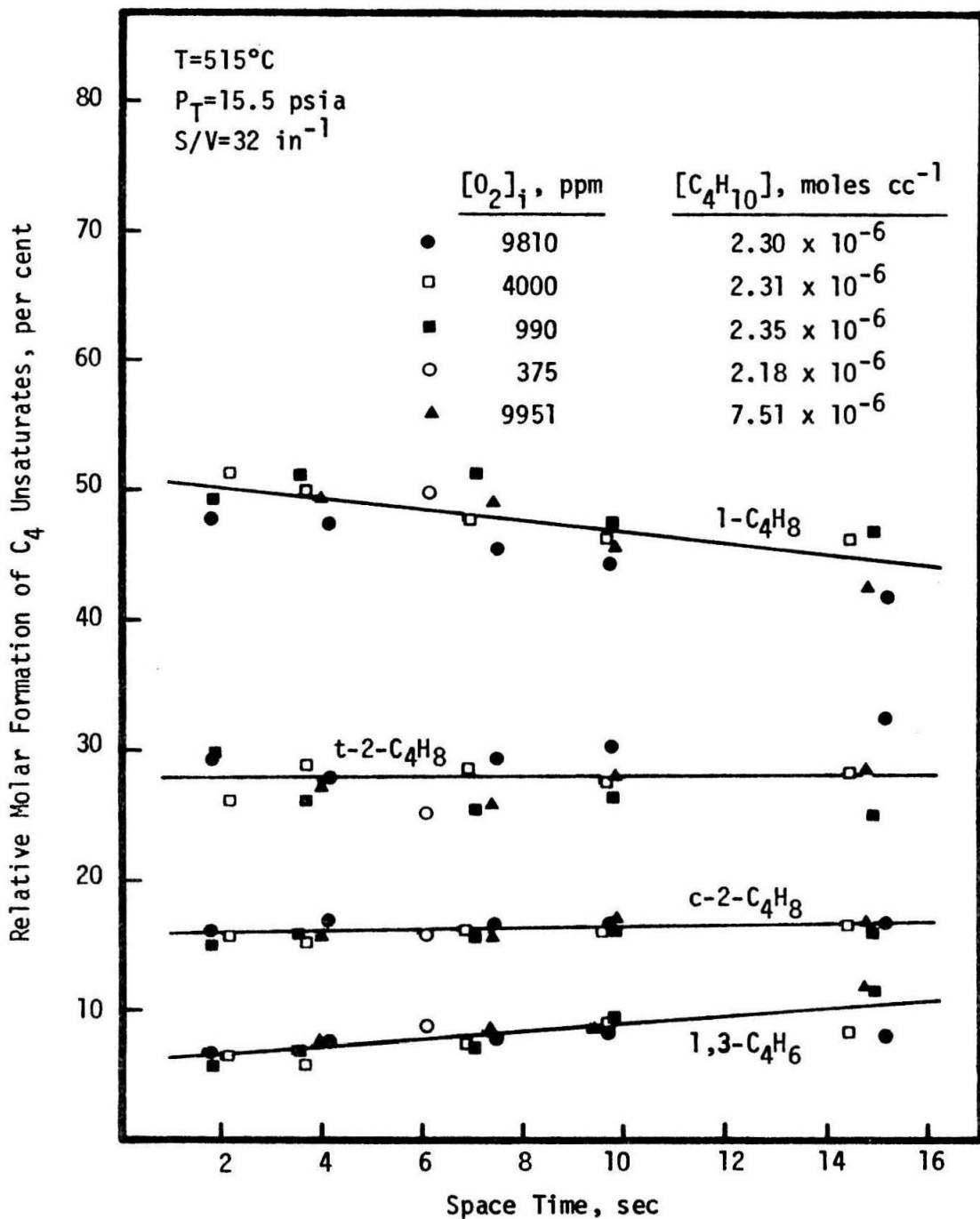
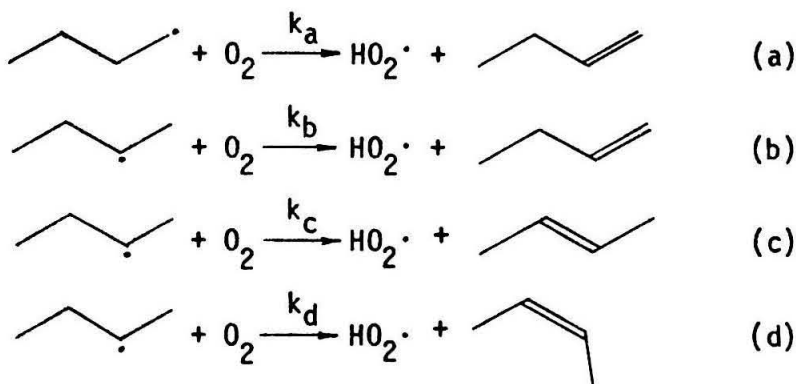


Figure 61. Relative formation of C_4 unsaturates as a function of space time for the oxidative dehydrogenation of butane.

independent of the concentrations of butane and oxygen in the range studied.

Assume for the moment that the butenes were formed only by reaction of primary and secondary butyl radicals which had been formed by the abstraction of a hydrogen from butane. This could be diagrammed as follows:



Further assume that isomerization of $p\text{-C}_4\text{H}_9\cdot$ to $s\text{-C}_4\text{H}_9\cdot$ is slow. Benson (61) has estimated that this isomerization would have to proceed intramolecularly through a four-centered transition state. The strain energy associated with such a ring is $27 \text{ kcal mole}^{-1}$. This coupled with an energy of 8 kcal mole^{-1} for the abstraction of a hydrogen atom would yield an activation energy of at least $35 \text{ kcal mole}^{-1}$. Thus it would seem probable that the radical isomerization is slow.

Kupperman and Larson (58) and McNesby and Gordon (59) observed that at 515°C the relative rates of abstraction of primary to secondary hydrogens were 0.45 and 0.40 respectively. Taking a value of 0.43 for k_p/k_s and assuming that

$$k_p/k_s = k_b/k_c = k_b/k_d \quad ,$$

the ratio of 1-butene to 2-butene in the products was calculated to be 1.10. This compared favorably with the experimentally observed values of 1.15 to 1.00 for space times of 2 and 15 seconds respectively.

If the $s\text{-C}_4\text{H}_9\cdot$ can be considered to be in equilibrium with respect to the cis-trans configurations, an estimate of the ratio of t-2-butene to c-2-butene may be made on the basis of equilibrium data. For 515°C Scott, et al (62) reported a value of 1.59 for the equilibrium ratio of t-2-butene to c-2-butene. Voge and May (63) gave a somewhat lower value of 1.30. These may be compared with the value of 1.75 calculated for the products from the data of Figure 61. Under the conditions of the reaction, c-2-butene, once formed, would not isomerize to t-2-butene to any extent. Experimental verification of this fact was provided by flowing 99.97 mole-per-cent pure c-2-butene through the gold reactor at 470°C. At contact times near 5 seconds, the t-2-butene in the effluent of the reactor was less than 0.05 per cent of the c-2-butene. Cundall and Palmer (64) reported an activation energy of 63 kcal mole⁻¹ for the isomerization. The ratio of t-2-butene to c-2-butene in the products varies slightly with temperature. The Arrhenius plot of Figure 62 reveals an activation energy of -3300 cal mole⁻¹. Scott, et al (62) reported a value of -718 cal mole⁻¹ at 515°C at equilibrium. As activation energies are difficult to obtain within ± 2 kcal mole⁻¹, the difference is not unexpected for such small activation energies.

With increasing space time, the relative formation of 1,3-butadiene increased by approximately the same amount as the 1-butene decreased.

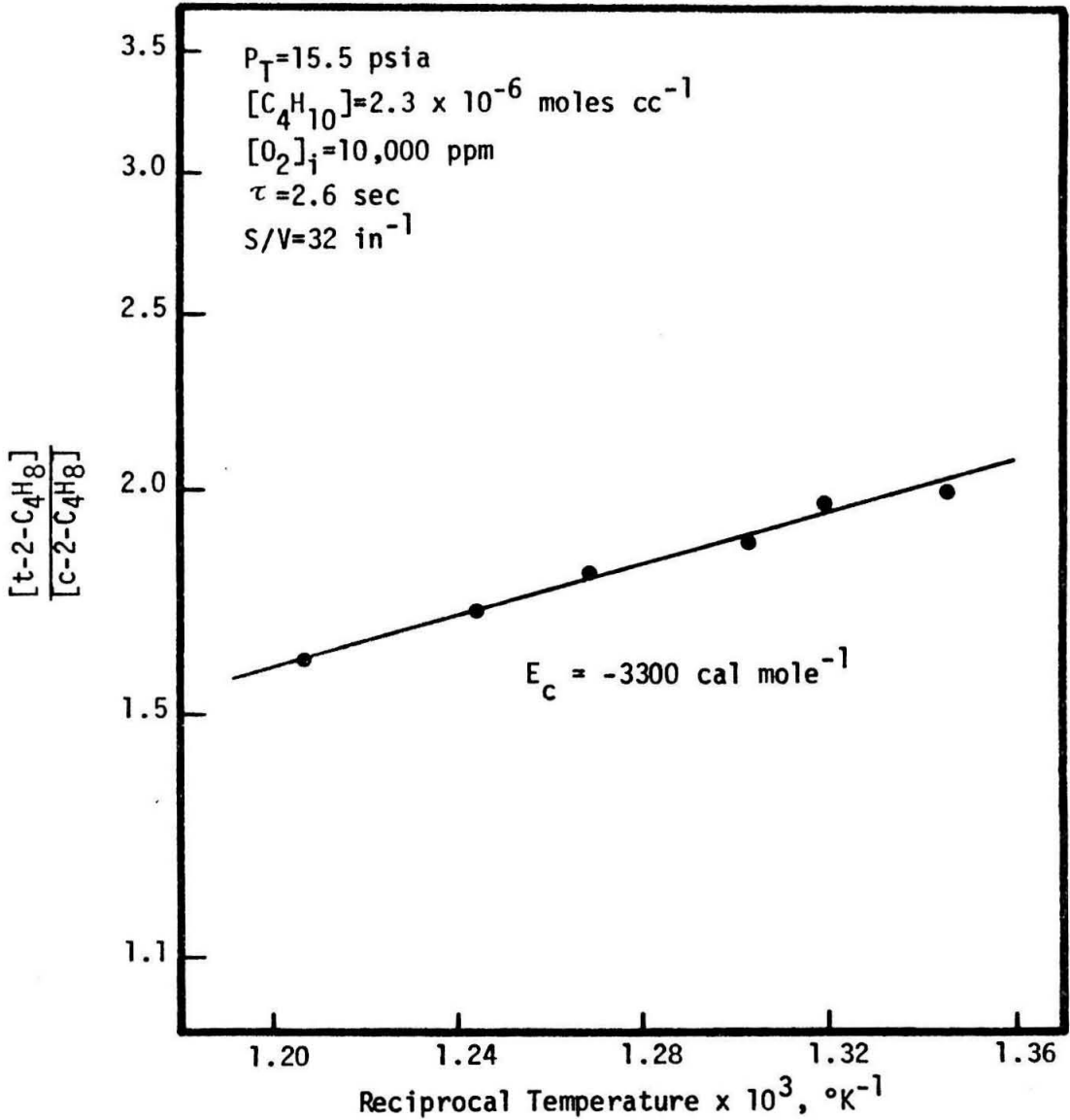


Figure 62. Arrhenius plot of the t-2-butene/c-2-butene yield for the oxidative dehydrogenation of butane.

This suggests the possibility that 1-butene is a precursor of 1,3-butadiene.

Relative formation of the cracked products

The relative molar formation of methane, ethylene, ethane and propane are presented in Figures 63 and 64 for 515 and 555°C respectively. The distribution of cracked products varied only slightly with contact time. With increasing temperature, the fraction of methane increased with a corresponding decrease in the fraction of ethylene. This is primarily a result of increased participation of the alkyl radicals in unimolecular decomposition reactions at the higher temperatures.

A comparison of the results of the pyrolysis in the absence of oxygen (Figure 19) reveals that the relative amount of ethylene increased with increasing amounts of oxygen. At 515°C and 9810 ppm of oxygen in the reactants, the ethylene fraction was 2.5 times that for the oxygen-free pyrolysis under similar conditions. The proportion of methane and ethane decreased with increasing oxygen.

The increased ethylene in the oxidation may be explained by considering the reaction of ethyl radicals with oxygen to form ethylene and a hydroperoxide radical. This alternate reaction would also lower formation of ethane which is primarily formed by abstraction of hydrogen by an ethyl radical.

For the pyrolysis, it was assumed that the methane and propylene were formed from the same precursor, butyl radical. Methane is

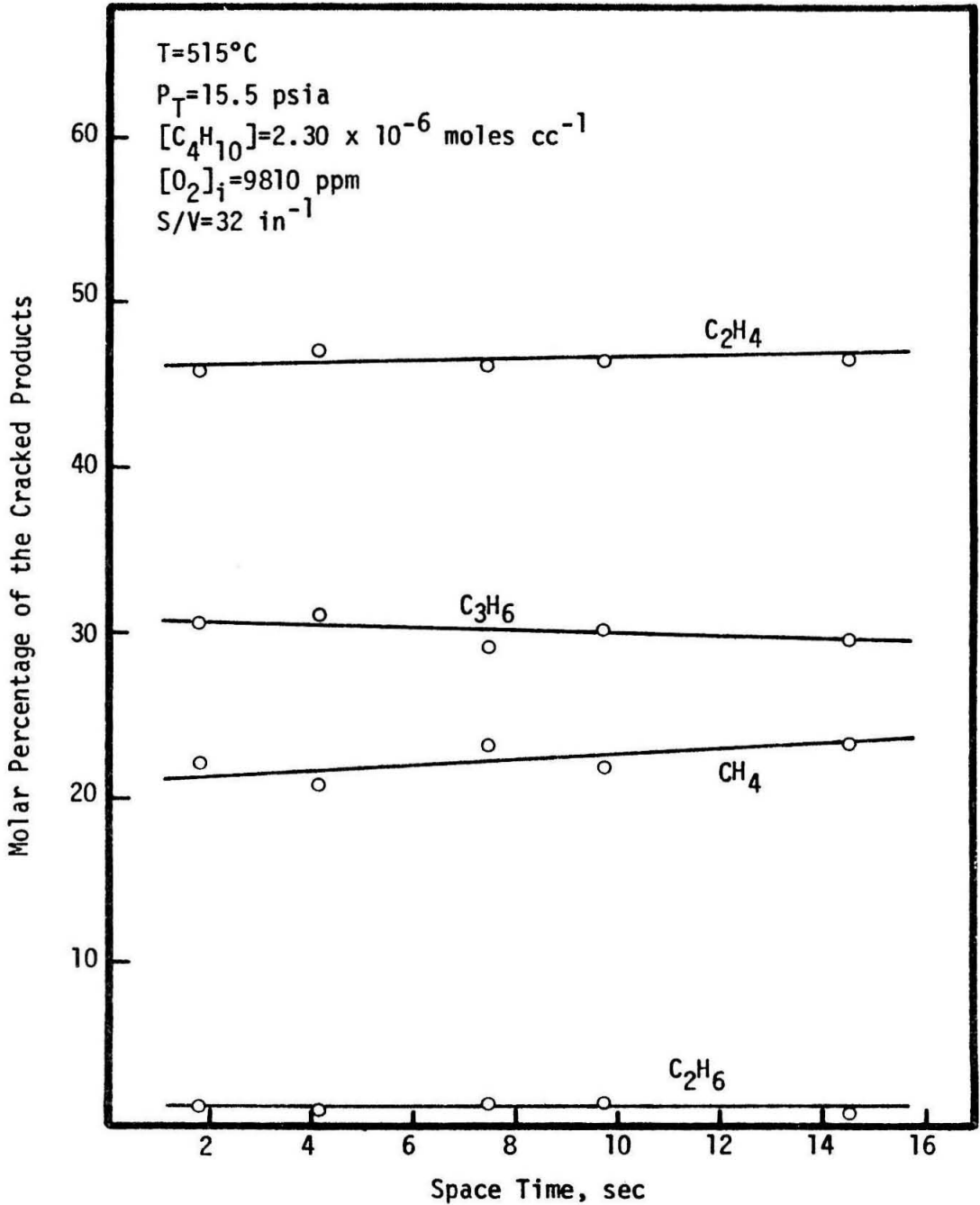


Figure 63. Relative formation of the cracked products as a function of space time for the oxidative dehydrogenation of butane at 515°C .

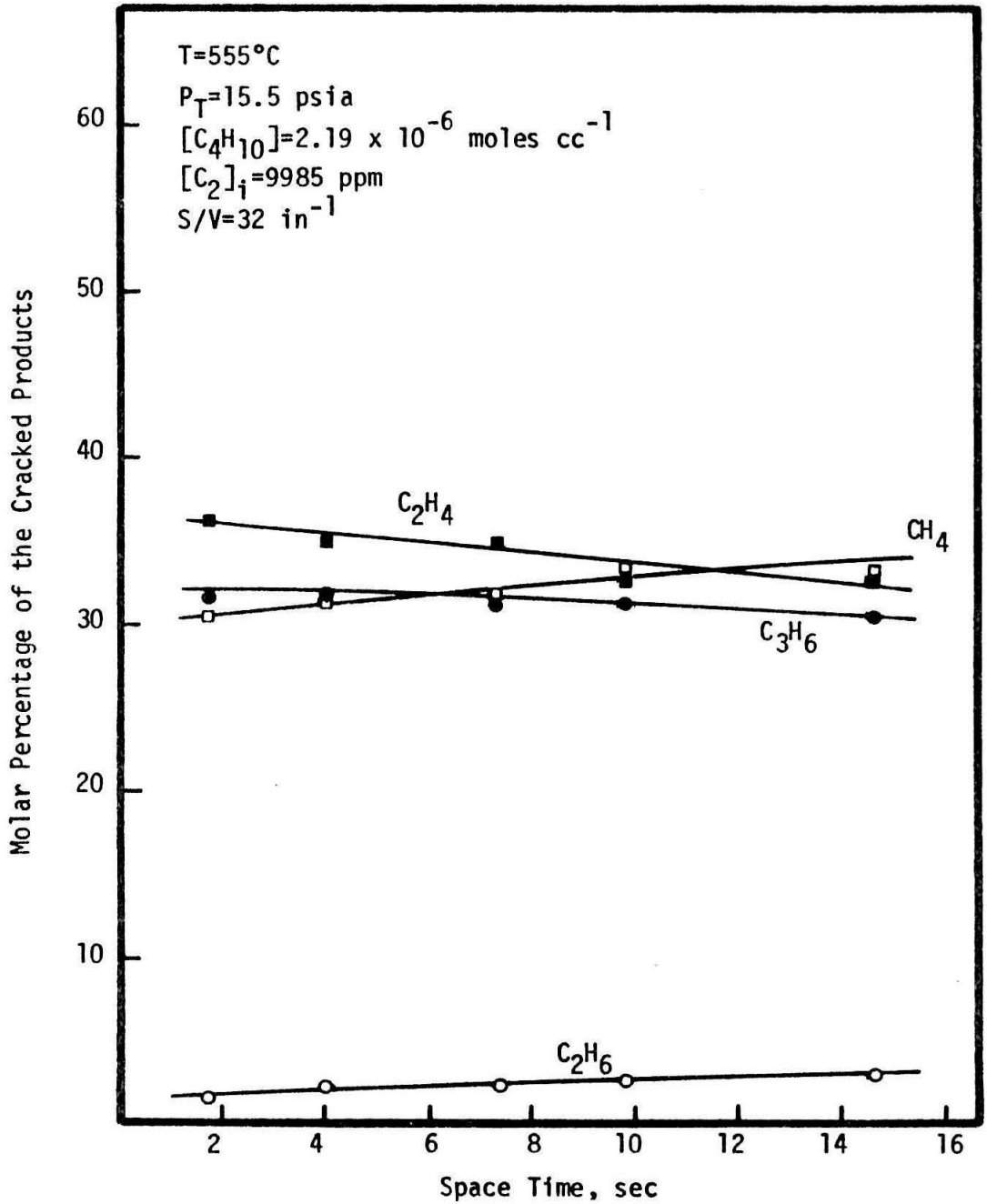


Figure 64. Relative formation of the cracked products as a function of space time for the oxidative dehydrogenation of butane at 555°C .

formed at lower proportions than propylene for the oxidation at temperatures below 530°C. A reaction of the methyl radical in addition to the abstraction of a hydrogen must be important under these conditions. A possible route could be the reaction of the methyl radical with oxygen leading to carbon dioxide and water.

Stoichiometry of the overall reaction

The moles of oxygen consumed per mole of butane reacted, defined as q , provided a measure of the stoichiometry of the reactants for the overall reaction. The variation of q with space time was random and was within ± 3 per cent of the mean value. A similar random drift in q over a period of several weeks was also observed.

Figure 65 presents the dependence of q on temperature in the range 470 to 530°C. The points were obtained by an average of q over space times from 1.5 to 15 seconds. Lower temperature favored higher values of q . For example, q varied from 3.0 at 530°C to 5.5 at 470°C, an increase of 85 per cent.

The composition of the reactants also influence the value of q . In Figure 66, q is presented as a function of the ratio of the initial concentrations of oxygen to butane. For $[O_2]_i/[C_4H_{10}]_i$ from 0.002 to 0.10, q can be described by the following equation for a temperature of 515°C:

$$q = 18.4 \left(\frac{[O_2]_i}{[C_4H_{10}]_i} \right)^{0.5} \quad (22)$$

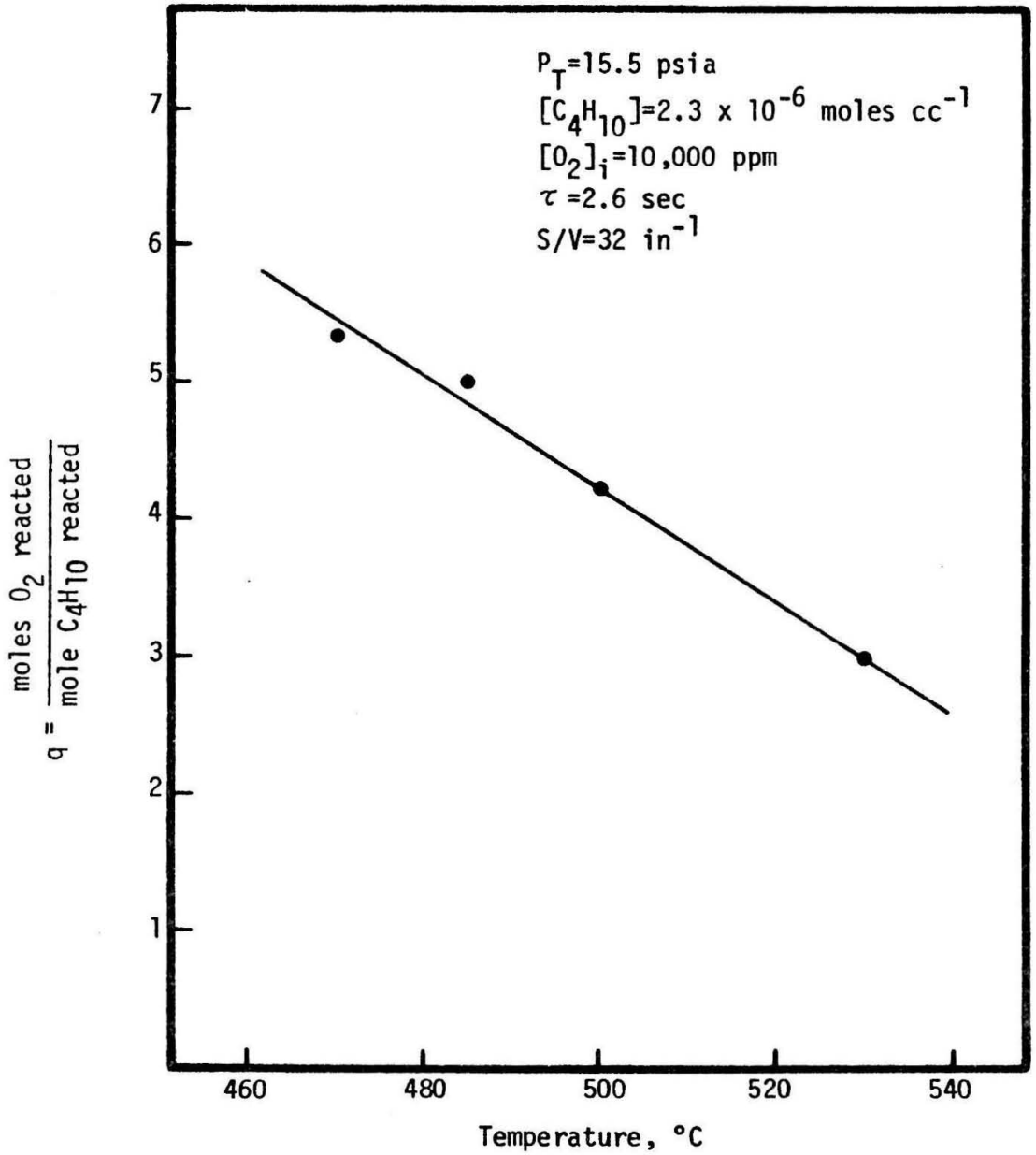


Figure 65. Moles of oxygen consumed per mole of butane reacted as a function of temperature.

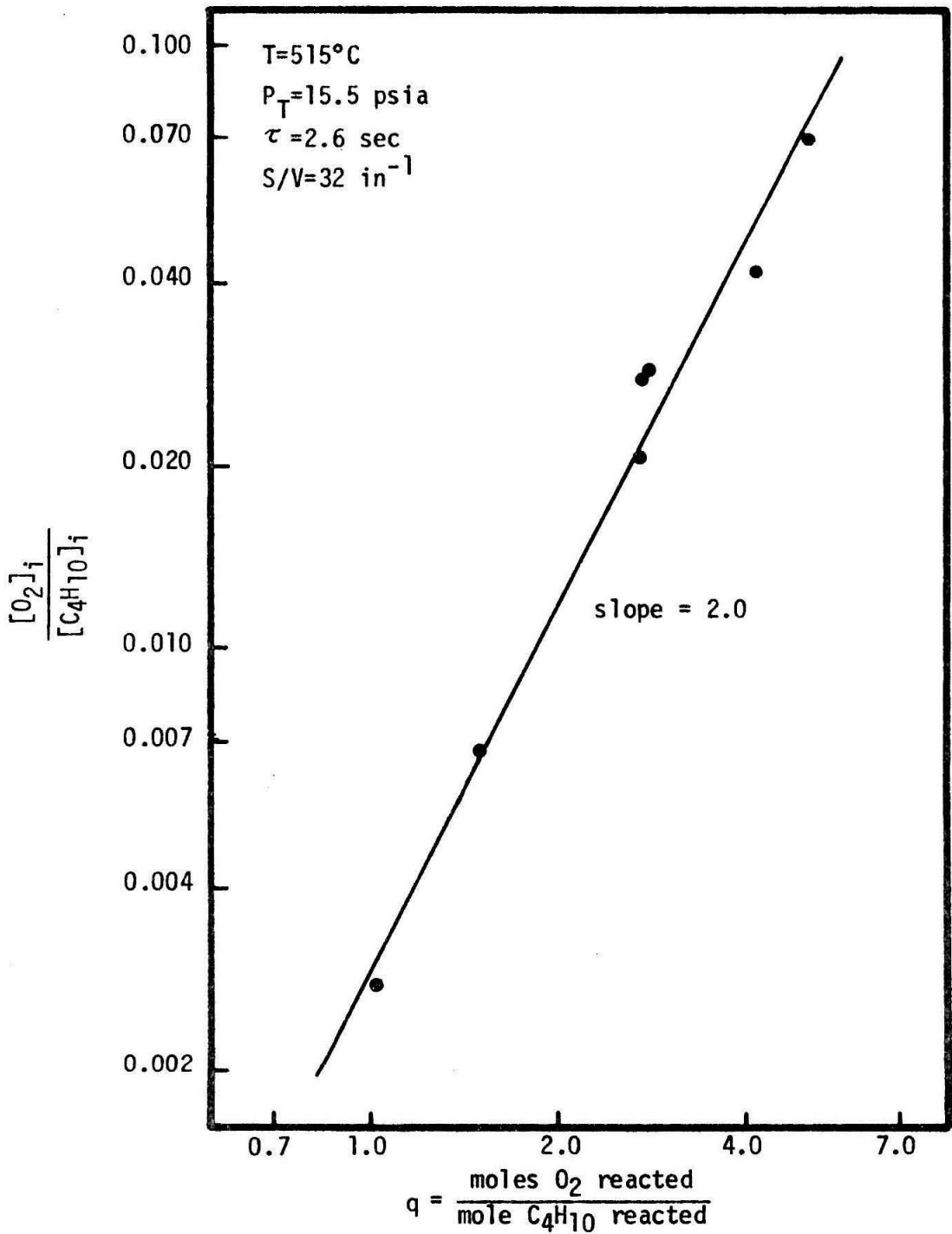


Figure 66. Moles of oxygen consumed per mole of butane reacted as a function of the initial concentrations of oxygen and butane.

This change of q with temperature and initial conditions may be taken as evidence that the overall oxidation is composed of competing processes of different stoichiometry.

Overall rate of the reaction

In order to describe the kinetics of the reaction between butane and oxygen, the following rate expression was assumed for the disappearance of butane:

$$-R_{C_4H_{10}} = k [C_4H_{10}]^m [O_2]^n \quad (23)$$

where

$$k = A \exp [-E_c/RT] \quad (24)$$

Equations (23) and (24) were then substituted into equations (7) through (10) and the constants m , n , E_c and A were evaluated from the experimental data. It should be recalled that the assumptions of an ideal gas, isothermal plug flow, constant pressure and constant density throughout the reactor were employed. In conjunction with the above equations, the stoichiometry of the overall reaction was assumed to be of the following form:



The coefficient, q , as discussed in the previous section, was found to be a function of the temperature and the initial conditions of the reaction; however, it was relatively independent of the residence time.

In order to evaluate the order, n , of the overall reaction with respect to oxygen, the disappearance of oxygen was measured as a function of the space time for a given temperature and initial mixture of reactants. An integral test of the rate expression was then made by assuming various values of n . Knowledge of the order, m , of the reaction with respect to butane was not required as the concentration of butane varied less than one per cent throughout the reactor.

A comparison of the data and rate expression for $n = 0.5$ is shown in Figure 67 for 515°C. The slopes of the lines are equal to $k [C_4H_{10}]^m$. Agreement with the data was within 8 per cent in extreme cases; however, average deviation was less than 4 per cent.

The order, m , of the reaction with respect to butane could be calculated from a log-log plot of the slopes of Figure 67 against the concentration of butane. This is shown in Figure 68. A value of 1.4 ± 0.15 was obtained for m .

Because of the relatively large error associated with the order with respect to butane, a value of m was obtained by a second method. The consumption of butane was calculated from the products by means of a mass balance. The formation of carbon in the reactor as a result of the oxidation was neglected as no physical evidence of its presence was ever observed under the operating conditions employed. The disappearance of butane was plotted as a function of space time for several initial concentrations of butane. The temperature and initial concentration of oxygen were held constant. An initial rate of reaction for

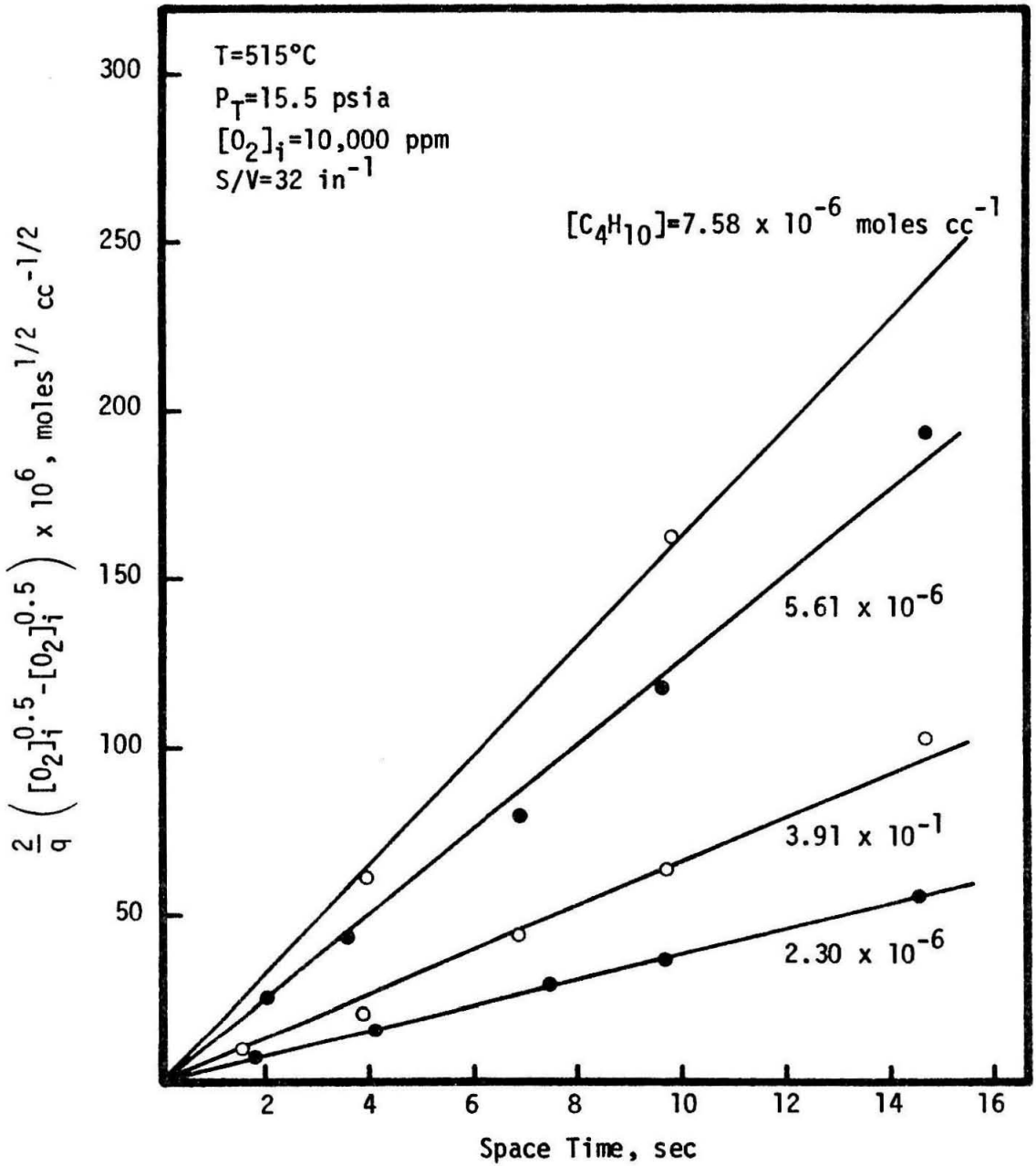


Figure 67. Integral test of the rate expression for an order with respect to oxygen at 0.5.

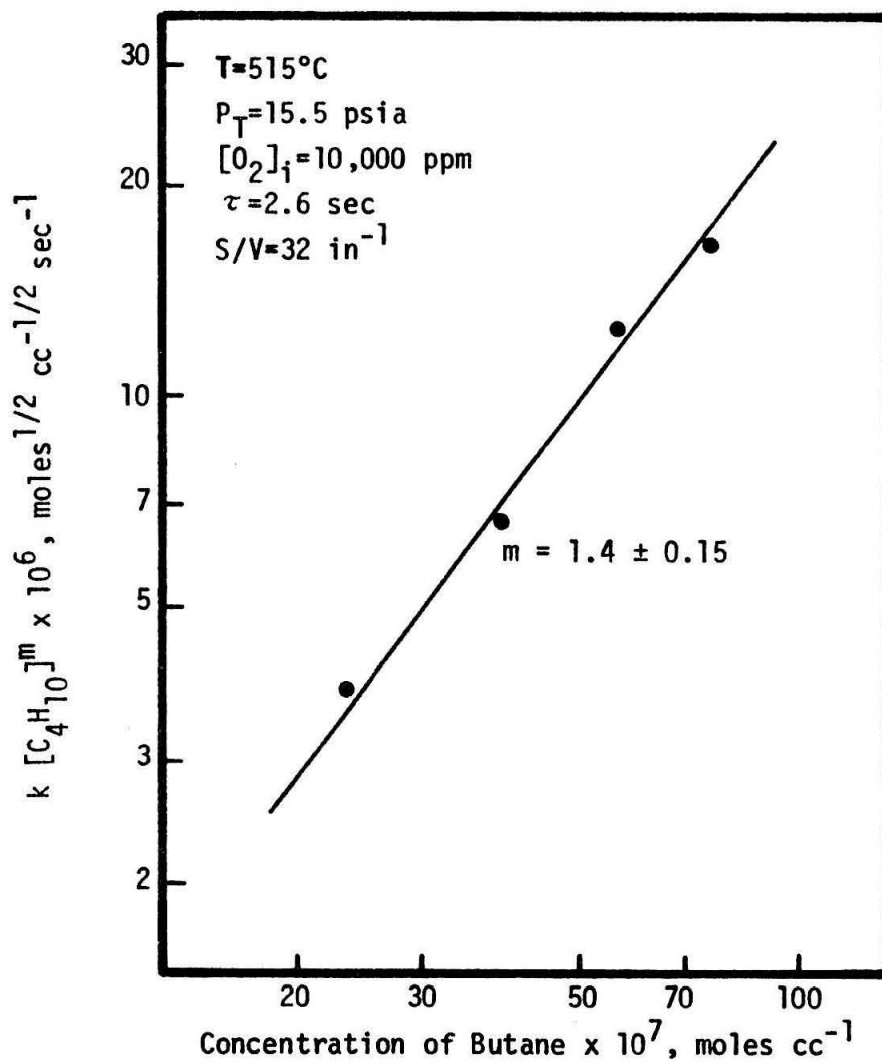


Figure 68. Determination of the order with respect to butane of the oxidative dehydrogenation by the method of successive slopes.

butane could then be obtained by graphical differentiation of the resulting curves at $\tau = 0$. Evaluation of the order with respect to butane could then be accomplished using the following equation:

$$\left(\frac{d [C_4H_{10}]}{d \tau} \right)_{\tau=0} = k [C_4H_{10}]_i^m [O_2]_i^n \quad (26)$$

The slope of a log-log plot of the initial rate against the concentration of butane would correspond to the order, m.

The procedure is illustrated in Figures 69 and 70 for 515°C and an initial concentration of oxygen of 1.0 per cent by volume. A value of m of 1.50 ± 0.05 was calculated.

Having determined the constants m and n, application of the rate expression was made over a variety of initial concentrations of butane and oxygen. Equation (7) may be integrated to yield the following expression:

$$k \tau = \frac{-2}{[C_4H_{10}]_i^{0.5} [O_2]_i^{0.5} (a-1)} \left\{ \left(\frac{1-aX_B}{1-X_B} \right)^{0.5} - 1 \right\}, \quad (27)$$

where

$$a = q \frac{[C_4H_{10}]_i}{[O_2]_i} \quad (28)$$

The right hand side of equation (27) is plotted against the space time in Figure 71 for 515°C and initial concentrations of oxygen from 375 to 10,075 parts-per-million and concentrations of butane from 2.2×10^{-6}

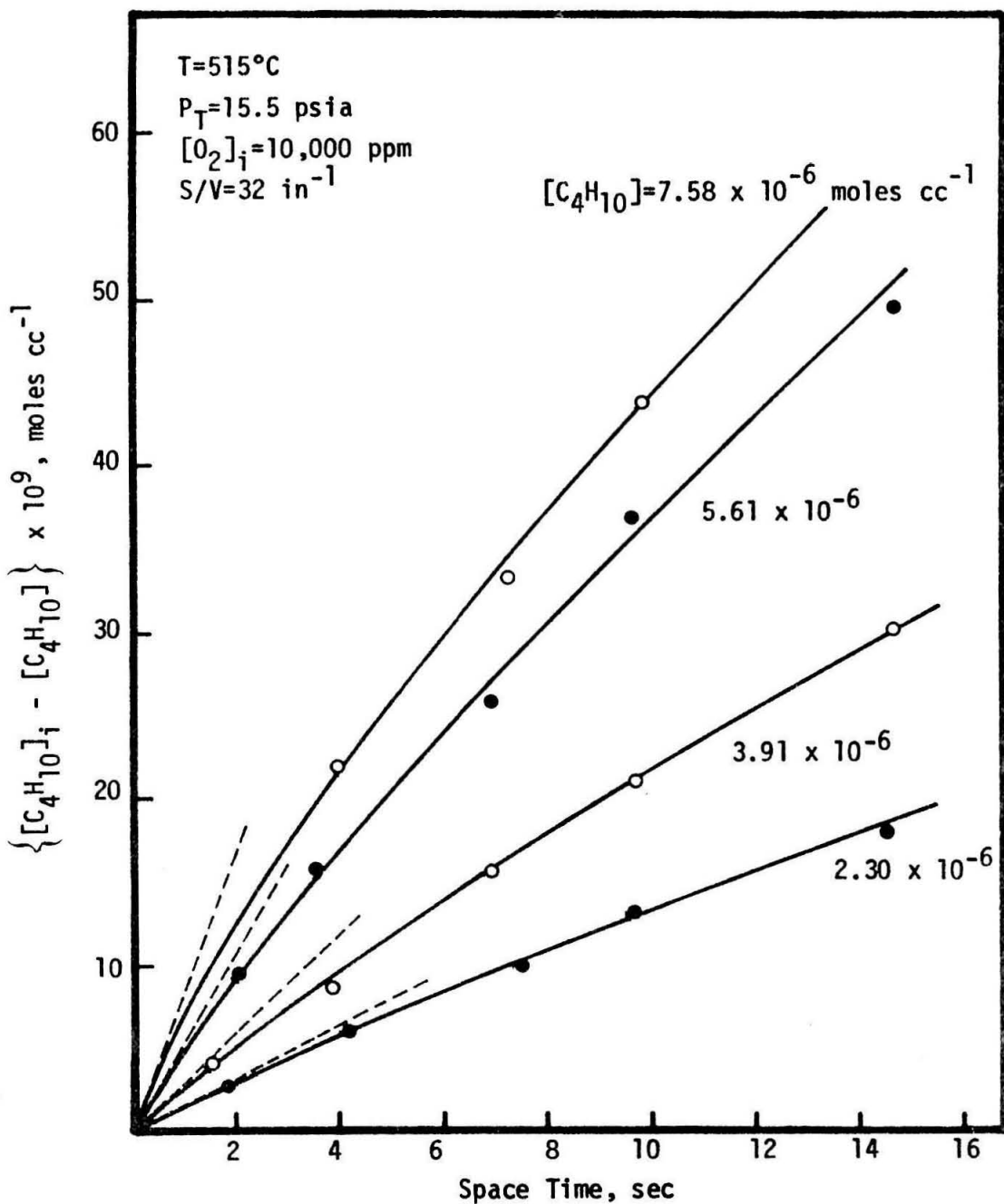


Figure 69. Determination of the initial rate of disappearance of butane as a function of the concentration of butane.

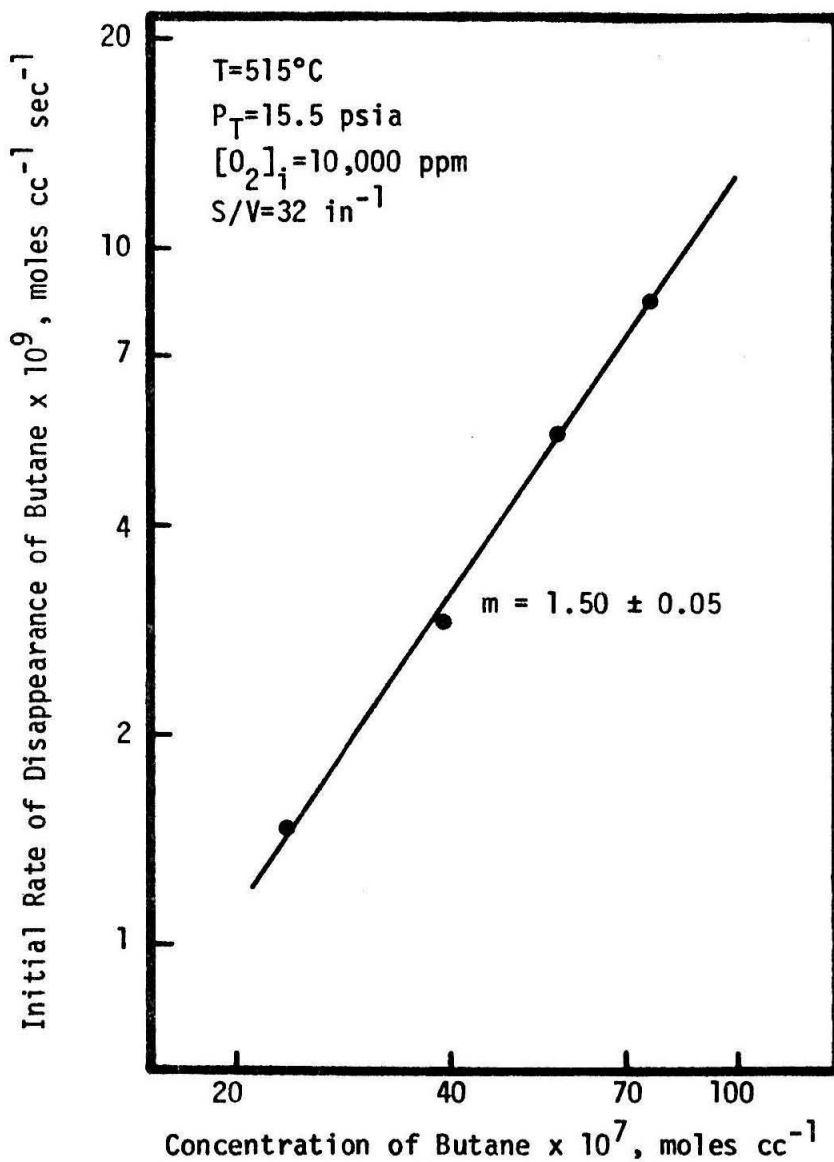


Figure 70. Determination of the order with respect to butane of the oxidative dehydrogenation by method of initial rates.

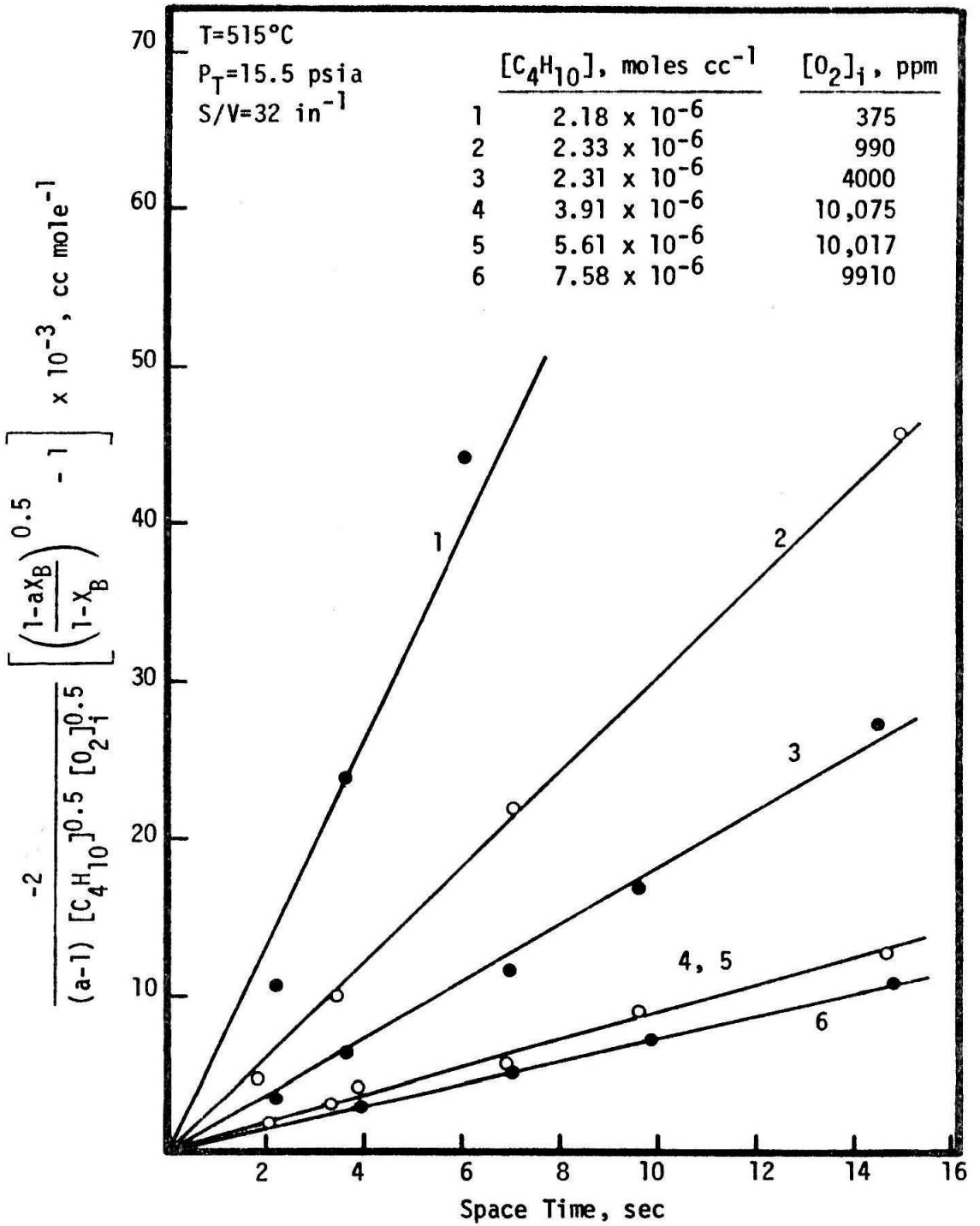


Figure 71. Integral test of rate expression over a range of initial concentrations.

to 7.6×10^{-6} moles cc^{-1} . The rate constant, k , varied from 0.73×10^{-3} to 6.57×10^{-3} $\text{cc mole}^{-1} \text{sec}^{-1}$ depending upon the initial concentrations of butane and oxygen.

Ideally, a rate constant is desired which is only a function of temperature. Closer inspection of the data of Figure 71 reveals that k is relatively independent of the concentration of butane but is approximately inversely proportional to the square root of the initial concentration of oxygen. Thus, the following rate constant was defined:

$$k' = k [O_2]_i^{0.5} \quad (29)$$

Equation (27) then becomes

$$k' \tau = \frac{-2}{[C_4H_{10}]^{0.5} (a-1)} \left\{ \left(\frac{1-a\chi_B}{1-\chi_B} \right)^{0.5} - 1 \right\} \quad (30)$$

A comparison of k and k' as a function of the initial mixture of reactants is given in Table 3. The average deviation of k' from a mean value of $0.39 \text{ cc}^{1/2} \text{ moles}^{-1/2} \text{ sec}^{-1}$ was 14 per cent. Variations of up to 20 per cent were observed in the rate over a period of four or five weeks.

The variation of the rate constant, k' , with temperature is presented in Figure 72 for initial concentrations of butane and oxygen of 2.3×10^{-6} moles cc^{-1} and 1.0 per cent by volume, respectively. Figure 73 is an Arrhenius plot of the rate constant, k' . An activation energy, E_c , for the oxidative dehydrogenation was calculated as $23.1 \pm 0.5 \text{ kcal mole}^{-1}$. The frequency factor, A' , based on the rate constant

Table 3. Rate Constants, k and k' , at 515°C.

$[C_4H_{10}]$, (moles cc^{-1})	$[O_2]_i$, (ppm)	k , ($cc \text{ moles}^{-1} \text{ sec}^{-1}$)	k' , ($cc^{\frac{1}{2}} \text{ moles}^{-\frac{1}{2}} \text{ sec}^{-1}$)
2.18×10^{-6}	375	6.75×10^{-3}	0.50
2.33×10^{-6}	990	3.04×10^{-3}	0.38
2.31×10^{-6}	4000	1.81×10^{-3}	0.45
3.91×10^{-6}	10,075	0.91×10^{-3}	0.35
5.61×10^{-6}	10,017	0.92×10^{-3}	0.37
2.30×10^{-6}	9810	1.13×10^{-3}	0.45
7.58×10^{-6}	9910	0.73×10^{-3}	0.29

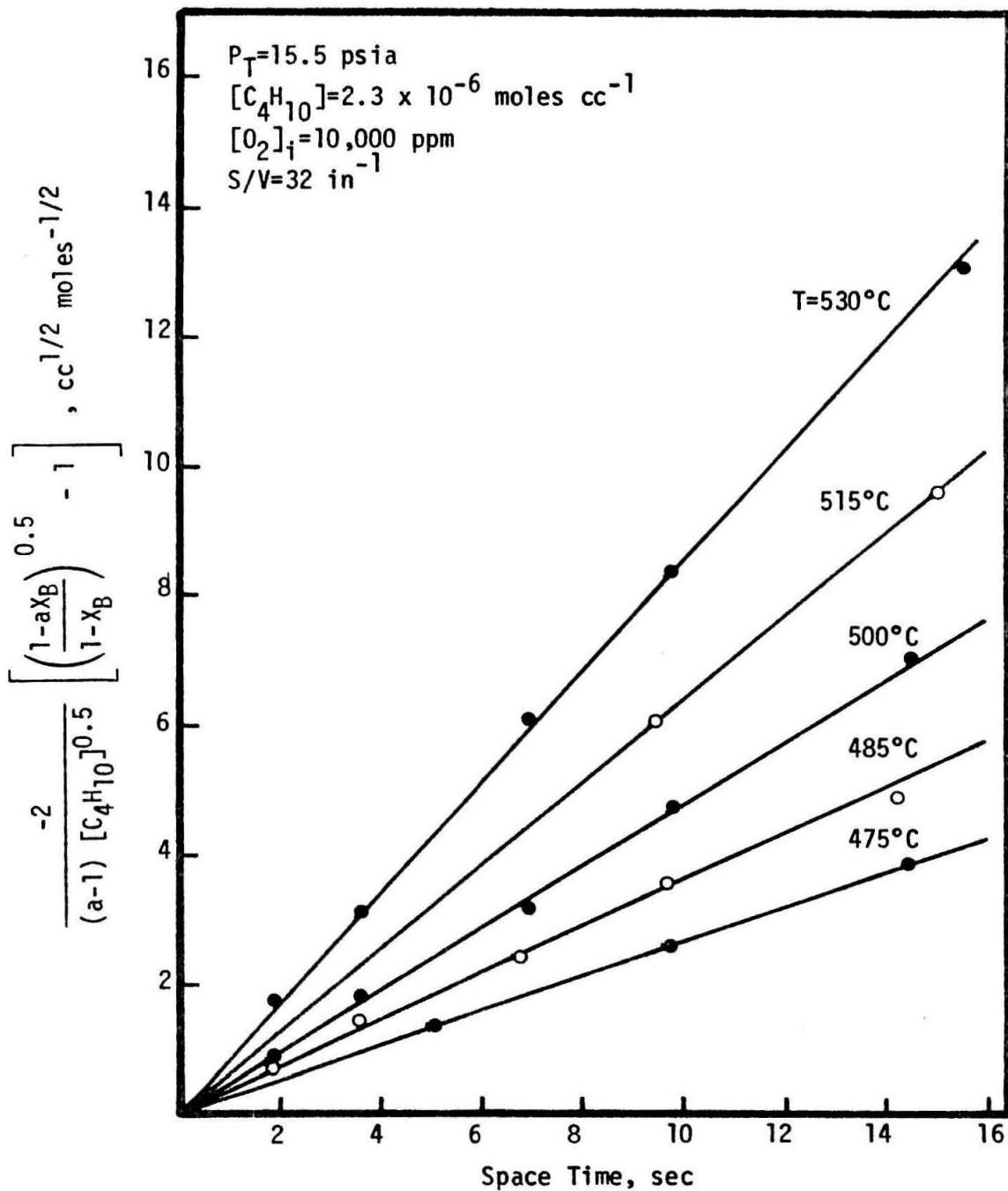


Figure 72. Variation of the rate constant, k' , as a function of temperature.

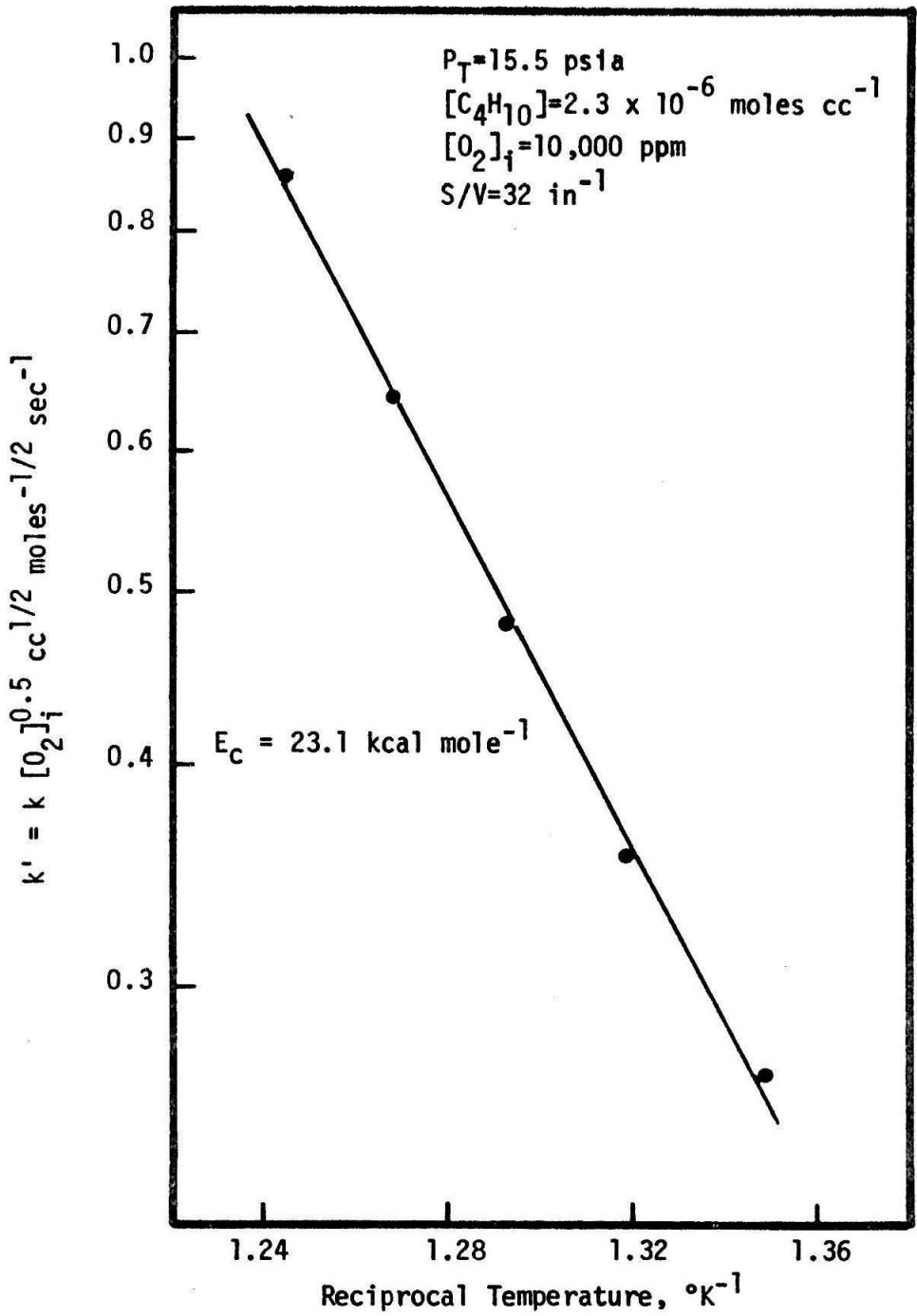


Figure 73. Arrhenius plot for the oxidative dehydrogenation of butane.

k' , was $1.6 \pm 0.2 \times 10^6 \text{ cc}^{1/2} \text{ moles}^{-1/2} \text{ sec}^{-1}$. Based on the rate constant k , a frequency factor of $4 \pm 3 \times 10^9 \text{ cc moles}^{-1} \text{ sec}^{-1}$ resulted.

Appleby, et al (17) also concluded that the orders of the reaction with respect to butane and oxygen were approximately 1.5 and 0.5, respectively. A value of $21 \text{ kcal mole}^{-1}$ was computed for the activation energy. However, as previously discussed, the distribution of products was different in the pyrex reactor of $S/V = 6.7 \text{ in}^{-1}$.

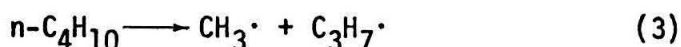
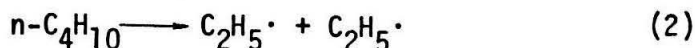
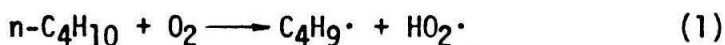
Before concluding the discussion on the rate of the oxidation, it should be mentioned that there is no reason that a simple power-law expression of the rate is warranted. However, until a detailed mechanism of the oxidation is established, the power-law expression has been demonstrated to approximate the experimental results for the initial reaction.

The mechanism of the oxidative decomposition of butane

In view of the complex dependence of the distribution of products on temperature, concentrations of the reactants and space time, additional data are required before a detailed reaction mechanism may be established. The gas-phase oxidation of hydrocarbons is recognized as a complex free-radical process (37, 46, 65). The nature and extent of the surface are also quite important in oxidations (22, 37). For the oxidative decomposition of butane, the influence of the surface is apparent from a comparison of the present work with that of Appleby, et al (17). Appleby, using a pyrex reactor ($S/V = 6.7 \text{ in}^{-1}$), detected no carbon dioxide at conversions of butane below 8 per cent. In the present work carbon dioxide was observed at conversions of butane as

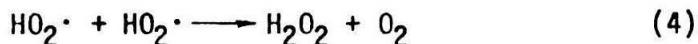
low as 0.1 per cent. The moles of butane combined with each mole of oxygen, when all of the oxygen was consumed, were reported to vary from ratios of 2 to 15. This should be compared with values of 0.2 to 1 in the present work. With these considerations in mind, possible schemes for the formation of the observed products have been suggested below.

Initiation of the chains may occur by the following steps.



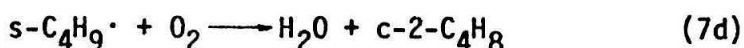
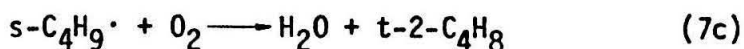
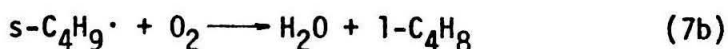
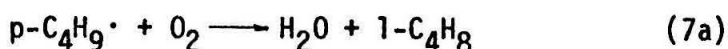
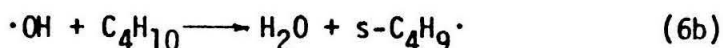
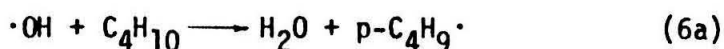
As step (1) is 30 to 40 kcal mole⁻¹ more favorable than either step (2) or step (3), initiation by the reaction of oxygen and butane to form butyl and hydroperoxide radicals will predominate (66) unless the concentration of oxygen is extremely low (several parts-per-million).

As evidenced by Knox (37), the abstraction of hydrogen by hydroperoxide radicals is thought to be a very slow reaction. Thus a means of converting the hydroperoxide radicals into more active chain carriers is required. This may be accomplished by a degenerate branching process involving hydrogen peroxide.

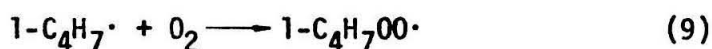
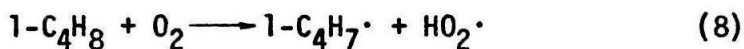


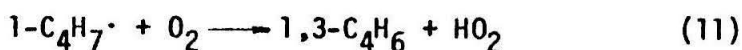


Step (5) is known to be catalyzed by the surface of a reactor (67); however, the homogeneous reaction is thought to occur rapidly above 470°C (37). The hydroxyl radicals may abstract a hydrogen from butane to form water and either a primary or secondary butyl radical, and the following chain of events may take place.

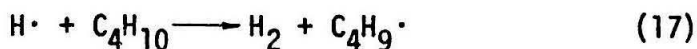
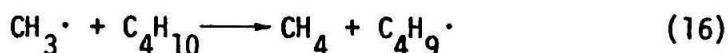
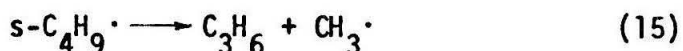
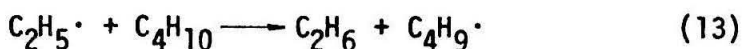
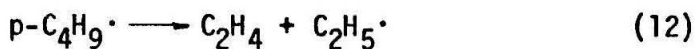


The isomerization of primary and secondary butyl radicals is assumed to be slow as suggested by Benson (61). The above scheme satisfactorily accounts for the distribution of butenes observed in the products. 1,3-Butadiene may be formed by the subsequent oxidation of 1-butene in the following manner.

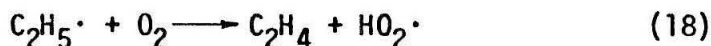




Alternate to steps (6a) through (7d), the butyl radicals may decompose as in the pyrolysis.



In addition, the ethyl radical may react with oxygen to form ethylene and a hydroperoxide radical.



Whenever sufficient oxygen is present, the reaction of the ethyl and butyl radicals with oxygen will be preferred to decomposition of the radical. This accounts for the increase yield of ethylene and butenes in the oxidations.

In the apparent absence of carbon monoxide from the products, the oxidation of carbon monoxide must be extremely fast under the experimental conditions or carbon dioxide must be formed by an alternate

route. Karmilova, et al (68) studied the oxidation of methane at 574°C in the presence of $^{14}\text{C}\text{O}$. Only negligible amounts of carbon dioxide were formed from the labelled carbon monoxide. Thus, direct formation of carbon dioxide without intermediate formation of carbon monoxide is probable. The oxidation of formyl and acetyl radicals arising from aldehydes is a possible direct route for the formation of carbon dioxide. Aldehydes are primary products of the oxidation of butane at temperatures from 250 to 350°C (69, 70) and may be formed from the reactions of peroxy radicals. Aldehydes may be readily oxidized at temperatures below 300°C, a fact which may explain the absence of aldehydes from the product mixture at 500°C. The oxidations of aldehydes are extremely sensitive to the surface and in the presence of a high surface area, carbon dioxide is formed to near-total exclusion of carbon monoxide (71).

Termination of the chains occur whenever two radicals combine to form stable products. Destruction of free radicals on the surface of the reactor also aids termination of the chains. In particular, oxygenated radicals are thought to be easily destroyed on surfaces.

In conclusion, the above discussion of the mechanism of the oxidative dehydrogenation of butane in the temperature range from 470 to 600°C presents feasible routes to the formation of the observed products. However, the mechanism is not intended to be all-inclusive. For a better understanding of the mechanism, oxidations should be performed employing radioactive tracer techniques. Study of the reaction

using mass spectroscopy might reveal intermediate species such as aldehydes.

Partial oxidation of butane at lower temperatures

For temperatures of 440 and 400°C, tests were conducted in a gold microreactor, $S/V = 32 \text{ in}^{-1}$, in order to ascertain the initial products of the oxidation. An initial concentration of oxygen of 10,000 ppm, concentrations of butane from 1.0×10^{-6} to 7.0×10^{-6} moles cc^{-1} and space times of 20 sec were employed. Aldehydes and other oxygenated compounds characteristic of the low-temperature oxidation of paraffins were not observed in the effluent of the reactor. Their presence in concentrations of several parts-per-million would have been detected. At 440°C, slight formations of butenes were observed as a result of dehydrogenation; however, no reaction was noted at 400°C.

The low-temperature oxidation is either totally suppressed in a gold reactor of $S/V = 32 \text{ in}^{-1}$ or an induction period in excess of 20 sec is required for a measurable rate of reaction. Jones, et al (25) reported total suppression of the low-temperature oxidation of propane in a packed-bed reactor, viz. a reactor of high surface-to-volume ratio.

CONCLUSIONS

The pyrolysis of n-butane was investigated in a gold microreactor of $S/V = 64 \text{ in}^{-1}$ under the following conditions:

Temperature: 535 to 595°C,

Total pressure: 15 to 16 psia,

Concentration of butane: 5×10^{-7} to 1×10^{-5} moles cc^{-1} ,

Conversion of butane: less than 2.5 per cent,

Space time: 1 to 5 sec.

The rate of disappearance of butane was accurately described by the following equation:

$$-R_{\text{C}_4\text{H}_{10}} = k [\text{C}_4\text{H}_{10}]^{1.50} \text{ moles cc}^{-1} \text{ sec}^{-1}. \quad (31)$$

For an untreated reactor,

$$k = 1.75 \times 10^{-7} \exp(-66,000/RT) \text{ cc}^{1/2} \text{ moles}^{-1/2} \text{ sec}^{-1}, \quad (32)$$

and for an acid-treated reactor,

$$k = 2.45 \times 10^{16} \exp(-63,000/RT) \text{ cc moles}^{-1/2} \text{ sec}^{-1}. \quad (33)$$

Considering experimental error, kinetics in untreated and acid-treated reactors were approximately the same. Departure from kinetics of three-halves order was not observed at concentrations of butane below 4×10^{-6} moles cc^{-1} as had been reported in earlier work. This discrepancy in the earlier work was shown to be a result of undesirable energy transfer.

Equal molar quantities of methane and propylene were observed.

Ethylene, ethane, and hydrogen constituted the remainder of the products. Higher temperatures and lower concentrations of butane favored increased formation of ethylene at the expense of ethane. A comparison of these results with the work of previous investigations indicated similar kinetics for the pyrolysis in gold, pyrex, or quartz reactors. This indicated that the reaction primarily occurs homogeneously.

The influence of small quantities of oxygen on the pyrolysis of n-butane had not been previously investigated. Trace quantities of oxygen, 5 to 500 ppm, drastically effected the pyrolysis. Although formation of the cracked products was decreased approximately 70 per cent relative to the pyrolysis in the absence of oxygen, the distribution of the cracked products remained unchanged. Yields of 1-butene, t-2-butene, c-2-butene, 1,3-butadiene, and water increased with increasing concentrations of oxygen. Increased proportions of butenes in the products were favored at lower temperatures and lower concentrations of butane.

A study of the reaction between oxygen and butane was conducted in gold microreactors of $S/V = 32 \text{ in}^{-1}$ under the following conditions:

Temperature: 470 to 595°C,

Total pressure: 15 to 16 psia,

Concentration of butane: 7×10^{-5} to 8×10^{-6} moles cc^{-1} ,

Initial concentration of oxygen: 375 to 10,000 ppm,

Conversions of butane: less than 1.0 per cent,

Conversions of oxygen: 5 to 100 per cent,

Space time: 1 to 16 sec.

The surface of the reactor had been washed repeatedly with nitric acid and heated to 500°C to remove impurities in the gold that might chemisorb oxygen. No previous study of the oxidative dehydrogenation of n-butane had been reported for conversions of butane less than 8 per cent. In the present investigation, conversions of butane, always less than one per cent, were generally between 0.2 and 0.5 per cent. Even at these low conversions, secondary reactions of olefin products were significant.

The rate of disappearance of butane was described on the basis of the following equation:

$$-R_{C_4H_{10}} = k [C_4H_{10}]^{1.50} [O_2]^{0.5} \text{ moles cc}^{-1} \text{ sec}^{-1} \quad (34)$$

where

$$k = 4 \times 10^9 \exp(-23,100/RT) \text{ cc moles}^{-1} \text{ sec}^{-1} . \quad (35)$$

The frequency factor varied within 75 per cent of the above value depending upon the initial concentrations of the reactants. Improved agreement with the data, ± 14 per cent, was achieved by defining a new rate constant as follows:

$$k' = [O_2]_i^{0.5} k . \quad (36)$$

The initial reaction was the oxidative dehydrogenation of the butane with primarily formation of isomers of butene and water. As the reaction progressed, carbon dioxide, 1,3-butadiene, and the cracked

products increased. Aldehydes and other oxygenated compounds that result from the low-temperature partial oxidation of butane were not detected in the products.

Increased yields of the cracked products were generally observed at higher temperatures, longer space times, higher concentrations of butane, and lower concentrations of oxygen. The stoichiometry of the overall reaction was also a function of the operating conditions. The moles of oxygen consumed per mole of butane reacted was proportional to the square root of the initial concentrations of oxygen to butane and inversely proportional to the temperature. Changes in the stoichiometry and the distribution of products with temperature, concentrations of reactants, and space time was interpreted in terms of competitive reactions of the alkyl radicals.

At temperatures below 440°C, no reactions between oxygen and butane were observed at space times up to 20 sec. It was concluded that either the low-temperature partial oxidation of butane is completely suppressed in a gold reactor of relatively high surface-to-volume ratio or an induction period in excess of 20 sec is required for the reaction to occur.

RECOMMENDATIONS FOR FUTURE STUDY

Without modification of the analytical system, several projects could be undertaken that would contribute to a better understanding of hydrocarbon reactions. The co-pyrolysis of n-butane and propane is of possible interest as commercial thermal-cracking processes use these materials as feedstocks for the production of olefins. Since the pyrolysis of propane requires higher temperatures than the cracking of butane, optimum control of the cracking process for increased selectivity in the formation of products would be important.

Along similar lines, commercial processes of the pyrolysis of paraffins are operated at high conversions of the paraffin. Olefins appearing in the products are known to inhibit the reaction. Thus, a study of the co-pyrolysis of n-butane and a low-molecular-weight olefin would be of commercial interest. With the olefin in the reactants, a controlled study of the inhibition at low conversions of n-butane could be made and the results compared with inhibition of the pyrolysis of n-butane at high conversions. The co-pyrolysis of n-butane and ethylene might reveal information on the minor formation of the butenes in the pyrolysis of n-butane.

The influence of small quantities of oxygen on the pyrolysis of butane at relatively high conversions as might be encountered in industry has not been defined. In the initial stages of the reaction, oxygen appears to act either as an inhibitor or a catalyst depending upon the nature and extent of the surface. In talking with research people

in industry, consensus was that small quantities of oxygen had no influence on the inhibited pyrolysis of high conversion of paraffin.

With regard to the partial oxidation of n-butane, numerous areas of research remain untouched. A study of the dehydrogenation has not been made in vessels of various surfaces or over a range of surface-to-volume ratios. The oxidative dehydrogenation of n-butane has not been studied in the presence of trace quantities of hydrogen peroxide or formaldehyde, compounds that are predicted to have a significant influence on the reaction from the proposed mechanism. The selective formation of carbon monoxide or carbon dioxide under various conditions in the oxidative dehydrogenation of butane has not satisfactorily been explained. Although the use of radioactive tracer techniques would require additional investment in equipment, the origin of the carbon oxides could be elucidated by a study of this nature.

Extension of the present work to include the partial oxidation of n-butane at lower temperatures could be achieved with the use of longer reactors for increased residence times. Should the low-temperature reaction be totally suppressed in reactors of relatively high surface-to-volume ratios, reactors of larger diameter as well as length would be necessary. Gold tubing of larger diameter would have to be special ordered. The present analytical system was designed with the analysis of the oxygenated products of the low-temperature oxidation in mind.

As olefins are more easily oxidized than the analogous paraffin, secondary reaction of the olefin products with oxygen may be significant

in the partial oxidation of alkanes. Using the existing equipment and analytical network, studies of the oxidation of c-2-butene, t-2-butene, 1-butene, and propylene could be accomplished. A comparison of the relative rates of oxidation of olefin and paraffin could be accomplished using co-oxidation experiments employing mixtures of olefin, paraffin, and oxygen in the reactants.

The areas of endeavor that have been discussed, and undoubtedly the list could have been lengthened especially in the oxidation, present a tremendous challenge for definitive research. In part, the obstacles are a result of the complexity of the product mixtures and their possible dependence upon the reactor surface.

NOMENCLATURE

A	frequency factor of an Arrhenius rate constant
E_C	activation energy of an Arrhenius rate constant
P_T	total pressure of the reactor
R	universal gas constant
$-R_{C_4H_{10}}$	rate of disappearance of n-butane by reaction
S	surface area of the reactor
T	temperature of the reactor
V	volume of the reactor
X_B	fractional conversion of n-butane
a	$q [C_4H_{10}]_i / [O_2]_i$
k	Arrhenius rate constant
m	order of the reaction with respect to butane
n	order of the reaction with respect to oxygen
q	moles of oxygen consumed per mole of butane reacted
α	ratio of ethylene to ethane in the products
β	ratio of C_2 hydrocarbons to the sum of the methane and propylene in the products
τ	space time or mean contact time

REFERENCES

1. J. R. Barker and W. H. Corcoran, Ph. D. Thesis, California Institute of Technology, 1969.
2. J. H. Purnell and C. P. Quinn, Proc. Roy. Soc., 270A, 267 (1962).
3. N. H. Sagert and K. J. Laidler, Can. J. Chem., 41, 838 (1963).
4. F. O. Rice, J. Am. Chem. Soc., 53, 1959 (1931).
5. R. N. Pease and E. S. Durgan, J. Am. Chem. Soc., 52, 1262 (1930).
6. E. W. R. Steacie and I. E. Puddington, Can. J. Res., 16B, 260 (1938).
7. V. A. Crawford and E. W. R. Steacie, Can. J. Chem., 31, 937 (1953).
8. H. J. Hepp and F. E. Frey, Ind. Eng. Chem., 45, 410 (1953).
9. M. Nehaus and L. F. Marek, Ind. Eng. Chem., 24, 400 (1932).
10. B. G. Gowenlock, Prog. React. Kin., 3, 173 (1965).
11. C. P. Quinn, Symposium on the Kinetics of Pyrolytic Reactions, Ottawa, 1964.
12. J. H. Purnell and C. P. Quinn, Nature, Lond., 189, 656 (1961).
13. J. H. Purnell and C. P. Quinn, J. Chem. Soc., 4128 (1961).
14. J. H. Purnell and C. P. Quinn, Can. J. Chem., 43, 720 (1965).
15. Y. L. Wang, R. G. Rinker and W. H. Corcoran, Ind. Eng. Chem. Fund., 2, 161 (1963).
16. Y. L. Wang and W. H. Corcoran, Ph. D. Thesis, California Institute of Technology, 1963.
17. W. G. Appleby, W. H. Avery, W. K. Meerbott and A. F. Sartor, J. Am. Chem. Soc., 75, 1809 (1953).

18. V. V. Voevodsky, Trans. Far. Soc., 55, 65 (1959).
19. R. Martin, M. Niclause and M. Dzierzynski, Compt. Rend., 254, 1786 (1962).
20. R. Martin and M. Niclause, J. Chim. Phys., 61, 802 (1964).
21. M. Niclause, R. Martin, A. Combes and M. Dzierzynski, Can. J. Chem., 43, 1120 (1965).
22. M. Niclause, R. Martin, A. Combes, J. Fusy and M. Dzierzynski, Ind. Chim. Belge, 32, 674 (1967).
23. J. J. Kalvinskas and W. H. Corcoran, Ph. D. Thesis, California Institute of Technology, 1959.
24. R. R. Baldwin and R. W. Walker, Trans. Far. Soc., 60, 1236 (1964).
25. J. H. Jones, T. E. Daubert and M. R. Fenske, Ind. Eng. Chem. Proc. Des. Dev., 8, 17 (1969).
26. R. Sampson, J. Chem. Soc., 5095 (1963).
27. A. Steitz, J. W. Palm and P. K. Garetson, Hydro. Proc. Petrol. Refiner, 41 (6), 167 (1962).
28. R. C. Lemon, D. Scott, P. C. Johnson and J. M. Berty, U. S. Patent 3, 132, 156 (May 5, 1964).
29. C. R. Harris, U. S. Patent 2,533,581 (Dec. 12, 1950).
30. J. F. Skrivan, Ph. D. Thesis, The Johns Hopkins University, 1959.
31. Y. D. Norikov and E. A. Blyumberg, Izv. Akad. Nauk SSSR, Otd. Khim. Nauk, 8, 1357 (1962).
32. Y. D. Norikov, A. V. Boblev and E. A. Blyumberg, Izv. Akad. Nauk SSSR, Ser. Khim, 5, 826 (1964).

33. N. A. Slavinskaya, E. F. Gribova, G. G. Demidova, S. A. Kamenetskaya and S. Y. Pshezhetskii, Zhur. Fiz. Khim., 37 (7), 1549 (1963).
34. M. B. Nieman and A. F. Lukovinkov, Zhur. Fiz. Khim., 29, 1410 (1955).
35. L. F. Albright and E. M. Winter, Ind. Eng. Chem. Prod. Res. Dev., 5, 244 (1966).
36. C. N. Satterfield and R. C. Reid, J. Chem. Eng. Data, 6, 302 (1961).
37. J. H. Knox, Comb. Flame, 9, 297 (1965).
38. J. H. Knox, R. F. Smith and A. F. Trotman-Dickenson, Trans. Far. Soc., 54, 1509 (1958).
39. R. R. Baldwin, D. Jackson, R. W. Walker and S. J. Webster, "Tenth Symposium (International) on Combustion, p 423, Combustion Institute: Pittsburg, 1965.
40. J. H. Knox and C. H. J. Wells, Trans. Far. Soc., 59, 2786 and 2801 (1963).
41. J. H. Knox, Trans. Far. Soc., 56, 1225 (1960).
42. J. Hay, J. H. Knox and J. M. C. Turner, "Tenth Symposium (International) on Combustion," p 361, Combustion Institute: Pittsburg, 1965.
43. A. P. Zeelenberg and A. F. Bickel, J. Chem. Soc., 4014 (1961).
44. L. F. Albright, Chem. Eng., 74, 197 (1967).

45. C. N. Satterfield and R. C. Reid, "Fifth Symposium (International) on Combustion," Reinhold, New York, 1955.
46. N. N. Semenov, "Photochemistry and Reaction Kinetics," p 229, Cambridge University Press, Cambridge, 1967.
47. P. A. Hersch, Anal. Chem., 32, 1030 (1960).
48. M. Trombetta and J. Happel, A.I.Ch.E. J., 11, 1041 (1965).
49. N. Bortner and G. Parravano, J. Am. Chem. Soc., 78, 4533 (1956).
50. B. M. W. Trapnell, Proc. Roy. Soc., 218A, 566 (1953).
51. J. T. Kummer, J. Phys. Chem., 63, 460 (1959).
52. B. L. Crynes and L. F. Albright, Ind. Eng. Proc. Des. Dev., 8, 25 (1969).
53. A. F. Trotman-Dickenson, "Gas Kinetics," p 125, Butterworth Scientific Publication, London, 1955.
54. K. J. Laidler, N. H. Sagert and B. W. Wojciechowski, Proc. Roy. Soc., 270A, 242 (1962).
55. P. Goldfinger, M. Letort and M. Niclause, "Contribution a l'etude de la structure moleculaire," Victor Henri Commemorative Volume, p 283, Desoer, Liege, 1948.
56. L. F. Loucks and K. J. Laidler, Can. J. Chem., 45, 2795 (1967).
57. H. O. Pritchard, R. G. Sowden and A. F. Trotman-Dickenson, Proc. Roy. Soc., 217A, 563 (1953).
58. A. Kuppermann and J. G. Larson, Long abstracts of papers presented at American Chemical Society meeting, Washington, D. C., March 21-24, 1962.

59. J. R. McNesby and A. S. Gordon, J. Am. Chem. Soc., 78, 3570 (1956).
60. J. H. Purnell and C. P. Quinn, "Photochemistry and Reaction Kinetics," p 330, Cambridge University Press, Cambridge, 1967.
61. J. W. Benson, "Thermochemical Kinetics," p 166, John Wiley and Sons, Inc., New York, 1968.
62. R. B. Scott, W. J. Ferguson and F. G. Brickwedde, J. Res. Natl. Bur. Standards, 33, 1 (1944).
63. H. H. Voge and N. C. May, J. Am. Chem. Soc., 68, 550 (1946).
64. R. B. Cundall and T. F. Palmer, Trans. Far. Soc., 57, 1936 (1961).
65. S. W. Benson, "Thermochemical Kinetics," p 146, John Wiley and Sons, Inc., New York, 1968.
66. J. O. Edwards, "Peroxide Reaction Mechanisms," p 111, Interscience Publishers, New York, 1962.
67. R. R. Baldwin and D. Bratten, "Eighth Symposium (International) on Combustion," p 110, Williams and Wilkins: Baltimore, 1962.
68. L. V. Karmilova, N. S. Enikolopyan and A. B. Nalbandyan, J. Phys. Chem. USSR, 35, 1458 (1961).
69. M. B. Neiman and G. I. Feklisov, J. Phys. Chem., 30, 1126 (1956).
70. A. F. Lukovnykov and M. B. Neiman, J. Phys. Chem. USSR, 29, 1410 (1955).
71. J. F. Griffiths and G. Skirrow, Oxid. and Comb. Rev., 3, 47 (1968).

APPENDIX A

A tabular summary of data taken on the pyrolysis and partial oxidation of n-butane is presented. By convention, if the yield of a compound was identically zero, i.e. it was not observed as a product, then its value will be given as 0.0000. If a minor product was detected but in a relatively minute amount, its value will be given as .0000. Asterisks denote that a particular compound was detected but not measured.

Series A. Pyrolysis of butane in an untreated reactor, S/V = 64 in⁻¹.

Run	Temp. (°C)	Total Pressure (psia)	Butane Pressure (psia)	Space Time (sec)	CH ₄	Moles Product per 100 Moles of Butane in Effluent C ₂ H ₆	C ₂ H ₄	C ₃ H ₆
1	580	15.20	8.78	1.01	.2890	.1068	.1638	.3080
2	580	15.18	8.79	1.01	.2610	.0922	.1202	.3050
3	580	15.20	8.78	1.02	.3329	.1243	.1961	.3586
4	580	15.24	5.27	1.07	.2080	.0964	.1816	.2670
5	580	15.24	5.27	1.07	.2872	.0993	.1778	.3109
6	580	15.25	5.29	1.09	.3756	.1159	.2156	.3702
7	580	15.25	3.39	1.10	.2910	.0980	.1814	.3120
8	580	15.25	3.39	1.10	.3219	.0915	.2002	.3251
9	580	15.30	1.68	1.17	.1924	.0548	.1584	.2475
10	580	15.30	1.68	1.17	.2485	.0418	.1751	.2494
11	580	15.30	1.51	1.14	.2110	.0498	.1514	.2196
12	580	15.30	1.51	1.14	.2470	.0575	.1668	.2532
13	580	15.32	.63	1.22	.1896	.0387	.1358	.1954
14	595	15.16	9.45	.98	.6556	.1943	.3759	.6524
15	595	15.17	9.45	.97	.6103	.2104	.3601	.6340
16	595	15.17	9.45	.97	.6088	.2080	.3378	.6069
17	595	15.15	9.47	.98	.6312	.2112	.3678	.6040
18	595	15.27	5.12	.98	.4945	.1476	.2962	.4729
19	595	15.24	5.13	.98	.4875	.1550	.3124	.5053
20	595	15.27	5.11	.99	.5044	.1466	.3074	.4880
21	595	15.33	3.32	.94	.4526	.1246	.2818	.4377
22	595	15.30	3.31	.96	.4297	.1162	.2734	.4236
23	595	15.35	1.45	.89	.3549	.0706	.2523	.3557
24	595	15.33	1.45	.89	.3692	.0795	.2505	.3583

Series A, continued.

Run	Temp. (°C)	Total Pressure (psia)	Butane Pressure (psia)	Space Time (sec)	CH ₄	C ₂ H ₆	C ₂ H ₄	C ₃ H ₆
25	595	15.35	1.44	.89	.3524	.0735	.2334	.3565
26	595	15.40	.74	.88	.2865	.0515	.2107	.2949
27	595	15.37	.74	.88	.2959	.0516	.2093	.2881
28	595	15.40	.73	.88	.2615	.0484	.1996	.2862
29	565	15.22	9.02	1.02	.1732	.0605	.0916	.1640
30	565	15.19	9.00	1.01	.1645	.0626	.0889	.1701
31	565	15.20	8.99	1.01	.1701	.0590	.0881	.1757
32	565	15.34	4.46	1.06	.1242	.0415	.0670	.1238
33	565	15.30	4.46	1.05	.1196	.0421	.0693	.1253
34	565	15.30	2.27	1.15	.0915	.0242	.0481	.0955
35	565	15.33	2.26	1.16	.1010	.0292	.0615	.1009
36	565	15.34	2.28	1.17	.0994	.0281	.0635	.1047
37	565	15.37	.97	1.22	.0656	.0188	.0513	.0755
38	565	15.34	1.01	1.21	.0747	.0172	.0501	.0778
39	550	15.24	8.71	1.01	.0804	.0326	.0377	.0783
40	550	15.26	8.72	1.02	.0619	.0237	.0324	.0661
41	550	15.25	8.72	1.01	.0772	.0282	.0380	.0728
42	550	15.24	8.77	1.00	.0504	.0222	.0276	.0632
43	550	15.30	4.24	1.09	.0545	.0188	.0315	.0605
44	550	15.30	4.24	1.09	.0515	.0167	.0263	.0503
45	550	15.30	4.23	1.09	.0558	.0189	.0309	.0581
46	550	15.30	2.29	1.14	.0330	.0133	.0237	.0465
47	550	15.33	2.28	1.15	.0415	.0128	.0222	.0414
48	550	15.35	2.30	1.15	.0346	.0141	.0258	.0438

Series A, continued.

Run	Temp. (°C)	Total Pressure (psia)	Butane Pressure (psia)	Space Time (sec)	CH ₄	Moles Product per 100 Moles of Butane in Effluent		
						C ₂ H ₆	C ₂ H ₄	C ₃ H ₆
49	550	15.34	1.22	1.23	.0252	.0095	.0230	.0388
50	550	15.32	1.27	1.21	.0326	.0085	.0192	.0332
51	535	15.21	8.55	1.02	.0336	.0118	.0168	.0346
52	535	15.24	8.56	1.03	.0320	.0118	.0154	.0320
53	535	15.25	8.56	1.04	.0336	.0122	.0161	.0340
54	535	15.33	4.35	1.08	.0219	.0086	.0134	.0236
55	535	15.30	4.36	1.07	.0229	.0077	.0112	.0226
56	535	15.33	2.17	1.19	.0170	.0072	.0118	.0193
57	535	15.31	2.18	1.18	.0187	.0058	.0100	.0187

Series B. Pyrolysis of butane in a reactor, S/V = 64 in⁻¹, pretreated with oxygen.

Run	Temp. (°C)	Total Pressure (psia)	Butane Pressure (psia)	Space Time (sec)	Moles Product per 100 Moles of Butane in Effluent			
					CH ₄	C ₂ H ₆	C ₂ H ₄	C ₃ H ₆
1	580	15.17	7.73	1.11	.0943	.0235	.0669	.0911
2	580	15.20	7.74	1.12	.0939	.0321	.0510	.0904
3	580	15.22	7.72	1.13	.1048	.0358	.0597	.0914
4	580	15.19	7.88	1.09	.0968	.0303	.0512	.0915
5	580	15.25	3.94	1.09	.1166	.0277	.0564	.0832
6	580	15.29	3.92	1.11	.0880	.0253	.0502	.0828
7	580	15.40	1.87	1.08	.0698	.0170	.0452	.0650
8	580	15.37	1.87	1.07	.0646	.0158	.0391	.0599

-189-

Note: Reactor was exposed to oxygen at a temperature of 550°C for a period of several hours, subsequently purged with argon.

Series C. Pyrolysis of butane subsequent to Series B, $S/V = 64 \text{ in}^{-1}$.

Run	Temp. (°C)	Total Pressure (psia)	Butane Pressure (psia)	Space Time (sec)	Moles Product per 100 Moles of Butane in Effluent			
					CH ₄	C ₂ H ₆	C ₃ H ₆	
1	580	15.20	8.00	1.12	.0880	.0303	.0516	.0827
2	580	15.22	8.04	1.14	.0867	.0293	.0483	.0821
3	580	15.36	3.61	1.06	.0555	.0167	.0369	.0566
4	580	15.33	3.61	1.05	.0481	.0156	.0313	.0494

Note: Vacuum of less than 10 microns was exerted on reactor that had been pretreated with oxygen before Series C was begun.

Series E. Start-up behavior in an acid-treated reactor, S/V = 64 in⁻¹.

Run	Temp. (°C)	Running Time (min)	Total Pressure (psia)	Butane Pressure (psia)	Space Time (sec)	Moles Product per 100 Moles of Butane in Effluent		
						CH ₄	C ₂ H ₆	C ₂ H ₄ C ₃ H ₆
1	575	15.5	15.17	8.62	1.00	.0836	.0267	.0506 .0673
2	575	37.5	15.16	8.90	1.02	.0797	.0261	.0433 .0672
3	575	52.0	15.15	8.87	1.02	.0831	.0282	.0495 .0712
4	575	75.5	15.14	8.78	1.00	.0847	.0251	.0435 .0639
5	575	85.0	15.14	8.87	1.01	.0978	.0274	.0486 .0746
6	575	200.0	15.14	8.85	1.01	.1170	.0252	.0425 .0647
7	575	235.0	15.14	8.84	1.02	.2045	.0254	.0428 .0652
8	575	315.0	15.12	8.84	1.01	.2349	.0253	.0438 .0680
9	575	363.0	15.12	8.84	1.01	.2310	.0271	.0430 .0690
10	575	485.0	15.14	8.84	1.02	.2318	.0302	.0497 .0767
11	575	543.0	15.10	8.82	1.01	.2250	.0310	.0509 .0771
12	575	615.0	15.13	8.85	1.02	.2312	.0305	.0521 .0835
13	575	697.0	15.12	8.84	1.01	.2216	.0304	.0512 .0829
14	575	841.0	15.14	8.84	1.02	.2298	.0383	.0656 .1050
15	575	867.0	15.13	8.81	1.01	.2229	.0356	.0575 .0991
16	575	904.0	15.12	8.85	1.02	.2320	.0411	.6095 .1110
17	575	1339.0	15.14	8.88	1.02	.2314	.0505	.0831 .1379
18	575	1362.0	15.12	8.89	1.02	.2263	.0486	.0783 .1370
19	575	1498.0	15.14	8.86	1.02	.2469	.0556	.0900 .1563
20	575	1652.0	15.13	8.80	1.02	.2452	.0662	.1037 .1764
21	575	1735.0	15.10	8.78	1.01	.2588	.0657	.1059 .1818
22	575	1769.0	15.10	8.77	1.01	.2647	.0687	.1159 .1883
23	575	2826.0	15.16	8.86	1.03	.2912	.0871	.1363 .2288
24	575	2869.0	15.15	8.85	1.02	.2936	.0803	.1286 .2309

Series E, continued.

Run	Temp. (°C)	Running Time (min)	Total Pressure (psia)	Butane Pressure (psia)	Space Time (sec)	Moles Product per 100 Moles of Butane in Effluent			
						CH ₄	C ₂ H ₆	C ₂ H ₄	C ₃ H ₆
25	575	3105.0	15.13	8.85	1.02	.3191	.0945	.1490	.2502
26	575	3170.0	15.13	8.78	1.02	.3353	.1018	.1687	.2794
27	575	3401.0	15.16	8.86	1.03	.3359	.1012	.1606	.2912
28	575	3407.0	15.16	8.81	1.03	.3435	.1109	.1674	.2917
29	575	9167.0	15.09	8.80	1.02	.2818	.0944	.1522	.2493
30	575	9197.0	15.12	8.81	1.02	.2821	.0928	.1469	.2651
31	575	9227.0	15.14	8.80	1.03	.3149	.1027	.1643	.2789
32	575	9300.0	15.12	8.76	1.03	.3354	.1001	.1566	.2843
33	575	9350.0	15.10	8.75	1.03	.3283	.1067	.1681	.2793

Series E, continued.

Run	Running Time (min)	Moles Product per 100 Moles of Butane in Effluent			
		1-C ₄ H ₈	t-2-C ₄ H ₈	c-2-C ₄ H ₈	1,3-C ₄ H ₆
1	15.5	.1064	.0576	.0495	.0098
3	52.0	.1005	.0493	.0374	.0078
5	85.0	.0718	.0366	.0279	.0055
10	485.0	.0474	.0176	.0138	.0034
12	615.0	.0456	.0205	.0153	.0034
14	841.0	.0347	.0159	.0143	.0026
17	1339.0	.0335	.0142	.0106	.0029
20	1652.0	.0384	.0128	.0132	.0017
23	2826.0	.0247	.0161	.0118	.0012
28	3407.0	.0220	.0146	.0129	.0018
31	9227.0	.0328	.0169	.0131	.0027

Series F. Pyrolysis of butane in an acid-treated reactor, S/V = 64 in⁻¹.

Run	Temp. (°C)	Total Pressure (psia)	Butane Pressure (psia)	Space Time (sec)	CH ₄	Moles Product per 100 Moles of Butane in Effluent	C ₂ H ₆	C ₂ H ₄	C ₃ H ₆
1	575	15.15	7.33	1.28	.2884	.0955	.1505	.2679	.2679
2	575	15.15	7.68	1.23	.2946	.0992	.1592	.2756	.2756
3	575	15.15	8.12	1.15	.2954	.0958	.1520	.2705	.2705
4	575	15.15	3.50	1.11	.1921	.0526	.1018	.1610	.1610
5	575	15.15	3.80	1.09	.1929	.0525	.0962	.1644	.1644
6	575	15.15	.64	1.15	.1644	.0189	.0456	.0579	.0579
7	575	15.15	.78	1.13	.1514	.0200	.0472	.0635	.0635
8	585	15.35	7.42	1.26	.4818	.1510	.2543	.4433	.4433
9	585	15.35	7.29	1.28	.4496	.1480	.2850	.4286	.4286
10	585	15.35	7.10	1.31	.4237	.1417	.2362	.4116	.4116
11	585	15.35	4.97	1.25	.3933	.1062	.1985	.3305	.3305
12	585	15.35	4.38	1.31	.3571	.1034	.2101	.3273	.3273
13	585	15.35	2.09	1.25	.2462	.0563	.1328	.2046	.2046
14	585	15.35	2.26	1.24	.2579	.0605	.1445	.2110	.2110
15	585	15.35	.78	1.25	.2100	.0614	.0625	.1159	.1159
16	585	15.35	.82	1.24	.1962	.0320	.0920	.1294	.1294
17	595	15.53	.93	1.01	.2014	.0404	.1242	.1628	.1628
18	595	15.53	.94	1.01	.1988	.0385	.1345	.1646	.1646
19	595	15.53	1.77	1.02	.2691	.0612	.1659	.2366	.2366
20	595	15.53	1.78	1.03	.2716	.0640	.1722	.2358	.2358
21	595	15.53	3.04	1.03	.3629	.0891	.2087	.3181	.3181
22	595	15.53	3.05	1.02	.3639	.1033	.2255	.3240	.3240
23	595	15.53	4.71	1.05	.4690	.1320	.2610	.4219	.4219
24	595	15.53	4.69	1.05	.4704	.1386	.2824	.4217	.4217

Series F, continued.

Run	Temp. (°C)	Total Pressure (psia)	Butane Pressure (psia)	Space Time (sec)	CH ₄	Moles Product per 100 Moles of Butane in Effluent	C ₂ H ₆	C ₂ H ₄	C ₃ H ₆
25	595	15.53	8.29	1.10	.6733	.2110	.3643	.6192	
26	595	15.53	8.27	1.09	.6401	.2100	.3680	.6259	
27	535	15.53	7.05	1.04	.0429	.0130	.0172	.0363	
28	535	15.53	7.03	1.04	.0443	.0136	.0195	.0353	
29	535	15.53	5.43	1.03	.0413	.0108	.0154	.0304	
30	535	15.53	5.43	1.03	.0422	.0114	.0165	.0298	
31	535	15.53	3.91	1.04	.0398	.0088	.0124	.0233	
32	535	15.53	3.90	1.04	.0420	.0092	.0146	.0242	
33	535	15.53	2.38	1.03	.0385	.0057	.0093	.0165	
34	545	15.61	.92	1.04	.0305	.0048	.0120	.0146	
35	545	15.61	2.46	1.03	.0412	.0088	.0164	.0282	
36	545	15.61	2.44	1.04	.0437	.0092	.0179	.0292	
37	545	15.61	3.88	1.01	.0501	.0124	.0195	.0362	
38	545	15.61	3.86	1.00	.0518	.0121	.0203	.0363	
39	545	15.61	5.38	1.03	.0626	.0170	.0244	.0477	
40	545	15.61	5.37	1.03	.0647	.0171	.0232	.0466	
41	545	15.61	7.23	1.04	.0731	.0225	.0325	.0578	
42	555	15.70	7.03	1.07	.1080	.0347	.0558	.0930	
43	555	15.70	7.03	1.06	.1064	.0354	.0498	.0953	
44	555	15.70	5.70	1.05	.0984	.0287	.0445	.0824	
45	555	15.70	5.69	1.05	.1031	.0296	.0516	.0859	
46	555	15.70	4.10	1.04	.0836	.0220	.0366	.0658	
47	555	15.70	4.09	1.04	.0835	.0221	.0398	.0596	
48	555	15.70	2.62	1.05	.0744	.0185	.0291	.0560	

Series F, continued.

Run	Temp. (°C)	Total Pressure (psia)	Butane Pressure (psia)	Space Time (sec)	CH ₄	Moles Product per 100 Moles of Butane in Effluent		
						C ₂ H ₆	C ₂ H ₄	C ₃ H ₆
49	555	15.70	2.62	1.05	.0709	.0151	.0318	.0483
50	555	15.70	.96	1.05	.0528	.0080	.0181	.0260
51	555	15.70	.96	1.05	.0662	.0075	.0187	.0246
52	565	15.63	7.32	1.06	.1699	.0566	.0828	.1561
53	565	15.63	7.31	1.07	.1744	.0592	.0926	.1557
54	565	15.63	5.64	1.04	.1457	.0447	.0698	.1286
55	565	15.63	5.64	1.04	.1510	.0476	.0792	.1293
56	565	15.63	4.18	1.04	.1261	.0348	.0606	.1073
57	565	15.63	4.17	1.04	.1298	.0378	.0688	.1080
58	565	15.63	2.53	1.04	.1092	.0234	.0463	.0786
59	565	15.63	2.50	1.05	.1071	.0243	.0530	.0838
60	565	15.63	1.39	1.04	.0923	.0162	.0360	.0543
61	565	15.63	1.39	1.04	.0926	.0165	.0389	.0555
62	565	15.63	.71	1.05	.0853	.0113	.0283	.0367
63	565	15.63	.73	1.03	.0967	.0120	.0284	.0392

Series G. Pyrolysis of butane in an acid-treated reactor, S/V = 64 in⁻¹.

Run	Temp. (°C)	Total Pressure (psia)	Butane Pressure (psia)	Space Time (sec)	CH ₄	C ₂ H ₆	C ₂ H ₄	C ₃ H ₆
1	575	15.68	4.34	1.07	.2553	.0764	.1464	.2233
2	575	15.68	4.24	1.08	.2520	.0750	.1372	.2237
3	575	15.68	3.43	1.06	.2068	.0605	.1116	.1877
4	575	15.68	3.42	1.06	.2155	.0636	.1209	.1834
5	575	15.68	2.39	1.06	.1949	.0483	.1043	.1671
6	575	15.68	2.35	1.05	.1995	.0534	.1140	.1765
7	575	15.68	1.23	1.04	.1620	.0325	.0870	.1332
8	575	15.68	1.23	1.04	.1692	.0357	.0953	.1340
9	575	15.68	.66	1.06	.1567	.0220	.0811	.1106
10	575	15.68	.64	1.06	.1542	.0239	.0831	.1065
11	575	15.68	.63	1.05	.2028	.0389	.1020	.1288
12	575	15.68	.64	1.04	.2103	.0384	.0997	.1313
13	595	15.40	.61	1.03	.1705	.0274	.1285	.1670
14	595	15.40	.58	1.03	.1644	.0261	.1253	.1578
15	595	15.40	.51	1.04	.1566	.0235	.1157	.1475
16	595	15.40	.46	1.05	.1507	.0220	.1174	.1463
17	595	15.40	1.35	1.00	.2430	.0520	.1612	.2255
18	595	15.40	1.34	1.00	.2512	.0349	.1410	.2464
19	595	15.40	2.42	1.01	.3349	.0867	.2021	.3110
20	595	15.40	2.43	1.01	.3308	.0827	.2144	.2986
21	595	15.40	4.43	1.02	.4474	.1311	.2606	.4265
22	595	15.40	4.40	1.02	.4449	.1305	.2696	.4059
23	595	15.40	6.53	1.02	.5240	.1680	.2926	.4989
24	595	15.40	6.51	1.02	.5063	.1658	.2684	.4969

Series G, continued.

Run	Temp. (°C)	Total Pressure (psia)	Butane Pressure (psia)	Space Time (sec)	CH ₄	Moles Product per 100 Moles of Butane in Effluent	C ₂ H ₆	C ₂ H ₄	C ₃ H ₆
25	555	15.63	.31	1.01	.0229	.0029	.0112	.0145	.0145
26	555	15.63	.73	1.04	.0319	.0062	.0178	.0258	.0258
27	555	15.63	.71	1.04	.0298	.0057	.0167	.0251	.0251
28	555	15.63	1.30	.96	.0407	.0101	.0227	.0367	.0367
29	555	15.63	1.28	.97	.0381	.0097	.0220	.0346	.0346
30	555	15.63	2.86	1.07	.0613	.0177	.0309	.0550	.0550
31	555	15.63	2.83	1.07	.0623	.0193	.0339	.0575	.0575
32	555	15.63	5.31	.97	.0802	.0259	.0381	.0730	.0730
33	555	15.63	5.25	.97	.0792	.0279	.0406	.0719	.0719
34	575	15.63	.82	1.06	.1053	.0146	.0540	.0732	.0732
35	575	15.80	1.72	1.07	.1368	.0292	.0774	.1087	.1087
36	575	15.82	1.75	1.06	.1414	.0297	.0790	.1139	.1139
37	575	15.85	3.87	1.06	.1896	.0551	.1013	.1734	.1734

Note: Runs 1, 2, 11, 12, were for 100% dilution at entrance of reactor.
 Runs 3, 4, 5, 6, 7, 8, 9, 10 were for 70% dilution at entrance of reactor.
 Runs 34, 35, 36, 37 were for 0% dilution at entrance of reactor.
 Others are for primarily premixed reactants.

Series J. Pyrolysis of butane in an acid-treated reactor, S/V = 32 in⁻¹. Effect of trace amounts of oxygen.

Run	Temp. (°C)	Total Pressure (psia)	Butane Pressure (psia)	Initial Oxygen (ppm)	Space Time (sec)	CH ₄	C ₂ H ₆	C ₂ H ₄	C ₃ H ₆
1	575	16.19	.44	8	2.68	.0387	.0051	.0338	.0410
2	575	16.11	1.65	8	2.71	.0841	.0220	.0555	.0753
3	575	15.93	3.04	8	2.66	.1181	.0358	.0757	.1023
4	575	15.88	5.38	8	2.67	.1636	.0542	.0885	.1410
5	575	15.73	7.58	8	2.61	.2050	.0676	.1114	.1719
6	565	16.19	.48	8	2.67	.0194	.0029	.0187	.0227
7	565	16.13	.82	8	2.70	.0277	.0067	.0231	.0275
8	565	16.08	1.67	8	2.67	.0447	.0110	.0294	.0429
9	565	15.89	3.06	8	2.66	.0632	.0182	.0386	.0568
10	565	15.78	5.29	8	2.62	.0869	.0284	.0479	.0751
11	565	15.66	7.50	8	2.60	.1099	.0374	.0593	.0965
12	555	16.08	.66	8	2.65	.0122	.0033	.0108	.0122
13	555	15.94	1.86	8	2.64	.0210	.0062	.0146	.0204
14	555	15.78	3.36	8	2.66	.0316	.0100	.0188	.0285
15	555	15.70	5.23	8	2.62	.0426	.0152	.0236	.0375
16	555	15.56	7.45	8	2.63	.0500	.0174	.0274	.0471
17	545	16.06	.96	8	2.68	.0081	.0020	.0066	.0074
18	545	15.92	1.59	8	2.66	.0117	.0032	.0072	.0095
19	545	15.87	2.87	8	2.61	.0144	.0046	.0069	.0140
20	545	15.70	4.42	8	2.65	.0202	.0066	.0106	.0167
21	545	15.59	7.33	8	2.59	.0279	.0097	.0145	.0245
22	535	16.02	1.46	8	2.65	.0043	.0016	.0042	.0053
23	535	15.88	2.59	8	2.64	.0069	.0025	.0048	.0064
24	535	15.78	4.40	8	2.61	.0096	.0032	.0053	.0088

Series J, continued.

Run	Effluent Oxygen (ppm)	Moles Product per 100 Moles of Butane in Effluent						H ₂ O
		1-C ₄ H ₈	t-2-C ₄ H ₈	c-2-C ₄ H ₈	1,3-C ₄ H ₈	CO ₂		
1	0	.0072	.0024	.0009	0.0000	0	.0583	
2	0	.0046	.0030	.0011	0.0000	0	.0156	
3	0	.0026	.0004	.0008	0.0000	0	.0084	
4	0	.0029	.0025	.0012	0.0000	0	.0047	
5	0	.0017	.0031	.0020	0.0000	0	.0033	
6	0	.0085	.0025	.0016	0.0000	0	.0544	
7	0	.0049	.0009	.0014	0.0000	0	.0314	
8	0	.0047	.0023	.0007	0.0000	0	.0154	
9	0	.0022	.0031	0.0000	0.0000	0	.0083	
10	0	.0020	.0016	.0005	0.0000	0	.0048	
11	0	.0010	.0022	.0016	0.0000	0	.0033	
12	0	.0058	.0013	.0007	0.0000	0	.0388	
13	0	.0041	.0026	.0001	0.0000	0	.0137	
14	0	.0011	.0024	0.0000	0.0000	0	.0075	
15	0	.0016	.0015	.0005	0.0000	0	.0048	
16	0	.0002	.0024	0.0000	0.0000	0	.0033	
17	0	.0047	.0031	.0006	0.0000	0	.0267	
18	0	.0024	.0015	0.0000	0.0000	0	.0160	
19	0	.0011	0.0000	0.0000	0.0000	0	.0089	
20	0	.0014	.0019	0.0000	0.0000	0	.0057	
21	0	.0006	.0012	0.0000	0.0000	0	.0034	
22	0	.0042	.0022	.0005	0.0000	0	.0175	
23	0	.0017	.0018	.0008	0.0000	0	.0098	
24	0	.0015	.0016	0.0000	0.0000	0	.0057	

Series J, continued.

Run	Temp. (°C)	Total Pressure (psia)	Butane Pressure (psia)	Initial Oxygen (ppm)	Space Time (sec)	CH ₄	C ₂ H ₆	C ₂ H ₄	C ₃ H ₆
25	535	15.58	7.25	8	2.58	.0136	.0050	.0070	.0125
26	585	16.01	.39	8	2.64	.0720	.0079	.0593	.0682
27	585	15.91	.72	8	2.67	.0928	.0149	.0725	.0866
28	585	15.89	1.37	8	2.63	.1328	.0287	.0916	.1177
29	585	15.74	2.39	8	2.63	.1838	.0448	.1216	.1624
30	585	15.63	4.60	8	2.59	.2538	.0790	.1454	.2182
31	585	15.43	7.61	8	2.57	.3481	.1196	.1934	.3147
32	595	16.02	.30	8	2.69	.1398	.0103	.1217	.1275
33	595	15.92	.46	8	2.66	.1643	.0178	.1385	.1448
34	595	15.98	.80	8	2.68	.2141	.0360	.1593	.1944
35	595	15.82	1.49	8	2.62	.2920	.0623	.1976	.2485
36	595	15.79	2.72	8	2.65	.3846	.0979	.2416	.3445
37	595	15.59	4.66	8	2.59	.5190	.1565	.3108	.4502
38	595	15.50	7.71	8	2.59	.6785	.2186	.3832	.6571
39	605	15.96	.27	8	2.60	.2156	.0151	.2000	.2301
40	605	15.98	.49	8	2.66	.3049	.0342	.2525	.2976
41	605	15.79	1.34	8	2.64	.4540	.0933	.3331	.4262
42	605	15.41	7.69	8	2.58	1.0456	.3149	.6277	1.0113
43	615	16.09	.29	8	2.66	.4458	.0267	.3852	.4043
44	615	15.88	.50	8	2.65	.5310	.0476	.4364	.4987
45	615	15.88	.91	8	2.64	.7005	.0982	.5205	.6375
46	615	15.74	1.75	8	2.64	.9195	.1864	.6480	.8141
47	615	15.62	3.80	8	2.60	1.2686	.3365	.8365	1.2832
48	615	15.40	7.86	8	2.57	1.7925	.5338	1.1125	1.7535

Series J, continued.

Run	Effluent Oxygen (ppm)	Moles Product per 100 Moles of Butane in Effluent					
		1-C ₄ H ₈	t-2-C ₄ H ₈	c-2-C ₄ H ₈	1,3-C ₄ H ₈	CO ₂	H ₂ O
25	0	0.0000	.0004	0.0000	0.0000	0	.0034
26	0	.0091	.0032	.0034	0.0000	0	.0660
27	0	.0047	.0019	.0021	0.0000	0	.0352
28	0	.0035	.0044	.0015	0.0000	0	.0186
29	0	.0022	.0039	.0018	0.0000	0	.0106
30	0	.0034	.0037	.0023	0.0000	0	.0054
31	0	.0026	.0052	.0038	0.0000	0	.0032
32	0	.0123	.0053	.0042	0.0000	0	.0841
33	0	.0087	.0043	.0021	0.0000	0	.0554
34	0	.0055	.0063	.0027	0.0000	0	.0320
35	0	.0043	.0063	.0034	0.0000	0	.0170
36	0	.0064	.0068	.0036	0.0000	0	.0093
37	0	.0043	.0099	.0039	0.0000	0	.0054
38	0	.0062	.0079	.0053	0.0000	0	.0032
39	0	.0104	.0075	.0022	0.0000	0	.0931
40	0	.0119	.0108	.0046	0.0000	0	.0523
41	0	.0073	.0077	.0046	0.0000	0	.0188
42	0	.0115	.0173	.0005	0.0000	0	.0032
43	0	.0127	.0093	.0099	0.0000	0	.0884
44	0	.0091	.0104	.0023	0.0000	0	.0507
45	0	.0161	.0088	.0050	0.0000	0	.0280
46	0	.0100	.0123	.0080	0.0000	0	.0144
47	0	.0163	.0169	.0109	.0016	0	.0066
48	0	.0190	.0220	.0166	.0010	0	.0031

Series J, continued.

Run	Temp. (°C)	Total Pressure (psia)	Butane Pressure (psia)	Initial Oxygen (ppm)	Space Time (sec)	Moles Product per 100 Moles of Butane in Effluent			
						CH ₄	C ₂ H ₆	C ₂ H ₄	C ₃ H ₆
49	625	15.91	.32	8	2.66	.7668	.0548	.6583	.7240
50	625	15.86	.89	8	2.64	1.1400	.1548	.8762	1.0339
51	625	15.72	1.79	8	2.61	1.5051	.2721	1.0593	1.3372

Series J, continued.

Run	Effluent Oxygen (ppm)	Moles Product per 100 Moles of Butane in Effluent					
		1-C ₄ H ₈	t-2-C ₄ H ₈	c-2-C ₄ H ₈	1,3-C ₄ H ₈	CO ₂	H ₂ O
49	0	.0139	.0139	.0095	0.0000	0	.0795
50	0	.0148	.0138	.0079	0.0000	0	.0286
51	0	.0216	.0209	.0083	0.0000	0	.0140

Note: Yield of H₂O was calculated from a mass balance on oxygen.

Series P. Pyrolysis of butane in an acid-treated reactor, S/V = 32 in⁻¹. Effect of trace amounts of oxygen.

Run	Temp. (°C)	Total Pressure (psia)	Butane Pressure (psia)	Initial Oxygen (ppm)	Space Time (sec)	CH ₄	C ₂ H ₆	C ₂ H ₄	C ₃ H ₆
1	595	15.32	7.43	15	2.61	.4676	.1458	.2622	.4398
2	595	15.40	5.37	14	2.58	.3959	.1236	.2300	.3437
3	595	15.60	3.12	14	2.59	.3009	.0792	.1903	.2633
4	595	15.70	1.55	14	2.64	.2443	.0514	.1681	.2105
5	595	15.92	.80	14	2.63	.1612	.0297	.1238	.1400
6	595	15.94	.42	14	2.67	.1281	.0133	.1056	.1171
7	575	15.50	7.35	14	2.62	.1423	.0493	.0742	.1235
8	575	15.63	4.55	14	2.61	.1153	.0357	.0673	.1017
9	575	15.86	2.34	14	2.63	.0766	.0202	.0466	.0670
10	575	15.90	1.26	14	2.67	.0566	.0110	.0379	.0492
11	575	16.03	.64	14	2.66	.0414	.0060	.0317	.0375
12	555	15.50	7.53	15	2.77	.0483	.0169	.0282	.0412
13	555	15.70	4.72	15	2.74	.0333	.0105	.0179	.0280
14	555	15.80	2.36	15	2.77	.0236	.0058	.0147	.0164
15	555	15.95	1.20	15	2.78	.0167	.0038	.0116	.0142
16	535	15.51	7.11	14	2.63	.0123	.0041	.0064	.0105
17	535	15.74	4.38	14	2.62	.0087	.0028	.0048	.0076
18	535	15.87	2.23	14	2.69	.0064	.0020	.0039	.0056
19	535	15.18	1.11	15	5.01	.0073	.0015	.0051	.0065
20	615	15.70	2.40	14	2.61	1.0557	.1983	.5847	.7590
21	615	15.83	1.25	13	2.64	.7981	.1369	.5520	.7100
22	615	15.83	.59	14	2.65	.6866	.0801	.8060	.5898
23	615	15.92	.27	14	2.64	.5459	.0335	.4436	.4768

Series P, continued.

Run	Effluent Oxygen (ppm)	Moles Product per 100 Moles of Butane in Effluent					
		1-C ₄ H ₈	t-2-C ₄ H ₈	c-2-C ₄ H ₈	1,3-C ₄ H ₈	CO ₂	H ₂ O
1	0	.0123	.0085	.0040	.0010	0	.0060
2	0	.0142	.0096	.0050	.0008	0	.0079
3	0	.0202	.0101	.0048	.0009	0	.0144
4	0	.0285	.0150	.0072	.0012	0	.0285
5	0	.0401	.0270	.0159	.0021	0	.0565
6	0	.0645	.0280	.0168	.0036	0	.1053
7	0	.0094	.0039	.0024	.0004	0	.0061
8	0	.0133	.0081	.0038	.0004	0	.0097
9	0	.0215	.0086	.0054	.0009	0	.0194
10	0	.0320	.0141	.0077	.0013	0	.0362
11	0	.0517	.0233	.0121	.0033	0	.0707
12	0	.0075	.0058	.0018	.0002	0	.0061
13	0	.0123	.0042	.0026	.0004	0	.0099
14	0	.0228	.0116	.0053	.0012	0	.0197
15	0	.0371	.0196	.0086	.0022	0	.0386
16	0	.0062	.0046	.0009	.0003	0	.0060
17	0	.0107	.0044	.0017	.0005	0	.0099
18	0	.0216	.0091	.0040	.0011	0	.0192
19	0	.0388	.0164	.0083	.0024	0	.0401
20	0	.0237	.0143	.0088	.0014	0	.0179
21	0	.0379	.0217	.0131	.0022	0	.0341
22	0	.0555	.0282	.0154	.0033	0	.0759
23	0	.0999	.0356	.0242	.0071	0	.1652

Note: Yield of H₂O was calculated from a mass balance on oxygen.

Series Q. Pyrolysis of butane in an acid-treated reactor, S/V = 32 in⁻¹. Effect of trace amounts of oxygen.

Run	Temp. (°C)	Total Pressure (psia)	Butane Pressure (psia)	Initial Oxygen (ppm)	Space Time (sec)	Moles Product per 100 Moles of Butane in Effluent			
						CH ₄	C ₄ H ₆	C ₂ H ₄	C ₃ H ₆
1	595	15.52	7.53	39	2.62	.8078	.2516	.4555	.7481
2	595	15.57	7.51	15	2.61	.7634	.2471	.4224	.6988
3	595	15.50	7.52	7	2.60	.7418	.2288	.3993	.7196
4	595	15.52	7.52	72	2.60	.7793	.2457	.4437	.7475
5	595	15.49	7.53	169	2.60	.4502	.1394	.2561	.4005
6	595	15.53	7.54	61	2.63	.4546	.1416	.2508	.4252
7	595	15.49	7.42	62	2.63	.4684	.1441	.2642	.4278
8	595	15.50	7.53	312	2.64	.5385	.1667	.3058	.4996
9	595	15.50	7.46	310	2.65	.5046	.1477	.2826	.4563
10	595	15.55	7.34	872	2.67	.5609	.1664	.3196	.5245

Series Q, continued.

Run	Effluent Oxygen (ppm)	Moles Product per 100 Moles of Butane in Effluent						H ₂ O
		1-C ₄ H ₈	t-2-C ₄ H ₈	c-2-C ₄ H ₈	1,3-C ₄ H ₈	CO ₂		
1	0	.0239	.0178	.0116	.0006	0		.0161
2	0	.0114	.0135	.0076	.0002	0		.0062
3	0	.0059	.0101	.0036	0.0000	0		.0029
4	0	.0358	.0131	.0106	.0005	0		.0299
5	0	.0416	.0408	.0180	.0014	0		.0693
6	0	.0241	.0305	.0117	.0013	0		.0251
7	0	.0292	.0336	.0156	.0017	0		.0258
8	0	.0758	.0487	.0250	.0049	0		.1283
9	0	.0912	.0382	.0249	.0090	0		.1290
10	0	.1916	.0739	.0485	.0272	0		.3696

Note: Yield of H₂O was calculated from a mass balance on oxygen.

Series R. Partial oxidation of butane in an acid-treated reactor, S/V = 32 in⁻¹.

Run	Temp. (°C)	Total Pressure (psia)	Butane Pressure (psia)	Initial Oxygen (ppm)	Space Time (sec)	CH ₄	Moles Product per 100 Moles of Butane in Effluent	C ₂ H ₆	C ₂ H ₄	C ₃ H ₆
1	595	15.58	7.49	10251	2.65	1.1929	.2136	.9177	1.1352	
2	595	15.92	2.21	10022	2.61	.2206	.0182	.2173	.2065	
3	595	16.04	.66	9997	2.69	.1729	.0106	.2141	.1604	
4	595	16.04	.62	4067	2.65	.1762	.0123	.1877	.1618	
5	595	15.93	2.15	4062	2.64	.2818	.0329	.2402	.2478	
6	595	15.62	7.41	4186	2.69	.9243	.2057	.6171	.8677	
7	595	15.54	7.50	1025	2.62	.4760	.1408	.2788	.4395	
8	595	15.96	2.21	999	2.64	.3258	.0662	.2462	.2907	
9	595	15.98	.65	980	2.63	.1565	.0224	.1867	.1676	
10	595	16.12	.66	404	2.68	.2089	.0256	.1915	.1935	
11	595	15.82	2.15	393	2.63	.2798	.0627	.2047	.2421	
12	595	15.58	7.56	403	2.71	.4846	.1447	.2789	.4591	
13	595	15.56	7.49	101	2.61	.4624	.1486	.2639	.4251	
14	595	15.97	2.20	99	2.67	.2706	.0654	.1757	.2352	
15	595	16.03	.67	98	2.67	.1751	.0253	.1446	.1640	
16	595	16.13	.64	40	2.73	.1581	.0232	.1275	.1461	
17	595	15.90	2.18	42	2.61	.2276	.0602	.1708	.2254	
18	595	15.58	7.59	42	2.63	.4749	.1495	.2706	.4702	
19	595	15.53	7.50	99	2.66	.4929	.1535	.2711	.4462	
20	595	15.16	7.32	101	5.08	.8153	.2627	.4532	.7707	
21	595	15.07	6.90	131	7.02	1.1895	.3638	.6647	1.1079	
22	595	14.94	7.14	99	9.63	1.5325	.4833	.8657	1.4414	
23	595	14.89	7.25	98	14.84	2.3656	.7719	1.3295	2.2273	
24	595	15.01	2.23	92	9.73	1.1198	.2661	.6908	1.0428	

Series R, continued.

Run	Effluent Oxygen (ppm)	Moles Product per 100 Moles of Butane in Effluent						H ₂ O	
		1-C ₄ H ₈	t-2-C ₄ H ₈	c-2-C ₄ H ₈	1,3-C ₄ H ₆	CO ₂	Observed	Computed	
1	****	.3319	.1479	.1122	.0654	.2964	1.0150	*****	
2	****	.3295	.1575	.1038	.0750	.2646	2.3349	*****	
3	****	.3137	.1519	.0912	.0621	.3736	1.0601	*****	
4	****	.2560	.1111	.0742	.0533	.0833	.9333	*****	
5	****	.2480	.1118	.0719	.0498	.0695	.7775	*****	
6	****	.2637	.1062	.0702	.0455	.0876	.6083	*****	
7	0	.1766	.0929	.0505	.0270	.0048	.2829	.4150	
8	****	.3065	.1305	.0867	.0667	.0331	.7824	*****	
9	****	.3535	.1535	.0968	.0726	.0032	1.3152	*****	
10	****	.2975	.1239	.0859	.0611	0.0000	*****	*****	
11	0	.2198	.1008	.0619	.0318	0.0000	*****	.5771	
12	0	.0907	.0320	.0242	.0084	0.0000	*****	.1662	
13	0	.0353	.0156	.0114	.0022	0.0000	*****	.0421	
14	0	.0765	.0301	.0209	.0053	0.0000	*****	.1440	
15	0	.1572	.0617	.0388	.0163	0.0000	*****	.4730	
16	0	.1008	.0380	.0225	.0063	0.0000	*****	.1988	
17	0	.0488	.0195	.0145	.0023	0.0000	*****	.0608	
18	0	.0174	.0071	.0064	.0008	0.0000	*****	.0171	
19	0	.0340	.0171	.0112	.0019	0.0000	*****	.0408	
20	0	.0348	.0187	.0125	.0031	0.0000	*****	.0417	
21	0	.0434	.0248	.0168	.0034	0.0000	*****	.0574	
22	0	.0235	.0191	.0146	.0015	0.0000	*****	.0414	
23	0	.0318	.0255	.0195	.0018	0.0000	*****	.0404	
24	0	.0311	.0192	.0142	0.0000	0.0000	*****	.1240	

Series R, continued.

Run	Temp. (°C)	Total Pressure (psia)	Butane Pressure (psia)	Initial Oxygen (ppm)	Space Time (sec)	CH ₄	Moles Product per 100 Moles of Butane in Effluent	C ₂ H ₆	C ₂ H ₄	C ₃ H ₆
25	595	15.12	2.09	96	7.47	.8500	.2369	.5665		.7920
26	595	15.27	2.14	100	5.06	.6611	.1569	.4250		.5743
27	595	16.39	2.27	99	2.04	.2765	.0662	.1756		.2395
28	595	15.16	7.30	9988	5.06	2.4313	.5051	1.5916		2.4664
29	595	15.05	7.18	9989	7.38	1.5586	.3635	1.0606		1.4703
30	595	14.96	7.20	9583	9.76	1.5838	.3807	1.0153		1.4384
31	595	14.88	7.20	9868	14.65	2.6423	.7579	1.5677		2.4662
32	595	14.90	1.85	9816	14.76	1.4652	.2523	1.1200		1.3538
33	595	15.02	2.18	9906	10.05	.9628	.1572	.8139		.9114
34	595	15.08	2.08	9837	7.36	.7322	.0893	.6926		.6367
35	595	15.30	2.15	9934	5.04	.5406	.0569	.5253		.5030
36	595	16.69	2.28	10007	1.66	.1819	.0160	.1954		.1774
37	595	15.12	2.06	9785	7.42	.8522	.1087	.8182		.8117
38	555	15.60	7.18	10215	2.64	.1587	.0201	.1282		.1320
39	555	15.98	2.07	9934	2.65	.0342	.0025	.0460		.0369
40	555	16.03	1.08	9969	2.68	.0229	.0007	.0389		.0266
41	555	16.04	1.07	4043	2.67	.0277	.0029	.0398		.0322
42	555	15.97	2.12	3994	2.62	.0417	.0052	.0454		.0452
43	555	15.66	7.29	3970	2.64	.1535	.0303	.1083		.1538
44	555	15.57	7.19	1013	2.63	.2139	.0659	.1198		.1891
45	555	16.00	2.11	1004	2.67	.0473	.0078	.0415		.0423
46	555	15.98	1.09	995	2.65	.0247	.0048	.0345		.0291
47	555	16.09	1.06	410	2.70	.0298	.0050	.0330		.0325
48	555	15.90	2.06	402	2.65	.0558	.0124	.0451		.0518

Series R, continued.

Run	Effluent Oxygen (ppm)	Moles Product per 100 Moles of Butane in Effluent						Observed H_2O	Computed H_2O
		1-C ₄ H ₈	t-2-C ₄ H ₈	c-2-C ₄ H ₈	1,3-C ₄ H ₆	CO ₄			
25	0	.0704	.0323	.0223	.0066	0.0000	*****	.1393	
26	0	.0721	.0342	.0210	.0079	0.0000	*****	.1432	
27	0	.0722	.0263	.0186	.0065	0.0000	*****	.1437	
28	***	.2815	.1347	.0934	.0544	.4322	.8100	*****	
29	0	.5608	.1989	.1674	.1715	.3960	1.7205	3.3929	
30	0	.5109	.2605	.1852	.1972	.3653	2.2219	3.2496	
31	0	.5102	.2520	.1795	.1842	.3172	2.0938	3.4445	
32	0	.8625	.4898	.3380	.4320	2.0920	6.2732	*****	
33	0	.8522	.4571	.3134	.5140	1.7671	4.5138	*****	
34	0	.8187	.4460	.2955	.4122	2.0833	5.1735	*****	
35	***	.6917	.3476	.2122	.2228	1.2677	3.3850	*****	
36	***	.3177	.1315	.0896	.0485	.1107	1.2041	*****	
37	***	.7824	.7727	.2135	.2852	*****	*****	*****	
38	6700	.1188	.0550	.0368	.0198	.1635	.4773	1.2003	
39	8100	.1482	.0710	.0476	.0270	.2422	.8149	2.3423	
40	8500	.1805	.0934	.0540	.0319	.1965	.8912	3.9616	
41	3500	.1479	.0735	.0453	.0252	.0584	.7991	1.5134	
42	3025	.1326	.0641	.0427	.0209	.0557	.7700	1.3459	
43	2380	.1046	.0404	.0300	.0138	.1270	.7628	.4285	
44	257	.0587	.0266	.0188	.0083	.0265	.1862	.2745	
45	580	.1253	.0543	.0376	.0201	.0324	.5042	.5772	
46	762	.1559	.0702	.0450	.0263	.0345	.5616	.6142	
47	182	.1324	.0591	.0388	.0207	0.0000	.5799	.6933	
48	95	.1109	.0481	.0316	.0157	0.0000	.3876	.4745	

Series R, continued.

Run	Temp. (°C)	Total Pressure (psia)	Butane Pressure (psia)	Initial Oxygen (ppm)	Space Time (sec)	CH ₄	Moles Product per 100 Moles of Butane in Effluent	C ₂ H ₆	C ₂ H ₄	C ₃ H ₆
49	555	15.57	7.15	414	2.65	.1295	.0393	.0755	.1255	
50	555	15.55	7.13	103	2.66	.0605	.0169	.0332	.0490	
51	555	15.97	2.16	99	2.66	.0442	.0123	.0286	.0372	
52	555	15.98	1.07	99	2.67	.0384	.0071	.0309	.0355	
53	555	16.03	1.07	39	2.69	.0262	.0059	.0202	.0239	
54	555	15.85	2.11	42	2.64	.0334	.0053	.0236	.0279	
55	555	15.54	7.05	43	2.67	.0651	.0223	.0334	.0548	
56	555	16.38	2.24	100	2.04	.0482	.0127	.0341	.0448	
57	555	15.34	2.23	99	5.07	.0575	.0152	.0361	.0517	
58	555	15.08	2.14	99	7.37	.0761	.0207	.0479	.0678	
59	555	15.01	2.07	102	9.97	.0874	.0243	.0528	.0787	
60	555	14.88	2.06	94	14.51	.0882	.0218	.0554	.0738	
61	555	16.81	2.32	9967	1.71	.0386	.0019	.0457	.0400	
62	555	15.48	2.17	10118	4.09	.0984	.0067	.1093	.0989	
63	555	15.08	2.21	9894	7.39	.1832	.0131	.2009	.1795	
64	555	14.98	2.13	9784	9.86	.2367	.0185	.2305	.2214	
65	555	14.87	2.12	10159	14.66	.3776	.0333	.3777	.3452	
66	555	14.80	6.95	10169	14.31	.5281	.1439	.3470	.4899	
67	555	14.85	7.16	9825	9.88	.3239	.0732	.2320	.2839	
68	555	14.92	7.26	10081	7.49	.2858	.0521	.2103	.2691	
69	555	15.19	7.22	10289	4.11	.2143	.0311	.1741	.1917	
70	515	15.66	6.83	10283	2.65	.0142	.0013	.0167	.0161	
71	515	15.75	4.50	10061	2.60	.0078	.0007	.0125	.0098	
72	515	15.99	1.99	10057	2.67	.0044	.0004	.0106	.0070	

Series R, continued.

Run	Effluent Oxygen (ppm)	Moles Product per 100 Moles of Butane in Effluent					H ₂ O	
		1-C ₄ H ₈	t-2-C ₄ H ₈	c-2-C ₄ H ₈	1,3-C ₄ H ₆	CO ₂	Observed	Computed
49	0	.0752	.0246	.0192	.0103	.0060	.1365	.1682
50	0	.0206	.0063	.0048	.0029	0.0000	.0512	.0451
51	0	.0611	.0231	.0159	.0059	0.0000	.1380	.1465
52	0	.0991	.0362	.0235	.0088	0.0000	.4913	.2949
53	0	.0525	.0206	.0133	.0040	0.0000	.3560	.1166
54	0	.0170	.0058	.0039	.0012	0.0000	.1369	.0630
55	0	.0162	.0092	.0055	.0007	0.0000	.0376	.0189
56	0	.0099	.0043	.0026	.0007	0.0000	.1015	.1464
57	0	.0523	.0210	.0133	.0058	0.0000	.1970	.1361
58	0	.0593	.0227	.0144	.0064	0.0000	.2903	.1404
59	0	.0550	.0211	.0141	.0076	0.0000	.3698	.1477
60	0	.0463	.0205	.0143	.0083	0.0000	.2799	.1355
61	9220	.0623	.0309	.0228	.0075	.0639	.3476	.9569
62	7570	.1324	.0677	.0439	.0210	.2477	.6232	3.1403
63	5620	.2040	.1206	.0747	.0385	.6860	1.5521	4.4736
64	4426	.2686	.1569	.0981	.0525	1.0625	1.9737	5.4189
65	2433	.3387	.2140	.1319	.0827	2.5010	3.1967	5.8147
66	0	.3351	.1825	.1203	.1228	.6768	1.0859	2.9758
67	0	.4443	.2222	.1518	.1740	.6114	1.1145	2.8534
68	0	.4058	.2096	.1326	.1309	.5939	1.4671	2.9569
69	3594	.2786	.1318	.0874	.0608	.3803	1.0738	2.0581
70	8083	.0533	.0248	.0187	.0088	.1056	.2459	.7973
71	8377	.0608	.0339	.0207	.0086	.1150	.2915	.9492
72	8798	.0771	.0425	.0252	.0117	.1263	.4673	1.7736

Series R, continued.

Run	Temp. (°C)	Total Pressure (psia)	Butane Pressure (psia)	Initial Oxygen (ppm)	Space Time (sec)	CH ₄	C ₂ H ₆	C ₂ H ₄	C ₃ H ₆
73	515	15.95	1.98	4214	2.65	.0059	.0006	.0101	.0083
74	515	15.76	4.60	4083	2.62	.0133	.0016	.0144	.0141
75	515	15.58	6.83	4070	2.65	.0217	.0036	.0196	.0220
76	515	15.64	6.81	1027	2.67	.0444	.0149	.0265	.0392
77	515	15.71	4.65	983	2.62	.0292	.0067	.0204	.0273
78	515	15.96	2.00	995	2.64	.0117	.0020	.0116	.0130
79	515	15.96	2.03	396	2.70	.0171	.0037	.0140	.0171
80	515	15.75	4.59	391	2.63	.0339	.0097	.0201	.0311
81	515	15.57	6.81	415	2.65	.0540	.0169	.0303	.0495
82	515	15.64	6.88	101	2.62	.0139	.0048	.0077	.0131
83	515	15.75	4.63	98	2.63	.0134	.0043	.0082	.0120
84	515	15.99	2.06	98	2.66	.0105	.0026	.0077	.0097
85	515	16.01	2.01	41	2.67	.0090	.0019	.0060	.0075
86	515	15.81	4.57	41	2.61	.0081	.0026	.0048	.0073
87	515	15.61	6.56	40	2.52	.0065	.0021	.0036	.0057
88	515	16.50	2.21	104	2.17	.0067	.0014	.0055	.0060
89	515	15.37	2.20	102	5.04	.0094	.0023	.0065	.0082
90	515	15.17	2.14	101	7.45	.0099	.0026	.0068	.0085
91	515	15.02	2.18	98	9.96	.0099	.0033	.0074	.0089
92	515	14.92	2.03	99	14.41	.0100	.0031	.0069	.0087
93	515	16.81	2.29	10032	1.83	.0036	.0002	.0075	.0050
94	515	15.52	2.26	9769	4.11	.0078	.0004	.0176	.0116
95	515	15.10	2.18	9610	7.48	.0153	.0009	.0304	.0192
96	515	15.00	2.13	9953	9.72	.0190	.0012	.0402	.0262

Series R, continued.

Run	Effluent Oxygen (ppm)	Moles Product per 100 Moles of Butane in Effluent							H ₂ O	
		1-C ₄ H ₈	t-2-C ₄ H ₈	c-2-C ₄ H ₈	1,3-C ₄ H ₆	CO ₂	Observed	Computed		
73	3364	.0672	.0338	.0222	.0097	.0425	.4933	1.2821		
74	2960	.0535	.0242	.0155	.0071	.0474	.2014	.6756		
75	2772	.0453	.0256	.0169	.0065	.0521	.2132	.4885		
76	400	.0316	.0113	.0100	.0039	.0096	.1163	.2686		
77	431	.0374	.0193	.0123	.0050	.0089	.1015	.3546		
78	519	.0492	.0260	.0152	.0064	.0043	.2638	.7531		
79	185	.0402	.0217	.0120	.0057	.0010	.3167	.3306		
80	117	.0318	.0131	.0103	.0042	.0005	.1288	.1869		
81	79	.0298	.0155	.0092	.0032	.0007	.0557	.1521		
82	0	.0138	.0055	.0045	.0018	0.0000	.1158	.0457		
83	0	.0231	.0115	.0063	.0021	0.0000	.0670	.0668		
84	15	.0428	.0199	.0122	.0053	0.0000	.1257	.1280		
85	0	.0239	.0118	.0070	.0028	0.0000	.0899	.0654		
86	0	.0126	.0058	.0034	.0014	0.0000	.0493	.0282		
87	0	.0073	.0053	.0026	.0012	0.0000	.0538	.0189		
88	30	.0496	.0214	.0130	.0054	0.0000	.0964	.1097		
89	0	.0450	.0214	.0138	.0062	0.0000	.2272	.1435		
90	0	.0392	.0182	.0109	.0052	0.0000	.3388	.1438		
91	0	.0396	.0185	.0119	.0056	0.0000	.4058	.1350		
92	0	.0377	.0162	.0112	.0074	0.0000	.4824	.1451		
93	9482	.0469	.0288	.0156	.0067	.0848	.2073	.6383		
94	7942	.0868	.0509	.0312	.0141	.2129	.5549	2.0890		
95	6369	.1293	.0839	.0475	.0227	.4976	.9707	3.4885		
96	5619	.1551	.1071	.0590	.0286	.7832	2.5022	4.5443		

Series R, continued.

Run	Temp. (°C)	Total Pressure (psia)	Butane Pressure (psia)	Initial Oxygen (ppm)	Space Time (sec)	CH ₄	Moles Product per 100 Moles of Butane in Effluent	C ₂ H ₆	C ₂ H ₄	C ₃ H ₆
97	515	14.88	2.08	9767	14.52	.0282	.0006	.0562	.0358	.0358
98	515	14.80	6.96	10206	14.80	.0659	.0084	.0631	.0575	.0575
99	515	14.85	7.25	9766	9.83	.0472	.0064	.0480	.0448	.0448
100	515	14.93	7.11	9915	7.29	.0302	.0037	.0332	.0303	.0303
101	515	15.20	7.25	9788	3.96	.0161	.0019	.0192	.0163	.0163

Series R, continued.

Run	Effluent Oxygen (ppm)	Moles Product per 100 Moles of Butane in Effluent						H ₂ O	
		1-C ₄ H ₈	t-2-C ₄ H ₈	c-2-C ₄ H ₈	1,3-C ₄ H ₆	CO ₂	Observed	Computed	
97	3932	.1904	.1490	.0776	.0366	1.2457	3.3175	5.8534	
98	385	.1875	.1262	.0731	.0528	.6902	.9795	2.7966	
99	2111	.1665	.1021	.0628	.0343	.5500	.9375	2.0348	
100	3699	.1455	.0768	.0487	.0258	.4062	.7991	1.7978	
101	6028	.1055	.0584	.0335	.0163	.1569	.4892	1.2624	

Series S. Partial oxidation of butane in an acid-treated reactor, S/V = 32 in⁻¹

Run	Temp. (°C)	Total Pressure (psia)	Butane Pressure (psia)	Initial Oxygen (ppm)	Space Time (sec)	CH ₄	Moles Product per 100 Moles of Butane in Effluent	C ₂ H ₆	C ₂ H ₄	C ₃ H ₆
1	515	16.91	2.25	1010	1.83	.0083	.0011	.0086	.0086	.0090
2	515	15.71	2.30	997	3.59	.0204	.0031	.0184	.0184	.0219
3	515	15.18	2.20	980	7.07	.0464	.0085	.0382	.0382	.0450
4	515	15.03	2.18	983	9.82	.0774	.0149	.0597	.0597	.0762
5	515	14.94	2.18	936	14.94	.1172	.0259	.0832	.0832	.1175
6	515	15.28	2.21	371	6.06	.0341	.0082	.0263	.0263	.0345
7	515	15.67	1.93	360	3.63	.0193	.0042	.0160	.0160	.0199
8	515	16.43	2.26	392	2.22	.0123	.0026	.0099	.0099	.0120
9	515	16.48	2.23	3975	2.20	.0046	.0007	.0099	.0099	.0082
10	515	15.58	2.23	3906	3.63	.0137	.0012	.0178	.0178	.0148
11	515	15.15	2.18	4071	7.01	.0282	.0022	.0365	.0365	.0309
12	515	14.98	2.24	3908	9.65	.0397	.0038	.0489	.0489	.0429
13	515	14.88	2.11	4133	14.48	.0700	.0077	.0795	.0795	.0719
14	515	17.01	3.82	10048	1.56	.0036	.0005	.0062	.0062	.0056
15	515	15.45	2.79	11141	3.89	.0082	.0011	.0166	.0166	.0123
16	515	15.04	3.64	10172	6.91	.0222	.0020	.0314	.0314	.0245
17	515	14.89	3.57	10023	9.71	.0334	.0023	.0469	.0469	.0359
18	515	14.80	3.84	10097	14.64	.0501	.0043	.0622	.0622	.0492
19	515	16.20	5.34	9984	2.06	.0058	.0005	.0080	.0080	.0069
20	515	15.43	5.34	10027	3.58	.0111	.0009	.0149	.0149	.0127
21	515	15.07	5.38	9859	6.93	.0237	.0024	.0297	.0297	.0251
22	515	14.90	5.30	10084	9.65	.0315	.0030	.0415	.0415	.0353
23	515	14.82	5.32	9924	14.70	.0436	.0059	.0505	.0505	.0425
24	470	14.74	2.10	10350	14.42	.0013	.0001	.0046	.0046	.0021

Series S, continued.

Run	Effluent Oxygen (ppm)	Moles Product per 100 Moles of Butane in Effluent						H ₂ O	
		1-C ₄ H ₈	t-2-C ₄ H ₈	c-2-C ₄ H ₈	1,3-C ₄ H ₆	C ₂	Observed	Computed	
1	830	.0358	.0218	.0110	.0042	.0265	.3482	.2170	
2	594	.0655	.0336	.0201	.0087	.0664	.2522	.4176	
3	268	.1079	.0536	.0326	.0154	.1743	.2801	.6343	
4	30	.1226	.0683	.0418	.0247	.2853	.5157	.7444	
5	0	.1426	.0766	.0484	.0356	.3001	.5107	.6818	
6	0	.0929	.0471	.0297	.0167	.0899	.3941	.3331	
7	91	.0782	.0377	.0227	.0134	.0524	.2496	.3329	
8	236	.0541	.0237	.0147	.0066	.0128	.1445	.2019	
9	3538	.0534	.0274	.0164	.0068	.0800	.3084	.4847	
10	3076	.0831	.0478	.0255	.0098	.1403	.3990	.8815	
11	2455	.1253	.0750	.0422	.0194	.3619	.7281	1.5221	
12	1862	.1555	.0931	.0558	.0302	.5741	.7737	1.5834	
13	690	.1856	.1133	.0674	.0342	.8821	1.3181	3.0810	
14	9111	.0436	.0202	.0125	.0052	.0433	.0896	.7479	
15	8642	.0966	.0561	.0315	.0178	.2843	.5301	2.2035	
16	5888	.1233	.0721	.0427	.0254	.4144	.8872	2.7083	
17	4451	.1537	.1013	.0607	.0326	.6200	.9275	3.4065	
18	2178	.1864	.1332	.0767	.0423	.9153	1.5610	4.2763	
19	8564	.0690	.0323	.0216	.0105	.1050	.1890	.6515	
20	7268	.1040	.0596	.0339	.0199	.1759	.2741	1.2436	
21	4970	.1477	.0829	.0526	.0326	.4069	.4971	1.9255	
22	3352	.1918	.1210	.0726	.0448	.7233	.7823	2.3406	
23	860	.2281	.1559	.0939	.0833	1.0403	1.0322	2.9654	
24	6256	.0942	.0886	.0434	.0144	1.1302	1.3495	3.4996	

Series S, continued.

Run	Temp. (°C)	Total Pressure (psia)	Butane Pressure (psia)	Initial Oxygen (ppm)	Space Time (sec)	CH ₄	Moles Product per 100 Moles of Butane in Effluent C ₂ H ₆	C ₂ H ₄	C ₃ H ₆
25	470	14.82	2.13	10146	9.74	.0016	0.0000	.0033	.0016
26	470	15.19	2.12	9973	5.11	.0008	.0001	.0018	.0007
27	530	16.55	2.14	10032	1.91	.0051	.0002	.0096	.0065
28	530	15.51	2.17	10004	3.60	.0103	.0002	.0198	.0136
29	530	15.01	2.10	9847	6.93	.0203	.0016	.0412	.0268
30	530	14.89	2.20	9854	9.76	.0309	.0024	.0558	.0383
31	530	14.77	2.08	10031	14.53	.0493	.0011	.0822	.0542
32	500	16.80	2.23	10045	1.91	.0012	.0001	.0032	.0022
33	500	15.61	2.18	10088	3.64	.0031	.0004	.0066	.0044
34	500	15.13	2.12	9849	6.96	.0050	.0004	.0131	.0079
35	500	14.95	2.15	9979	9.77	.0062	.0003	.0174	.0105
36	500	14.87	2.15	10048	14.49	.0110	.0006	.0266	.0152
37	485	16.79	2.17	9985	1.90	.0007	0.0000	.0011	.0007
38	485	15.52	2.11	9984	3.60	.0010	.0002	.0023	.0013
39	485	15.07	2.21	9932	6.84	.0013	.0002	.0031	.0024
40	485	14.87	2.09	9996	9.68	.0018	.0003	.0068	.0033
41	485	14.71	2.07	10360	14.25	.0025	.0002	.0095	.0045

Series S, continued.

Run	Effluent Oxygen (ppm)	Moles Product per 100 Moles of Butane in Effluent						H ₂ O	
		1-C ₄ H ₈	t-2-C ₄ H ₈	c-2-C ₄ H ₈	1,3-C ₄ H ₆	CO ₂	Observed	Computed	
25	7259	.0878	.0718	.0291	.0144	.6634	.6990	2.6814	
26	8486	.0618	.0411	.0212	.0113	.2714	.0700	1.5844	
27	9055	.1085	.0558	.0337	.0174	.1347	.2672	1.2412	
28	8145	.1564	.0825	.0492	.0306	.4272	.2695	1.8044	
29	6328	.2446	.1467	.0872	.0522	.9388	.8655	3.1514	
30	5111	.2679	.1783	.1008	.0636	1.6491	1.5801	3.1102	
31	3543	.2977	.2510	.1396	.0793	2.6619	1.8208	3.8848	
32	9126	.0573	.0321	.0178	.0085	.0786	.1831	1.2281	
33	8712	.0900	.0555	.0281	.0143	.2863	.3388	1.3950	
34	7353	.1225	.0847	.0467	.0205	.6409	.7114	2.2778	
35	6065	.1561	.1175	.0625	.0296	1.0427	.7138	3.3569	
36	4627	.1783	.1390	.0733	.0344	1.7877	.7410	3.9172	
37	9268	.0456	.0260	.0136	.0071	.0694	.1369	.9697	
38	8503	.0702	.0475	.0246	.0101	.2381	.3112	1.6983	
39	7477	.0976	.0681	.0345	.0179	.5130	.7777	2.3285	
40	6579	.1182	.0941	.0447	.0198	.8252	.9050	3.2157	
41	5596	.1300	.1105	.0575	.0314	1.2579	1.1256	4.2387	

APPENDIX B

A summary of the chromatograph network is given. Included are molar response values for the various detectors, calibration procedures and a description of the columns selected for use in the analysis.

Chromatography consists of the physical separation of two or more materials based on their differential distribution between a mobile and a stationary phase. In the case of gas chromatography, the mobile phase is a gas. Either a liquid or a solid is employed as the stationary phase. Once separated, the compounds are eluted to a detector with which a quantitative measurement of the amount of material is made. For this study, three flame ionization and two thermal conductivity detectors were employed.

The thermal conductivity detectors (TCD) employed heated filaments to detect changes in the thermal conductivity of the carrier gas when diluted by components of the sample. A TCD responds in varying degrees to all compounds. Response is strongest for compounds whose thermal conductivity is most different from that of the carrier gas. For this reason, helium is commonly used as a carrier gas because of its relatively high thermal conductivity; however, with helium as a carrier, the response for hydrogen is quite low. As a result, helium was used in the present work as a carrier in a chromatograph for the detection of water, carbon dioxide and formaldehyde. Argon was used as a carrier to a second chromatograph for measurement of hydrogen, oxygen, nitrogen and carbon monoxide.

Flame ionization detectors (FID) measure the minute current generated when a combustible material enters a hydrogen-air flame. A DC potential of 300 to 400 volts is applied across two electrodes positioned near the flame. The ionized species are collected and the

current generated is amplified by an electrometer to values suitable for millivolt recorders.

The FID possesses high sensitivity (approximately 1000 times the sensitivity of a TCD under similar conditions) and a wide range of linearity of response. Linearities of the FID used in this study were checked by successively diluting a sample of pure butane and noting the response. For all detectors, the response was observed to be linear with sample size through 100 μ l.

A disadvantage of the FID is that it does not respond to all compounds. Inorganic compounds and carbon oxides yield no response while compounds such as formaldehyde exhibit very weak responses. Response is a function of the number and type of burnable carbon atoms in a compound. Greater response is observed for compounds of greater carbon content.

Sensitivity of the detector is also influenced by the ratio of the flow rates of hydrogen to air fed to the flame. The optimum flows are influenced by the design of the detector and must be determined by trial. Values of 15 ml/min of hydrogen and 250 ml/min were optimum for the Loenco FID used in this work whereas the corresponding figures for the F&M FID were 42 ml/min and 500 ml/min, respectively.

Because the response of a given detector varies from compound to compound, calibration of each detector was required. Standard mixtures of known composition were prepared of the hydrocarbons, carbon oxides, water and fixed gases expected in the reaction. Responses of samples

of the standard mixtures were recorded for each detector and the average relative molar response on the basis of peak area was calculated. Table 1 is a list of the relative molar responses for each detector. These values have a precision of about ± 3 per cent (± 5 per cent for the CEC TCD).

The goal of the chromatograph program was the development of a system capable of measuring possible products in the pyrolysis and partial oxidation of butane. These included low-molecular-weight paraffins, olefins, aldehydes, alcohols, esters, ketones, organic acids, fixed gases, carbon oxides and water. The appropriate stationary phases, column lengths and operating conditions to produce the required separations were determined by trial and error using the available literature as a guide. Table 2 is a summary of the columns and operating conditions selected for use in the chromatograph network.

In addition to the columns selected, a variety of polar and non-polar liquid phases were evaluated. Among these were adiponitrile, silicone oil, dioctyl phthalate, Carbowax 1500 and triethylene glycol. Other porous polymers tried were Porapak QS, Porapak S, Porapak T and Porapak N. Chromosorb P coated with 25 per cent adiponitrile separated the low-molecular-weight olefins and paraffins with much the same success of the two part column (column number 1) selected for the task. In general, the Porapaks possessed similar retention characteristics. All gave an approximately symmetrical peak for water, a difficult compound to resolve well on a liquid-loaded column.

Table 1. Relative Molar Response Values (Peak Area).

Compound	Relative Molar Response Based on Peak Area			
	Loenco FID Helium Carrier	F&M FID Helium Carrier	CEC TCD Argon Carrier	Loenco TCD Helium Carrier
CH ₄	0.265	0.247	(1.00)	---
C ₂ H ₆	0.505	0.494	---	0.758
C ₂ H ₄	0.505	0.491	---	0.704
C ₃ H ₆	0.745	0.748	---	0.961
C ₃ H ₈	0.750	0.750	---	---
1-C ₄ H ₈	1.00	1.00	---	---
t-2-C ₄ H ₈	0.98	---	---	---
c-2-C ₄ H ₈	0.98	---	---	---
1,3-C ₄ H ₆	1.00	---	---	---
n-C ₄ H ₁₀	(1.00)	(1.00)	---	(1.00)*
i-C ₄ H ₁₀	0.98	---	---	---
H ₂ O	---	---	---	0.485
CO ₂	---	---	---	0.704
CO	---	---	0.369	---
H ₂	---	---	4.74	---
O ₂	---	---	0.448	---
N ₂	---	---	0.398	---

*Butane peak was slightly overloaded.

Table 2. Summary of Chromatograph Network.

<u>No.</u>	<u>Column</u>	<u>Stationary Phase</u>	<u>Carrier Gas</u>	<u>Column Temp., °C</u>	<u>Detector</u>
1	I. 48 ft of 0.0625" ID copper tubing	22% β - β' oxydipropionitrile on 60/80 mesh Chromosorb P	Helium at 22 ml/min	21	FID
	II. 40 ft of 0.0625" ID copper tubing	32% Carbowax 400 on 60/65 mesh Chromosorb P			
2	10 ft of 0.093" ID stainless-steel tubing	Molecular Sieve 5A, 30/60 mesh	Argon at 11 ml/min	65	TCD
3	10 ft of 0.093" ID stainless-steel tubing	Porapak Q, 80/100 mesh	Helium at 35 ml/min	95	TCD
4a	10 ft of 0.093" ID stainless-steel tubing	Porapak Q, 80/100 mesh	Helium at 35 ml/min	94	FID
4b	10 ft of 0.093" ID stainless-steel tubing	Porapak Q, 80/100 mesh	Helium at 35 ml/min	150	FID
5	10 ft of 0.093" ID stainless-steel tubing	Porapak R, 80/100 mesh	Helium at 35 ml/min	150	FID

Table 2, cont'd. Summary of Chromatograph Network.

No.	Compounds Separated	Analysis Time	Remarks
1	CH ₄ , C ₂ H ₆ , C ₂ H ₄ , C ₃ H ₈ , i-C ₄ H ₁₀ , C ₃ H ₆ , n-C ₄ H ₁₀ , 1-C ₄ H ₈ , t-2-C ₄ H ₈ , c-2-C ₄ H ₈ , 1-C ₅ H ₁₀ , 1,3-C ₄ H ₆	35 min	Good separations; no interference from oxygenated compounds; sensitivity reduced somewhat by long retention times
2	H ₂ , O ₂ , N ₂ , CH ₄ , CO	16 min	Good separation; low sensitivity; deterioration of column performance with time
3	(CH ₄ , Ar, CO), CO ₂ , C ₂ H ₄ , C ₂ H ₆ , H ₂ O, C ₃ H ₆ , (C ₃ H ₈ , HCHO), CH ₃ OH, CH ₃ CHO, (1-C ₄ H ₈ , n-C ₄ H ₁₀ , t-2-C ₄ H ₈ , c-2-C ₄ H ₈ , C ₂ H ₅ OH)	22 min	Adequate separation for CO ₂ and H ₂ O; HCHO elutes with C ₃ H ₈ ; adequate sensitivity; n-C ₄ H ₁₀ peak is overloaded under normal conditions of experiments
4a	CH ₄ , C ₂ H ₄ , C ₂ H ₆ , C ₃ H ₆ , C ₃ H ₈ , CH ₃ OH, CH ₃ CHO, C ₂ H ₅ OH, 1-C ₄ H ₈ , (n-C ₄ H ₁₀ , t-2-C ₄ H ₈ , c-2-C ₄ H ₈)	24 min	Good separation of low-molecular-weight oxygenated organics; high sensitivity
4b	CH ₃ OH, CH ₃ CHO, HCO ₂ H, C ₂ H ₅ OH, (C ₂ H ₅ CHO, CH ₃ COCH ₃), CH ₃ CO ₂ CH ₃ , CH ₃ CO ₂ H, 1-C ₃ H ₇ OH, CH ₃ COC ₂ H ₅ , (C ₂ H ₅ CO ₂ CH ₃ , 2-C ₄ H ₉ OH), CH ₂ :CHCH ₂ OH,	45 min	Propionaldehyde and acetone elute together as do ethyl acetate and 2-butanol; other separations are fair to good; high sensitivity

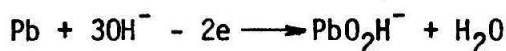
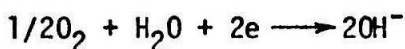
Table 2, cont'd. Summary of Chromatograph Network.

<u>No.</u>	<u>Compounds Separated</u>	<u>Analysis Time</u>	<u>Remarks</u>
5	$(\text{CH}_3\text{OH}, \text{CH}_3\text{OH}), \text{HCO}_2\text{H}, \text{C}_2\text{H}_5\text{OH},$ $(\text{C}_2\text{H}_5\text{CO}, \text{CH}_3\text{OCH}_3), \text{CH}_3\text{CO}_2\text{CH}_3,$ $2\text{-C}_2\text{H}_7\text{OH}, 1\text{-C}_3\text{H}_7\text{OH}, \text{CH}_3\text{COC}_2\text{H}_5,$ $\text{C}_2\text{H}_5\text{CO}_2\text{CH}_3, (2\text{-C}_4\text{H}_9\text{OH}, \text{CH}_2\text{:CHCH}_2\text{OH}),$ $1\text{-C}_4\text{H}_9\text{OH}, \text{CH}_3\text{CO}_2\text{H}, \text{C}_2\text{H}_5\text{COC}_2\text{H}_5$	43 min	Complements 4b in that ethyl acetate and 2-butanol are separated; other separations are fair to good; much better than 4b on lower-molecular-weight oxygenated organics

APPENDIX C

A description of the Hersch cell is presented. Included are the design of the cell, its operating characteristics and a discussion of the continuous and pulse modes of operation.

P. A. Hersch, in 1960, proposed a galvanic cell for the continuous trace monitoring of oxygen in gases (1). The Hersch cell consists of a silver anode and a lead cathode in contact with an electrolyte containing hydroxide ions. Oxygen is reduced at the cathode with the generation of a galvanic current, the strength of which is dependent on the amount of oxygen reduced. The reactions occurring at the cathode and anode are, respectively:



The anode and cathode are connected by a microammeter to measure the response of the cell to the oxygen of a gas stream. Extreme sensitivity to oxygen, a wide range of linear response, a rapid response and good stability are factors responsible for the widespread adoption of the Hersch cell as an analytical tool.

The use of a Hersch cell as a detector in gas chromatography was advanced by R. W. Dickinson and developed by T. R. Phillips (2). A sample of the gas containing oxygen is injected into an oxygen-free carrier gas and transported to the cell where a galvanic response to the oxygen is obtained. The response, proportional to the amount of oxygen introduced into the cell, is symmetrical and peak heights, as opposed to the more rigorous treatment of peak areas, have been used in correlation of the oxygen concentration with the cell response (2, 3). Hillman (3) reported that oxygen concentrations of 20 ppm could be

detected within an error of 5 per cent and that the detector was linear for oxygen concentrations below 2 per cent by volume.

Several reasons may be listed for the use of the Hersch cell as a detector, in preference to continuous monitoring, for the determination of oxygen in the partial oxidation of n-butane.

(1) The upper range of linearity can be extended from 0.01 per cent to over 1.0 per cent oxygen without the use of sample splitting.

(2) Error in the oxygen analysis in the ppm range may be reduced since cell drift is minimized.

(3) The detector system may easily be used in sampling reactor systems that are operated below atmospheric pressure whereas continuous monitoring would require pumping equipment for the compression of the gas stream to slightly higher than atmospheric pressure.

A Hersch cell for use as a specific chromatographic detector for oxygen was designed and built. Figure 1 presents a schematic of the cell design, similar to that of Hersch. The cell consists of a lead-foil anode which is wrapped around a half-inch, stainless-steel tube. A silver-gauze cathode is separated from the anode by a 0.033 inch thick layer of Poron that is initially saturated with a 5N solution of KOH. The cell casing is made of Lucite. Entering the cell casing, the gas stream is bubbled through a 5N KOH solution in the saturator in order to reduce evaporation of the cell electrolyte. An adjustable reservoir of 5N KOH was connected directly to the saturator in order to extend the life of the cell. Gas samples of 200 μ l were injected

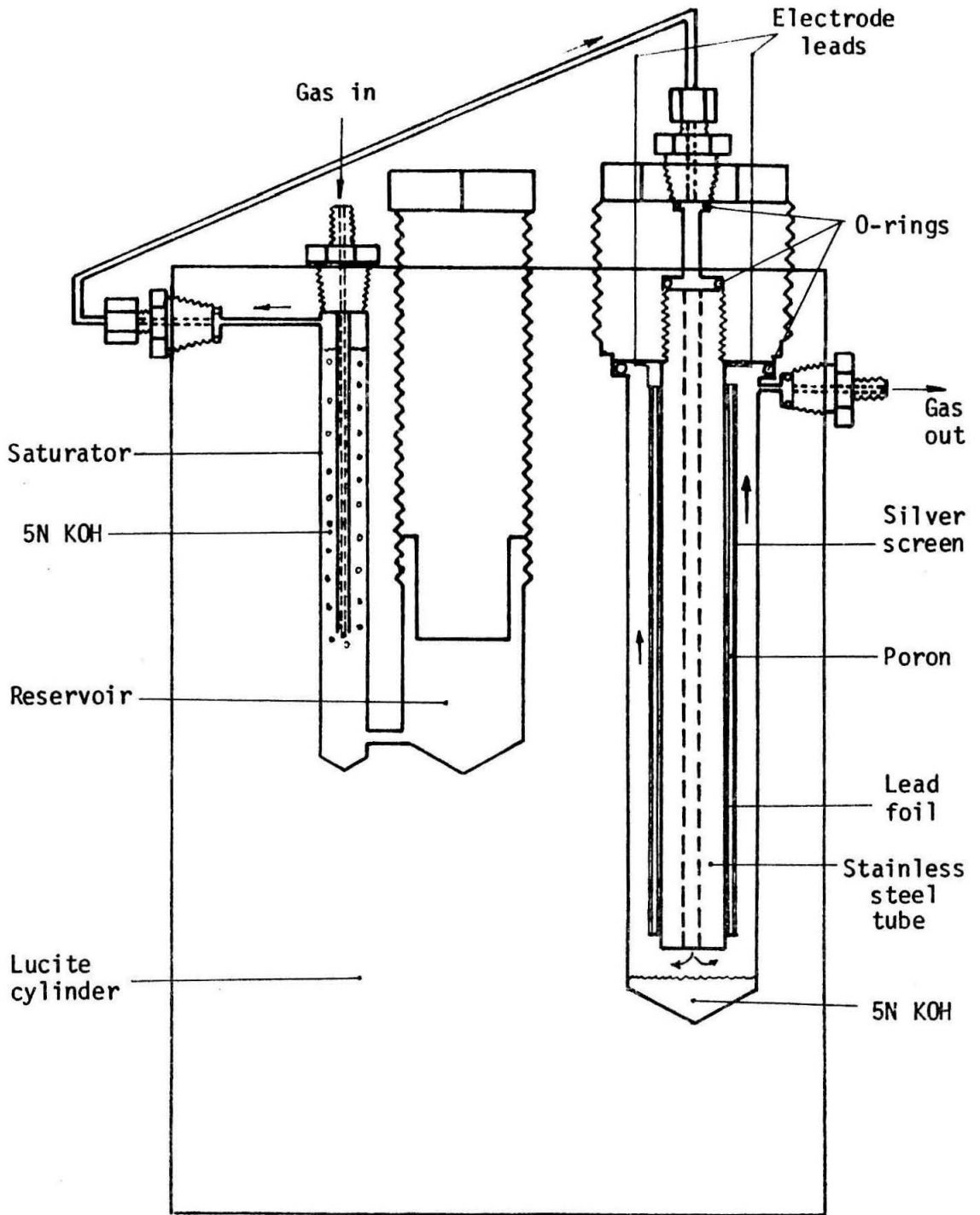


Figure 1. Schematic of the Hersch cell.

into an argon carrier gas for transport through the cell. Oxygen in the argon had been removed by means of a trap of manganous oxide.

A schematic of the electrical circuit for measuring the cell response is given in Figure 2. Provision was made for nulling background current which may result from leakage of oxygen into the cell. Normally, background currents of 2 to 6 microamps, corresponding to 1 or 2 ppm oxygen, were observed. The voltage drop across a known resistor was recorded on a millivolt recorder. By adjusting the value of the resistor, oxygen in concentrations of 0 to 4 per cent by volume of the sample could be measured within 3 per cent. Linear response of the cell was from 0 to 1 per cent oxygen in the sample. The variation of response with size of the resistor was determined by Smith (4) as

$$\frac{v_1}{v_2} = \frac{R_1}{R_2} \left[\frac{R_2 + \lambda}{R_1 + \lambda} \right]$$

where v_1, v_2 = cell output, mv,

R_1, R_2 = resistors, ohms,

λ = internal resistance of the cell, ohms.

Daily calibration of the cell with an argon-oxygen mixture of known composition was performed in order to insure accurate analyses. Changes in the calibration were observed from week to week because of changes in the cell itself, e.g. a decrease in efficiency resulting from loss of electrolyte.

Being an integral detector, the Hersch cell is expected to possess

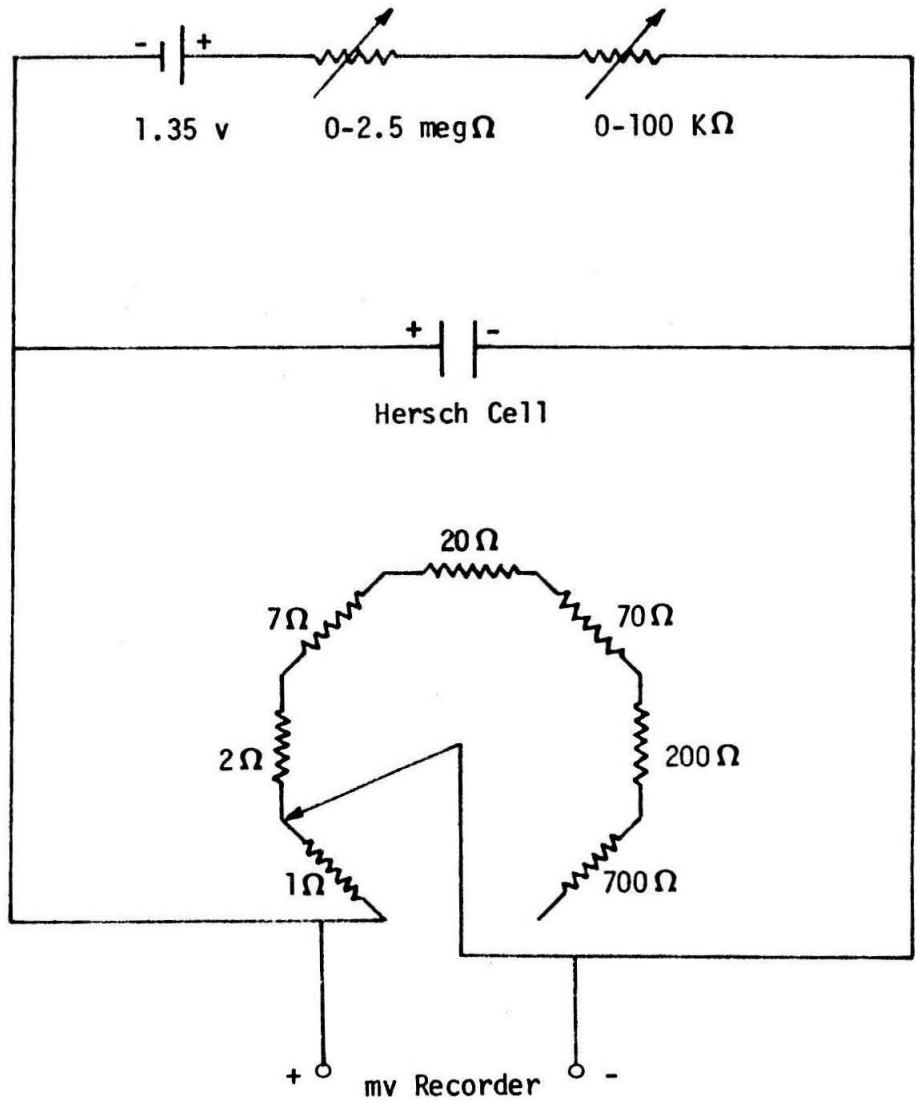


Figure 2. Electrical circuit for use with the Hersch detector.

a response (as measured by peak height) which is dependent upon the carrier gas flow rate. This was found to be the case. Using a sample of 153 ppm oxygen, the effect of carrier gas flow rate on the cell response was studied. Gas flow rates from 8.8 to 24.2 ml/min were employed. The peak height response of the cell was found to vary directly but in a non-linear manner with the carrier flow rate. A 50 per cent greater response was recorded at 20 ml/min than at 8.8 ml/min; however, higher rates of carrier flow contributed to shorter cell life. A standard flow rate of 20 ml/min was established for routine analysis. At this value, cell life, with daily use, was approximately one month.

No interference of the cell response is caused by hydrocarbons. Only materials reacting with silver or the electrolyte affect the sensitivity. Baker, et al (5) indicated that cathodes of gold or platinum perform satisfactorily and could be used in instances where materials in the sample interact with silver. The adverse effects of sample-electrolyte interference are reduced by the contact of the sample with the electrolyte prior to the cell, e.g. in the saturator.

Limited use of a continuous-monitor version of the Hersch cell was made in the pyrolysis and oxidation employing concentrations of oxygen below 100 ppm. Linearity of the cell was from 0 to 150 ppm and cell life averaged several months at these oxygen concentrations and a gas flow rate of 10 ml/min. Cell response was measured directly by a microammeter of 100 ohms internal resistance. Sensitivity of the cell was approximately 2.5 μ a/ppm of oxygen.

REFERENCES

1. P. A. Hersch, Anal. Chem., 32, 1030 (1960).
2. T. R. Phillips, E. G. Johnson and H. Woodward, Anal. Chem., 36, 450 (1964).
3. G. E. Hillman and J. Lightwood, Anal. Chem., 38, 1430 (1966).
4. R. L. Smith, Ph. D. Thesis, California Institute of Technology, 1970.
5. W. J. Baker, J. F. Combs, T. L. Zinn, A. W. Wotring and R. F. Wall, Ind. Eng. Chem., 51 (6), 727 (1959).

APPENDIX D

The validity of the steady-state assumption as it applies to the pyrolysis of n-butane is presented. Numerical integration of a set of ordinary differential equations indicate that the induction period is of the order of 3 milliseconds.

VALIDITY OF THE STEADY-STATE APPROXIMATION APPLIED TO THE PYROLYSIS OF *n*-BUTANE

J. E. BLAKEMORE AND W. H. CORCORAN

California Institute of Technology, Pasadena, Calif. 91109

A quantitative proof of the validity of the steady-state approximation in the mechanistic treatment of the pyrolysis of *n*-butane is given. The length of the induction period is noted, and the free-radical concentrations are predicted. Rate constants used for the individual steps in the mechanism were developed from a careful review of the literature.

IN THE kinetic treatment of chain reactions it is frequently assumed that the rates of formation of the free radicals or intermediate species are zero. It is apparent that this steady-state or pseudostationary-state assumption is not applicable to the induction period in which the free radicals increase from their initial concentrations, usually zero, to their steady-state values. The steady-state approximation is said to be valid if the duration of the induction period is much smaller than the over-all reaction time. Qualitatively, if the rates of destruction of the intermediate species are large compared with the over-all reaction rate, the intermediate species are present in the reaction mixture in relatively low concentrations, and the assumption of pseudostationary state is generally good.

Pyrolysis of *n*-Butane

Of special petrochemical interest are the pyrolyses of paraffin hydrocarbons and specifically that of *n*-butane. Experimental data have been collected on the pyrolysis of *n*-butane by several investigators (Barker and Corcoran, 1968; Purnell and Quinn, 1962; Sagert and Laidler, 1963; Wang, 1963). The steady-state assumption has been employed to correlate proposed mechanisms and experimental findings. Justification of the assumption has been based upon the satisfactory agreement of predicted results with experimental data—e.g., Wang *et al.* (1963). There has been no estimate of the induction period—i.e., the time required for the free radicals of the system to approach their steady-state concentrations. The existence of a short induction period is sufficient evidence that the pseudostationary-state approximation may be used in predicting product concentrations for systems whose reaction time is long relative to the induction period. If for some reason extremely fast pyrolysis reactions were desirable, it would be convenient to have a reliable estimate of the induction period. In the work presented here, the pseudo-steady state of radical concentrations in the pyrolysis of *n*-butane is found to be reached in a few milliseconds.

Several approximate mathematical tests (Giddings and Shin, 1962; Hirschfelder, 1957) have been proposed to test the validity of the steady-state hypothesis in individual cases; however, the most accurate method is to solve, simultaneously, the system of ordinary, coupled, first-order differential equations which govern the reaction system. By use of this method, a critical quantitative treatment of the steady-state assumption as applied to the pyrolysis

of *n*-butane has been made, and the length of the induction period and concentrations of free radicals have been estimated.

Procedure

Mechanisms involving the principal fundamental reactions have been proposed by previous investigators (Barker and Corcoran, 1968; Purnell and Quinn, 1962; Sagert and Laidler, 1963; Wang *et al.*, 1963). Wang *et al.* (1963) used the most elaborate scheme, 19 elementary reactions, while others chose to disregard the apparently less important reactions to give schemes of six to eight reactions. The shorter mechanisms were proposed with the intention of predicting the dependence of the reactions on the primary molecular products. To elucidate the roles of the free radicals quantitatively, more inclusive mechanisms must be used.

A mechanism similar to that of Wang *et al.* (1963) was chosen. A few additional steps illustrating the attack of free radicals on olefin products were included; however, these reactions should in general have little significance for low conversions. Equations 1 to 23 shown in Table I represent the mechanism. The selected rate constants for the individual reactions, also listed, represent selections based on data in the literature, some of which were not available to Wang *et al.* (1963).

In the selection of the rate constants for Equations 1 to 23 in Table I, the following scheme was used.

First, literature values of the rate constants were collected; then the experimental conditions under which the individual rate constants were measured were reviewed. Where there appeared to be equally correct values of the rate constants, presented values were averaged. Selected values of the rate constants were then tabulated and slight modifications made for consistency among related reactions. Finally, any modifications made were analyzed using the original references as a check to prevent unjustified modifications.

Rate constants are given in Table II for a pyrolysis temperature of 519°C. Activation energies are quoted in calories per gram mole while frequency factors have the units of reciprocal seconds for first-order reactions and liters/(gram mole)(second) for second-order reactions.

A feature of the mechanism is that free radicals of carbon number greater than 4 are not considered. They would lead to products such as hexane and heptene through combination and disproportionation reactions; however,

Table I. Proposed Mechanism for Pyrolysis of *n*-Butane

Chain-initiating reactions		
(1) $C_4H_{10} \rightarrow CH_3 \cdot + C_3H_7 \cdot$	$k_1 = 1.0 \times 10^{17} \exp -79000/RT$	Purnell and Quinn (1962) Wang <i>et al.</i> (1963)
(2) $C_4H_{10} \rightarrow 2 C_2H_5 \cdot$	$k_2 = 1.0 \times 10^{17} \exp -80,000/RT$	Purnell and Quinn (1962) Kerr and Trotman-Dickenson (1961) Wang <i>et al.</i> (1963)
Chain-propagating reaction		
(3) $C_4H_{10} + H \cdot \rightarrow C_3H_7 \cdot + H_2$	$k_3 = 6.3 \times 10^{10} \exp -8200/RT$	Henson and Demore (1965) Sagert and Laidler (1963) Schiff and Steacie (1951) Thruah (1965) Wang <i>et al.</i> (1963)
(4) $C_4H_{10} + CH_3 \cdot \rightarrow C_3H_7 \cdot + CH_4$	$k_4 = 1.0 \times 10^8 \exp -8300/RT$	Jones and Steacie (1953) Kerr and Trotman-Dickenson (1961)
(5) $C_4H_{10} + C_2H_5 \cdot \rightarrow C_3H_7 \cdot + C_2H_6$	$k_5 = 7.7 \times 10^8 \exp -10,400/RT$	Boddy and Steacie (1960) Purnell and Quinn (1962) Wang <i>et al.</i> (1963)
(6) $C_3H_7 \cdot \rightarrow C_2H_5 \cdot + H \cdot$	$k_6 = 2.6 \times 10^{14} \exp -39,500/RT$	Bywater and Steacie (1951) Loucks and Laidler (1967) Purnell and Quinn (1962)
(7) $C_3H_7 \cdot \rightarrow C_2H_5 \cdot + H \cdot$	$k_7 = 2.6 \times 10^{14} \exp -37,500/RT$	Jackson and McNesby (1961) Kerr and Trotman-Dickenson (1961) Wang <i>et al.</i> (1963)
(8) $C_3H_7 \cdot \rightarrow C_2H_4 + CH_3 \cdot$	$k_8 = 5.0 \times 10^{11} \exp -25,000/RT$	Lin and Laidler (1966) Kerr and Trotman-Dickenson (1961) Wang <i>et al.</i> (1963)
(9) $C_3H_7 \cdot \rightarrow C_2H_6 + H \cdot$	$k_9 = 1.0 \times 10^{12} \exp -31,000/RT$	Kerr and Trotman-Dickenson (1961) Wang <i>et al.</i> (1963)
(10) $C_3H_7 \cdot \rightarrow C_2H_4 + CH_3 \cdot$	$k_{10} = 1.0 \times 10^{12} \exp -24,500/RT$	Lin and Laidler (1966) Purnell and Quinn (1962) Sagert and Laidler (1963) Kerr and Trotman-Dickenson (1961)
(11) $C_3H_7 \cdot \rightarrow C_2H_4 + C_2H_5 \cdot$	$k_{11} = 1.6 \times 10^{11} \exp -22,000/RT$	Kerr and Trotman-Dickenson (1960) Kerr and Trotman-Dickenson (1961) Wang <i>et al.</i> (1963)
Secondary reactions		
(12) $C_3H_7 \cdot + H \cdot \rightarrow C_2H_5 \cdot$	$k_{12} = 6.3 \times 10^{10} \exp -4500/RT$	Kerr and Trotman-Dickenson (1961) Wang <i>et al.</i> (1963)
(13) $C_3H_7 \cdot + CH_3 \cdot \rightarrow C_2H_5 \cdot$	$k_{13} = 1.0 \times 10^8 \exp -5000/RT$	Wang <i>et al.</i> (1963)
(14) $C_3H_7 \cdot + CH_3 \cdot \rightarrow C_2H_7 \cdot$	$k_{14} = 1.0 \times 10^8 \exp -7000/RT$	Kerr and Trotman-Dickenson (1961)
(15) $C_3H_7 \cdot + C_2H_5 \cdot \rightarrow C_3H_8$	$k_{15} = 1.0 \times 10^8 \exp -6800/RT$	Kerr and Trotman-Dickenson (1961)
(16) $C_3H_7 \cdot + H \cdot \rightarrow C_2H_5 \cdot$	$k_{16} = 1.0 \times 10^{10} \exp -5500/RT$	Kerr and Trotman-Dickenson (1961)
Chain-terminating reactions		
(17) $H \cdot + H \cdot \rightarrow H_2$	$k_{17} = 6.0 \times 10^7$	Benson and DeMore (1965)
(18) $H \cdot + CH_3 \cdot \rightarrow CH_4$	$k_{18} = 1.0 \times 10^8$	Benson and DeMore (1965)
(19) $H \cdot + C_2H_5 \cdot \rightarrow C_2H_6$	$k_{19} = 1.0 \times 10^{12}$	Benson and DeMore (1965) Wang <i>et al.</i> (1963)
(20) $CH_3 \cdot + CH_3 \cdot \rightarrow C_2H_6$	$k_{20} = 1.0 \times 10^{14}$	Kerr and Trotman-Dickenson (1961)
(21) $CH_3 \cdot + C_2H_5 \cdot \rightarrow C_3H_8$	$k_{21} = 3.0 \times 10^{11}$	Kerr and Trotman-Dickenson (1961)
(22) $C_2H_5 \cdot + C_2H_5 \cdot \rightarrow C_4H_{10}$	$k_{22} = 1.8 \times 10^{10}$	Ivin and Steacie (1951) Kerr and Trotman-Dickenson (1961) Wang <i>et al.</i> (1963)
(23) $C_2H_5 \cdot + C_2H_5 \cdot \rightarrow C_2H_4 + C_2H_6$	$k_{23} = 1.8 \times 10^{10}$	Ivin and Steacie (1951) Kerr and Trotman-Dickenson (1960) Purnell and Quinn (1962) Sagert and Laidler (1963)

Table II. Elementary Rate Constants for 510° C.

$k_1 = 1.5 \times 10^7 \text{ sec.}^{-1}$	$k_{11} = 4.1 \times 10^6 \text{ l./ (g. mole) (sec.)}$
$k_2 = 6.8 \times 10^7 \text{ sec.}^{-1}$	$k_{12} = 1.1 \times 10^6 \text{ l./ (g. mole) (sec.)}$
$k_3 = 3.0 \times 10^8 \text{ l./ (g. mole) (sec.)}$	$k_{13} = 1.2 \times 10^6 \text{ l./ (g. mole) (sec.)}$
$k_4 = 5.0 \times 10^8 \text{ l./ (g. mole) (sec.)}$	$k_{14} = 3.0 \times 10^6 \text{ l./ (g. mole) (sec.)}$
$k_5 = 1.0 \times 10^9 \text{ l./ (g. mole) (sec.)}$	$k_{15} = 6.0 \times 10^7 \text{ l./ (g. mole) (sec.)}$
$k_6 = 2.5 \times 10^9 \text{ sec.}^{-1}$	$k_{16} = 1.0 \times 10^8 \text{ l./ (g. mole) (sec.)}$
$k_7 = 1.2 \times 10^9 \text{ sec.}^{-1}$	$k_{17} = 1.0 \times 10^{12} \text{ l./ (g. mole) (sec.)}$
$k_8 = 6.0 \times 10^9 \text{ sec.}^{-1}$	$k_{18} = 1.0 \times 10^{11} \text{ l./ (g. mole) (sec.)}$
$k_9 = 2.6 \times 10^9 \text{ sec.}^{-1}$	$k_{21} = 3.0 \times 10^{11} \text{ l./ (g. mole) (sec.)}$
$k_{10} = 1.6 \times 10^9 \text{ sec.}^{-1}$	$k_{22} = 1.6 \times 10^{10} \text{ l./ (g. mole) (sec.)}$
$k_{11} = 1.3 \times 10^9 \text{ sec.}^{-1}$	$k_{23} = 1.6 \times 10^{10} \text{ l./ (g. mole) (sec.)}$
$k_{12} = 3.5 \times 10^9 \text{ l./ (g. mole) (sec.)}$	

none of these higher-order molecular products have been detected experimentally. Alkyl radicals higher than $C_4H_9\cdot$ are thought to be extremely unstable under pyrolysis conditions and, if formed, to decompose rapidly to the more stable lower-alkyl radicals. The mechanism also does not consider tertiary and normal butyl radicals separately but lumps the two together.

An isothermal, constant-volume batch reactor was chosen as a basis for the calculations. The restriction to an isothermal system applies to cases where the effects of heats of reaction are small e.g., for low conversion. A material balance for species k in the system gives:

$$R_k = dc_k/dt \quad (24)$$

where c_k = concentration of species k , gram moles per cc., and R_k = rate of production of k by chemical reaction, gram moles/(cc.) (sec.)

Equation 24 coupled with reaction rates derived from Equations 1 to 23 yields the following set of differential equations governing the reaction system. The symbols listed below are used for brevity.

Component	Symbol	Component	Symbol
C_4H_{10}	A	$C_4H_9\cdot$	H
C_3H_8	B	$C_3H_7\cdot$	I
C_2H_6	C	$C_2H_5\cdot$	J
CH_4	D	$CH_3\cdot$	K
C_2H_4	E	H_2	L
C_2H_2	F	H_2	M
C_2H	G		

$$\frac{dc_A}{dt} = -k_1c_A - k_2c_A - k_3c_Ac_L - k_4c_Ac_K - k_8c_Ac_J + k_{23}c_J^2 \quad (25)$$

$$\frac{dc_H}{dt} = k_{21}c_Kc_J \quad (26)$$

$$\frac{dc_C}{dt} = k_5c_Ac_J + k_{10}c_Lc_J + k_{20}c_K^2 + k_{23}c_J^2 \quad (27)$$

$$\frac{dc_D}{dt} = k_4c_Ac_K + k_{18}c_Lc_K \quad (28)$$

$$\frac{dc_K}{dt} = k_9c_H \quad (29)$$

$$\frac{dc_F}{dt} = k_7c_I + k_{10}c_{II} - k_{12}c_Ic_L - k_{13}c_Ic_K \quad (30)$$

$$\frac{dc_O}{dt} = k_6c_J + k_8c_I + k_{11}c_{II} - k_{14}c_Kc_O - k_{18}c_Jc_O - k_{19}c_Lc_O + k_{22}c_J^2 \quad (31)$$

$$\frac{dc_H}{dt} = k_9c_Ac_L + k_4c_Ac_K + k_8c_Ac_J - k_9c_H - k_{10}c_H - k_{11}c_H + k_{11}c_Ic_K + k_{16}c_Jc_O \quad (32)$$

$$\frac{dc_I}{dt} = k_1c_A - k_7c_I - k_8c_I + k_{12}c_Ic_L + k_{14}c_Kc_O \quad (33)$$

$$\frac{dc_J}{dt} = 2k_2c_A - k_6c_Ac_J - k_6c_J + k_{11}c_H - k_{23}c_Kc_J - k_{10}c_Lc_J - 2k_{22}c_J^2 - k_{10}c_Jc_O + k_{10}c_Lc_O - 2k_{22}c_J^2 \quad (34)$$

$$\frac{dc_K}{dt} = k_1c_A - k_4c_Ac_K + k_8c_I + k_{10}c_H - k_{18}c_Lc_K - 2k_{20}c_K^2 - k_{21}c_Kc_J - k_{13}c_Ic_K - k_{14}c_Kc_O \quad (35)$$

$$\frac{dc_L}{dt} = -k_3c_Ac_L + k_6c_J + k_7c_I + k_9c_H - 2k_{17}c_L^2 - k_{10}c_Lc_K - k_{10}c_Lc_J - k_{12}c_Ic_L - k_{16}c_Lc_O \quad (36)$$

$$\frac{dc_M}{dt} = k_2c_Ac_L + k_{17}c_L^2 \quad (37)$$

These equations were then solved numerically employing a Runge-Kutta-Gill, Adams-Moulton differential equation subroutine on file in Caltech's computing center for use with an IBM 7094 computer. As pointed out by Hirschfelder (1957), equations of this type are often difficult to solve numerically; thus, extremely small increments in time had to be employed to prevent overflow on the computer. The subroutine was set up so that local truncation error was not allowed to exceed 1×10^{-8} (roughly equivalent to specifying significant figures to be preserved locally throughout the integration). The computer solution was interrupted periodically and carbon-atom and hydrogen-atom balances were made on the computed species concentrations as a check for continuity of the numerical integration. Approximate computing time for the solution was 15 minutes.

Results

In Figure 1, the free-radical concentrations are plotted as a function of time for a typical pyrolysis case in which the initial pyrolysis mixture is pure *n*-butane, the concen-

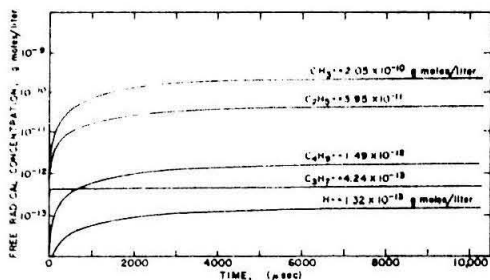


Figure 1. Free-radical concentrations as a function of reaction time for pyrolysis of *n*-butane at 519°C. in a batch reactor and with an initial concentration of 0.002035 mole per liter

tration of which is 0.002035 mole per liter, and the reaction is carried out at 519°C. Any comparison of experiment with calculations necessarily involves some error, since experimentally the initial butane possesses impurities. The induction period, arbitrarily chosen as the time within which the concentrations of free radicals are within 10% of their ultimate values, is seen to be approximately 3.5 milliseconds under these conditions. The over-all reaction times are normally from 1 second to 60 minutes. Only for reaction times as low as a few hundredths of a second does the induction period represent an appreciable fraction, 10%, of the total reaction time. The induction period can be expected to vary slightly with the initial butane concentration but remain in the milliseconds range. Although the absolute level of the free radicals increases with an increase in the initial concentration of butane, the rate of formation of free radicals also increases, as demonstrated by Equations 32 through 36.

A check may be made on the computed concentrations of free radicals by employing the steady-state assumption—i.e., setting Equations 32 through 36 equal to zero and introducing experimental product concentrations of the molecular species into the resulting set of five algebraic equations. In Table III, these calculated free-radical concentrations at steady state are compared with the values obtained by simultaneous numerical integration of Equations 25 through 37. Experimental product concentrations, taken from the work of Sagert and Laidler (1963), were used for the calculation. The average deviation of the free-radical concentrations computed with the assumption of steady state from the values obtained without that assumption is 6%. This result is additional proof of the validity of the steady-state assumption for the pyrolysis of the *n*-butane.

To integrate successfully the complete set of differential equations arising from the material balances for the free-radical reactions, very small increments in the independent variable, time, must be used. During the integration should the concentrations of free radicals approach the values calculated assuming steady state, these steady-state values should be inserted into the original set of differential equa-

Table III. Comparison of Computed Free-Radical Concentrations at 10 Milliseconds with Concentrations Calculated Using Steady-State Assumption

Radical	Computed Conc., Mole/Mole C ₄ H ₁₀ Initially	Calculated Conc. Using Steady-State Assumption, Mole/Mole C ₄ H ₁₀ Initially
CH ₃ ·	1.01 × 10 ⁻⁷	1.1 × 10 ⁻⁷
C ₂ H ₅ ·	1.94 × 10 ⁻⁸	2.0 × 10 ⁻⁸
C ₃ H ₇ ·	2.08 × 10 ⁻¹⁰	2.1 × 10 ⁻¹⁰
C ₄ H ₉ ·	7.32 × 10 ⁻¹⁰	6.4 × 10 ⁻¹⁰
H·	6.48 × 10 ⁻¹¹	6.9 × 10 ⁻¹¹

tions. Numerical integration could then continue, assuming steady state and using large increments in the independent variable.

Acknowledgment

Work reported here is part of a program on studies of the thermal decomposition and partial oxidation of *n*-butane. Partial support of the effort by the Shell Companies Foundation and by way of a National Science Foundation fellowship is gratefully acknowledged.

Literature Cited

- Barker, J. R., Corcoran, W. H., unpublished work, 1968.
 Benson, S. W., DeMore, W. B., *Ann. Rev. Phys. Chem.* **16**, 397 (1965).
 Boddy, P. J., Steacie, E. W. R., *Can. J. Chem.* **38**, 1576 (1960).
 Bywater, S., Steacie, E. W. R., *J. Chem. Phys.* **19**, 326 (1951).
 Giddings, J. C., Shin, H. K., *J. Chem. Phys.* **36**, 640 (1962).
 Hirschfelder, J. O., *J. Chem. Phys.* **26**, 271 (1957).
 Ivin, K. J., Steacie, E. W. R., *Proc. Roy. Soc. London* **A206**, 25 (1951).
 Jackson, W. M., McNesby, J. R., *J. Am. Chem. Soc.* **83**, 4891 (1961).
 Jones, M. H., Steacie, E. W. R., *Can. J. Chem.* **31**, 505 (1953).
 Kerr, J. A., Trotman-Dickenson, A. F., *J. Chem. Soc.* **1960**, 1802.
 Kerr, J. A., Trotman-Dickenson, A. F., *Progr. Reaction Kinetics* **1**, 119 (1961).
 Lin, M. C., Laidler, K. J., *Can. J. Chem.* **44**, 2927 (1966).
 Loucks, L. F., Laidler, K. J., *Can. J. Chem.* **45**, 2795 (1967).
 Purnell, J. H., Quinn, C. P., *Proc. Roy. Soc. London* **A270**, 287 (1962).
 Sagert, N. H., Laidler, K. J., *Can. J. Chem.* **41**, 838 (1963).
 Schiff, H. I., Steacie, E. W. R., *Can. J. Chem.* **29**, 1 (1951).
 Thrush, B. A., *Progr. Reaction Kinetics* **3**, 63 (1965).
 Wang, Y. L., Ph.D. thesis, California Institute of Technology, 1963.
 Wang, Y. L., Rinker, R. G., Corcoran, W. H. *Ind. Eng. Chem. Fundamentals* **2**, 161 (1963).

RECEIVED for review April 15, 1968

ACCEPTED October 18, 1968

PROPOSITIONS

PROPOSITION I

ESTIMATION OF OXYGEN CONTENT
OF GAS MIXTURES

ABSTRACT

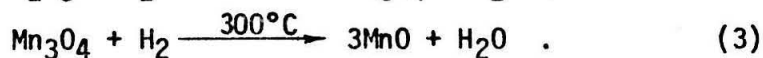
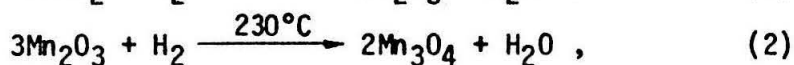
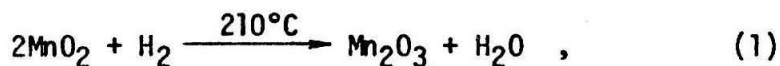
The concentration of oxygen in a gas mixture may be found by metering the gas through a small-bore glass tube containing manganous oxide. The rate of advance of the $\text{MnO} - \text{Mn}_3\text{O}_4$ interface is correlated with the oxygen concentration and flow rate.

INTRODUCTION

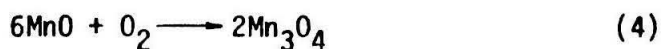
Gas-solid chemical reactions have been commonly used to purify inert gas streams contaminated with oxygen (1, 2, 3). The oxidation of the lower oxides of certain metals to more highly oxidized states are but one group of materials used in these processes. Manganous oxide (MnO) in the form of a fine green powder, may be oxidized rapidly at room temperature to a more stable oxide Mn_3O_4 , a brownish grey powder. If a small bore glass tube is filled with MnO and a gas containing oxygen is passed through the column, the MnO is oxidized at a rate proportional to the oxygen concentration of the sample. A sharp advancing MnO- Mn_3O_4 interface may be observed visually because of the color difference in reactant and product. By recording the gas flow rate and the time required for the interface to traverse a measured length of the tube, an estimate of the oxygen content of the inlet gas may be found.

ANALYSIS

Manganese dioxide (MnO_2), obtainable commercially from Baker Chemical Company, may be reduced to manganous oxide (MnO) with hydrogen at temperatures above $300^\circ C$ (3). The basic steps involved in the reduction are shown below:



MnO, near room temperature, will re-oxidize immediately to the Mn₃O₄ stage when exposed to oxygen according to equation (4).



If a mass balance is made on oxygen over a length of the test column for which the time has been recorded for the traverse of the moving interface, the following equation results.

$$FC_T x_A \phi - WAL = 0 \quad (5)$$

where F = inlet gas flow rate, [=] cm³ min⁻¹

C_T = total inlet concentration of gas, [=] mole cm⁻³

x_A = mole fraction oxygen of inlet gas

ϕ = time required for interface to travel distance L , [=] min

W = amount of oxygen absorbed per unit volume of bed,
[=] mole cm⁻³

A = inside cross-sectional area of tube, [=] cm²

L = length of bed traversed by interface in time ϕ , [=] cm.

The following assumptions were made in the derivation of equation (5).

1. All oxygen entering the column is absorbed rapidly by MnO at the interface.
2. The reactor bed of MnO is uniform.

Rearranging equation (5) yields the desired expression for the inlet oxygen concentration.

$$x_A = \frac{WAL}{FC_T \phi} \quad (6)$$

If C_T , A , and W are assumed constant, equation (6) becomes

$$x_A = k \frac{L}{F\phi} \quad (7)$$

where $k = (WA) / C_T$.

An expression for the amount of oxygen reacted per unit volume of bed, W , may be written as follows from consideration of equation (4).

$$W = \frac{\psi \rho_B}{6M} \quad (8)$$

where ψ = efficiency of MnO bed taken as the moles of MnO reacted in the test section divided by the total moles MnO present in the same section

ρ_B = bulk density of granular MnO bed, [=] gms cm⁻³

M = molecular weight of MnO.

If the gas is assumed ideal, an expression for C_T may be written in terms of the temperature and pressure of the inlet gas,

$$C_T = \frac{P}{RT} \quad (9)$$

where R = universal gas constant = 82.06 atm cm³ mole⁻¹ °K⁻¹

T = absolute temperature of the inlet gas, [=] °K

P = absolute pressure of the inlet gas, [=] atm.

Substitution of equations (8) and (9) into equation (6) yields

$$x_A = \frac{\psi \rho_B}{6MP} \frac{ART L}{F\phi} \quad (10)$$

and

$$k = \frac{\psi \rho_B \text{ ART}}{6\text{MP}} \quad (11)$$

PROCEDURE

Two six-inch lengths of 0.25 inch O.D. glass tubing having a 1.25 mm I.D. were selected for the test. A plug of glass wool was inserted into one end of each tube. Manganese dioxide (MnO_2) powder, approximately 100 mesh with an average bulk density of 2.83 g cm^{-3} , was carefully poured into the tubes. The ends of the tubes were gently tapped intermittently during the packing to obtain a uniform bed. After packing, another plug of glass wool was placed in the open end of each tube. The columns were then equipped with Swagelock fittings using Teflon ferrules.

The MnO_2 (black) in the tubes was then reduced to MnO (green) by passing hydrogen through the tubes at approximately 370°C for 24 hours. Upon cooling, a tube was placed vertically into the testing assembly as shown in Figure 1 and a run taken. After a test, the MnO was regenerated by reducing the Mn_3O_4 with hydrogen at 370°C for 6 hours.

Test gases were prepared using an available gas make-up apparatus in which a gas cylinder was initially evacuated. Oxygen was admitted into the cylinder until the desired pressure was attained. The cylinder pressure was then boosted to 48 psig with argon. Assuming that Dalton's law was valid for the gas mixture, the oxygen concentration

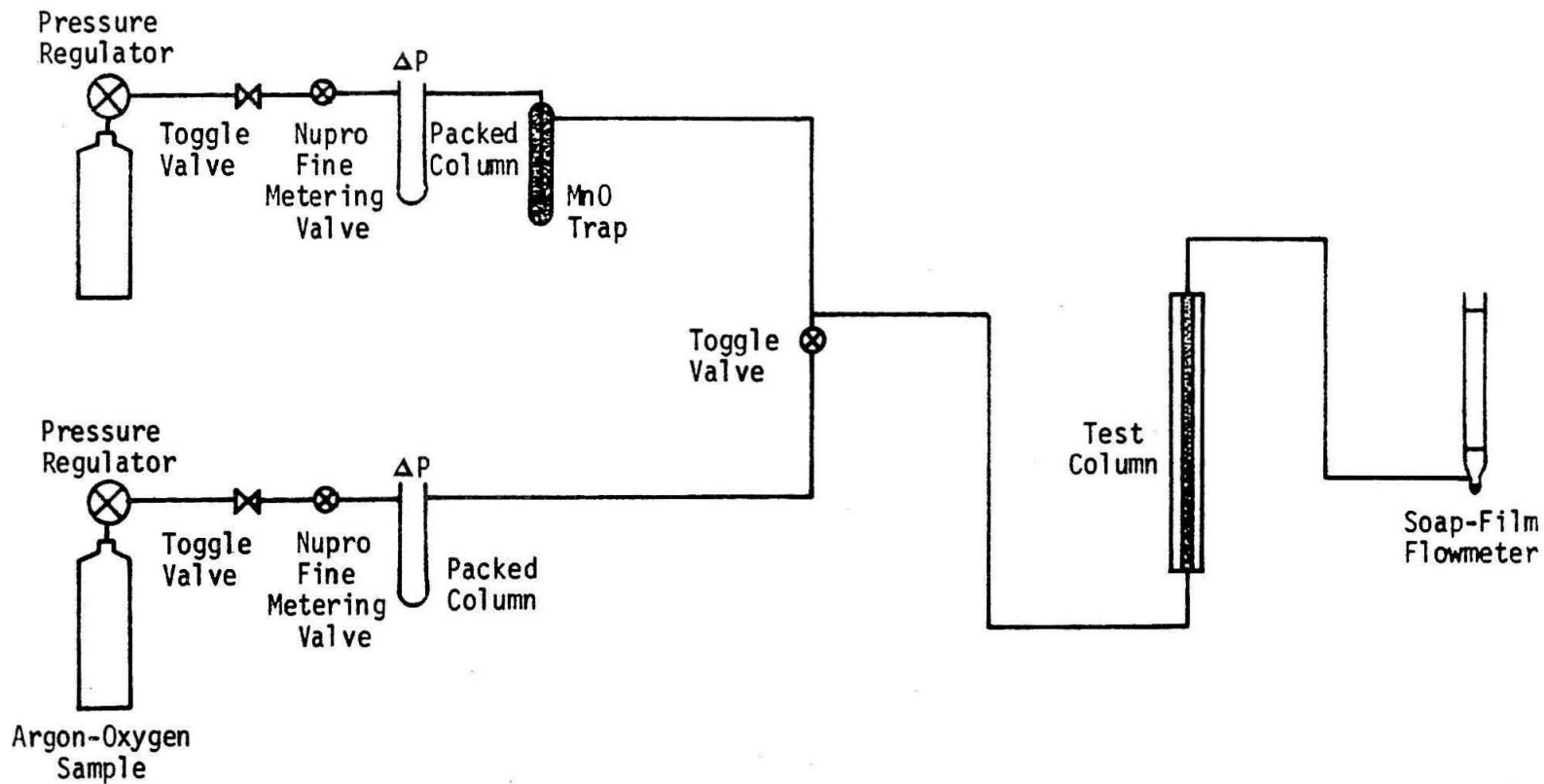


Figure 1. Schematic of testing apparatus.

could be calculated.

Oxygen-free argon was used as a purge gas in the test assembly. Prior to insertion of an MnO tube into the assembly, the system was purged to remove previous oxygen samples. The tube was placed in the assembly, the purge gas valve closed, and the test gas valve opened. After a short time (30 to 60 seconds) to allow the gas entering the tube to become representative of the sample, a position of the interface was noted by means of a cathetometer and simultaneously a stop-watch started. The cathetometer was then adjusted to a new position and the watch stopped as the interface advanced past this position. The difference in cathetometer readings and time were recorded as in Table 1. Gas flow was regulated by a Nupro fine-metering valve and measured by manometrically recording the pressure drop through packed columns of glass micro-spheres. The exit flow rate, F' , from the MnO tube was also measured with a soap-film flowmeter.

RESULTS

The data of Table 1, taken on gas mixtures from 0.39 to 4.1 mole per cent oxygen, were treated according to equation (7). Figure 2 is a plot of oxygen concentration versus $L/(F\phi)$. The experimental relationship between the mole fraction of oxygen in a mixture and $L/(F\phi)$ is seen to be in agreement with the linear theoretical analysis. The equation of the straight line representing the data is shown below:

$$x_A = 1.723 L/(F\phi) . \quad (12)$$

Table 1. Experimental Data.

Test Column	x_A , mole per cent	L , cm	ϕ , min	F' , cm^3/min	F , cm^3/min	$L/F\phi$, cm^{-2}	$(x_A)_C^*$, mole per cent	Per cent Error
1	0.39	7.02	7.16	3.70	3.72	0.263	0.45	15.4
1	0.39	7.03	7.31	3.72	3.74	0.257	0.44	12.8
1	0.39	7.04	6.75	3.76	3.78	0.276	0.47	20.5
2	1.8	5.46	1.25	3.60	3.66	1.19	2.05	11.4
2	1.8	5.65	1.28	3.68	3.75	1.17	2.02	11.2
2	1.8	6.69	1.86	3.70	3.77	0.96	1.66	-6.7
2	3.4	4.97	0.724	3.59	3.72	1.85	3.19	-6.2
1	4.1	3.55	0.405	3.60	3.75	2.33	4.02	-2.0
1	4.1	6.26	0.725	3.58	3.72	2.32	4.00	-2.4
1	4.1	4.40	0.483	3.62	3.77	2.42	4.17	1.7

* Calculated from equation (12)

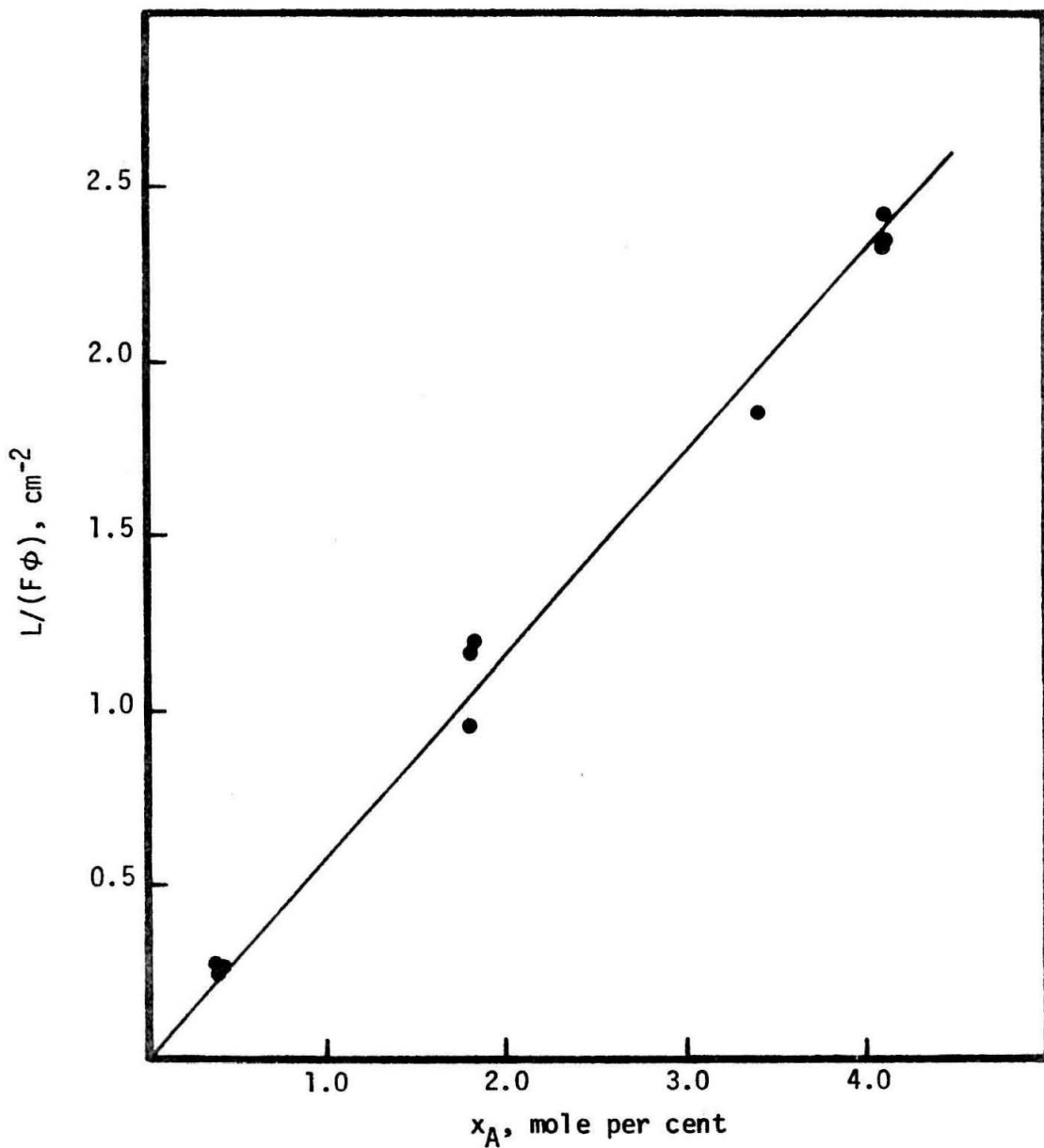


Figure 2. Oxygen concentration versus $L/(F\phi)$.

The average deviation of the data from the straight line is 9.0 per cent. The maximum and minimum deviations (13 to 20 per cent and 2 per cent) occur at the lowest (0.39 mole per cent) and the highest (4.1 mole per cent) concentrations of oxygen, respectively.

From equations (12) and (7), the value of k found experimentally from the particular test columns was $1.723 \text{ (cm}^2\text{) (mole per cent O}_2\text{)}$. From equation (11), a value of 0.012 was calculated for the efficiency of the MnO bed under the following conditions:

$$T = 295^\circ\text{C}$$

$$P = 1.15 \text{ atm}$$

$$\rho_B = 2.31 \text{ gms cm}^{-3}$$

$$A = 0.01227 \text{ cm}^2$$

Based on the experimental data, little difference in the analysis resulted from interchanging test columns. Regeneration of a column did not appear to change its reactivity.

DISCUSSION

The preliminary data indicate that, over the range of oxygen concentrations studied, the use of MnO columns as a means of measuring the oxygen concentration of a gas is feasible. The error in analysis was greatest at oxygen concentrations below 0.5 per cent; however, there is no reason to believe that with refined techniques and equipment the general method cannot be applied satisfactorily to gases containing less than 0.1 per cent oxygen.

Quite probably, a reduction in the error of the analysis can be achieved by improvements in the testing arrangement. In the assembly used, a significant dead space was present between the sample source and the inlet to the test column. Reduction of this space would effectively reduce error resulting from the mixture of the sample gas with the purge gas. Longer test sections and the choice of an optimum tube diameter may also improve results.

The rather low column efficiency observed is a striking point. The variation of this parameter, a distinct possibility, with column size and flow rate was not investigated. Channeling of the gas stream through the MnO bed is probably the greatest source of low column efficiency. Lack of sufficient time during an analysis for the diffusion of oxygen to the centers of the MnO particles is another possibility. Increasing the temperature of the column from room temperature to 150°C might improve the efficiency as the reaction rate would be increased.

White and Smith (3), in removing oxygen from contaminated inert atmospheres, found that MnO beds upon repeated regeneration (20 to 30 cycles) crumbled and lost efficiency for absorbing oxygen. Because of the limited number of runs in the present experiment, this problem was not encountered; however, the problem may be overcome by routinely discarding the MnO after an optimum number of cycles. Studies of the bed efficiency with repeated use would thus be desirable.

REFERENCES

1. H. A. Cockett, British Patent 757,037.
2. G. E. Hillman and J. Lightwood, Anal. Chem., 38 (10), 1430 (1966).
3. P. A. F. White and S. E. Smith, "Inert Atmospheres," Butterworths, Washington, 1962.

PROPOSITION II

A HIGH DEGREE OF SELECTIVITY IN THE
ABSORPTION OF OLEFINS USING SULFURIC ACID

ABSTRACT

Olefins may be absorbed from gas mixtures by contact with sulfuric acid. By careful control of the concentration of the absorbing sulfuric acid, a high degree of olefin selectivity may be exhibited. A simple scheme is presented for the laboratory preparation of research-quality mixtures of gases such as the permanent and inert gases with controlled traces of the lower olefins.

INTRODUCTION

The use of sulfuric acid as an olefin absorbent has been known for over fifty years. In 1949, F. R. Brooks, et. al., (1) developed a gas absorption apparatus for the analysis of gas mixtures commonly encountered in the petroleum industry. A degree of olefin selectivity obtained by the use of sulfuric acid solutions of different concentrations (65 and 87 per cent) was utilized in this scheme for the determination of the concentration of isobutene and the aggregate concentration of the n-butenes plus propylene.

In 1955, P. W. Mullen (2), in a discussion of olefin absorbents, concluded that sulfuric acid in various concentrations appeared to offer about the only available method of differentiating among types of olefins by absorptiometric techniques. To the author's knowledge, all work to date involving olefin absorptions in sulfuric acid has been limited to the total separation of ethylene, propylene and n-butenes, isobutene, and higher olefin fractions. It would seem, at least in principle, higher degrees of olefin selectivity could be obtained by careful control of the concentration of sulfuric acid. If feasible, the technique would be applicable to the laboratory preparation of research-quality hydrocarbon mixtures. Because of the destructive nature of the olefin absorption, the method would be limited to the preparation of mixtures of the lower olefins and compounds, such as cyclohexane, that are not reactive with sulfuric acid. To test the feasibility of the method, the absorption characteristics of a gas

mixture containing 1-butene, t-2-butene, c-2-butene and isobutane have been studied with different concentrations of sulfuric acid.

PROCEDURE

The gas mixture was prepared using C.P. grade cylinders of the pure compounds and an available gas make-up unit. A test cylinder was initially evacuated. The sample components were then introduced into the cylinder in the desired proportions by noting the pressure changes in the test cylinder upon the individual additions. Argon was added to the mixture as a diluent. Assuming Dalton's Law was valid for the mixture, the gas composition could be determined. The gas used in the preliminary experiments was of the following composition: argon, 80.0 per cent; isobutane, 10.5 per cent; 1-butene, 3.4 per cent; t-2-butene, 2.7 per cent; c-2-butene, 3.4 per cent.

The testing apparatus is shown in Figure 1. The test gas was bubbled through 500 ml of sulfuric acid at an average rate of 7.5 ml min^{-1} . A scrubber containing dilute solution of potassium hydroxide served to remove sulfur trioxide vapor that might have been introduced into the gas stream. Water-soluble absorption products such as alcohols which might have entered the gas train were removed in a second scrubber containing water. Before the emerging gas stream entered the gas-chromatography unit for analysis, water was removed from the gas by a trap of Drieite (anhydrous calcium sulphate). The scrubbed gas was analyzed using a 90 foot column of Carbowax 400 -- β , β' - oxydipropionitrile on Chromosorb P and a flame ionization detector.

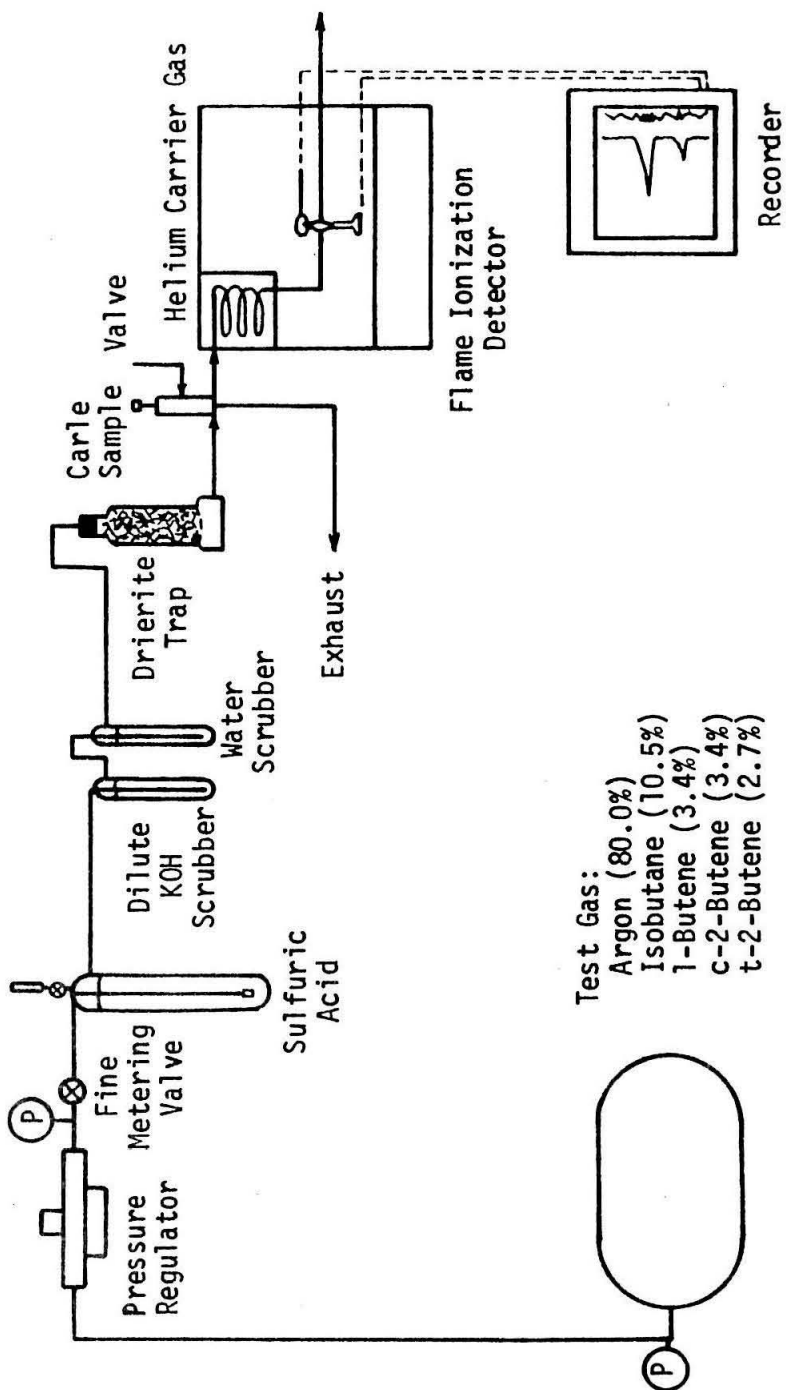


Figure 1. Schematic of experimental apparatus.

Six single-pass test runs were made using sulfuric acid in concentrations of 75.0, 82.0, 85.0, 87.5, 90.0 and 96.0 per cent by weight. Each run generally covered a 24 hour period and gas analyses were performed intermittently. Five to nine analyses were made per run, each analysis taking roughly 35 minutes. In addition, analyses of the test were made prior to beginning the series of tests and checked after the first four runs. No change in the test gas composition was observed.

The peak areas from the chromatograms of each run were used in the determination of the absorption of the components. Isobutane, which is not absorbed by sulfuric acid in the range of concentrations of acid studied, was used as a standard in analysis of the chromatograms. In order to place all the analyses in proper perspective, each analysis was adjusted to obtain the same peak area for isobutane.

RESULTS

In general, after a two to three hour period of initial operation in which the various vessels and connecting lines were purged of gases of the previous test, the compositions of the scrubbed gas did not change. The results of the olefin absorption tests are given in Table 1.

In the lower range of acid concentrations (70 to 77 per cent), the butenes were found to be absorbed in the following order: t-2-butene > c-2-butene > 1-butene. In contrast the relative absorptions at acid concentrations above 90 per cent were in the following order: c-2-butene > t-2-butene > 1-butene. In the intermediate area, c-2-butene was

Table 1. Experimental Results.

Sample Size, μ l	Sulfuric Acid Concentration, Weight Per Cent	Adjusted Peak Area			Per Cent Reduction			
		i-C ₄ H ₁₀	1-C ₄ H ₈	t-2-C ₄ H ₈	c-2-C ₄ H ₈	1-C ₄ H ₈	t-2-C ₄ H ₈	c-2-C ₄ H ₈
50	--	8,000	2,100	1,702	2,192	--	--	--
100	--	16,325	4,510	3,650	4,680	--	--	--
50	75.0	8,000	2,030	1,597	2,086	3.3	6.2	4.8
100	75.0	16,325	4,305	3,205	4,310	4.5	12.2	7.9
50	82.0	8,000	1,405	--	928	33.1	--	57.7
100	82.0	16,325	2,955	--	1,915	34.5	--	59.1
50	85.0	8,000	632	609	200	69.9	64.3	90.9
100	85.0	16,325	1,408	1,354	470	68.8	63.0	89.9
50	87.5	8,000	414	456	126	80.3	73.2	94.4
100	87.5	16,325	961	1,000	264	78.8	72.7	94.3
50	90.0	8,000	101	58	20	95.1	96.6	99.2
100	90.0	16,325	207	97	33	95.5	97.3	99.4
50	96.5	8,000	238	11	3	88.7	99.4	99.9
100	96.5	16,325	522	13	6	88.5	99.7	99.9

clearly absorbed in the greatest proportion; however, absorption of t-2-butene and 1-butene were approximately equal. A plot of the relative absorption versus the concentration of the absorbing acid is given in Figure 2.

Visual observations of the absorption process were noted during the runs. The color of the 96.5 per cent sulfuric acid solution after 19 hours of operation was a deep brownish-orange. The 75 per cent solution was still clear after 21 hours of operation while the solutions of intermediate concentrations varied from pale yellow to deep yellow to pale orange after 20 to 22 hours operation. No analyses of the compositions of these solutions were made.

DISCUSSION

The results may be rationalized by considering a probable reaction path during the absorption. The absorptions, as run, are unlikely to be equilibrium controlled because of the relatively short gas contact time in the acid absorber (approximately 3 to 5 seconds). Thus, olefin consumption may be examined on the basis of a kinetic-controlled reaction. The stability of intermediate species and steric effects would thus be important. If the absorption is considered as a cationic hydration or dimerization at the lower concentrations of acid and a cationic polymerization at the higher concentrations of acid, the first step of the absorption might be the electrophilic attack on the olefin of a hydrogen ion from the dissociated acid. Polymerization might then

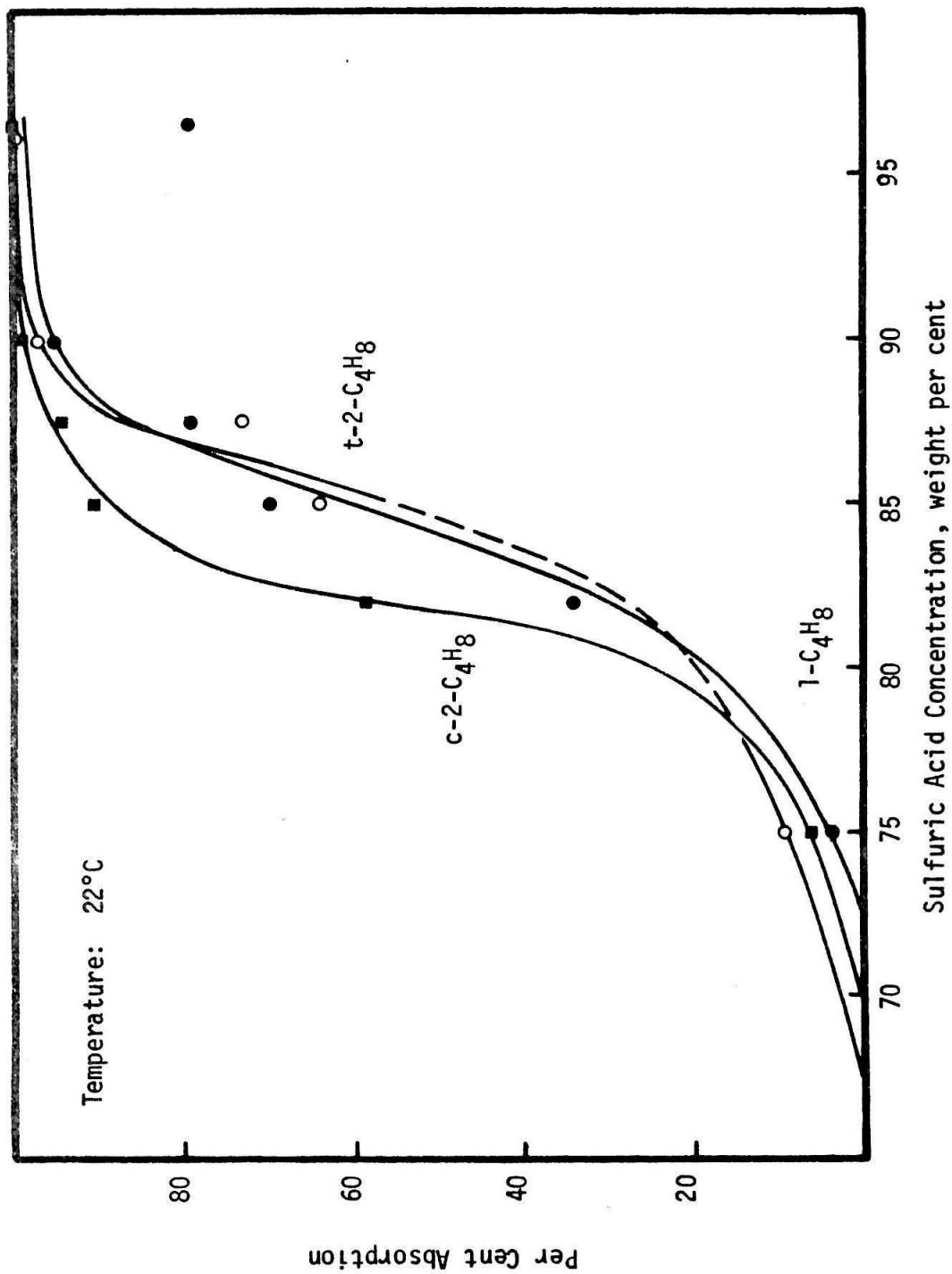
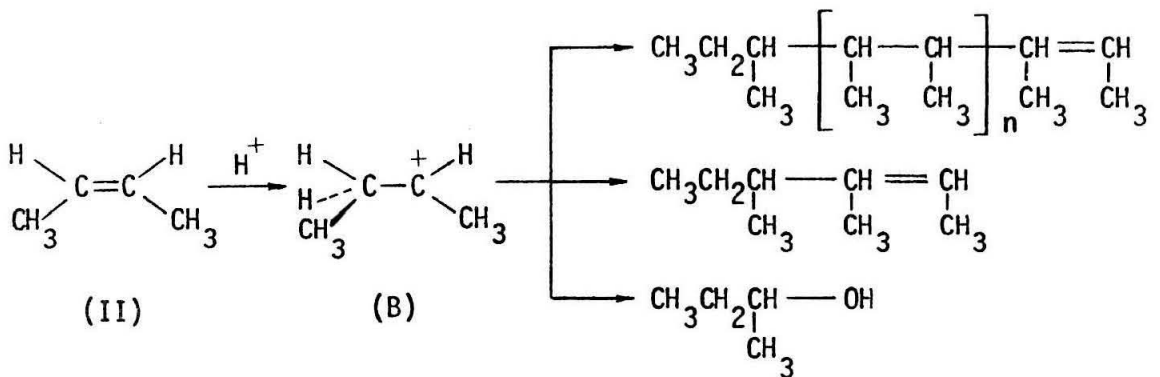
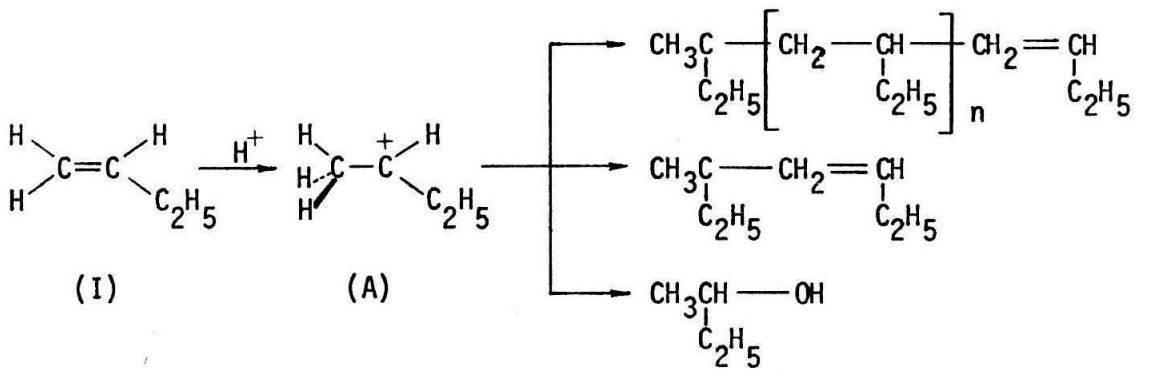
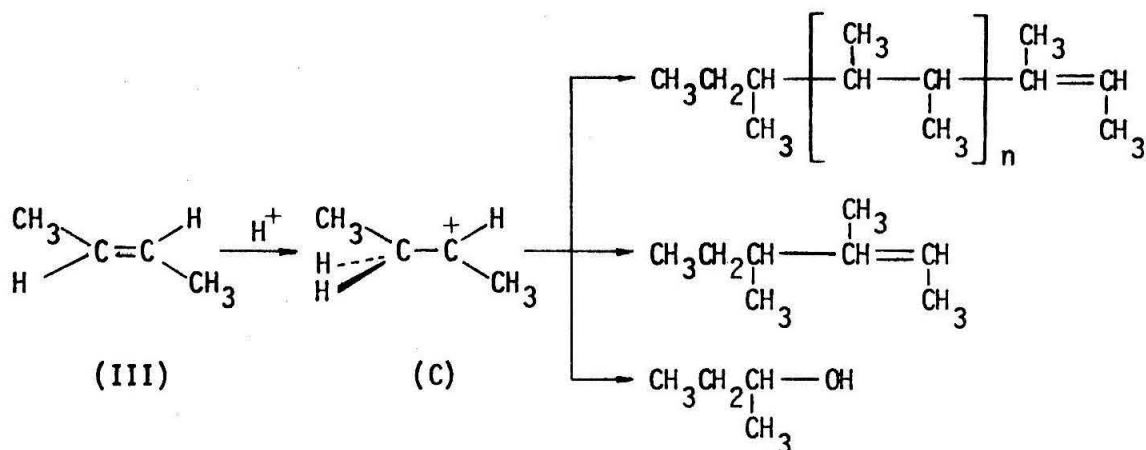


Figure 2. Absorption characteristics for the n-butenes in sulfuric acid.

take place in highly concentrated acid with the repeated attack on olefin molecules by growing cationic intermediates. Termination of a polymerization chain would occur with the loss of a proton to water. In less concentrated acids (higher water concentrations), the intermediate cationic species might lose a proton to water at an early stage, i.e., dimerization. In even less concentrated acid, hydration of a cationic species may result in alcohol formation. These reaction sequences are illustrated in the following steps for each of the three butenes.





Of the three cationic species initially formed, the order of increasing stability is $A < B < C$. This represents a possible explanation of the absorption characteristics in the lower concentrations of acid where the order of increasing absorption was observed as $I < II < III$. In the more concentrated acid where polymerization might take place, stereochemical effects might favor the absorption of II over III.

CONCLUSIONS

As a thorough study of the use of various concentrations of sulfuric acid for preferential absorptions of olefins on a preparative basis was not made, it cannot be concluded that this method is general. The preliminary data do sufficiently indicate the strong possibility of the success for the controlled preparation of mixtures of saturated hydrocarbons and olefins by selective absorption using sulfuric acid. The preliminary work was restricted to small scale operation and mixtures of the n-butenes. The effects of residence time in the sulfuric-acid absorber, composition of the inlet gas and temperature of operation

were not investigated.

On the basis of the experimental data, a large number of passes would be required for the near complete preferential absorption of the 2-butenes in a mixture of n-butenes. The sulfuric acid concentration would be critical in such a separation; however, such a purifying process should be possible.

REFERENCES

1. F. R. Brooks, L. Lykken, W. B. Milligan, H. P. Nebeker and V. Zahn, Anal. Chem., 21, 1105 (1949).
2. P. W. Mullen, "Modern Gas Analysis," Interscience, New York, 1955.
3. J. D. Roberts and M. C. Caserio, "Basic Principles of Organic Chemistry," W. A. Benjamin, Inc., New York, 1965.
4. D. A. Shirley, "Organic Chemistry," Hold, Rhinehart and Winston, New York, 1964.

PROPOSITION III

PARALLEL-COLUMN, GAS CHROMATOGRAPHY FOR THE
SEPARATION OF LIGHT GASES

ABSTRACT

A dual-column arrangement employing molecular sieve 5A and either Porapak T or Porapak S is proposed for the separation of hydrogen, oxygen, nitrogen, carbon monoxide, carbon dioxide, and other light gases in gas chromatography. Uniqueness of the proposal is the combined choice of stationary phases and the connection of the columns in parallel. Flexibility of the system is enhanced by temperature control of the columns individually.

INTRODUCTION

The use of gas chromatography as an analytical tool has been widely accepted in the past decade. In the course of the analysis of gas mixtures, the separation of hydrogen, oxygen, nitrogen, carbon monoxide, and carbon dioxide is frequently required. Such would be the case for the analysis of flue gases, combustion products, or in a study of the oxidation of carbon monoxide. A parallel column arrangement utilizing molecular sieve 5A and either Porapak T or Porapak S is proposed for use in the chromatographic analysis of these compounds. Proper choice of column dimensions, carrier flow rates, and column temperatures would allow extension of the analysis to include compounds such as nitric oxide, methane, ethane, water, and formaldehyde.

Previously, many stationary phases have been employed in the chromatography of these compounds. In addition, techniques of multiple columns, multiple detectors, solute trapping and column switching have been used. Since Kyriacos and Boord (1) first reported the separation of hydrogen, oxygen, nitrogen, and carbon monoxide on molecular sieve, the separation of mixtures containing oxygen and nitrogen has generally involved an analysis using some type of molecular sieve. Unfortunately, molecular sieve irreversibly absorbs carbon dioxide at normal operating temperatures (<300°C). Adsorption columns of silica gel (2) or activated charcoal (3) have commonly been used in series with a column of molecular sieve for the complete analysis. Either two detectors or a column selector valve are required for the series column approach. Each

elective may add several hundred dollars to the cost of the analytical unit.

Hollis (4), in 1966, reported the use of porous-polymer beads (Porapak) as a solid adsorbent with the separating properties of a liquid phase, e.g. reduced tailing of peaks caused by solute-adsorbent interaction. The beads were synthesized from monomers such as styrene, tertiary-butylstyrene, and ethylvinylbenzene that were crosslinked with divinylbenzene. Using Porapak Q at -78°C , hydrogen, nitrogen, and oxygen can be resolved but temperature programming is required for elution of carbon monoxide and carbon dioxide within a reasonable time.

Obermiller, et al (5) described the use of porous polymers in the analysis of nitrogen, oxygen, argon, carbon monoxide, carbon dioxide, hydrogen sulfide, and sulfur dioxide using a novel dual column (connected in series) arrangement. Each element of a thermistor detector was alternately used as the reference and sensing element in the analysis. Analysis time was about 17 minutes.

Recently, Lorenzo (6) has reported the use of a three-column system in series employing column switching for the determination of mixtures of nitrogen, oxygen, carbon monoxide, methane, carbon dioxide, ethylene, and ethane. Molecular sieve 5A and Porapak Q were selected as stationary phases, and the analysis required 25 minutes.

PROCEDURE

A schematic of the proposed dual column system using a combination of molecular sieve and porous polymer as the adsorbents is shown in

Figure 1. A 1.5-foot column (0.125" O.D.) of molecular sieve 5A was placed in parallel with a 2.5-foot column (0.125" O.D.) of Porapak T. To avoid interference of peaks eluting early, a 6-foot length of 1/8" tubing was inserted in series with the Porapak column. For a total flow rate of carrier gas of 39.9 ml min^{-1} through the network, flow through the Porapak column was 11.0 ml min^{-1} . The temperature of each column could be controlled individually. The flow rate through each column was a function of the inlet pressure, the column temperatures, and the resistance to flow of each branch of the parallel network. If an adjustment of flow were desired with the only resultant change in the separation a result of that change in flow, a short length of tubing packed with glass beads could be added in series to the branch whose flow was to be decreased.

RESULTS

A chromatogram of a test gas is presented in Figure 2 for a total flow rate of 39.9 ml min^{-1} , a sample size of 0.5 ml, and temperatures of the Porapak T and molecular sieve columns of 23 and 55°C, respectively. A total time of 6 minutes was required for the analysis. The composition of the test gas is given below:

	<u>mole per cent</u>
Helium	71.96
Nitrogen	8.25
Hydrogen	6.68
Carbon monoxide	6.56
Carbon dioxide	4.36
Oxygen	2.19

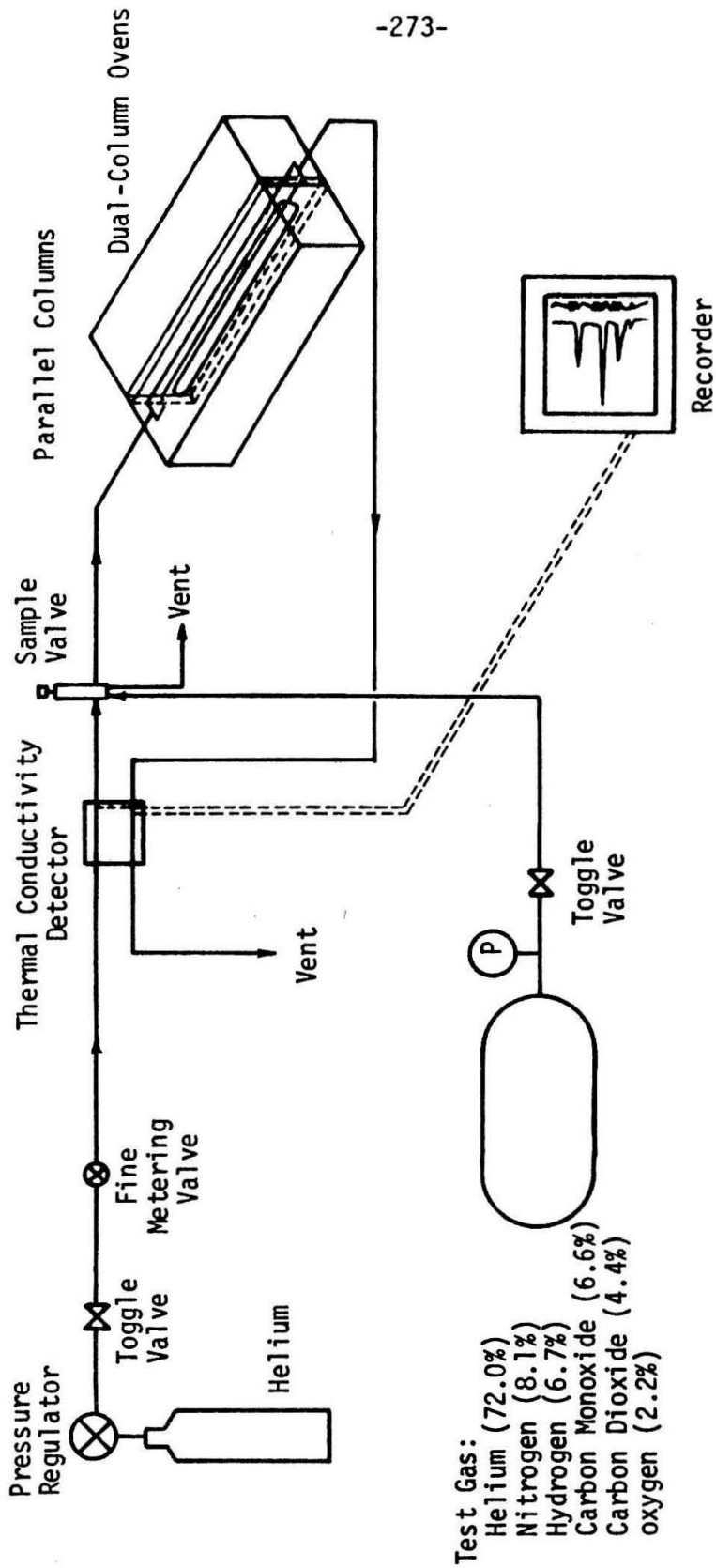


Figure 1. Schematic of the proposed dual-column network.

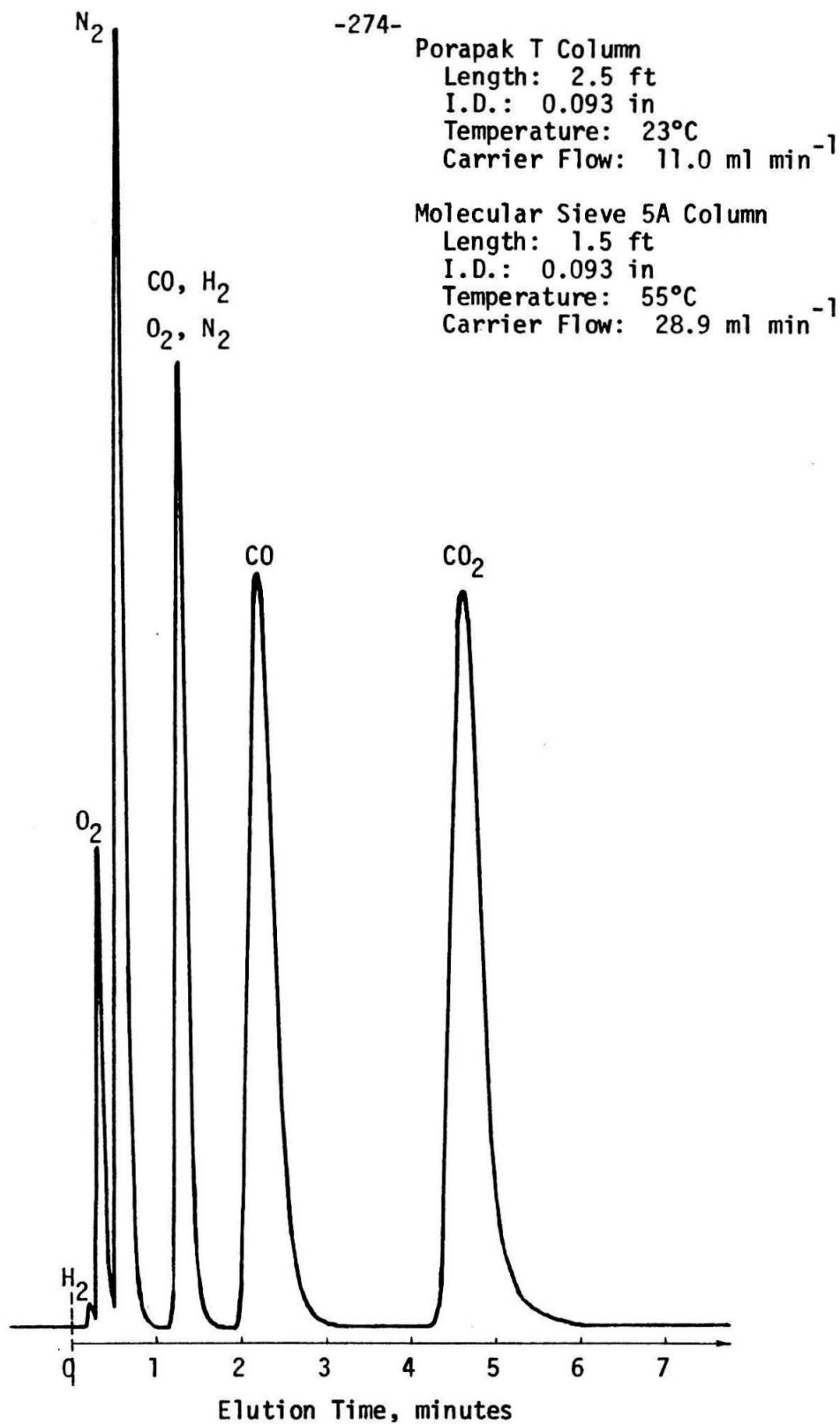


Figure 2. Chromatogram for parallel columns of Porapak T and molecular sieve 5A.

For instances in which small quantities of carbon monoxide, oxygen, and nitrogen are to be measured in the presence of an excessively large amount of carbon dioxide, the system just described is suitable. In other cases where trace analysis of hydrogen, oxygen, nitrogen, and carbon dioxide in carbon monoxide is required, elution of the peak for carbon monoxide last would be advantageous so as not to mask the smaller peaks. A 2.5-foot column (0.125" O.D.) of Porapak S in series with a 4-foot length of 1/8" tubing can be substituted for the column of Porapak T in the previous scheme. A chromatogram of the test gas on the Porapak S arrangement is presented in Figure 3. Total flow of helium carrier was 40.0 ml min^{-1} with 13.3 ml min^{-1} through the Porapak branch. The column of molecular sieve 5A was at 28°C while the column of Porapak S was at 23°C . Total time for the analysis was 6 minutes. As may be observed, the relative positions of the peaks for carbon monoxide and carbon dioxide have been reversed while retaining good peak shape.

Advantages of the parallel-column method over the series-column technique may be listed as follows:

1. Analysis time is decreased.
2. Base line shifts accompanying column switching are absent and the analysis is uninterrupted.
3. A single detector is required.
4. Temperature programming is not required although it may be utilized on each column individually for more complicated mixtures.
5. Flexibility of peak position is enhanced by the capability of independently varying the flow rate through each column.

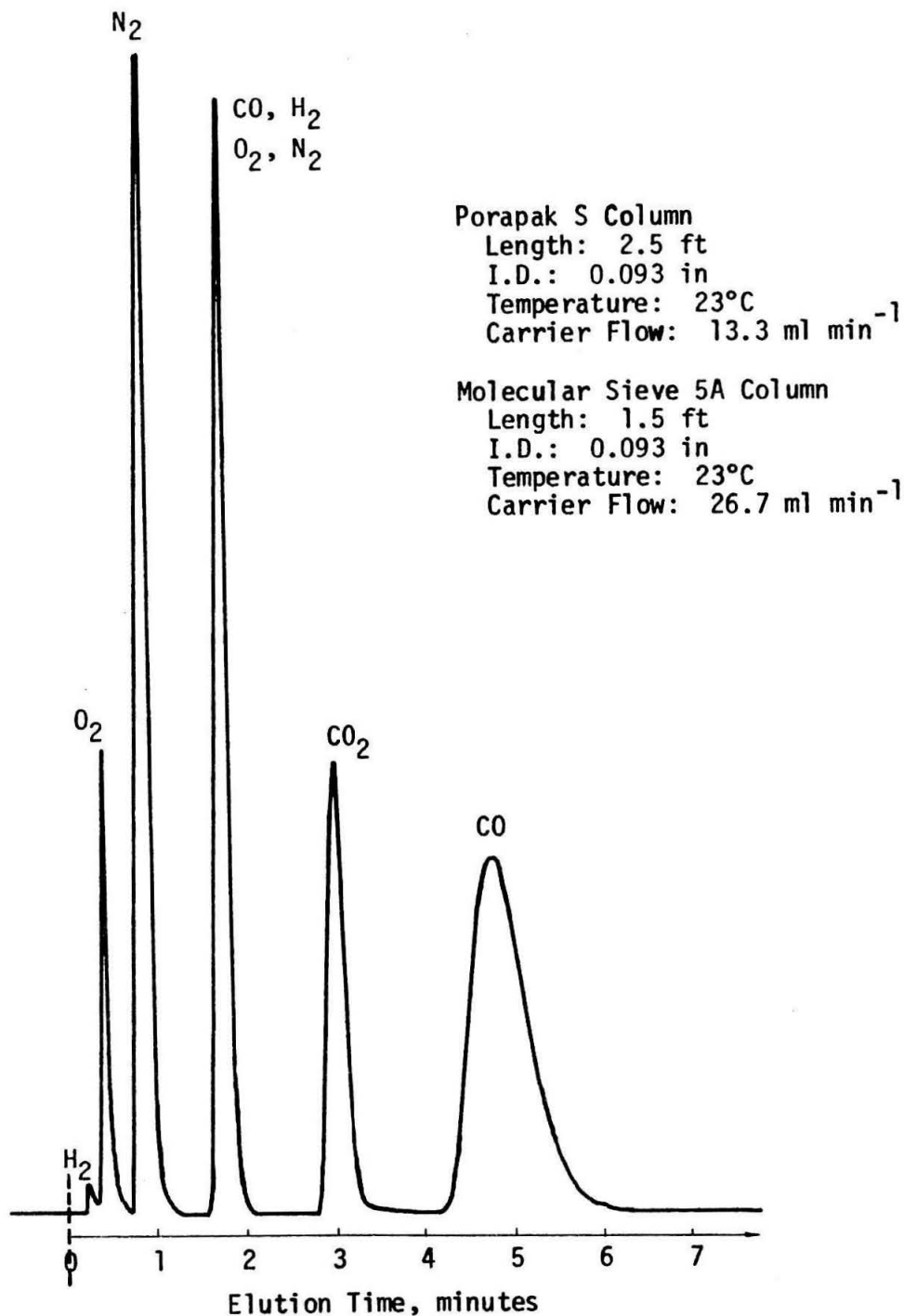


Figure 3. Chromatogram for parallel columns of Porapak S and molecular sieve 5A.

Apparent disadvantages may be summarized as follows:

1. Reproducible splitting of the sample is desirable.
2. Repeated adsorption of carbon dioxide on the molecular sieve may reduce the sensitivity and effective life of the column.

These disadvantages may be circumvented by following two relatively easy procedures. First, the composite peak for hydrogen, oxygen, nitrogen, and carbon monoxide that is eluted from the Porapak column may be compared to the total peak area for the individual peaks on the molecular sieve column. Variation in the sample split is thus noted and the appropriate correction made to the analysis. Secondly, it is recommended that the column of molecular sieve be re-conditioned frequently. This may be accomplished "in situ" by raising the temperature of the molecular sieve to 350°C for several hours while maintaining a low flow of carrier through the column.

By means of temperature programming and/or optimum choice of column parameters, the technique that has been successfully demonstrated in the separation of hydrogen, air, and carbon oxides may be applied to other compounds. Among these might be mixtures of other inorganic gases such as the oxides of nitrogen or sulphur as well as mixtures containing compounds such as water, methanol, and formaldehyde.

In conclusion, a chromatographic method based on parallel columns utilizing molecular sieve and porous-polymer beads as the stationary phases has been presented for the separation of the permanent gases. A complete, uninterrupted analysis using a single detector may be obtained

from one sample. Peaks are eluted with good shape and analysis time is minimized.

REFERENCE

1. G. Kyryacos and C. E. Boord, Anal. Chem., 29, 787 (1957).
2. A. S. Meyer and I. B. Rubin, U. S. At. Energy Comm. Rept., ORNL-2866, UC-4, Chem. General, TID-4500, 15th Ed., issued Feb. 18, 1960.
3. N. Takamiya and S. Mural, Kogyo Kagaku Zasshi, 63, 1935 (1960).
4. O. C. Hollis, Anal. Chem., 38, 309 (1966).
5. E. L. Obermiller and G. O. Charlier, J. Gas Chromatog., 6, 446 (1968).
6. A. D. Ottenstein, 13th Pittsburg Conf. Anal. Chem. Appl. Spectroscopy, March, 1962.